Newcastle University

The Formation and Development of Proglacial Overdeepenings at a Contemporary Piedmont Lobe Glacier: Skeiðarárjökull, South East Iceland

Andrew. R. Gregory
BSc (Hons)

August 2012

A thesis submitted to Newcastle University in partial fulfillment of the requirements for the degree of Doctor of Philosophy in the Faculty of Humanities and Social Sciences

DECLARATION

I hereby certify that the work described in this thesis is my own, except where otherwise acknowledged, and has not been submitted previously for a degree at this, or any other, university.

Andrew Robert Gregory

ABSTRACT

The genesis of overdeepenings in proglacial environments has been investigated within both the Quaternary and pre-Quaternary glacial-geologic record. These landforms are important as they can control the behaviour of glaciers and ice sheets through their impact upon subglacial meltwater routing and the glacial hydrological regime. The formation of such landforms has not been studied in detail at contemporary glacier margins, constituting a major gap in our understanding. This research aims to identify the processes that are responsible for the formation of overdeepenings at the margin of Skeiðarárjökull, south east Iceland, which is comparable to the outlet glaciers of the Quaternary and older glacial-geologic record. Through detailed sedimentological and geomorphological analysis, this thesis tests existing models for the formation of overdeepenings, and identifies a number of new processes which had not previously been attributed to the formation of these landforms within contemporary glacial environments. In addition to the erosive role of meltwater, this work has identified that sandur aggradation, ice stagnation, ice fracturing, variations in meltwater routing, and the formation of subglacial bedforms such as eskers can all play a key role in the formation of overdeepenings at contemporary glacier margins. The evidence presented within this thesis, which demonstrates that overdeepenings are not exclusively formed as a result of erosion, and that preferential deposition of sediments can lead to their genesis, is a huge leap from our current understanding. It has found that overdeepenings can form as a result of processes associated with the interactions of individual landforms within the wider proglacial landsystem, and that the development of the system as a whole is more important than individual processes.

ACKNOWLEDGEMENTS

I am indebted to my supervisor Prof Andy Russell, your continued energy and enthusiasm has helped to keep me going throughout this project and your advice has been invaluable. Thank you for all of your support during this long, long process and for pointing out some truly hilarious typos!!!

Mum, Dad and Ste; thank you for your love and support over the last few years and your amazing ability to always say the right thing, as always - you were right! Thank you also for the times when you knew it was better just to say nothing.

Rob Duller, Matt Burke, and Dave Blauvelt - my Icelandic Glaciers brothers. Thank you for your endless inspiration, humour, support, and distraction. Without you guys I would have probably succumb to the 'sandur madness' long ago.

Thanks also to my fellow Geography PhD's, Dave Blauvelt, Chris Leach, Chris Meikle, Rebecca Payne, and Pete Thomas. Your friendship has made the trials of this process even more rewarding. Thanks also to Flavia, because apparently, you can't have an acknowledgements section without mentioning the coffee machine!!

Thanks to all my colleagues at Royal Haskoning for your patience, I wasn't lying when I said I was doing a PhD!

Field assistance was provided by Kay Cocks, Rupy Sandhu, Kate Whitbread, and Jenny & Andrew McConkey, and numerous teams of Earthwatch volunteers - Thank you all for lightening the load on those cold, wet, summer days.

Fieldwork was conducted from March 2005 to March 2007 and was funded through the Earthwatch 'Icelandic Glaciers' project. This PhD was funded by a Newcastle University Graduate Teaching Assistantship and I was also awarded external research funds by the Quaternary Research Association, which contributed towards fieldwork and field assistance costs. Thank you also to all the staff at Skaftafell National Park for your warm hospitality.

TABLE OF CONTENTS

LIST OF FIGURES

1 INTRODUCTION AND JUSTIFICATION

This chapter introduces the main aims of the project, discusses the importance of topographic overdeepenings within contemporary glacial systems, and provides a rationale for the project. The specific objectives of this project are presented together with a summary of the thesis structure.

1.1 OVERALL AIM

The overall aim of this project is to investigate the origin of a series of overdeepenings within the contemporary glacial environment, to gain an understanding of the processes responsible for their formation, and increase understanding towards providing a modern analogue for the formation of similar landforms formed during the Quaternary and earlier Glaciations, such as tunnel channels or tunnel valleys.

1.2 INTRODUCTION AND PROJECT RATIONALE

Glaciers and ice sheets cover a large proportion of the Earth's surface, currently comprising approximately one tenth of its surface area, having a total volume close to 33×10^6 km^3 (Benn and Evans 1998; Eyles 2006). During the Quaternary period, ice volumes had been much greater, covering up to one third of the Earth's surface (Benn and Evans 1998). As these huge quantities of ice advanced and retreated during the Earth's history, they significantly sculpted much of the planet's surface and continue to be a source of landform modifying processes today.

Glaciers also act as sensitive monitors of global climate change, advancing and retreating as the Earth's climate fluctuates between colder (Glacial) periods and milder (Inter-glacial) periods (Benn and Evans 1998). Glacial landforms, the product of the glaciers interaction with its substrate, are

capable of recording glacier fluctuations and have long been used to reconstruct the dynamic nature of former glaciers and ice sheets (Clark 1997). By investigating the sedimentological and geomorphological legacy of palaeo ice masses, as well as the sediments and landforms found at the margins of contemporary glaciers, we are able to gain a detailed understanding of their internal behavioural mechanisms (Boulton 1978; Boulton 1982; Boulton 1987; Benn 1995; Clark et al. 2000). The aim of most glacial geomorphological and sedimentological investigations is to refine our understanding of these internal mechanisms, improving models used to predict the behaviour of former ice masses, thus reconstructing the former climate that controlled their formation and flow, and eventually understand the processes of global climate change (van Dijke and Veldkamp 1996; Boulton et al. 2001; Stokes and Clark 2001; Evans and Twigg 2002). However, in many cases, the processes that are responsible for the genesis of glacial landscapes are poorly understood. It is therefore necessary to study the processes and products of contemporary glaciers and ice sheets in order to better understand those found within the sedimentary and landform record (Benn and Evans 1998).

One of the many areas of glacial geomorphology that have been investigated in the past is the suite of landforms interpreted as tunnel channels and tunnel valleys. These landforms are common within the Quaternary landform and sedimentary record (Wright 1973; Ehlers and Linke 1989; Brennand and Shaw 1994; Clayton et al. 1999; Jørgensen and Sandersen 2006). They have also been identified within Late Ordovician and Late Palaeozoic successions (Ghienne and Deynoux 1998; Eyles and de Broekert 2001). Tunnel channels are semi sinuous troughs or valleys, up to 100 km long and 4 km wide, cut into bedrock or soft sediment (Ó Cofaigh 1996). Where they have been

infilled, they are commonly referred to as 'tunnel valleys' (Piotrowski 1994). Unfilled, open channels are referred to as 'tunnel channels' (Clayton et al. 1999). The term 'tunnel valley' has also been used to describe features which have been formed by non-bankfull flow conditions, which can cause confusion, as some features have been identified in terms of their morphology, whilst others have been identified depending on their processes of formation (Clayton et al. 1999) (**Figure 1-1**). Despite the ubiquity of these large topographic incisions, the common consensus is that they are of subglacial origin (Boulton and Hindmarsh 1987; Shaw and Gilbert 1990; Wingfield 1990; Brennand and Shaw 1994; Clayton et al. 1999; Beaney and Shaw 2000; Cutler et al. 2002; Smith 2004), although the exact process of formation is still under much debate. Boulton and Hindmarsh (1987) suggested that tunnel valleys formed by a steady state process of deforming subglacial sediment flowing towards low-pressure zones around conduits, allowing progressive evacuation of subglacial sediment. Whereas Piotrowski (1997; 1997), argued that for glacially-charged aquifers, groundwater flux alone was incapable of discharging large volumes of subglacial meltwater and suggested that subglacial meltwater accumulation resulted in periodic jökulhlaups (glacier outburst floods), which excavate subglacial sediments to produce tunnel valleys. Alternatively, Christiansen (1987) and Wingfield (1990) suggested tunnel channel formation was the result of headword erosion in the subglacial and subaerial environments respectively.

Our understanding of such over deepenings is crucial; where such landforms have become in-filled with glacial and glaciofluvial sediments they may act as groundwater aquifers and thus have great hydro-geological implications (Berry 1979; Sharpe et al. 2003). Where over deepened relief has been identified within the ancient geological record, they have been found to be

excellent sources of reservoir rocks which are of great importance to the oil and gas industry (Hirst et al. 2002). Furthermore, tunnel channels, which are one of a series of over deepened landforms, are believed to have played a significant role in controlling the behaviour of the large Quaternary ice sheets.

"They [Tunnel Valleys] are generally believed to have served as major subglacial drainage pathways for large volumes of meltwater, and are thus supposed to play a substantial role for the entire hydraulic system beneath glaciers. Because glacier behaviour largely reflects the subglacial hydraulic regime, the understanding of how tunnel valleys form and act is of crucial importance for the reconstruction and understanding of the former ice sheets." Jørgensen and Sandersen (2006).

Figure 1-1

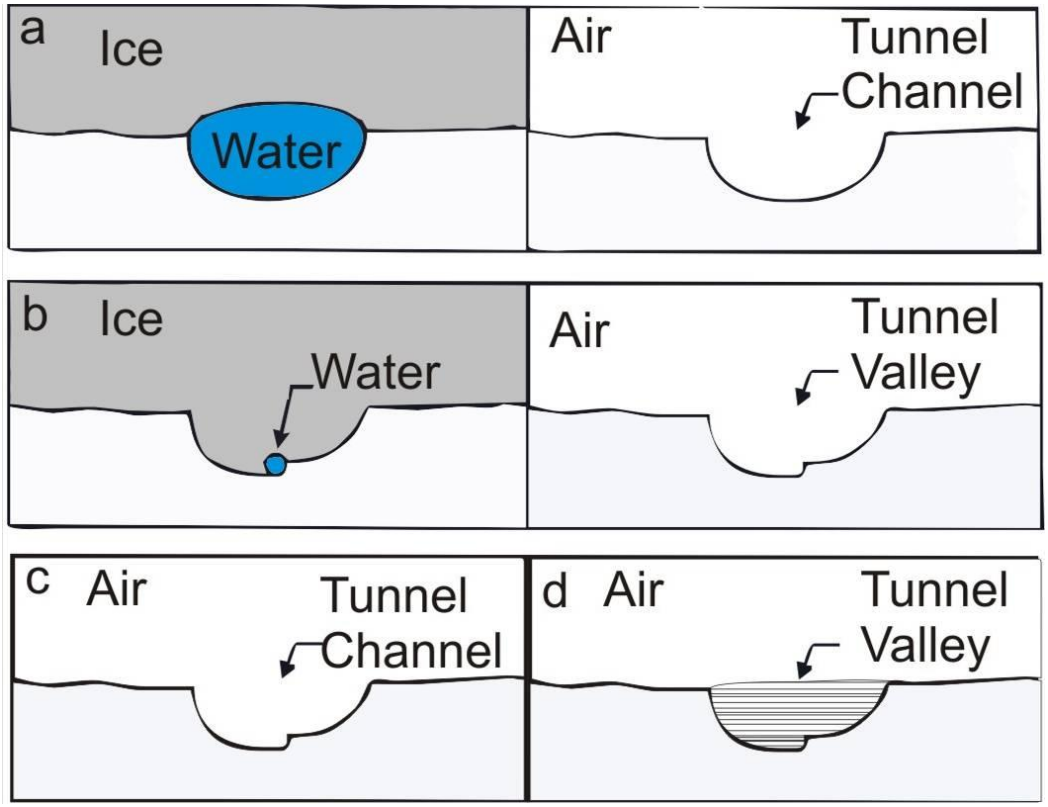

Hypothetical differences between tunnel channels and tunnel valleys based on processes of formation (a + b) or sedimentary infill (c + d). Modified from: Clayton et al., (1999).

Despite these works, no modern analogue for the formation of tunnel channels or valleys has been identified, which is a major gap in our knowledge. In addition to this gap in knowledge presented from the Quaternary literature, the presence of such topographic forms (negative relief) within glacierized catchments has the potential to impact greatly upon the glacial system within those catchments in a number of ways.

1.3 IMPACT OF SUBGLACIAL NEGATIVE RELIEF

Numerous authors have already found that negative relief within the subglacial environment can have major impacts on the glacier system (Kamb 1964; Shreve 1972; Kamb 1987; Alley et al. 2003). Hooke (1991) demonstrated that 'over-deepenings' can result in enhanced erosion as the result of positive

feedback mechanisms; over-deepenings produce crevassing in the ice surface that allows supra- and englacial meltwaters to reach the subglacial drainage system, increasing fluvial erosion of the bed (Hooke 1991). This increased erosion consequently increases the depth of the over-deepening and encourages further crevassing of the glacier surface, thus leading to increasing amounts of supraglacial meltwaters reaching the bed and further fluvial erosion (Hooke 1991). Alley et al.; (2003) demonstrated that erosion within subglacial over deepenings can become self stabilizing. Once the reverse slope of the over-deepening reaches a gradient eleven times the gradient of the glacier surface, meltwater capable of flowing up this reverse slope, due to subglacial hydrostatic pressure, becomes supercooled and freezes to the glacier bed preventing further erosion.

Subglacial negative relief also produces areas of low hydraulic potential capable of attracting vast amounts of meltwater and substantially impacting the subglacial hydrological regime (Röthlisberger 1972; Shreve 1972; Nye 1976) (**Figure 1-2**). Where such areas of low hydraulic potential remain stable, they may lead to the formation of subglacial lakes, most famously Lake Vostok beneath the east Antarctic Ice Sheet (Inman 2005). Where water collects, ice dammed subglacial lakes have the potential to have a huge impact on the glacial system, from influencing local ice flow (Tikku et al. 2004) (**Figure 1-3**), to sudden catastrophic drainage (Guðmundsson et al. 1997).

Figure 1-2

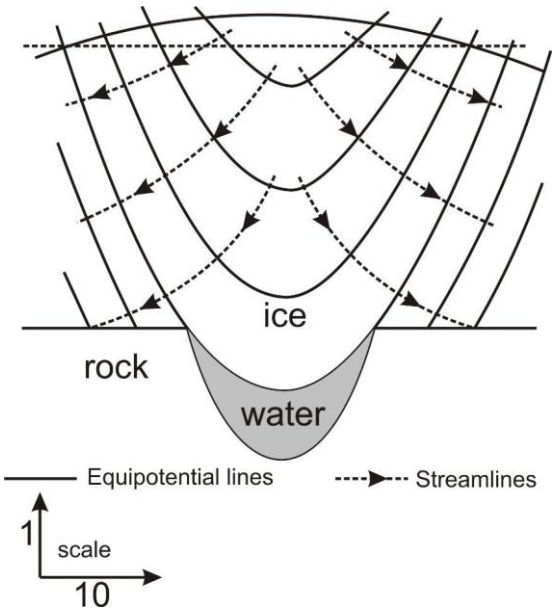

Lake formed within a subglacial depression beneath an ice dome. Source: Nye (1967).

Figure 1-3

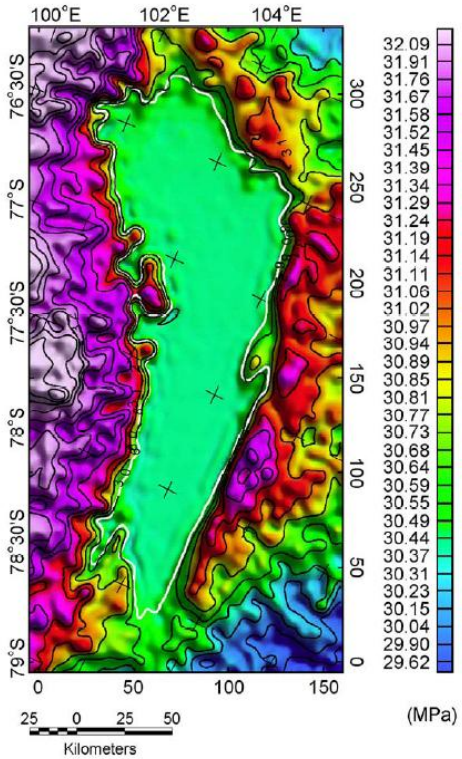

Map showing varying ice flow rates of the east Antarctic Ice Sheet influenced by the presence of subglacial Lake Vostok (Tikku et al. 2004).

1.4 IMPACT OF TOPOGRAPHIC LOWS IN AN ICE MARGINAL POSITION

Where areas of negative topography are found immediately in front of a glacier's ice margin, meltwater is likely to become ponded and form a proglacial lake. Lake formation within the proglacial environment, especially when in direct contact with glaciers, can have numerous affects, not only for the glacial system, but also for downstream fluvial and coastal systems. Where glaciers terminate in water, ice front calving becomes a prominent process (Lingle et al. 1993; Kirkbride and Warren 1999; Warren and Aniya 1999). Calving has the potential to greatly increase the glaciers rate of ablation and can promote the already increasing trend of negative mass balance seen in the majority of the Earth's glaciers at present (Kirkbride 1993). It also has the potential to increase ice flux and surface flow velocity as drawdown of ice increases to compensate for the greater rate of ablation, which may in turn lead to an increased subglacial erosion (Andrews et al. 1994). Glaciers that calve into proglacial lakes can become decoupled from the local climate signal, resulting in ice dynamic behaviour that differs from that which would be expected from the local climatic conditions (Chinn 1996).

Proglacial lakes act as sediment traps, producing new environments for lacustrine sedimentation as a result of debris entering from a variety of different sources. Supra-, en- or subglacial debris may enter proglacial lakes directly from the ice margin or from calved icebergs (Dowdeswell et al. 1995); debris from unconsolidated glacier beds can enter lakes at the grounding line as a result of local squeezing or large scale glacier bed deformation (Powell and Domack 1995); or glacial meltwater can carry sediment directly into proglacial lakes from either glacier portals or supraglacial meltwater streams (Benn and Evans 1998). Consequently, increased rates of deposition and the associated reduction in

proglacial sediment flux can have a large impact on the proglacial fluvial system and beyond. This impact has been seen at Breiðamerkurjökull in southern Iceland, where the formation of a tidal lagoon (Jökulsárlón) since the 1930's has lead to a dramatic reduction in sediment load in the river Jökulsá (Björnsson 1996). The present sediment transport rate from the glacier is approximately 10 × $10^6 m^3 a^{-1}$, of which only 30% is transported to the coast, the remaining 70% is transported to, then trapped within the lake (Björnsson 1996). This sediment storage has had a direct impact on the coastal area of Breiðamerkursandur, where coastal erosion has caused the shore line to retreat 4 km either side of the river outlet between 1904 and 1989 as a result of reduced sediment flux into the coastal system (

Figure 1-4).

Figure 1-4

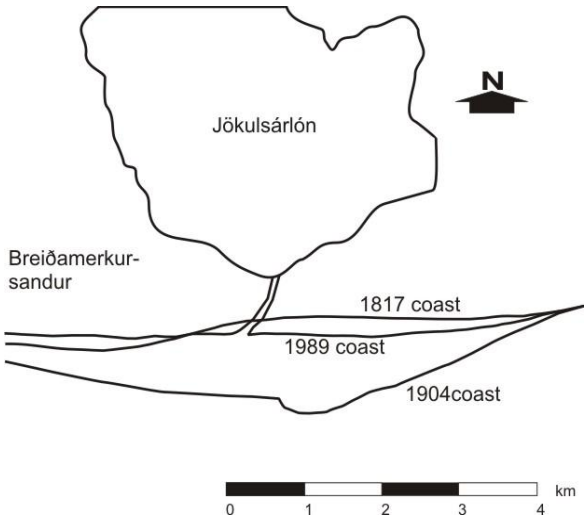

Map of the coastal area of Breiðamerkursandur, southern Iceland, showing coastal retreat between 1904 – 1989 due to sediment trapping in the glacial lake Jökulsárlón (Björnsson 1996).

From the examples described above, it is clear that areas of negative relief located within glaciated regions can have significant consequences for glaciated regions where areas of negative topography are located. Whether it is processes of subglacial erosion and deposition, ice flow dynamics over the large ice sheet

scale, or the downstream impacts of sedimentation, there is no doubt that negative relief plays an important role throughout the glacial system.

As stated in section 1.1, the overall aim of this project it to provide a modern model for the formation of over deepened, negative relief at the margins of contemporary, soft bed glaciers and to understand how these features are formed in relation to other landforms in the wider ice marginal land system.

1.5 SPECIFIC AIM AND OBJECTIVES

The aim of this thesis is to identify the processes that are responsible for the formation of overdeepenings within modern proglacial environments of soft-bedded glaciers, and to establish how these features interact with other landforms within the wider proglacial land system. To achieve these aims, a number of specific objectives have been identified:

Objective 1: Test diagnostic existing models / hypotheses for the formation of negative relief from existing literature.

Objective 2: Identify a suitable methodology to achieve objective 1, including identification of an appropriate field area and field techniques to test the diagnostic properties of pre-existing models.

Objective 3: Based on the observations of objective 2, produce a refined conceptual model, or models, for the formation of topographic overdeepenings within contemporary glacial settings.

1.6 THESIS STRUCTURE

Chapter 2 provides a detailed review of the current understanding of overdeepenings within the glacial land system. Over deepened negative relief from other systems will also be discussed where appropriate. Chapter 2

concludes with a list of models and hypothesis taken from the literature that will be tested in this study.

Chapter 3 introduces and justifies the choice of field area where this research was carried out and the methods utilized during this research. It begins with a justification for the choice of site and a brief description of the sites geographical context and history. A brief description of each method is provided, along with a justification for the choice of method and examples of where such methods have been employed successfully elsewhere.

Chapters 4 to 6 present results from three separate field sites within the ice proximal zone of Skeiðarársandur, Iceland. Each results chapter begins with a detailed description of the site, including time sequence aerial photography and geomorphological maps where appropriate. Results from geomorphological and sedimentological investigations follow, and each chapter is concluded with site-specific interpretations.

Chapter 7 draws together the interpretations of Chapters 4, 5 and 6 to discuss the formation of overdeepenings within the contemporary proglacial land system of Skeiðarárjökull. New models of overdeepening formation are presented, along with discussions of how overdeepenings are formed by the interactions of other proglacial and subglacial landforms, and comparisons to existing hypotheses are made.

Chapter 8 provides the conclusions and wider implications of this research, and suggests avenues for further study.

2 LITERATURE REVIEW

This chapter provides a detailed review of current understanding of the formative processes of topographic overdeepenings within pro-glacial systems. Processes of negative topography formation from other systems are also discussed where appropriate. Emphasis is given to the sedimentological and geomorphological characteristics that would be expected as a result of each process.

2.1 INTRODUCTION

Research into overdeepenings found within glacial environments has mainly focused on processes of subglacial erosion; such as glaciotectonic erosion of glacier beds to form 'Hill-hole' pairs (Evans & Wilson, 2006); subglacial fluvial erosion of tunnel channels and tunnel valleys (Piotrowski, 1994); or landforms that are the product of ice melt and stagnation, such as kettle holes (Maizels, 1992). In reality, the formation of negative topography can be achieved by a wider suite of processes from glacial abrasion (Boulton 1974; Hallet 1979) or meltwater corrasion (Drewry 1986) within the subglacial environment, to non-deposition associated with flow expansion (Baker 1984) within the subaerial fluvial environment, or by the interaction of landforms within the wider pro-glacial land system (Evans & Twigg, 2002).

Where material is deposited and the land surface built up, negative relief can be formed along the flanks of newly deposited positive relief. Thus, it is important to understand the processes that are responsible for the formation of both positive and negative relief, as well as the interactions between these features to fully understand the wider land system.

This chapter provides a review of the current understanding of process that result in the formation of overdeepenings and negative relief found within

glacial environments. It will outline the process or processes that are responsible for forming such landforms, and will identify diagnostic sedimentological and geomorphological signatures that one would expect to be associated with each process.

2.2 LANDFORMS OF SUBGLACIAL EROSION

Glasser and Bennett (2004) provided a detailed review of landforms of glacial erosion, identified over various spatial (**Figure 2-1**). It is clear from their review that many of the most common landforms of subglacial erosion have been identified within hard-bedded glacial environments, and far fewer have been investigated within glacial catchments underlain by soft, unconsolidated sediments which are more directly applicable to this research. Landforms of negative relief that have been investigated within soft sediments and that are of relevance to this research are tunnel channels and valleys; which are believed to have formed by a variety of subglacial erosive processes, and Hill Hole Pairs, which have a glaciotectonic origin.

Where processes result in the formation of positive relief, there is the potential for overdeepenings to form along the flanks of such features, especially where their formation is not uniform along the ice margin. As such, it is essential to provide a brief review of proglacial fans, which are deposited radially from point sources at intervals along the ice margin, and additionally, drumlins that can form as a result of proglacial fan over riding. A review of both of these positive relief landforms is provided in the following sections.

Figure 2-1

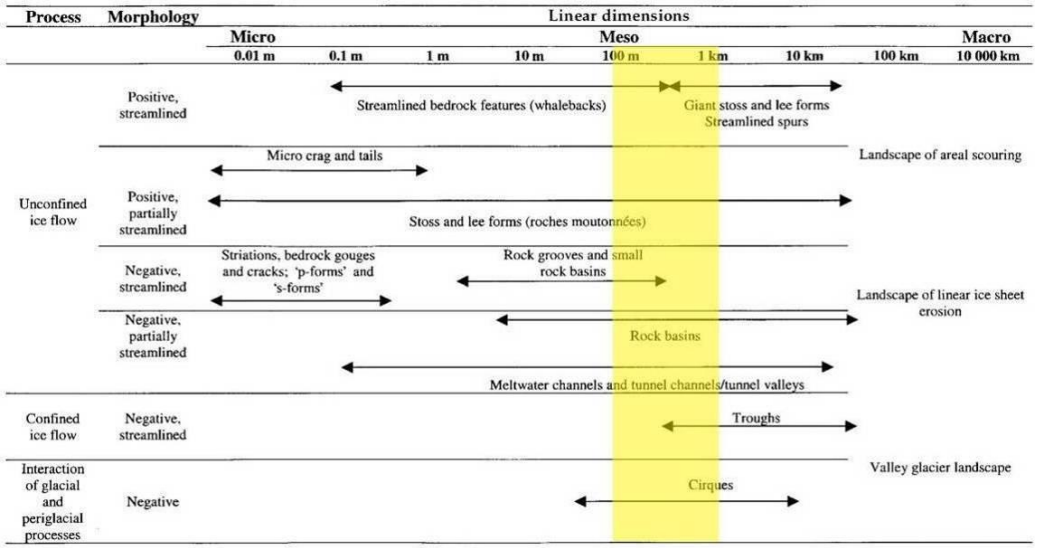

Classification of the principle landforms of glacial erosion and the spatial scales over which they occur. Yellow box highlights those applicable to this research. Modified from Glasser and Bennett (2004).

2.2.1 GLACITECTONICS & OVER-DEEPENED NEGATIVE RELIEF

Glacitectonic deformation of pro or subglacial sediments results from the normal stresses produced by the weight of the glacier becoming transferred into lateral stresses within the materials. When lateral stresses exceed the basal shear strength of the materials comprising the glacier bed, these materials bulge outwards and push laterally against adjacent materials. These stresses, in addition to the basal shear stress of the glacier, can result in significant deformation or shearing of sub and proglacial materials along failure plains (Evans and Wilson, 2006).

Aber et al., (1989) and van der Wateren, (1994) provide excellent models for the removal of sediments in the proglacial area revered to as the 'gravity-spreading model'. This model accounts for the movement of sub and proglacial materials when normal and basal shear stresses force wedges of such materials away from the glacier, upward, enabling wedges of sediment or slabs of bedrock to ride up over one another in a '*proglacial stress field*". The lateral shunting of

sediments below the glacier snout, within an area of extension results in the excavation of an overdeepening, whereas the compression of materials beyond the glacier margin results in the stacking of glacitectonic moraine. As the lateral stresses reduce with distance from the glacier, the size and extent of displaced materials also reduce, resulting in landforms with asymmetric cross profiles.

These processes have been found to be responsible for the formation of three distinctive glacitectonic landforms at the margins of many ancient and contemporary glaciers; 1) Composite Ridges, 2) Hill Hole Pairs, and 3) Cupola Hills, which are glacially overridden versions of the former two landforms (Figure 2-2).

Figure 2-2

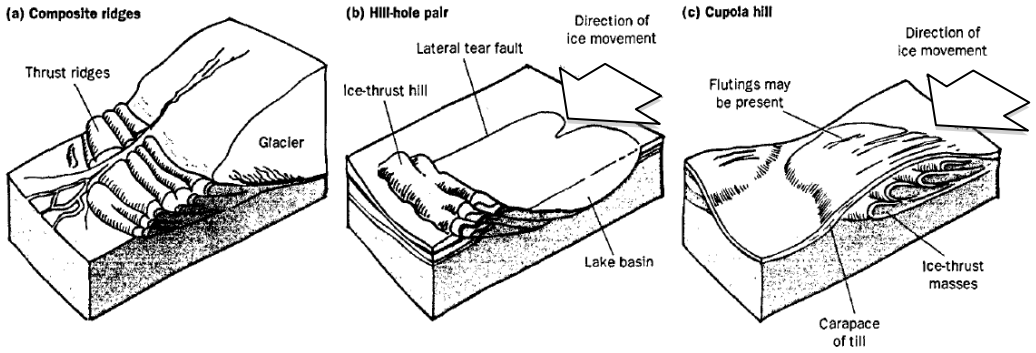

Conceptual sketches of the three main proglacial glacitectonic landforms (Evans & Wilson, 2006).

Of the glacitectonic landforms described above, Hill Hole Pairs and Cupola Hills have the potential to be linked with associated negative relief which is of interest to this research. The processes responsible for the formation of these landforms are discussed in detail below.

2.2.2 HILL HOLE PAIRS

Hill Hole Pairs, as the name suggests, are glacitectonic landforms where a discrete hill or ice-thrust material, often slightly crumpled, is situated a short distance down glacier from a depression (the 'hole') of similar size and shape

(Bluemle and Clayton, 1984). Instances have been noted where the 'hill' is located up to 5km from the originating depression (Bluemle, 1970; Clayton et al, 1980; Bluemle and Clayton, 1984), although they are usually considerably closer.

The typical morphology of a hill-hole pair as described by Aber et al, (1989) consists of four distinctive elements: (1) hills have a arcuate planform which is concave up glacier; (2) the surface of the hill is traversed by a series of transverse, sub-parallel ridges and depressions; (3) the hill has an asymmetric cross-profile, with the highest point and steeper slopes on the convex or down glacier side; and (4) the topographic depression is approximately the same shape and area as the hill, located on the concave or up-glacier side.

Where significant post formation sub-glacial modification has occurred, these morphologic features may be less obvious. In some cases, the source depressions have been known to become infilled with younger sediments, resulting in only the hill remaining visible. In addition, glacitectonic depressions have been identified without associated hills as a result of the positive relief features becoming removed by subglacial erosion (Ruszczynska-Szenajch, 1976).

Examples of Hill-Hole Pairs have been identified in various quaternary and contemporary glacial environments, from the Wolf Lake Hill-Hole Pair in Alberta Canada (Andriashek & Fenton, 1988) to the modern margins of Breiðamerkurjökull in South-east Iceland (Evans & Twigg, 2002).

An excellent Icelandic example of a Hill-Hole Pair within the contemporary setting is that in the Brennhola-Alda region of the Breiðamerkurjökull foreland in South-east Iceland. Evans & Twigg (2002) describe a series of wide and arcuate, low amplitude ridges that are aligned parallel to Little Ice Age recessional push moraines. Standing more than 30m above the surrounding terrain, Brennhola-Alda comprises a chain of

asymmetrical ridges with heavily dissected slopes. Earlier analyses of Brennhola-Alda reveled that the internal structure was also unique for the foreland moraines of Breiðamerkurjökull (Todtmann, 1960; Howarth, 1968). A number of exposures at the top of the moraine show more than 10m of interbedded sands, silts and fine gravels that Howarth (1968) believed to have been deposited as horizontal beds on a braid plain at the margin of an infilling lake. Lower facies include layers of cobbles suspended in silts and clays, interpreted to have been deposited by ice rafting events and reworked into palimpsest lags by traction currents across the lake bottom. The whole sequence is shown to dip towards the glacier and contains significant evidence for internal glacitectonic disturbance including; low amplitude folds, low angle shear faults and associated liquifaction structures and drag folds.

Even without the confirmation of internal glacitectonic structures, Thórarinsson (1956) and Todtmann (1960) suggested that Brennhola-Alda was a "Stauchmorane" or glacitectonically thrust mass. Howarth (1968) provided support for this interpretation with documented evidence of glacitectonic deformation within the internal sediments and linked them to compression from the northeast.

Figure 2-3

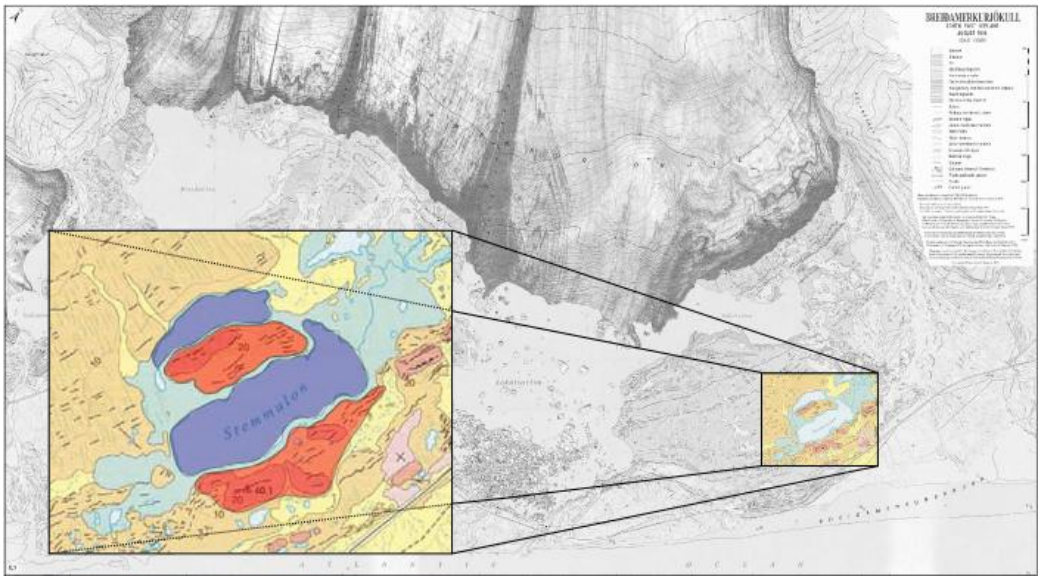

Map illustrating the location of hill-hole pairs on the foreland of Breiðamerkurjökull, Southeast Iceland. (Modified from Evans & Twigg, 2002). Hills shaded RED, Holes Shaded BLUE.

2.2.3 CUPOLA HILLS

Coined by Smed (1962) during work on the classification of Denmark's glacitectonic landforms, the term Cupola Hill refers to the glacially over-ridden remnants of a Hill-Hole pair. Such features exhibit very similar internal stratigraphic signatures to Hill-Hole pairs, made of heavily deformed glacial and glaciofluvial sediment, although evidence of glacitectonic deformation is often more pronounced. These features often have a till cover, or carapace (Jakobsen, 1996) and often have a more streamlined and smoothly undulating cross profile as illustrated in Figure 2-4.

Figure 2-4

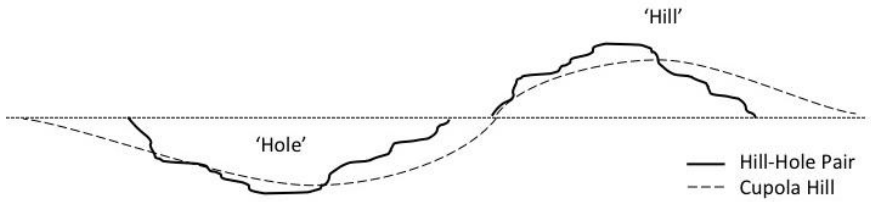

Idealised cross sections of Hill-Hole Pair compared with Cupola Hill

As has been clearly illustrated, both Hill-Hole Pairs and Cupola hills have the potential to form topography that is over deepened in comparison to the surrounding landscape, and thus an understanding of their formation is essential to this research.

2.2.4 PROGLACIAL FANS

Pro-glacial alluvial fans also have to potential to form topography that is over deepened in comparison to the surrounding landscape. These features form as the result of glaciofluvial sedimentation from point source melt-water outlets at glacial margins. Where such outlets exit onto an unconfined surface, such as the outwash plains of many typical piedmont lobe glaciers, sediments that are transported by subglacial meltwaters are deposited at the mouth of the outlet as flow expands and flow energy drops. These sediments are then redistributed across the outwash surface as the melt waters diverge across the unconfined surface to produce a distinctive fan shaped landform. The elevation of the fan is highest at its apex where the meltwater exits the glacier, and grades radially to the sandur surface (Church and Gilbert, 1975).

Where the deposition of such sediments occurs against an ice-contact slope, a feature that is common at many Icelandic glaciers including Skeiðarárjökull and Breiðamerkurjokull, the intervening areas will become

completely enclosed, resulting in the formation of areas that are overdeepened in comparison to their surroundings as is illustrated in Figure 2-5.

Figure 2-5

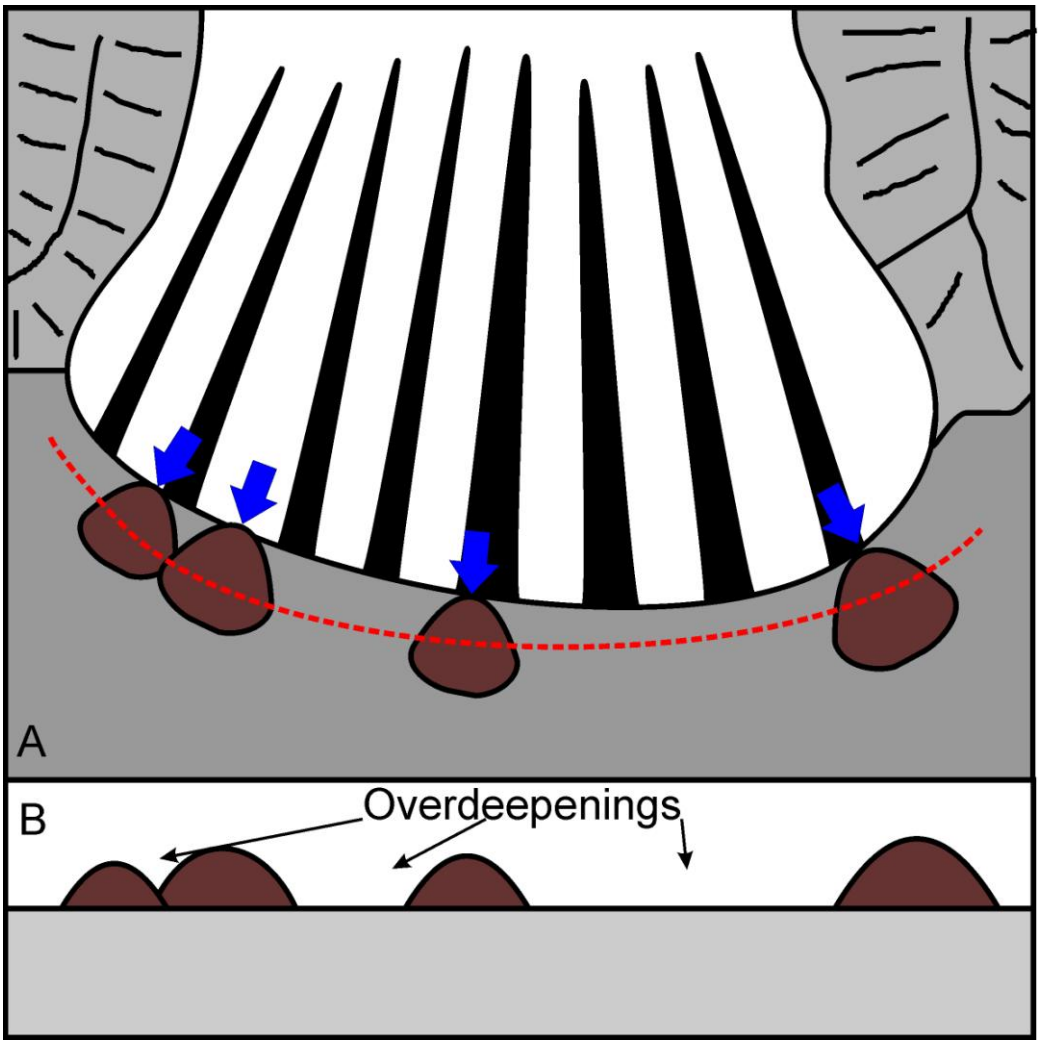

Schematic model of overdeepenings formed in-between ice-contact proglacial fans.

The formation of such features can vary significantly as a result of temporal and spatial variations in the ice margin position and sub-glacial hydrological regime, be it as a result of changes in diurnal meltwater flow, or seasonal variations in the position of the glacier front. Proglacial fans can also form as a result of single events, such as glacier out-burst floods (jökulhlaups) or following short-lived flood events succeeding the end of glacier surges (Russell et al, (2001), van Dijk, T. (2001).

van Dijk, T. (2001) noted the development of a series of ice contact fans along the margin on Skeiðarárjökull during the 1991 surge event. These landforms were found to be deposited against push moraines composed predominantly of deformed surge-related fluvial sediment and were noted to be regularly spaced along the glacier snout, reflecting the reorganization of the subglacial drainage system during surges (Figure 2-6).

Figure 2-6

Regularly spaced proglacial fans formed at the margin of Skeiðarárjökull, South East Iceland, during the 1991 surge event. Russell et al, (2001)

Furthermore, the formation of large fans has been noted as a consequence of sediment deposition following large-scale meltwater evacuation from glaciers during outburst floods. Russell and Knudson (2009) note that large scale alluvial fans were formed during the 1996 jökulhlaup of Skeiðarárjökull, comprised of upward-coarsening sequences of horizontally bedded sands, gravels, boulders and debris-rich ice blocks, which suggest deposition varied from of rising-limb fluvial flows to hyperconcentrated and debris-flow.

2.2.5 DRUMLINS

Drumlins are one of the most recognisable and most intensely investigated landforms of a glacial origin, having been studied for over 120 years (Upham, 1892). Over the past 120 years, a huge collection of literature focusing on drumlins and many theories of their formation has been amassed.

Consequently, a full review of the formation and composition of drumlins would likely make up the requirement of a thesis in its own right, and is far beyond the needs of this research. For this reason, this review is going to concentrate on the theories of drumlin formation which are most credibly recognised, and that are most appropriate to the setting of this research in South East Iceland.

2.2.5.1 Drumlin Morphology

Menzies (1979) defined drumlins as:

"Typically smooth, oval-shaped hills of hillocks of glacial drift resembling in morphology an inverted spoon or an egg half-buried along its long axis. Generally the steep, blunter end points in an up-ice direction and the gentler sloping, pointed end faces in the down-ice direction"

The long axes of drumlins are orientated parallel to that of the forming ice flow, with the highest and widest part of the feature located towards the stoss (up-ice) end. Where drumlins have a very narrow and long plan form they have been referred to as spindle forms, while broad, asymmetric forms are referred to as parabolic form s (Shaw, 1983; Shaw 1998).

As research into the formation of drumlins has advanced, as has the identification of more complex drumlinoid forms including superimposed drumlins (Rose and Letzer, 1977) and asymmetrical spindle drumlins with overdeepened hollows along one margin (Clapperton, 1989). These latter forms

are of particular relevance to this research due to their formation with an associated overdeepening.

Figure 2-7

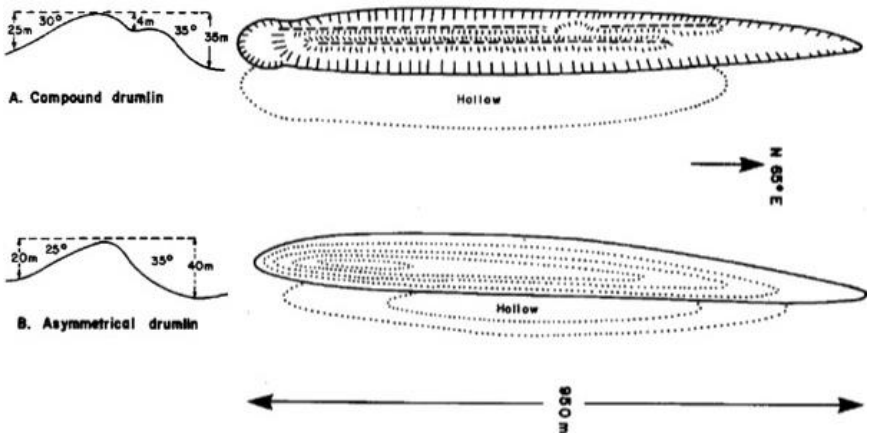

Cross section and plan form of Compound and Asymmetric Drumlins. Modified from Clapperton, (1989).

2.2.5.2 Drumlin Composition

The exact composition of drumlins is particularly varied, in fact Menzies (1979) states that "the internal composition of a drumlin varies from stratified sand, to unstratified till, to solid bedrock, with every possible permutation between".

Thus, the range and number of articles dealing with the subject is just as vast. However, Stokes et al, (2011) reported that drumlin composition could be distilled into five basic types;

1. Mainly bedrock
2. Part bed-rock / part till
3. Mainly till
4. Part till / part sorted sediments
5. Mainly sorted sediments.

2.2.5.2.1 Bedrock Drumlins

Bedrock Drumlins are some of the least well studies types of drumlin within the drumlin composition literature (Stokes et al,. 2011). First reported by Fairchild (1907), they are found in a variety of rock types, from Precambrian

shield rocks, to younger sedimentary rocks (Dionne, 1987), although they are most often seen in harder, crystalline rocks (Graham et al., 2009).

The morphology of such drumlins is often similar to that of other bedrock erosional features such as rouch moutonnées and whalebacks, and these features are often referred to as 'rock drumlins'. However, Evans (1996) highlights the fact that they differ in long profile, as rock drumlins are asymmetrical where as whalebacks have a symmetrical long profile.

2.2.5.2.2 Bedrock & Till Drumlins

Initially reported in 1883 by Chamberlin (Menzes, 1979), these drumlins are composed by a combination of rock and till. Although the proportion of these to components varies significantly, it is accepted that 25% of the drumlin should be composed of till for it to be differentiated from a Bedrock Drumlin (Dionne, 1987).

Some have a core of consolidated rock, surrounded and entirely covered by unconsolidated sediments, which can comprise one or several units of till, and/or glaciofluvial sediments, which has lead to the term 'rock cored' drumlins.

The position of this core has been reported throughout the structure, but appears to most frequently reside in the stoss of the structure (Boyce and Eyles, 1991; Fuller and Murray, 2002).

Stokes et al., (2011) note that in some cases it is not possible to determine the limit of the bedrock 'core' and, depending on the size of the exposure, it could be easy to mistake large boulders as bedrock. In addition, Patterson and Hooke (1995) illustrate that in some drumlinised areas, small bedrock protuberances are present in drumlin fields that are not associated with drumlins.

2.2.5.2.3 Mainly Till Drumlins

First investigated by Upham (1892), till drumlins are the most frequently investigated of all drumlin types (Stokes et al, 2011). These drumlins are composed entirety of unconsolidated diamicton (till), however, the exact composition or structure of these tills has been shown to be extremely variable. Wright (1962) described drumlins from Minnesota that were composed of a single unit of homogenous till, where as other have found drumlins composed of numerous layers of tills, some displaying evidence of deformation (Nenonen, (1994).

In some studies, the relative ages of the till units have been established based upon the thickness and relative density of the units in question. Cores comprised of 'older' till suggest that different subglacial processes are responsible for their deposition over time. For example, Aario and Peuraniemi (1992) describe a densely-packed underlying till covered by a less dense till unit and suggested that dense core was deposited by lodgement and melt-out, where as the overlying till was the result of melt-out and flow processes throughout deglaciation.

Johnson et al. (2010) noted that up to five till units were present within two drumlins at the active glacier margin of Múlajökull in Iceland. They investigations found that the upper three till units were separated by small lenses of sorted sediment, and that the highest till unit in the sequence could be traced between the present-day ice margin and the 1992 surge end moraine. The upper till unit also covered an erosional surface that represented the drumlins shape before the till was deposited during the 1992 surge. Other studies have shown that till units do not always correspond to the underlying drumlin surface (Stea and Brown, 1989).

Where layers do correspond to the drumlin surface, it has been implied the layers have been deposited cumulatively over time, which has resulted in the eventual drumlin formation (Fairchild, 1929; Newman and Mickelson, 1994). Alternatively, where tills do not correspond to the drumlins surface, it is often suggested that the shape of the drumlin has been produced by erosion.

2.2.5.2.4 Till & Sorted Sediment Drumlins

First discussed by Kupsch (1955), sorted sediment / till drumlins have become the most commonly reported type of drumlins since the late 1970's (Stokes et al, 2011). With in such drumlins, the location of the sorted sediments can vary, will some drumlins possessing a central 'core' of sand and gravel (Boulton, 1987) and others exhibiting sorted sediments inter-bedded between layers of till (Kerr and Eyles, 2007).

Hart (1995) found that drumlins in northwest Wales were composed of a relatively more resistant core of glaciofluvial sand and gravel, which was surrounded by a thin layer of till. In some cases the core appeared to have been deformed. Hart (1995) also found that the till was often thinnest, or some times stacked, at the stoss end of the drumlins.

Other studies have shown that sorted sediment can be preferentially deposited at the lee of the drumlin, suggesting that they have infilled a lee-side cavity within the ice which had formed as a result of the drumlin itself (Hanvey, 1989).

2.2.5.2.5 Sorted Sediment Drumlins

First reported by Upham in 1894 (Stokes et al, 2011) drumlins composed entirely of sorted sediments have received relatively little attention in

comparison to drumlins composed from till. These features, often overlain with a very thin veneer of till, differ greatly from till drumlins in that they very rarely exhibit evidence of internal deformation (Shaw, 1983; Sharpe, 1987; McCabe, 1989).

Menzies and Brand (2007) reported a large exposure of proglacial and deltaic sediments with a drumlin at Port Byron, New York State. These sediments exhibited no evidence of deformed. Menzies and Brand (2007) suggested that the drumlin formed by the precipitation of calcium carbonate, which cemented the stratified sediments. These consolidated sediments then acted as an obstacle around which a thin veneer of till was deposited.

Shaw (1983) presents an alternative theory for the deposition of sorted sediment drumlins in which case such sediments are deposited within subglacial cavities by large subglacial floods.

2.2.5.3 Drumlin Formation

Related to the scale of literature available, Sugden and John (1976) suggested that there might be as may theories for the formation of drumlins as there are drumlins themselves, and as stated earlier, a full review of all of these theories is far beyond the scope of this thesis.

However, despite the huge number of individual theories, most can be characterised within three types of processes;

1. The erosion of intervening areas,
2. The accretion of sediment into hills,
3. A combination of the above.

The most widely accepted model of drumlin formation relies on the erosion and redistribution of sediments with the deforming glacier substrate (Boulton, 1987). It is suggested that stiffer materials will not deform, or will

deform more slowly than weaker sediments, thus leading to the weaker sediments becoming streamlined around the stiffer, immobile sediments.

Boulton (1987) provides the example of an initial bed of course grained gravel bodies within finer grained sediments. Due to the course nature of the gravels, theses are better drained, and have higher sediment strength due to their low pore water. As such, the surrounding finer sediments undergo pervasive deformation, producing sheaths of attenuated glacitectonite and deformation till around the stiffer gravel cores (Figure 2-8).

Figure 2-8

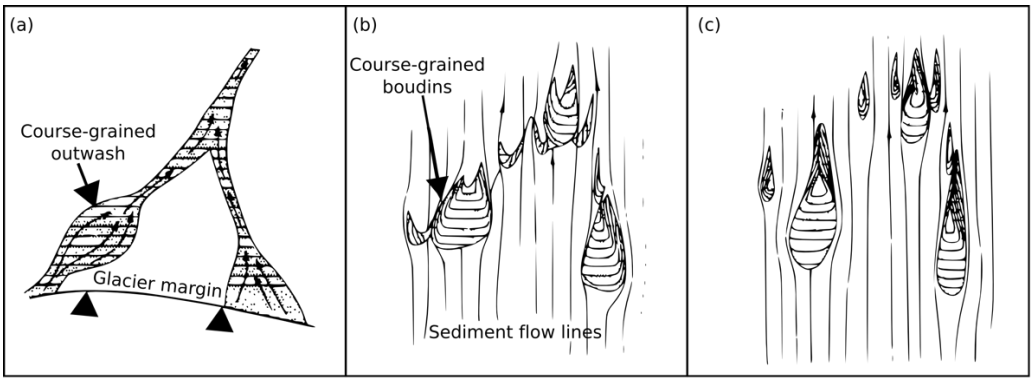

The formation of drumlins as a result of varying sediment properties overridden by a glacier: (a) Initial distribution of coarse-grained proglacial sediments, (b) + (c) progressive development of drumlins from coarse-grained sediment masses and rapid deformation of weaker sediments. (Boulton, 1987).

Further evidence suggests that Boulton's (1987) theory can be applied to many types of drumlins with solid rock, till, or sorted sediment cores, each of which can form resistant regions within the glacier substrate around which softer sediments can be deformed. Figure 2-9 provides a schematic review of the deforming bed processes that can result in the formation of drumlins.

Although widely discredited, the formation of drumlins, particularly sorted sediment drumlins, has been interpreted as a product of the infilling of large scours that have been excavated into the basil ice of glaciers by catastrophic subglacial floods (Shaw, 1983, Fisher and Shaw, 1992). Support for this hypothesis is provided by the similarity in the form of some drumlins, with scout marks such as spindle flutes and other longitudinal P-forms.

Figure 2-9

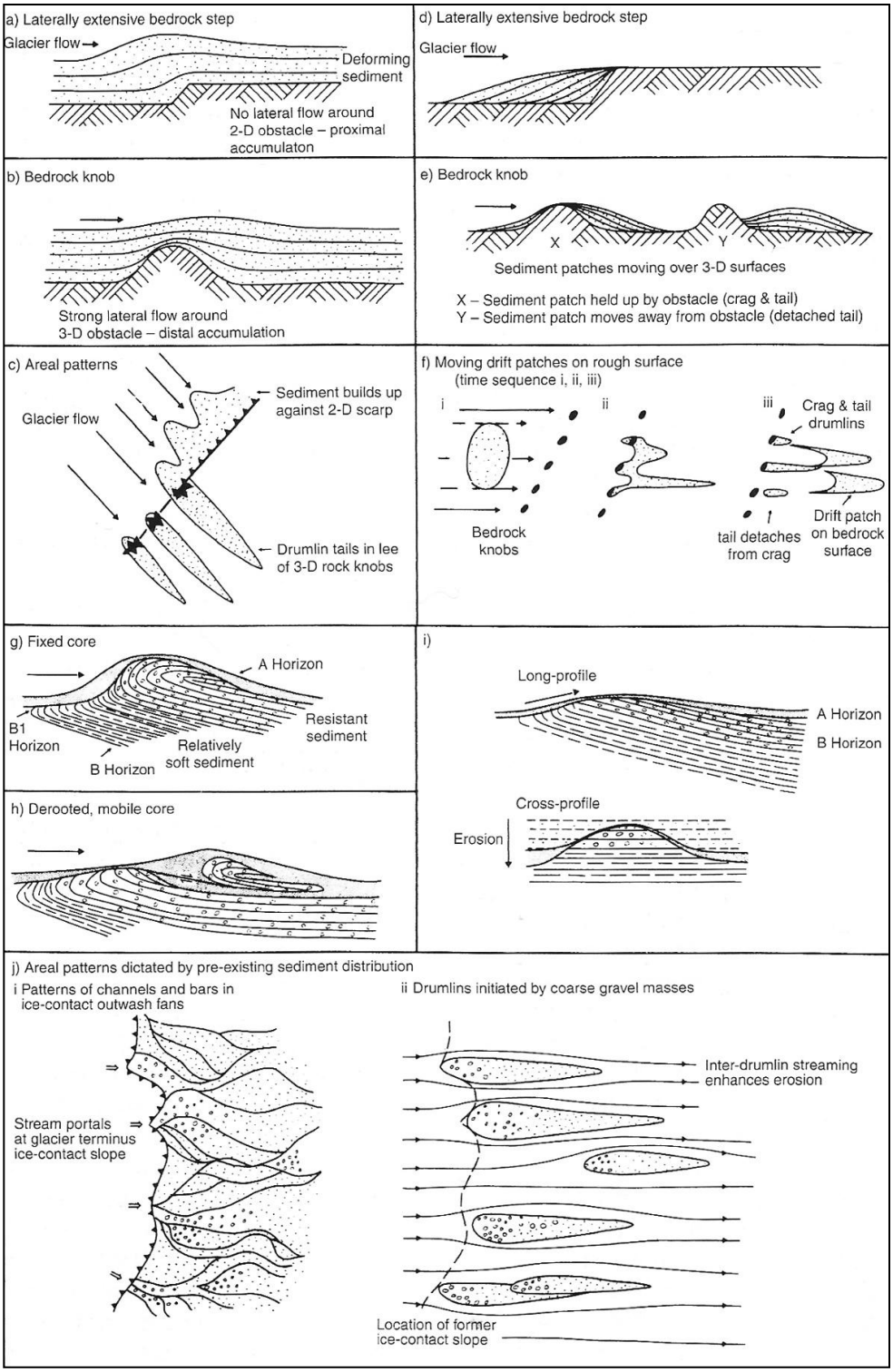

Summary of deforming bed drumlin formation processes (Boulton, 1987).

Support for the sub-glacial flood model is provided by Sharpe (1987), who suggest that the sediments that make up these drumlins are deposited

within subglacial cavities during the waning stage of the flood, thus producing stratified sediments that have been observed within many documented drumlins.

Figure 2-10 -

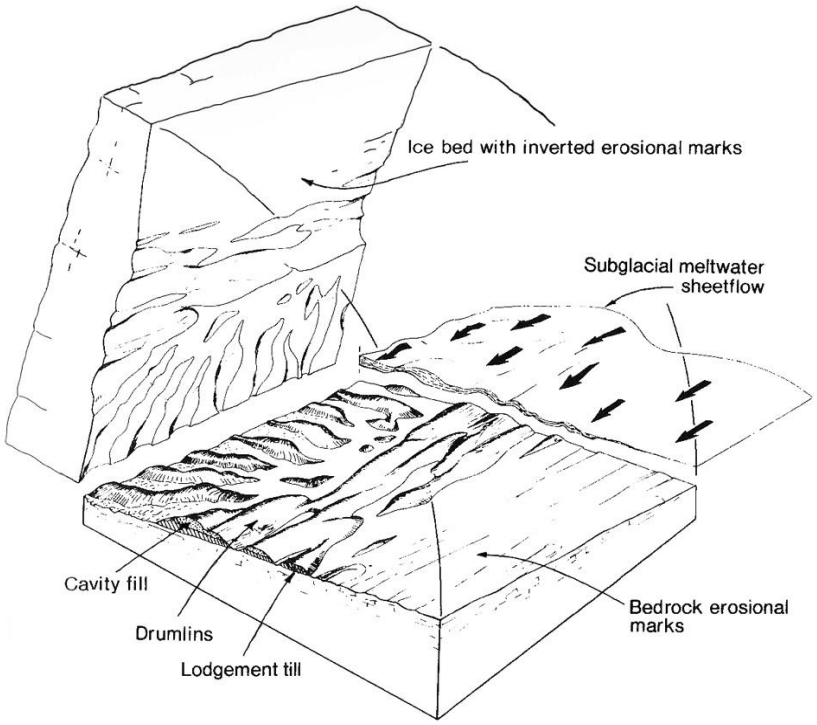

Schematic diagram of the formation of Drumlins by subglacial sheet floods (Fisher and Shaw, 1992).

Shaw et al, (1989) and Shaw (1993) have also suggested that the flood model can also explain the formation of till-cored drumlins. In this instance, it is suggested that such drumlins are purely erosional and that subglacial floods are responsible for their formation by eroding the substrate in the intervening areas between each bedform.

These theories have been widely criticised in the past (Benn and Evans, 1996; Evans et al, 2006) as the megaflood hypothesis attempts to explain too much. If the drumlins are made up of sorted sediments are interpreted as scour infilling and if they are made up of tills, they are considered erosional. As such,

the hypothesis cannot be falsified and is thus considered as a number of ideas that could result in the formation of drumlins, rather then a testable scientific theory (Benn and Evans, 1996).

2.3 TUNNEL CHANNELS AND VALLEYS

Tunnel channels are elongate topographic depressions with steep sides that are cut into bedrock or unconsolidated sediment (Ó Cofaigh 1996). In many respects their topography resembles that of a river valley except for their greater depths, steeper flanks and undulating long profiles (Piotrowski 1994). The common consensus is that they are formed by subglacial fluvial erosion (Boulton and Hindmarsh 1987; Boyd et al. 1988; Piotrowski 1994; Ó Cofaigh 1996; Piotrowski 1997; Clayton et al. 1999; Beaney 2002; Hooke and Jennings 2006; Jørgensen and Sandersen 2006). This is on account of their anastomosing plan form, the identification of subglacial bedforms such as eskers and drumlins on channel floors and that the bed gradient of many tunnel channels is opposed to regional gradient, meaning that meltwater flow would have been up hill, which can only be explained by the hydrostatic pressures of the subglacial drainage system (Shreve 1972). However, the specific nature of subglacial fluvial erosion responsible for tunnel channel formation is still under much debate. Most hypotheses for tunnel channel formation can be categorised into a) steady state; b) catastrophic, or c) polygenetic, the latter suggesting both meltwater erosion and direct glacial abrasion. A full description of each of the above will be provided once the terminology used within the tunnel channel literature and scales of formation for tunnel channels have been explained.

The terminology used to describe tunnel channels and valleys within the literature is often confusing. Many different terms have been used to describe large (meso / mega-scale) elongate landforms within the glacial literature; glacial

troughs, tunnel channels, tunnel valleys, linear incisions and valley channels have all been employed (Boulton and Hindmarsh 1987; Boyd et al. 1988; Wingfield 1990; Ó Cofaigh 1996; Clayton et al. 1999). Where channels are in-filled with sediments, they are preserved within the sedimentary record as 'tunnel valleys' and are often filled with unconsolidated glaciofluvial sands, gravels, and glacial diamicton (till). For the sake of consistency, the term 'tunnel channel' will be used to refer to over-deepenings that do not contain a sedimentary infill. As tunnel valleys are in-filled and no longer provide an area of negative topography, their processes of formation will be discussed but they too will be referred to as tunnel channels. Further confusion associated with the terminology within the literature comes from the use of 'channel' to mean formed from bank-full conditions and 'valley' formed from smaller channels. Hence, as described in **Section 1.2 (Figure 1-1)**, some features are named based on their process of formation, whilst others their degree of infill. For the sake of clarity, all features described within the literature as tunnel channels, tunnel valleys or subglacial channels etc, will be referred to as tunnel channels.

The spatial scale over which tunnel channels form can be considerable. Shaw and Gilbert (1990) describe an anastomosing system of tunnel channels near eastern Lake Ontario, USA, which shows channels up to 8 km wide stretching over a course for over 40 km. Piotrowski (1994) described tunnel channels in northwest Germany as being at least 13 km long and 222 m deep (191 m b.s.l.). These tunnel channels are clearly larger than the meso-scale features that are under investigation, however the processes of formation are no less applicable.

2.3.1 STEADY STATE TUNNEL CHANNEL FORMATION

Boulton and Hindmarsh (1987) provided the first theoretical hypotheses for the formation of tunnel channels, stating that they are the result of steady state unconsolidated subglacial sediment deformation into R-channels (Röthlisberger channels) under high porewater conditions. This model proposed a steady state process of formation where higher porewater pressures in subglacial sediment in comparison to the overlying, overburden pressure and hydrostatic pressure within subglacial channels, lead to the deformation of subglacial materials into meltwater conduits at the glacier bed. The material that is deformed into the conduit is subsequently removed by fluvial erosion, which leads to the drawdown of the glacier sole as its substrate is removed from below (**Figure 2-11**). This processes allows the formation of very deep (hundreds of metres) and very wide (kilometres) tunnels channels by the steady state evacuation of material from much smaller subglacial conduits (Ó Cofaigh 1996).

Figure 2-11

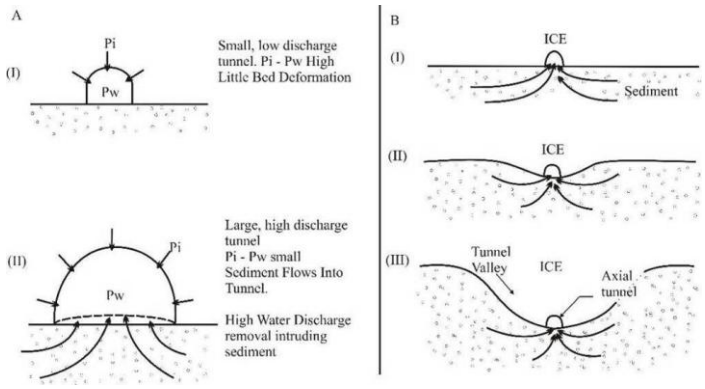

The formation of tunnel channels by steady state removal of subglacial deforming sediment and lowering of the glacier bed. (Boulton and Hindmarsh 1987)

More specifically, Boulton and Hindmarsh (1987) suggested that where glaciers overlie soft sediments with low hydraulic transmisivity, the bulk of meltwater is not able to be removed by groundwater flow alone, and this may

lead to groundwater pressures that are equal to the ice over burden pressure. If friction between particles is low, as a result of low effective pressures, sediment may liquefy and flow towards the ice margin due to its unconfined position, potentially producing 'pipes' within subglacial sediments. This scenario is initiated within the marginal zone where discharges and hydraulic gradients are highest. Boulton and Hindmarsh (1987) suggested that pipes formed within subglacial sediments would form drainage conduits that will reduce potentials within the aquifer, allowing stable deformation to occur. Subsequent removal of subglacial sediments is the result of deformation into subglacial conduits, which is immediately eroded by rapid meltwater flow. Evidence used in support of this hypothesis is the identification of eskers occupying tunnel channel floors. Boulton and Hindmarsh (1987) believed eskers to be blocked remnants of immature meltwater channels, where sediment was deformed into the channel but has not been subsequently removed by meltwater.

The processes responsible for the formation of tunnel channels by this hypothesis allow one to speculate about the potential sedimentary and geomorphologic signatures that would be expected as a result. Firstly, one would expect to find evidence of extensive deformation and shearing of the material comprising the tunnel channel walls and floor as the primary processes of formation is deformation into a subglacial conduit. One would also expect to find extensive evidence of 'piping' throughout the sediments, or pipe collapse or infill structures as Boulton and Hindmarsh (1987) stated that pipes form within subglacial materials to relieve pressure within saturated sediments. Ó Cofaigh (1996) also described the potential to find 'esker-like' features composed of subglacial diamicton with evidence of deformation along their flanks, following the thalweg of tunnel channels (**Figure 2-12**).

Figure 2-12

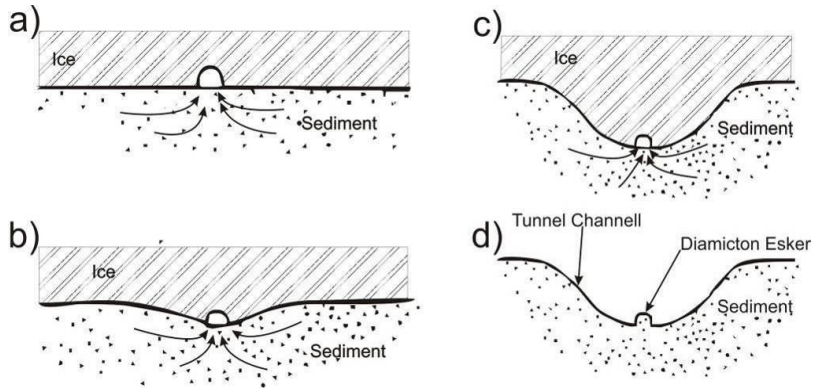

Theoretical formation of diamicton cored Eskers as a result of subglacial sediment deformation into subglacial R-channels. A) – C) Shows the steady state removal of subglacial sediment and lowering of the glacier bed. D) Shows a de-glaciated remnant of the subglacial channel, unfilled with deformed glacier bed sediments forming a diamicton cored Esker. Model modified from Boulton and Hindmarsh (1987) as discussed by Moores (1989) and Ó Cofaigh (1996).

Support for the Boulton and Hindmarsh (1987) model is provided by Evans et al. (2010) who presented evidence of eskers composed of subglacial till on the foreland of Sandfellsjökull, Iceland. However in this case, the eskers were not formed within a topographic trench or tunnel channel, and were interpreted as having been formed by the deformation of sediments into a subglacial conduit after meltwater evacuation.

Further support for the steady state hypothesis was proposed by Moores (1989), who suggested a steady state process for the formation of tunnel channels in central Minnesota, USA. Contrary to other works in this region (Wright 1973; Clayton et al. 1999), Moores (1989) suggested that tunnel channels are the result of supraglacial meltwaters that have penetrated the ice surface through moulins during deglaciation and have eroded channels in the glacier substrate in a processes similar to that described by Boulton and Hindmarsh (1987) (**Figure 2-11**). The evidence for this hypothesis is the formation of tunnel channels located behind moraine ridge systems and the presence of eskers that are initiated at moulin kames within tunnel channels.

Moores (1989) suggests the tunnel erosion was achieved by a mechanism similar to that proposed by Boulton and Hindmarsh (1987), and that the presence of eskers within tunnels was due to a reduction in discharge, resulting in a switch from erosion to deposition within subglacial conduits. As many of the eskers in question are initiated at moulin kames, Moores (1989) suggests this is evidence for the meltwater having a supraglacial origin, and that tunnel channels and eskers form time transgressively as ice sheets retreat (**Figure 2-13**).

Figure 2-13

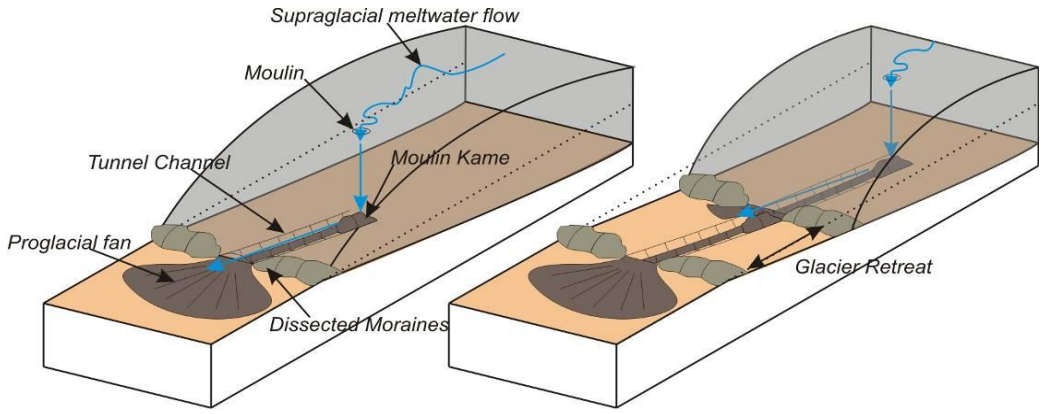

Simplified block diagram of time transgressive tunnel channel formation based on the processes described by Moores (1989).

To identify evidence of these processes occurring within the modern environment, one would expect to see a suite of features including tunnels intersecting breached end moraines, with associated outwash fans (Moores 1989). One would also expect to see eskers within tunnel bottoms that are composed of either deformed subglacial sediments or sand and gravel derived from debris rich basal ice. Eskers are likely to be associated with kames derived of supra- or englacial debris.

In order to falsify Moores (1989) hypothesis, the following observations must be made;

1) The termination of a tunnel channel at locations other than breached end moraines;
2) The absence of kames within tunnel channels or the presence of sub-glacially transported materials within the tunnel channel.

Support for the formation of tunnel channels by steady state processes was provided by Praeg (2003). Based on seismic imaging of tunnel channel infills in the North Sea basin, Praeg (2003) found that the seismic reflections of the deepest channel infills were consistent with the reflections of glaciofluvial sands and gravels. This is in direct contrast to previous works that found the deepest infills to be characterised by chaotic reflections (Wingfield 1990). These chaotic reflections were interpreted as catastrophic flood deposits (hyperconcentrated flows). Praeg (2003) suggests that the presence of glaciofluvial sands and gravels in the bottom of tunnel channels is evidence of their formation by steady state subglacial meltwater erosion. Although tenuous, Praeg (2003) accepted that this hypothesis required further testing.

2.3.2 'CATASTROPHIC' TUNNEL CHANNEL FORMATION

Many authors have described the formation of tunnel channels as a result of short lived 'catastrophic releases' of meltwater, where discharges are greatly in excess of the upper perennial boundary of glacier melt dominated flow (Roberts et al. 2005). These outbursts and their associated erosion events are commonly described as occurring within either the subaerial (proglacial) or subglacial environments.

2.3.2.1 Subaerial catastrophic tunnel channel formation

Wingfield (1990) described the formation of tunnel channels as the product of subaerial jökulhlaup plunge pool erosion. Seismic profiles of incisions into Pleistocene strata and older rock of the British continental shelf in the North Sea revealed a series of incisions with morphology down cut 100-360

m deep (150-450 m below m.s.l), with widths from 2-5 km and lengths of 6-30 km. Wingfield (1990) stated that these 'incisions' [tunnel channels], which are up to 100km long, are composites formed by individual features less than 30km long, and that they are the result of mass evacuation of subglacial meltwater that was dammed up behind a frozen ice sheet margin. Wingfield (1990) suggested that evacuation of meltwater through the ice sheets substrate was inhibited due to the low hydraulic conductivity of the clay-rich Quaternary deposits on which the glacier lay, leading to the build up of subglacial hydrostatic pressure. Ponded meltwater was subsequently released once subglacial hydrostatic pressure exceeded ice over-burden pressure, leading to hydrostatic jacking of the glacier bed from the substrate. Formation of the tunnel channel was then initiated at the ice margin, where floodwaters flowed through a subglacial tunnel and produced a plunge pool where waters spilled out onto a proglacial sandur. Tunnel channel growth continued as the plunge pool eroded headword, into the glacier, leading to collapse of the subglacial tunnel roof, increasing erosion and causing further channel growth (**Figure 2-14**).

Figure 2-14

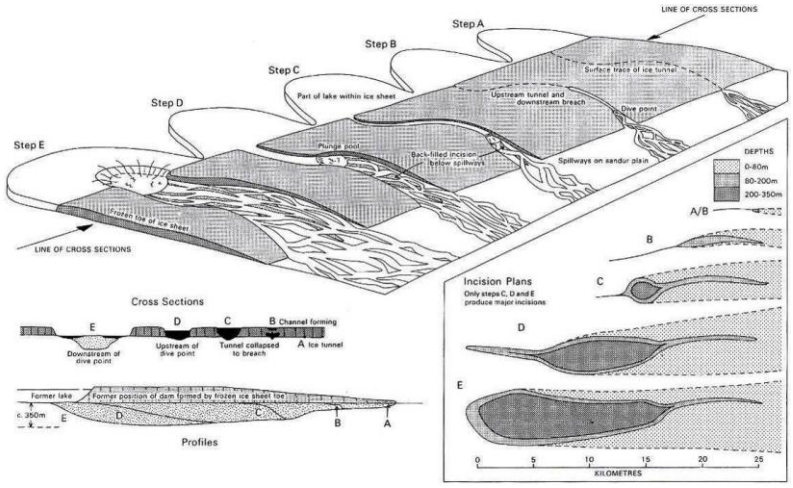

Schematic model of the formation and immediate infilling of Tunnel Channels by the headword erosion of an ice marginal jökulhlaup plunge pool. From Wingfield (1990).

Support for this hypothesis was presented by Christiansen (1987), who described the Verendrye Valley in Saskatchewan, Canada. The Verendrye Valley is a 100 km long, 1km wide, and 225 m deep channel, which Christiansen (1987) states formed time transgressive by head ward meltwater erosion under the margin of the Laurentide Ice Sheet during final deglaciation, whilst the ice margin remained stationary.

Although significant support has been provided for the subaerial hypothesis, as is shown in Figure 2-14, such features become instantly infilled, and thus do not present a process for the formation of over deepenings of negative relief, which is the focus of this study.

2.3.2.2 Subglacial catastrophic tunnel channel formation

The preferred hypothesis for the formation of tunnel channels by most authors is as a result of subglacial catastrophic flooding. However, the exact nature of these floods is still under much debate. Controversially, Shaw and others stated that tunnel channel genesis was the product of cataclysmic subglacial *sheet floods* (Shaw and Archer 1979; Shaw 1983; Shaw 1988; Sharpe and

Shaw 1989; Shaw and Gilbert 1990; Brennand and Shaw 1994; Beaney and Shaw 2000; Shaw et al. 2000; Shaw et al. 2000; Rains et al. 2002; Shaw 2002). Shaw and Gilbert (1990) used tunnel channels, drumlins and other erosional forms in southern Ontario, Canada, as evidence to support the hypothesis of catastrophic subglacial sheet floods, however the evidence presented is highly speculative. Shaw and Gilbert (1990) identified a number of features as tunnel channels based on their orientation being opposed to the regional gradient, thus stating that meltwater flow must have been under hydrostatic pressure. Shaw and Gilbert (1990) also stated that flutes in bedrock were formed by floodwaters that emerged out of tunnel channels as 'over-bank' flooding during times of peak discharge, and that tunnel channels would have carried the total discharge during the rising and falling stages of the flood; however they neglect the specific processes of fluvial erosion stating only that water flowed through such channels. One can only speculate that the processes of erosion would be plucking, abrasion and cavitation of the bed by flood waters which are commonly discussed within fluvial literature (Knighton 1998; Whipple et al. 2000).

Brennand and Shaw (1994) clarify this hypothesis by the use of theoretical modelling of ice sheet hydrology to show that tunnel channel formation is a result of progressive channelisation of meltwater during the collapse of sheet floods. Based on the work of Shoemaker (1992), who stated that sheet floods are extremely unstable and rapidly collapse into more stable channelised systems, Brennand and Shaw (1994) suggested that tunnel channels are the result of progressive channelisation and flow diversion processes that are governed by the geometric interactions between the ice base and bed (**Figure 2-15**). Brennand and Shaw (1994) stated that the presence of eskers within

tunnel channels are a record of "a return to seasonally driven meltwater drainage". They also highlight the phenomenon of channels following major fault systems and lithological boundaries, which emphasizes the importance of geological control. Brennand and Shaw (1994) use channel path, adverse to contemporary regional gradient, and striations superimposed on S-forms, to suggest that glacial abrasion caused at least ornamentation, to emphasis the potential for water flow beneath ice. They also correctly state that it is difficult to rationalize an anabranched channel pattern with glacial erosion as the primary formative agent. Whether or not these examples are evidence for subglacial sheet floods is still under much debate (Evans et al. 2006), however, these hypotheses do provide an important context for the study of subglacial meltwater in the formation of tunnel channels.

Figure 2-15

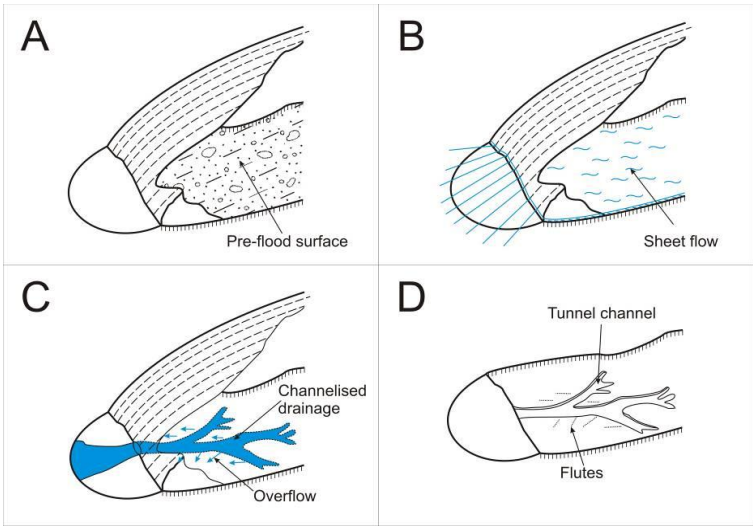

Theoretical model for the formation of tunnel channels based on the descriptions of Brennand and Shaw (1994). A) Glacier on bedrock substrate prior to flood. B) Subglacial sheet flood inundates the entire glacier bed. C) Instability of subglacial sheets causes flood to collapse into channels. During channelised flow, meltwater spills over the channel sides. D) Following deglaciation, anabranched tunnel channels are revealed with flutes emanating from channel sides caused by over flow events.

Sjogren et al., (2002) provided an excellent understanding of the formation of a suite of hummocky landforms which have a similar morphology to

tunnel channels interpreted as having a subglacial catastrophic origin. The term 'incipient' tunnel channel is used to describe a suite of landforms on a spectrum from hummocky terrain, to well defined tunnel channels, which are shown to have formed by subglacial fluvial erosion associated with the catastrophic release of subglacially stored meltwaters. Sjogren et al., (2002) identified three types of landform each with increasing degrees of channelisation. Type 1 channels (**Figure 2-16**) do not show distinct channel morphology but are an amalgamation of deep, aligned, hollows within areas of hummocky topography. The hollows are circular or elliptical in plan form, separated by hummocks or transverse ridges. Type 2 channels (**Figure 2-16**) resemble interlinked beaded potholes with low cols formed by transverse ridges. Type 3 channels (**Figure 2-16**) have sharply defined margins and flat bottoms with convex-up long profiles (Sjogren et al. 2002).

Figure 2-16

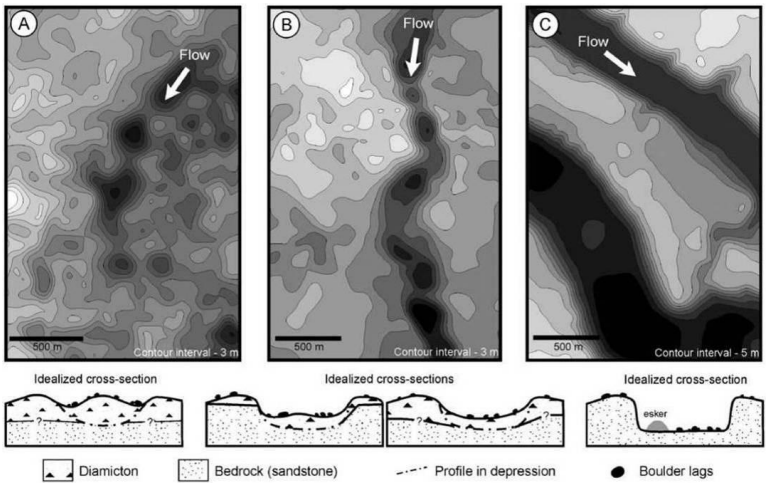

Morphology of incipient tunnel channels with idealized cross-sections. A = Type 1 channels. B = Type 2 Channels. C = Type 3 channels. Source: Sjogren et al., (2002).

The three channel types described above are believed to represent different stages of the same developmental sequence, a sequence that is primarily controlled by hydrodynamic conditions, although the nature of the substrate

appears to have some influence. Where the till cover is thick over bedrock, channels are generally narrower, with more pronounced hummocks along their base (Types 1 and 2). When till cover is thin or non-existent, channels have flatter bottoms, steeper margins, and may contain depositional landforms (Type 3) (Sjogren et al. 2002).

Drawing on comparisons with the Channelled Scablands (Baker 1978; O'Connor and Baker 1992), Sjogren et al., (2002) state that following flow initiation (removal of a frozen toe), roughness at the ice / bed interface created various scales of longitudinal and transverse flow expansions and constrictions (**Figure 2-17**). Flow deflection over bed irregularities resulted in near-vertical return flow in the lee of obstacles, resulting in the formation of macro turbulent flow structures known as "kolks" (**Figure 2-17**) (Sjogren et al. 2002). These kolks became locally fixed, forming a larger flow impediment that accentuated the flow structure. Linked potholes began to form as some depressions were enlarged resulting in the formation of Type 1 channels (**Figure 2-17**). Continued erosion caused breaching of cols between potholes, leading to the formation of intermediate, Type 2 channels (**Figure 2-17**). Increased channelisation emphasised erosion in the channel and as the discharge dropped, the channels carried all of the meltwater. This resulted in reattachment of ice to the bed adjacent to the channel and the formation of the familiar tunnel channel form, with a nearly flat bottom and steep margins (**Figure 2-17**), where the flow duration was able to remove the intra-channel cols.

Figure 2-17

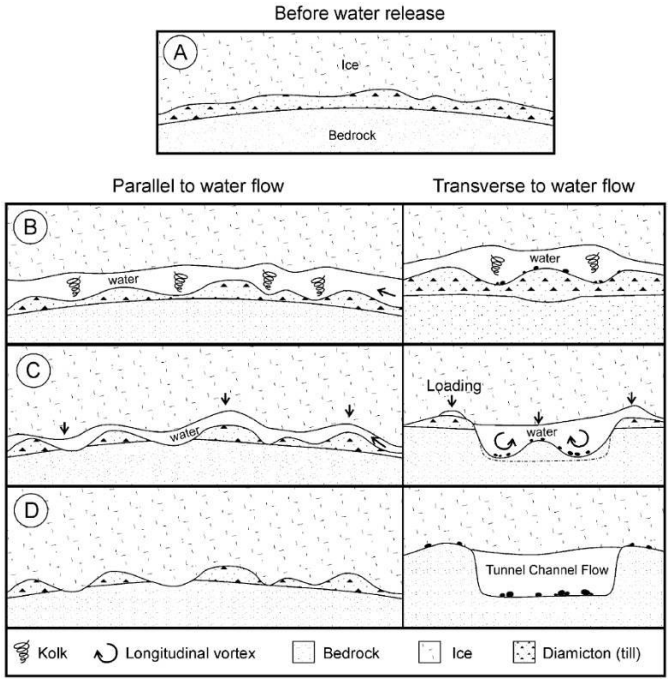

Developmental sequence of incipient tunnel channel formation. A = Subglacial roughness is related to the configuration of the ice and substrate. B = Vertical vortices (kolks) form which accentuate bed roughness as meltwater is released. Positive feedback concentrates erosion in depressions. C = As discharge drops, water is increasingly concentrated in channels. D = Once ice is re-attached, all the flow is concentrated in the channel, creating the 'classic' channel form. Source: Sjogren et al, (2002).

Cutler et al., (2002) provide further support for the formation of tunnel channels by subglacial catastrophic flooding when describing exposures of a very large boulder bed (boulders in excess of 2 m) within fans that have an apex located at the mouth of tunnel channels. Based on the presence of a finer sand and gravel unit beneath the boulder bed, Cutler et al., (2002) propose that channel formation is initiated by normal meltwater flows, and that the channel is enlarged by the outburst flood. They suggest that outburst floods are triggered following the thawing of a permafrost seal at the ice margin which has allowed the build up of subglacial meltwater over several thousand years (**Figure 2-18**).

Figure 2-18

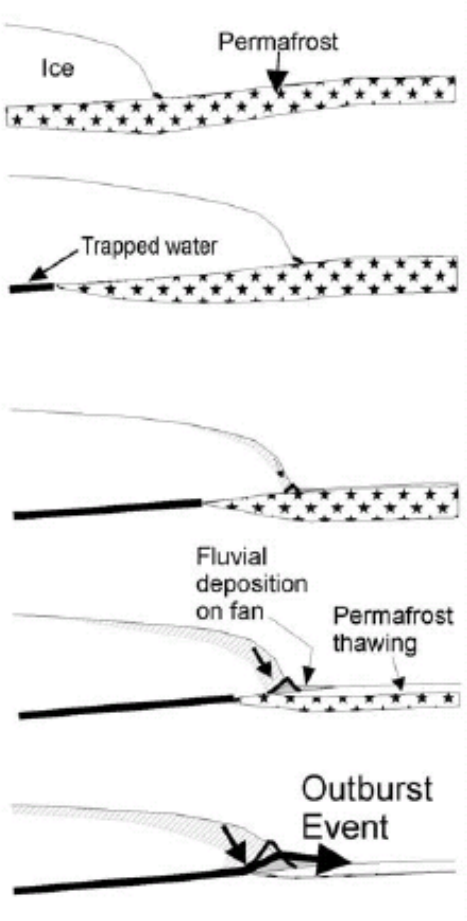

The formation of proglacial fans and tunnel channels by the release of meltwater following the thawing of permafrost. Modified from Cutler et al., (2002).

Hooke and Jennings (2006) proposed a more simplified model of tunnel channel formation based on field evidence from the southern Laurentide Ice Sheet. They suggest that tunnel channel formation is initiated by the catastrophic release of a large subglacial reservoir, through the substrate that has built up behind a frozen ice margin or 'frozen toe' (as also proposed by Wingfield (1990) and Piotrowski (1994; 1997; 1997). Hooke and Jennings (2006) state that meltwater dammed behind the frozen ice margin will build up until water pressures are high enough to allow water to percolate through the substrate to the ice margin, where headword erosion of a conduit through the substrate could tap the reservoir leading to a massive outburst with enough

power to erode the channel. Hooke and Jennings (2006) also suggest that following the outburst, the subglacial conduit would rapidly become clogged with sediment and ice, therefore closing, leading to further build up of water and subsequent catastrophic releases, which in turn lead to further tunnel channel erosion and deepening. In this case, the hypothesis is considered a 'composite' as tunnel channels are developed by the repeated process of subglacial flooding and are not formed by a single event.

The field evidence for this hypothesis is based on the observations of down flow areas of tunnel channels which are commonly composed of fluvially eroded landscapes, or grade onto proglacial gravel fans. The sediments within these fans are often of boulder size, implying large discharges. In some instances, the stratigraphy highlights different overlapping fans which suggest that waters were transported through the channels more than once (Hooke and Jennings 2006). However, it has been shown that very large floods can deposit fans comprising fine sediment in areas where sediment size is controlled by sediment availability rather than stream power, thus sediments size cannot always be used as a direct proxy for flood magnitude (Maizels 1993; Duller et al. 2008). It is also shown that the lack of continuity between valleys formed at one ice margin and those formed at a subsequent recessional margin, are evidence that tunnel channels are probably not continually exploited (Hooke and Jennings 2006).

2.3.3 POLYGENETIC FORMATION OF TUNNEL CHANNELS

Composite models for the formation of tunnel channels suggest that tunnel channels have been formed as a result of a number of different processes such as subglacial meltwater and direct glacial abrasion (Piotrowski 1994; Jørgensen and Sandersen 2006). Piotrowski (1994; 1997; 1997) proposed a

polygenetic model for the formation of tunnel channels as a result of direct glacial erosion and subglacial flooding. Flooding associated with this hypothesis is based on variations of subglacial groundwater transmisivity. Piotrowski's (1994; 1997; 1997) model is based on geological evidence from the Bornhöved lakes, north west Germany, and states that tunnel channels form in areas of increased groundwater flow, coupled with a strong geological control. Piotrowski (1994) proposed that tunnel channels in this area of Germany are polygenetic features, formed over three glacial cycles (**Figure 2-19**). The series of events begins with the glaciotectonic removal of deformable subglacial sediment located in-between two salt diapirs which act as the geological control, creating a preferential flow direction for subsequent erosive processes (Piotrowski 1994). Subsequent ponding of subglacial meltwater due to low porosity of subglacial sediments and the freezing of the ice sheet margin to its bed (a result of cold wave penetration through thinner ice at its margin), lead to high porewater pressure and reduced shear strength of subglacial sediments. Following water build up, catastrophic meltwater release is initiated following the removal of the 'frozen toe' as a result of ice sheet retreat. This enormous release of meltwater along the preferential flow path removed large quantities of unconsolidated subglacial sediment as a result of its low shear strength (**Figure 2-20**). Further excavation and expansion of the tunnel channel results from lowering of the glacier sole into the channel, leading to deformation of the substrate into subglacial channels and subsequent removal by meltwater (**Figure 2-19**). In support of the groundwater hypothesis for tunnel channel formation, Piotrowski (1997) modelled the groundwater balance for the area around the Bornhöved tunnel valley and showed that the total groundwater discharge was much lower than the calculated basal meltwater production rate for the basin, thus much

more water was produced than could be removed through the substrate alone. Consequently, other means were needed to explain the transfer of the remaining meltwater. It was suggested that this excess meltwater could have drained through other regions outside the study area, but this was rejected as adjacent regions had even lower hydraulic conductivities than the study area (Piotrowski 1997). Alternatively, it was suggested that the excess water may have discharged as a film flow at the ice / bed interface. This hypothesis was rejected because it would have had to be very thick (E.g. (Shaw and Gilbert 1990; Shoemaker 1992)) and no evidence for massive sheet floods exists. Thus, it is stated that discharge through tunnel channels is the only remaining possibility. Piotrowski concludes that tunnel valleys were initiated along higher energy groundwater flow paths and shows that tunnel channels occurred in areas of increased ground water flow activity and that there are no tunnel valleys in areas of little ground water flow.

Figure 2-19

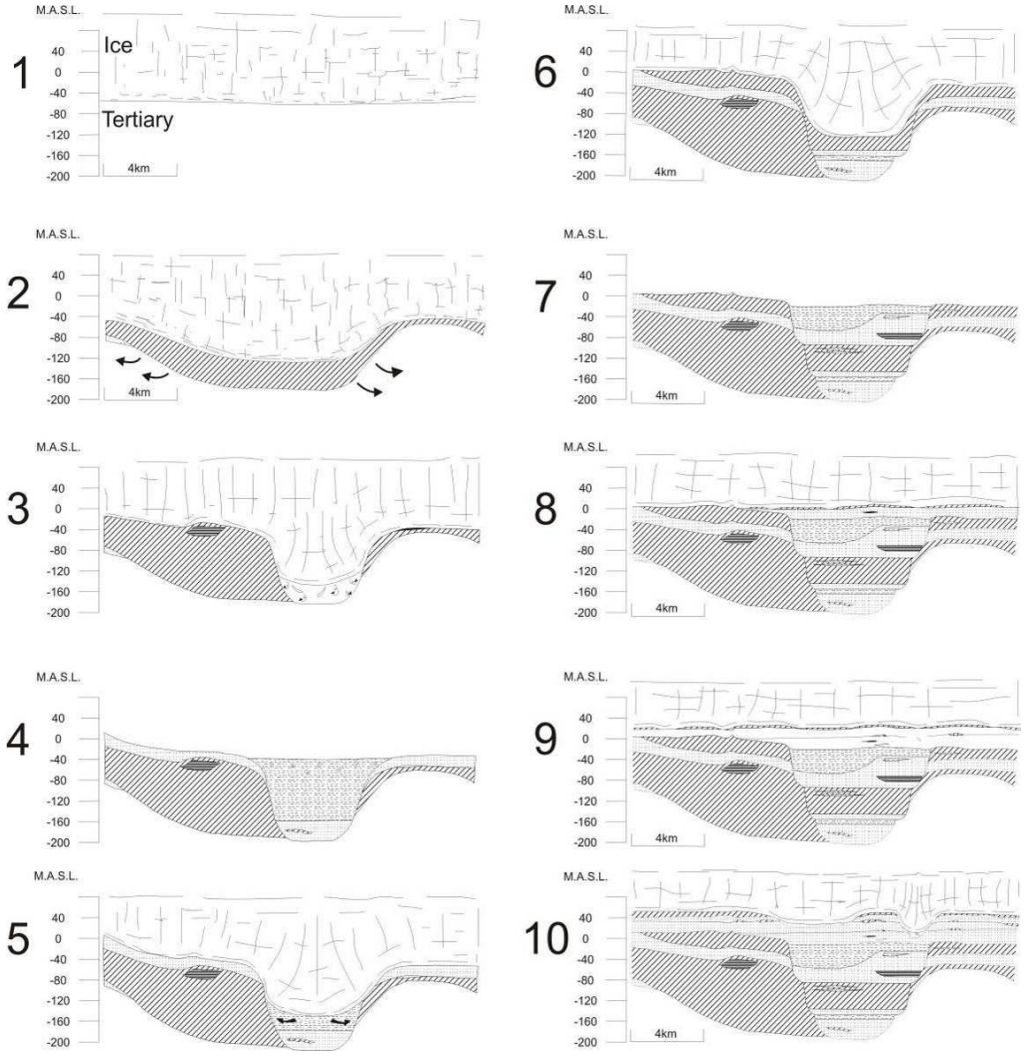

Simplified model of tunnel valley genesis and infill through three cycles of glacier advance and retreat. Source: Piotrowski (1994).

Figure 2-20

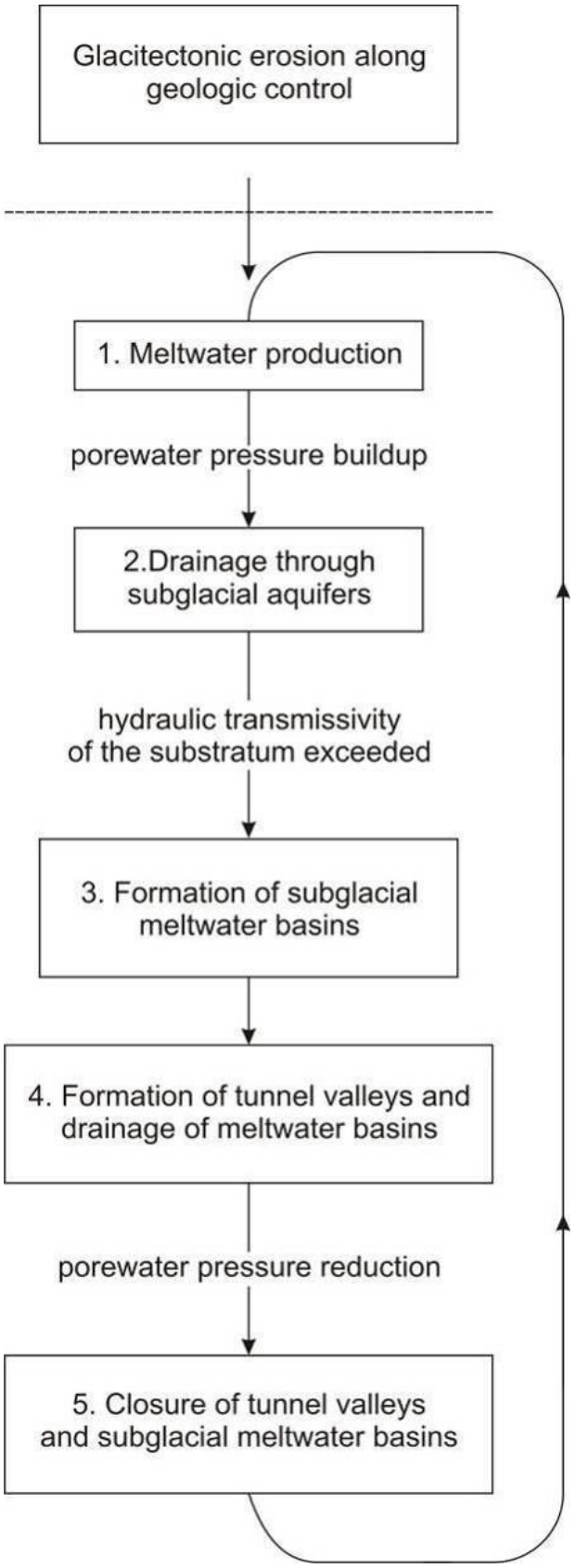

Formation of tunnel channels through a cycle of subglacial meltwater build up and high energy outburst through tunnel channels. Modified from Piotrowski (1994; 1997)

This hypothesis is based on the premise that subglacial sediment is removed as a result of subglacial groundwater flow through sediment with high hydraulic transmisivity and low shear strength, and that in the case of the Bornhöved tunnel channel system, this is aided by the presence of two highly resistant salt diapers which promote the initial erosion of the unconsolidated sediments found between them.

Boulton & Caban (1995) provide support for the subglacial ground water hypothesis based on modelling of European Ice sheets including Breiðamerkurjökull, in Southern Iceland. This modelling found that such ground water flow can lead to hydrofracturing and liquefaction of subglacial sediments, which can contribute to tunnel channel formation.

However, Piotrowski fails to account for or describe in his interpretation the lack of channels or canals at the ice bed interface, only dismissing ice / bed interface flow within a film or sheet due to the lack of evidence for subglacial sheet flows. Piotrowski (1994) neglects the possibility of meltwater flowing at the ice / bed interface within smaller R-channels which would have left no lasting impression on the land surface (Röthlisberger 1972). One would imagine that once drainage through subglacial aquifers was exhausted, following the exceedance of subglacial transmisivity, the next logical step would be the formation of more efficient channels at the ice / bed interface, rather than storage. One could speculate that if conditions were unsuitable for channelised flow due to freezing, then they would be similarly unsuitable for pore water flow. Despite the potential problems with this model, it is still essential that the appropriate field evidence be systematically identified to attempt to falsify it.

Despite the sight specific nature of Piotrowski's (1994) model, being associated with a geologic control, this geologic control is not the crux of the

hypothesis, and Piotrowski (1997) provides a model which has a number of easily testable criteria. Piotrowski (1994; 1997) states that channels form in areas of higher ground water movement. It would be expected that there be a variation in hydraulic conductivity between the areas in which channels originate and their immediate surroundings. However, there is no obvious solution to the problem associated with the inability to measure the properties of the materials within which channels are formed which has been removed as a result of channel formation. As a result, this portion of the hypothesis remains un-testable, and so emphasis must be placed on the character of the remaining sediments and channel morphology. Piotrowski (1997) also states increased porewater pressure leads to a reduction in subglacial sediment shear strength, allowing materials to be more easily eroded. Thus, one might expect to see evidence of dilation between pore spaces, piping, and deformation in the sediments which make up the channel walls. A lack of such sedimentary structures within the walls of such channels may be used as evidence to reject this hypothesis. Piotrowski (1997) also states that channel erosion occurs as a result of high magnitude drainage of subglacially ponded water. Coarse grained, rounded sediments are indicative of high discharge flows (Powers 1953; Collinson et al. 2006), thus the presence of fine sediments within channel bottoms may be used as evidence to reject this hypothesis. Finally, due to the proposed polygenetic nature of tunnel channels, the glacier's sole in believed to have deformed into the channel following erosion by meltwater. Thus, one would expect to see evidence of deformation within sediments making up the walls of the channel. A lack of subglacial deformation or lodgement tills would suggest that the channel has not been occupied by ice since its initial formation.

Support for Piotrowski's (1994; 1997; 1997) cyclic model is provided by Jørgensen and Sandersen (2006) for tunnel channel formation based on data from tunnel channels in Denmark, where "tunnel valleys were primarily eroded by subglacial meltwater and direct glacial erosion is considered to have played an important, but secondary role".

If tunnel channels are to form as a result of catastrophic drainage of a subglacial reservoir via piping through the glacier substrate, there are number of key sedimentological and geomorphological criteria one would expect to observe in the field. First, one would expect the areas downstream of the tunnel to be fluvially eroded or to be composed of large gravel fans, the volume of sediments of which would be of an appropriate size for the magnitude of the flood. The lack of such a fan or lack of evidence for downstream fluvial erosion could be used as evidence to reject this hypothesis. Second, you might expect to see evidence of piping within the sediments which make up the channel walls, although the preservation potential for such features is expected to be low due to the erosive power of the flood waters following breach of the reservoir. As such, a lack of pipe features may not be enough to reject this hypothesis. You might also expect to observe large rounded boulders within the bottoms of tunnel channels as is experienced within many flood channels.

2.4 LANDFORMS OF ICE STAGNATION

Where ice becomes stagnant, in most cases it will become buried by supraglacial debris or proglacial outwash (Thwaites 1926; Johnson 1992; Everest and Bradwell 2003). Once stagnant ice begins to melt, the former positive topography can become inverted, leading to the formation of a variety of landforms of negative topography. Kettle holes are some of the most commonly identified landforms of ice stagnation that result in the formation of distinct overdeepened topography (Price 1969; Maizels 1992; Fay 2002; Fay 2002). Where large numbers of kettle holes occur within close proximity, landforms of kame and kettle topography can develop (Price, 1969). Similarly, much larger masses of stagnating ice melting in-situ can result in the development of dead-ice sinks and moats (Fleisher, 1986). These larger complexes of ice stagnation topography are beyond the scale of this research and thus a review of their formation is considered unnecessary.

2.4.1 KETTLE HOLES

Kettle holes are enclosed hollows that form by the melt-out of buried ice (Bennett and Glasser 1996). However, there a number of different processes that can form kettle holes, and a number of different kettle hole morphologies. Maizels (1992) used field evidence of kettle holes formed following jökulhlaups in southern Iceland and laboratory experiments to classify the formation of four types of kettle holes depending upon the degree of burial, and the concentration of debris within the forming ice block. 'Normal' (Type 1) kettle holes were formed from sediment starved ice blocks and are characteristically identified by normal faulting of sediments along the flanks of the hollow as aggraded material slumps into the hollow as the ice block melts (**Figure 2-21**). As the sediment

concentration within the ice block increased and the depth to which the ice block was buried decreased, three other types of kettle were identified. Firstly, Type 2: 'Rimmed' kettles (**Figure 2-21**) are characterised by deep hollows and have a characteristic three-unit stratigraphy. The lowest unit composed basal, granular floods gravels, over which lies a thin diamicton drape which has been produced by melt out of debris within the ice block, and which produced a discontinuous 'boulder ring' on the surface as a result of material washing off the edges of the ice block, concentrating build up of material around the periphery of the block. The final unit was consisted of laminated sand and silts which was deposited within standing water once the ice block has completely melted (**Figure 2-22**) (Maizels 1992). As the amount of sediment within the ice block increases and / or the depth of burial decreases, kettles Type 3 and Type 4 begin to develop (**Figure 2-21**). These are 'crater' kettles, which have thick units of diamicton and shallow hollow bottoms which are at a higher elevation to the surrounding sandur, and 'Till fill' kettles, which are entirely filled with think units of diamicton, leaving a large mound on the surface and no evidence of the underling hollow (Maizels 1992). The relationship between debris concentration and burial is shown in **Figure 2-23**.

Figure 2-21

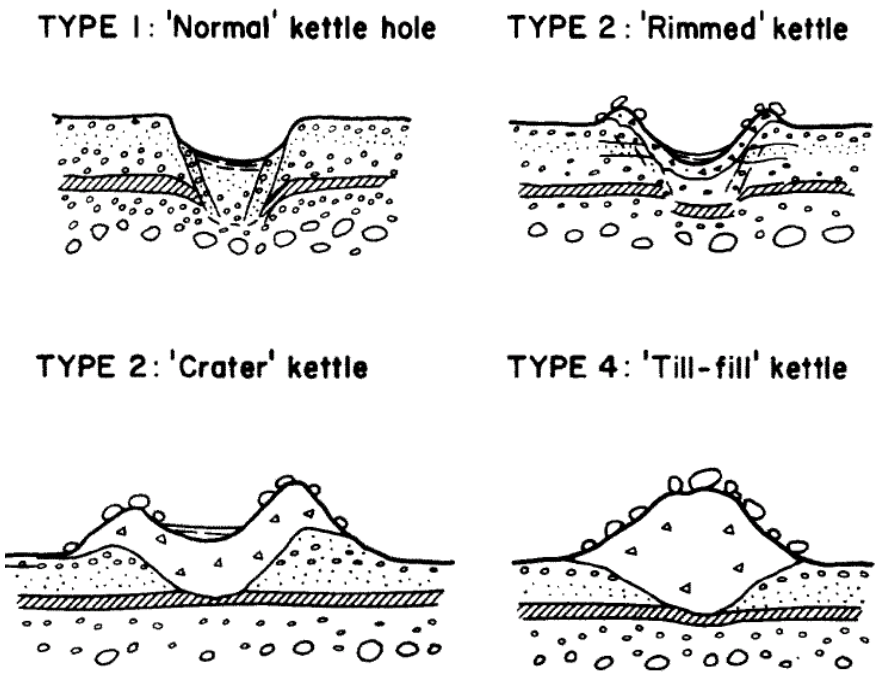

Schematic diagrams of the four types of kettle / ring structures produced from melting ice blocks in a laboratory environment. Kettle / ring structures vary from type 1 through to type 4 with progressive increases on ice block debris concentration and / or reducing burial depth. Source: Maizels (1992)

Figure 2-22

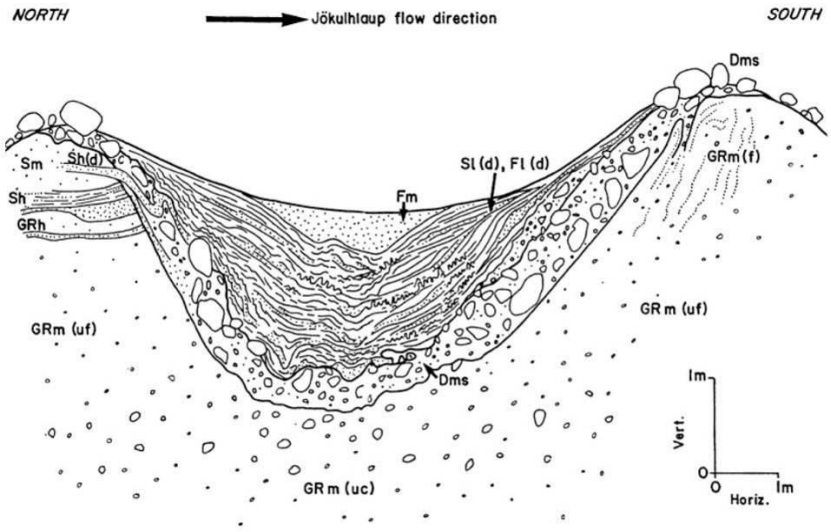

Typical stratagraphic cross-section of a kettle / ring structure showing three sedimentary units. Basal granular flood gravels (GRm); diamicton (Dms) and upper laminated sands and silt (Sl and Fl). Source: Maizels (1992).

Figure 2-23

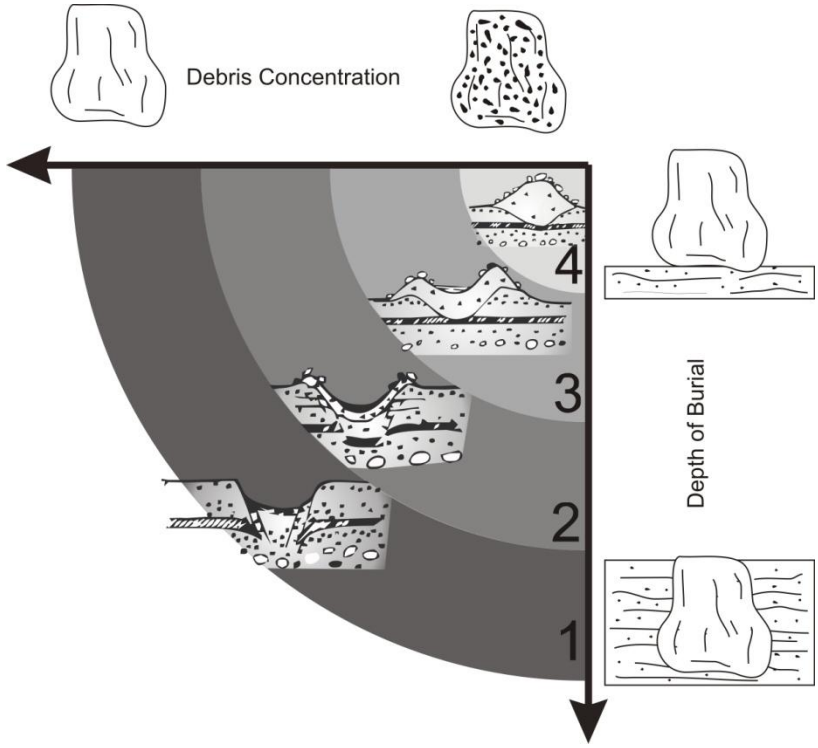

Idealised relationships between kettle / ring structure types 1 – 4 depending on variations on burial depth and debris concentration.

Maizels (1992) provided an excellent set of criteria for one to be able to identify and test for the formation of landforms believed to have formed as a result of ice block melt out. Fay (2002; 2002) built upon this work in identifying a number of sedimentary signatures associated with kettle holes and ice block obstacle marks. Fay (2002) identified the formation of longitudinal and transverse kettle 'chains' up to 270 m in length, formed by the grounding of a single dominant ice block, which led to the further grounding due to decreased flow within the blocks shadow. Areas of 'hummocky topography' comprising numerous closely spaced hollows with raised rims were also observed in areas of back water conditions during the rising stage of the floods and lower fan locations during the waning stage (Fay 2002), thus emphasising the importance of flood flow conditions on kettle hole geomorphology.

Fay (2002) identified two morphologically distinct kettle hole types; steep-walled and inverse-conical kettles, of which Steep-walled kettles have two types. Type A are shallow circular depressions formed within coarse grained clast supported sediments which have vertical to inward dipping walls and a base consisting of a block of stream bed sediment. Type B are up to 4.5 m deep, circular pits within coarse grained matrix supported sediments, or exclusively fine sediments, with steeply dipping or overhanging walls.

Both steep-walled and inverse-conical kettles are formed within close proximity to flood outlets where sediment flux was highest (Fay 2002). By examining the walls of kettle holes on Skeiðarársandur, Fay (2002) identified sedimentary signatures that could be related to kettle hole morphology. Type B kettles form within competent sediments such as matrix supported or fine grained materials, which allow the formation of a cavity beneath the sediments. Thus Type B kettles form as a result of the vertical collapse of the cavity. Type A kettles form in less competent sediments as a result of sliding or avalanching down the kettle walls. Molewski (1996) also found that kettles formed as a result of the vertical collapse of sediments above an ice block melt out cavity (**Figure** 2-24). In addition, Fay (2002) identified sedimentary signatures that relate to the flow conditions of the flood which deposited the ice block in question. Fay (2002) found upstream dipping beds of open framework boulder gravel and clast supported pebble gravel (**Figure** 2-25**a**) along the internal flanks of some kettles, which were interpreted to have formed by the upstream migration of standing waves (antidunes) formed around an ice block (**Figure 2-26**). Fay (2002) also identifies large, coarse grained, anticlinal structures (**Figure** 2-25**b**) within the lee of ice blocks. These are interpreted as obstacle shadows formed by rapid aggradation during the rising stage of the jökulhlaup.

Figure 2-24

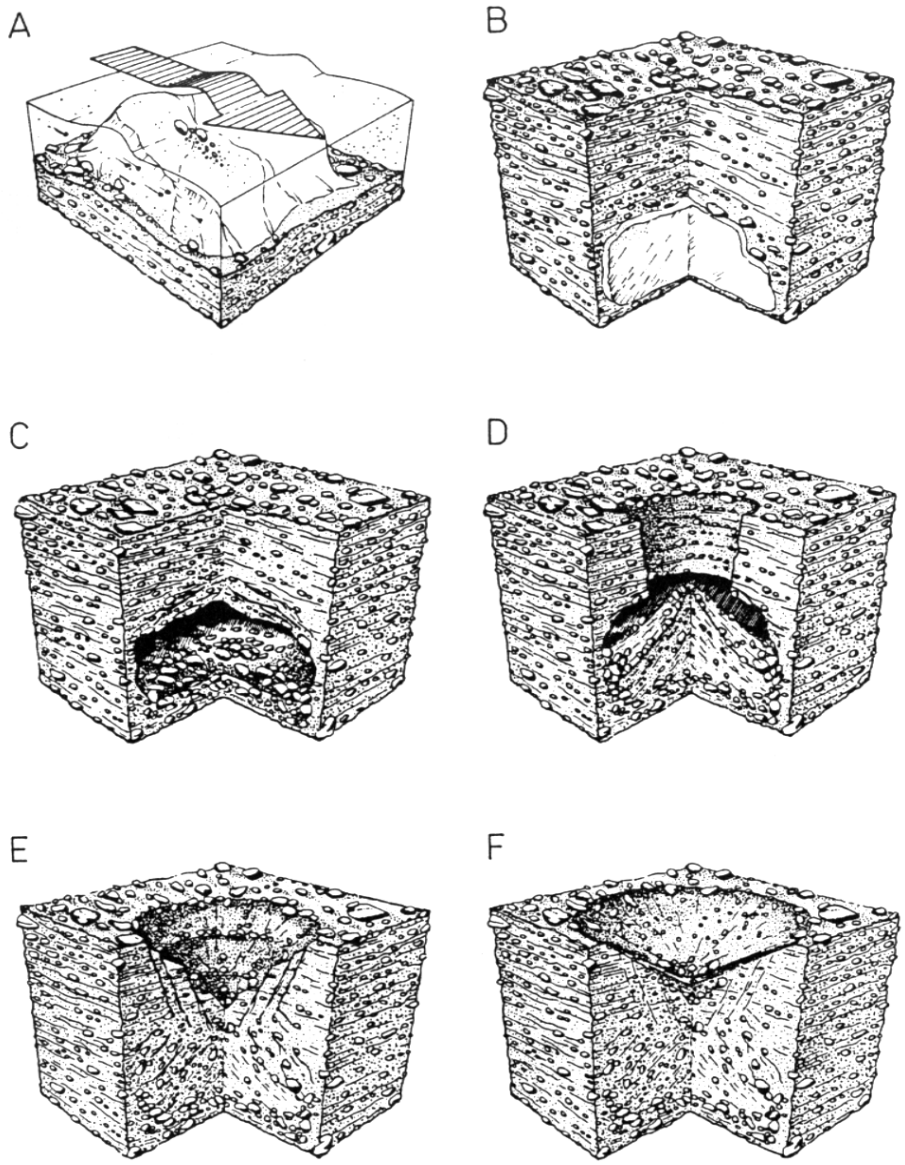

Conceptual model of the formation of kettle holes. A = Burial of ice block by glaciofluvial deposits. B = Buried ice block C = Melting of ice and formation of buried chamber. D = Formation of vertical well and talus cone following roof collapse. E = Collapse of kettle hole slopes. F= Smoothing of kettle hole by denotative processes. Source: Molewski (1996).

Figure 2-25

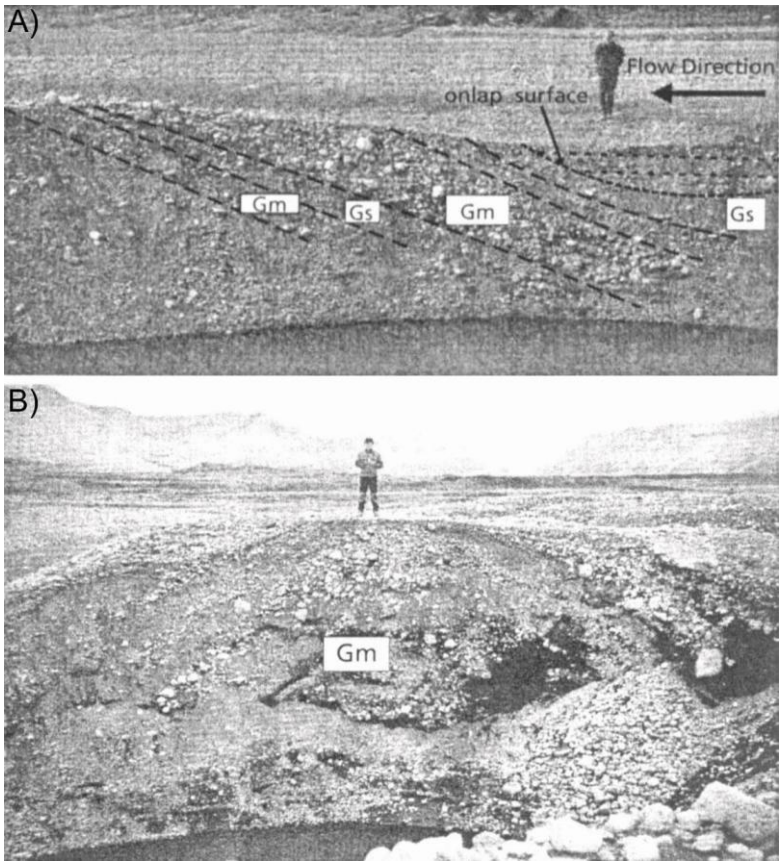

Sedimentary signatures identified within kettle holes formed as a result of high magnitude glacier outburst floods. A = upstream dipping beds of open framework boulder gravel and clast supported pebble gravel. B = coarse grained, anticlinal bedforms within the lee of ice blocks. Source (Fay 2002).

Figure 2-26

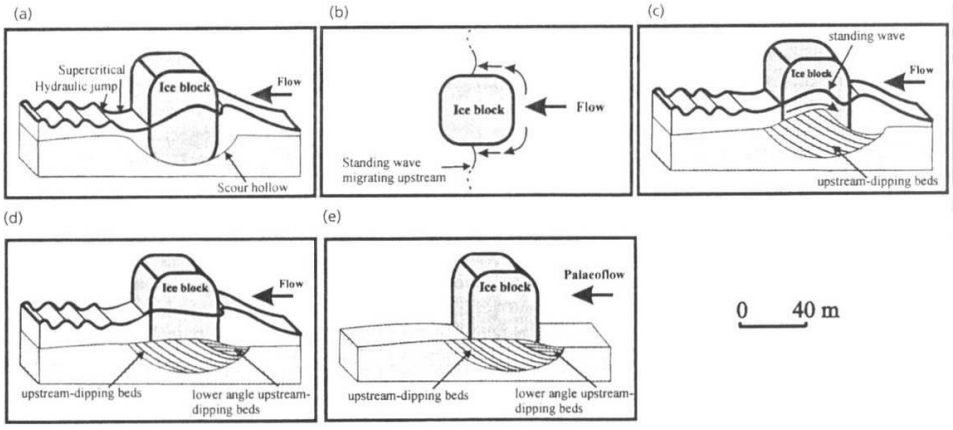

Model for the formation of standing waves (antidunes) and associated stoss-side strata around ice blocks. Source: Fay (2002).

2.5 CHAPTER SUMMARY

This literature review was provided a detailed review of the current understanding of the processes associated with the formation of overdeepenings at glacier margins within both ancient and contemporary systems. It has shown how overdeepenings can be the product of active processes of erosion such as a result of the glacitectonic removal of sediments associated with hill-hole pairs and along the flanks of drumlins. Alternatively, overdeepenings can result from more passive processes where they form as a result of the genesis of other landforms, such as kettle holes, or in-between other landforms of more positive relief.

This chapter has also provided an outline of the sedimentary and geomorphological signatures that one would expect to be associated with each process of formation.

An understanding of these signatures is essential for designing methods to critically test each hypothesis and form the basis for the design of the methodologies that follow in the next chapters. Table 2-1 provides a summary of the hypothesis discussed in this chapter, along with key references, sedimentological and geomorphological signatures, and critical tests which must be considered for the falsification of each hypothesis.

Table 2-1

Process	Diagnostic Geomorphology	Diagnostic Sedimentology	Selected References
Glacial meltwater erosion	Suite of landforms from semi-linear hollows to well defined channels; Undulating long profiles; Transected moraines; Downstream alluvial fans; Eskers or Kames within channel bottoms; P-forms on bedrock surfaces.	Large, well rounded cobbles / boulders; Deformed valley sides; Deformed, diamicton within eskers; Stratified, glaciofluvial deposits within eskers and kames.	Hindmarsh, (1987) Moores, (1989) Brennand and Shaw, (1994) Ó Cofaigh, (1996) Clayton et al., (1999) Sjogren et al., (2002) Jørgensen and Sandersen,(2006)
Direct glacier abrasion	Streamlined, polished bedrock surfaces; Micro scale lineations, striations, etc;	Lodgement till;	Goldthwait, (1979) Piotrowski, (1994) Glasser and Bennett, (2004)
Glacitectonics	Hill-Hole Pairs Cupola Hills	Heavily deformed glacial and glaciofluvial sediment	Bluemle, (1970) Clayton et al, (1980) Bluemle and Clayton, (1984) Todtmann, (1960) Howarth, (1968) Evans & Twigg, (2002)
Stagnating ice / melt out	Small scale kettle holes / kettle chains; Large-scale irregular topography, dead ice sinks / moats.	Diamicton mounds within high energy fluvial / hyperconcentrated flood deposits; Significant evidence of faulting or slumping; Heavily deformed / faulted fluvial deposits.	Fleisher, (1986) Maizels, (1992) Fay, (2002; 2002)
Formation of positive glacial landforms	Proglacial alluvial fans Drumlins	Bedded glaciofluvial sands and gravels Deformed glaciofluvial sediments – Deformation till	Church and Gilbert, 1975 Boulton (1978)

Table summarising the most common hypothesises for the formation of overdeepenings and the diagnostic geomorphology and sedimentology associated with those hypothesis.

3 INTRODUCTION TO THE FIELD SITE AND METHODOLOGY

This chapter provides an introduction to the field area where this research was carried out, including a justification for the choice of field area, as well as a description of the field techniques used in collecting data at the site. **Section 3.1** introduces the field area, including geographical context, morphological descriptions, a brief history and a detailed a justification for the choice of this field as an analogue for former ice sheet margins. **Section 3.2** discusses the methodology and field techniques utilised for this research. Justification of the choice of these techniques is provided by examples of cases when these techniques have been successfully utilised elsewhere.

3.1 INTRODUCTION TO THE FIELD SITE: SKEIÐARÁRJÖKULL, SOUTHEAST ICELAND

To test the diagnostic properties associated with models of the formation of negative relief in proglacial areas, Objective 2 requires the identification of a suitable field site. As tunnel channels and valleys are diagnostic of the large piedmont outlets of Quaternary ice masses such as the Green Bay lobe of the Laurentide Ice Sheet (Clayton et al. 1999) or the western margin of the Scandinavian Ice Sheet (Jørgensen and Sandersen 2006) it is considered appropriate that a field site be identified that could act as a modern analogue of these former ice sheet outlets.

Boulton (1987) states that modern piedmont lobe glaciers are believed to be much better analogues for the outlet glaciers of the former Laurentide and Scandinavian ice sheets than most smaller alpine glaciers, where most glaciological research has been carried out to date. We also understand from palaeo glaciological reconstructions that the outlets of Quaternary Ice Sheets were primarily temperate, exhibiting extremely dynamic behaviour, subject to

variations in ice flow velocity (surging / ice streaming) (Kehew et al. 2005) and intermittent catastrophic outburst floods (jökulhlaups) (Baker 2002). For these reasons, the field site chosen to carry out this study was Skeiðarárjökull, located approximately 70 miles north east of the town of Vik, on Iceland's south coast. Further details and justification for the choice of Skeiðarárjökull are provided in the following sections.

3.1.1 GLACIER MORPHOLOGY

Skeiðarárjökull is a large piedmont glacier located in southeast Iceland (Figure 3-1) It is one of the major outlet glaciers of Europe's largest ice cap, Vatnajökull, with an area of approximately 1400 km^2 (Roberts et al. 2005). It is also the source of Iceland's largest active outwash plain, Skeiðarársandur (Krigström 1962; Magilligan et al. 2002). Skeiðarárjökull has a total length of over 50 km from which it descends 1500 m from the centre of the Vatnajökull icecap to the unconfined expanse of Skeiðarársandur. The glacier is approximately 7.5 km wide where flow is constricted through the narrowest portions of the valley-confined upper section, and fans out to approximately 17 km where the glacier reaches the outwash plain, with a total ice margin length closer to 22 km, between the tall Eystrafjáll cliffs to the west and the Skaftafellsjöll massif to the east.

Figure 3-1

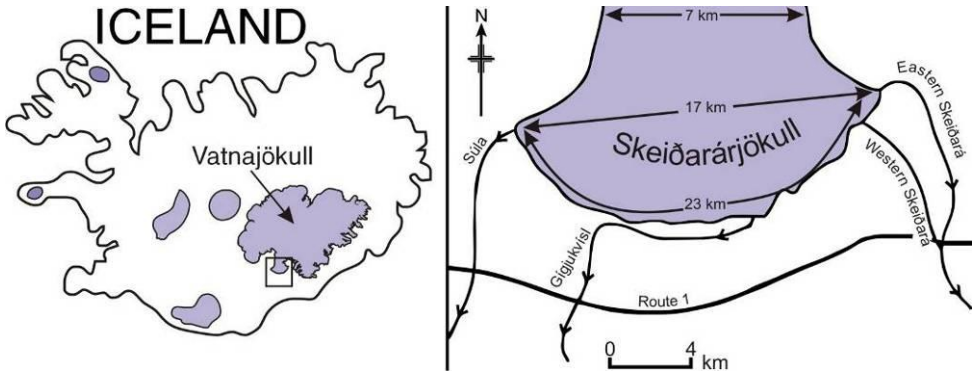

Location map showing Skeiðarárjökull in relation to Iceland and the major glacial river outlets. Modified from (Roberts et al. 2001).

The current ice margin lies at approximately 96 m a.s.l, although due to large accumulations of debris at the ice margin, substantial volumes of glacier ice are currently buried (Everest and Bradwell 2003), leading to large areas of ice melt out topography and difficulty in defining the true location of the ice margin at some locations.

Like many large glaciers in southern Iceland, Skeiðarárjökull occupies a large over-deepened basin (**Figure 3-2 - a**) (Björnsson et al. 1999; Roberts et al. 2002). Radio echo sounding surveys across the surface of the glacier have shown that its bed descends to a depth of approximately 200 m b.s.l at approximately 12 km up glacier from the present margin. This overdeepening does not span the entire width of the glacier; it is contained within two relatively narrow strips. The deeper of the two overdeepenings is located to the far west of the glacier, where the ice hugs the Eystrafjáll cliffs. The second of these over deepenings is much wider, approximately 5 km, to the east of the glaciers centre line. These overdeepenings result in maximum ice thicknesses of approximately 500 m (Björnsson et al. 1999; Roberts et al. 2005).

Figure 3-2

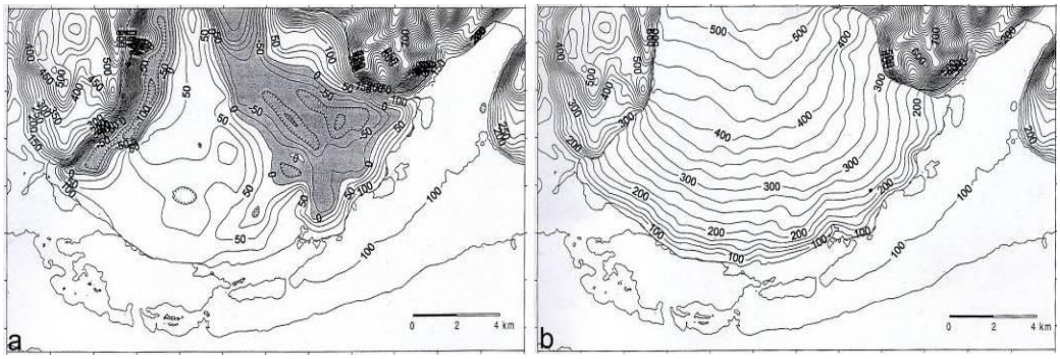

Map of Skeiðarárjökull showing a) subglacial topography. Note two large over deepenings, one to the western margin and a second larger over deepening stretching from the glaciers centre line to the eastern margin .b) Ice surface topography, showing ice thicknesses up to 500 m. Modified from Björnsson et al.,(1999).

Skeiðarárjökull, like most of Earth's large ice masses, is currently going through a period of negative mass balance and retreat (Sigurðsson 2005). The snout is currently retreating at a rate of approximately 100 m per year with an additional 10 m of vertical ablation.

3.1.2 GLACIER HYDROLOGY AND DRAINAGE

Skeiðarárjökull is a temperate glacier which produces a large amount of discharge especially during the summer months (Snorrason et al. 1997). Like many glacierized catchments, the moist maritime climate of southern Iceland results in prolonged rain storms which intensify melt and significantly increase discharge (Collins 1998; Wildt et al. 2003). These large volumes of meltwater are drained from the glacier into three main river outlets. The Skeiðará drains the eastern most margin of the glacier; the Gígjukvísl drains the central portion; and the Súla drains the western margin.

The Skeiðará originates from two well defined outlets at the far eastern margin of the glacier where water rises through a large zone of up-welling artesian vents (**Figure 3-3**) (Tweed et al. 2005). Meltwater from these vents flows southwards through the eastern and western Skeiðará River channels

before converging into a single channel upstream of the Skeiðará road bridge (Wadell 1935; Björnsson et al. 1999; Roberts et al. 2001). Beyond here, the river bifurcates as it braids across the outwash plain towards the Atlantic Ocean.

The Gígjukvísl does not have a single defined outlet, and instead is fed by many smaller outlets, many of which cannot be identified due to the formation of numerous ice contact lakes within recent years. The Gígjukvísl drains a large portion of the ice margin between the Western Sæluhúsavatn area in the east and an area a few kilometres from the western margin. Most waters in the Gígjukvísl exit the glacier and flow laterally west across the ice margin within large ice contact lakes and small interconnecting stream channels before abruptly flowing south where they are able to branch out and braid across the outwash plain.

The Súla, like the Gígjukvísl, does not have a well defined portal and is an amalgamation of small surface meltwater channels and up-welling vents. The area drained by this river is smaller than that of the Gígjukvísl, although the exact drainage divide between the Súla and Gígjukvísl is difficult to define. Flowing south from the far western margin, the Súla joins the freshwater (non-glacial) river Núpsá and becomes the River Núpsvötn (Krigström 1962). The average seasonal discharge of each of these rivers is provided in Table 3-1 below. However, flows have been recorded at much higher discharges during Skeiðarárjökull's many jökulhlaups.

Table 3-1

River	Average Summer Discharge (Q)	Average Winter Discharge (Q)
Skeiðará	200 - 400	15 - 80
Gígjukvísl	20 - 70	2 - 20
Súla	10 - 60	1 – 10

Average seasonal discharge of Skeiðarárjökull's three primary meltwater outlets. (Snorrason et al. 1997).

Figure 3-3

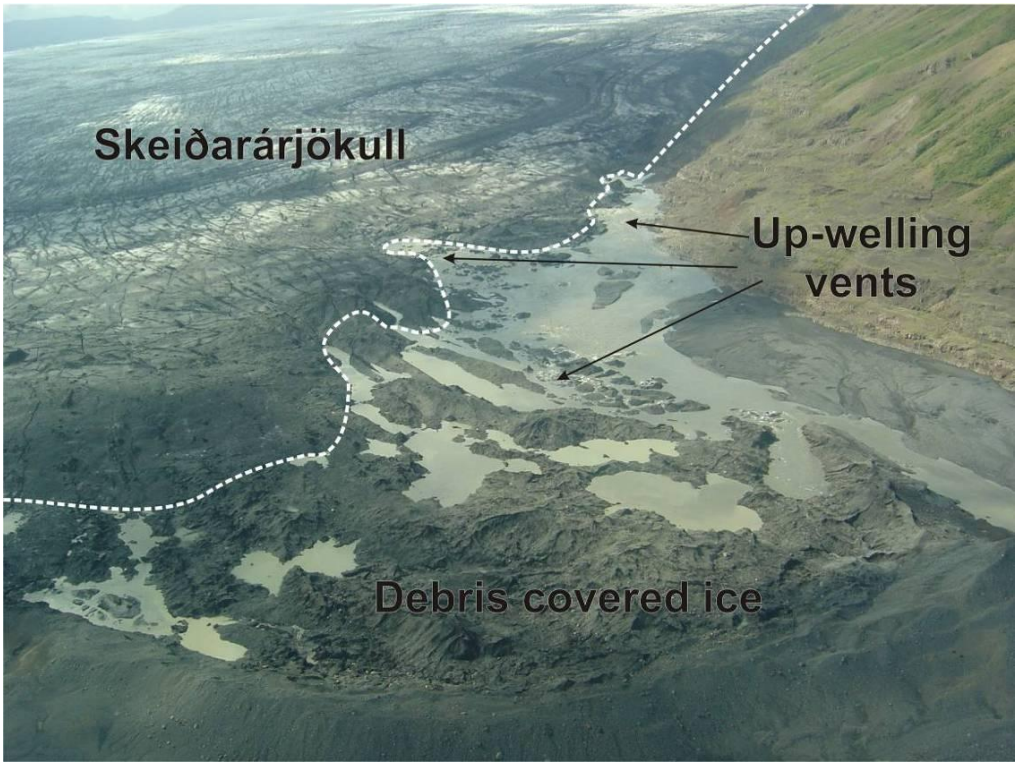

Oblique aerial photograph of up-welling artesian vents at the far eastern margin of Skeiðarárjökull. Photograph: Dr R. Duller.

3.1.3 JÖKULHLAUPS

Skeiðarárjökull's history is one that is dominated by the occurrence of high magnitude outburst floods or jökulhlaups (Wadell 1935; Thorarinsson 1939; Krigström 1962). The term Jökulhlaup is an Icelandic word, now used globally to describe floods caused by the release of water from glaciers. It is defined as "river discharges in excess of the upper perennial boundary of glacier melt dominated flow" (Roberts et al. 2005) and can have a large number of potential sources (Tweed and Russell 1999).

Large jökulhlaups have been reported in southern Iceland since records began following the first settlement of Iceland in approximately 870AD (Wadell 1935). Sagas of washed away farms and travellers disappearing into kettle holes date back to the 15th century (Þórarinsson 1974), although our greatest

understanding of jökulhlaups have only come about during the last eighty to a hundred years, when the first scientific investigations of jökulhlaups were undertaken (Thoroddsen 1893; Wadell 1935; Thorarinsson 1939). Table 3-2 provides a summary of the known floods from Skeiðarárjökull. It is beyond the scope of this thesis to review all of those known flood events; however it is important to understand the processes associated with such floods as they play a huge role in the sedimentological and geomorphological legacy of this region (Russell et al. 2006). For this reason, a brief review of the mechanisms that cause jökulhlaups and a description of the most recent catastrophic event are provided in **Section 0**.

Table 3-2

Year	Eruption	Date	Flow Discharge	Comments
1598	yes			Gísli biskup Oddson, 1637. Annalium in Islandia farrago.
1629	yes			Annáll Gísla biskups: A family was buried beneath the flood. It destroyed fertile land and flooded Skeiðarársandur.
1659	yes			
1697	yes			Eruption in Bárðabunga system
1725	yes	Mar - Apr		Eggert Ólafsson, 1756
1774	yes	February		Destroyed landing stage east of Ingólfshöfdi.
1784	yes	8 Apr		Both in the rivers Súla and Skeiðará. Jökulhlaup in Núpsvötn 1785, probably the drainage of the marginal lake Grænalón.
1796	no	June		Strong sulphuric smell that affected fertile land and animals.
1803	no			
1812	no			Probably jökulhlaup.
1861	(yes)	23 May	20,000 - 30,000 m3/s?	Large jökulhlaup, destroyed much land close to the farms Svínafell, Hof and Hofsnes. Icebergs and large quicksand areas formed in the flood path. Birds died. Probably this flood also reached Núpsvötn.
1867	yes	27 Aug	peak on 29 Aug	Quiet large jökulhlaup which diminished on the 4th day. Icebergs were carried down to Skeiðarársandur (~ 7 miles wide), which was all covered by water. Destroyed fertile land in the western part of the area "Öræfasveit".
1873	yes	6 Jan		Flow discharge in the river Súla increased half a day later, in all a smaller jökulhlaup than the last two. An eruption started on 8 Jan in Grímsvötn. Jökulhlaup also in river Djúpá (but probably different source).
1883	yes	13 Mar - 22 Mar	Peak on 21 Mar	No large flood, jökulhlaup followed eruption (Grímsvötn).
1887	(yes)			Maybe an eruption close to Thórdahyrna, the jökulhlaup only on western part of Skeiðarársandur (river Súla and Blautakvísl)
1892	(yes)	12 Mar - 16 Mar	Peak on 14 Mar ~30,000 m3/s?	The flow discharge increased slowly, during peak discharge icebergs were carried all the way to the sea (ca. 10 km). One of the largest jökulhlaups. No certain report of an eruption (most likely one in January 1892).
1897	no	13 Jan - 23 Jan	Peak on 19 Jan	This jökulhlaup increased slowly, burst out from beneath the glacier on 17 Jan, not far from Hörduskridu. It was diminishing late on 19 Jan and was smaller than the one 1982. On 17 Jan the flood reached Núpsvötn.
1903	yes	26 May - 31 May	Peak on 28 May	The river was dry until 25 May. Then it increased fast, the water covered half of the Skeiðarársandur on 27 May. The next night there were tremendous noises; icebergs were carried all the way to the ocean (ca.10 km).
1913	no	14 Apr - 26 Apr	Peak on 16 - 17 Apr	Descriptions are fairly unequal, but the jökulhlaup was large. Much ice was broken out of the glacier snout, icebergs as large as houses remained until June. The main flood went down on the eastern Sander.
1922	yes	22. Sep - 6 Oct	Peak on 4 Oct	Increase of flow-rate first 6 days before icebergs were carried downstream. Large jökulhlaup with its main outlet east of Hörduskridu. Volcanic eruption in Vatnajökull, 29 Sept - 23 Oct.
1934	yes 30 Mar - 15 Apr.	22 Mar - 1 Apr	25,000 - 30,000 m3/s (31 Mar)	On 28 Mar approx 10 times summer discharge, one outlet 2.5 km wide (near Skaftafell). Icebergs were carried all the way to ocean. Diminishes 1 Mar. 8 km telephone line swept away, vol. Then estimated to be 7 km3, now 4.5 km3.
1938	yes	23 May - 7 June	25,000-30,000 m^3/s (26 May)	On 25 May 3 km wide, during peak discharge almost all Skeiðarársandur (30 km2) was flooded. 7 km telephone line swept away, diminishing more slowly than 1934 with a lower peak discharge.
1939	no	~5 July - 21 July	Peak on 15 July	One outlet at the very least, damaged fences and fertile land near Bæjarstad. No detailed information exists, origin may not be Grímsvötn.

Year	Eruption	Date	Flow Discharge	Comments
1941	no	1 May -17 May	Peak on 16 May	Small jökulhlaup, Grímsvötn obviously with newly lowered lake level, fairly small icebergs broke out of glacier snout.
1945	no	16 Sept – 27 Sept	8,000 - 10,000 m^3/s (25 Sept)	Discharge increases slowly. On 22 Sept four times summer discharge, icebergs transported, about 4 major outlets beneath eastern glacier snout, flood reached Núpsvötn, Grímsvötn ice surface lowered by 70-80 (100) m.
1948	no	11 Feb - 27 Feb	~5,000 m^3/s ? (23 Feb)	11 Feb summer discharge, from 17 Feb obvious increase. Night to 20 Feb telephone line swept away, 21 Feb flood reached Sandgígjukvísl.
1954	no	8 July - 21 July	10,000 m^3/s (18 July)	On July 12 discharge was already about 1,000 m^3/s, telephone line swept away on 16 July and on 17 July the jökulhlaup exited Skeiðarárjökull at 9 locations (Súla and Sandgígjukvísl included).
1960	no	16 Jan - 26 Jan	5,000 - 6,000 m^3/s (24 Jan)	Smell noticed in late December, slow discharge increase. Flood reached Skeiðará, Sandgígjukvísl and Súla.
1965	no	31 Aug - 12 Sept	6,000 m^3/s	Sulphuric smell first noticed about mid August. Telephone line broke down on 6 Sept. Quite small jökulhlaup.
1972	no	13 Mar- 31 Mar	5,000 m^3/s (24 Mar)	Sulphuric smell first noticed on 1 march. Total volume first estimated to be 3.2 km3 (Thorarinsson, 1974), later corrected to 2.1 km3 (Guðmundsson et. al.1995). Flood reached Skeiðará, Sandgígjukvísl and Súla.
1976	no	September	3,500 - 4,000 m^3/s	Total Vol.: 1.7 km3
1982	no	February	2,000 m^3/s	Total Vol.: 1.2 km3
1983	no	December	600 m^3/s	Total Vol.: 0.6 km3
1986	no	August	2,000 m^3/s	Total Vol.: 1.15 km3
1991	no	November	2,000 m3/s	Total Vol.: 1.45 km3
1996	no	April	3,000 m3/s	Total Vol.: 1.15 km3
1996	yes	November	40,000 - 50,000 m3/s	Total Vol.: 3.6 km3
1998	no	February		Small Flood
1999	no	November		Small Flood
2000	no	July		Very small Flood

Summary table of jökulhlaups on Skeiðarársandur: Source; "Flood Dates in the river Skeiðará (almost exceptionally from Grímsvötn)" (Mahlmann 2002)

Jökulhlaups from Skeiðarárjökull originate from three main sources; (a) subglacial volcanic eruptions; (b) stored subglacial meltwater; and (c) ice-dammed marginal lakes. Less frequent, but usually more catastrophic flows originate from subglacial volcanic eruptions centred beneath the Vatnajökull ice cap. During the earliest recorded volcanically induced floods, eruptions were located at a volcanic cauldron named Sviagigur (Wadell 1935), in the north-eastern portion of Skeiðarárjökull's drainage catchment (**Figure 3-4**).

Figure 3-4

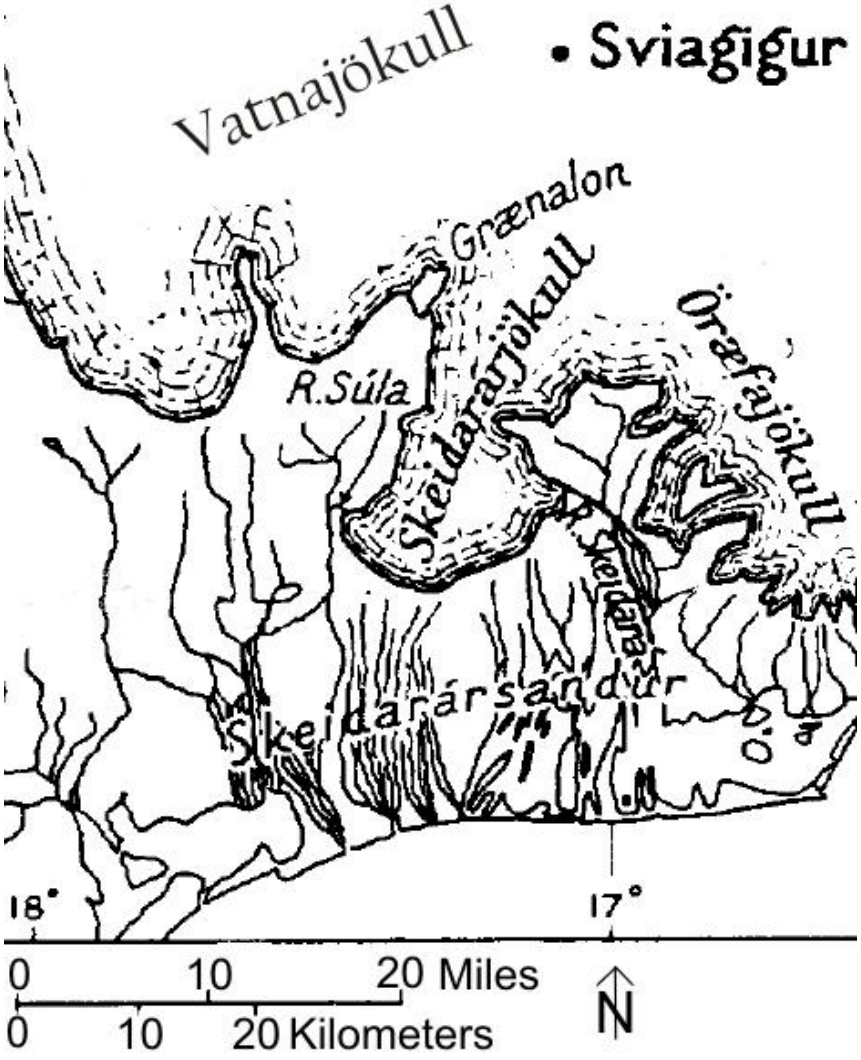

Map showing the location of the volcanic cauldron; Sviagigur to the northwest of Skeiðarárjökull. Map modified from: Waddell (1935)

More recently, floods have originated from the volcanic centre Gal (**Figure 3-5**), which is part of the same volcanic rift beneath Vatnajökull (the eastern Volcanic Zone). Volcanic eruptions beneath the icecap result in the melting of huge amounts of glacial ice, producing vast quantities of meltwater (Guðmundsson et al. 1997). In most cases, meltwaters produced by volcanic eruptions flow into the subglacial lake Grímsvötn, where the water is stored before being released, although the exact routing of this meltwater can vary.

The second source of jökulhlaups on Skeiðarársandur is the release of subglacially stored meltwater from Grímsvötn as a result of geothermal heating. Unlike meltwaters produced from volcanic eruptions, which are produced very quickly, geothermal heating beneath the icecap results in slow, continuous melting of ice at the glacier bed. This meltwater flows into the ice-dammed, subglacial lake Grímsvötn, where it is stored until the lake level reaches a critical level for drainage (Guðmundsson et al. 1997).

The final source of jökulhlaups on Skeiðarársandur is the ice dammed lake Grænalón, which occupies a small subaerial valley on the west side of Skeiðarárjökull (**Figure 3-6**) (Roberts et al. 2005). Dammed by the flank of Skeiðarárjökull to the east, and the mountains Grænafjall and Eggjar to the north and south, meltwater from the northwest margin of Skeiðarárjökull, and runoff from the surrounding peaks, flow into the ice dammed lake basin. The drainage mechanisms for the discharge of this lake are somewhat complicated and have evolved over the last few hundred years.

Morphologically, the impact that these floods have on the outwash plain is significant. It is believed that jökulhlaups on Skeiðarársandur are responsible for rapid rates of aggradation, which has almost completely buried the 1890 terminal moraines in the middle to east sections of the ice margin. At the

western side of the glacier, where the 1890 terminal moraines remain unburied, they reach elevations of 20 – 25 m (Wisniewski et al. 1997; Gomez et al. 2000). Through seismic surveys of the sediments that make up Skeiðarársandur, Guðmundsson et al., (2002) found that the existence of the outwash plain is primarily a result of repeated outburst floods and that such an accumulation of sediments could not have been deposited by 'normal' flow conditions within the time scale allocated. Thus, large outburst floods are known to have a lasting legacy in this region of Iceland. However, this view has been challenged by Smith et al., (2006).

Figure 3-5

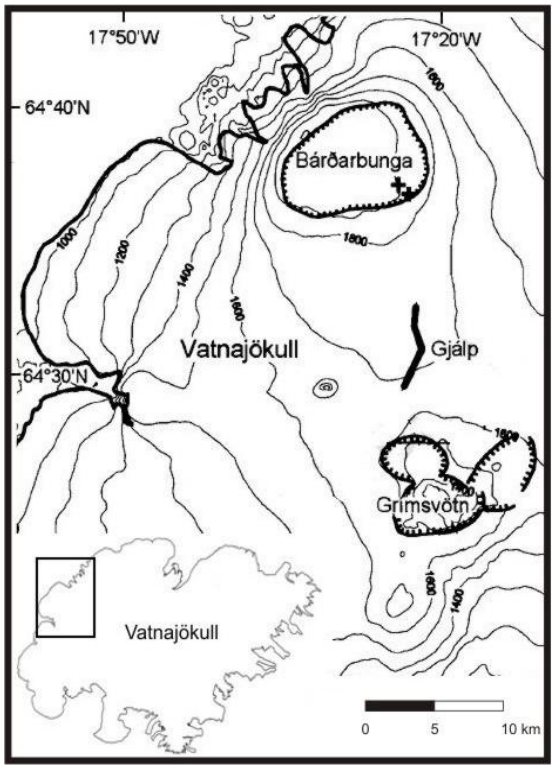

Map showing the location of the Gjálp volcanic fissure beneath Vatnajökull and the location of Grímsvötn in relation to the rest of the icecap. Modified from Guðmundsson et al., (1997)

Figure 3-6

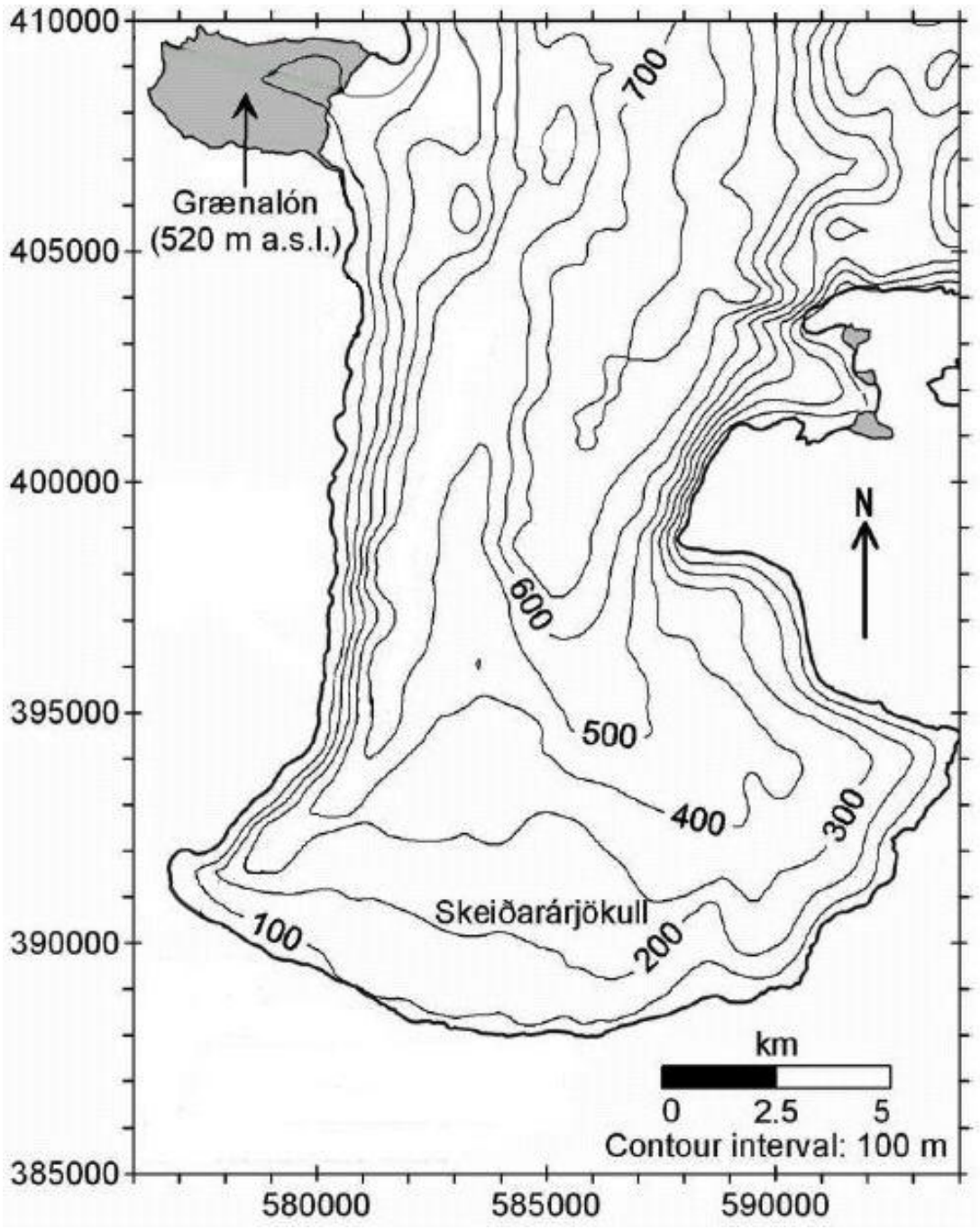

Contour map of Skeiðarárjökull showing the location of Grænalón ice dammed lake on the western flank. Modified from Roberts et al., (2005)

3.1.4 THE NOVEMBER 1996 JÖKULHLAUP

Following the onset of a subglacial volcanic eruption at Gjálp (**Figure 3-5**) at 22:00 on 30th September 1996, 3 km^3 of glacier ice was melted within 13 days as ice came into contact with freshly erupted volcanic material

(Guðmundsson et al. 1997). This water, under hydrostatic pressure, flowed subglacially for five weeks along a narrow conduit at the glacier bed into subglacial lake Grímsvötn. On 4th November 1996, hydrostatic pressure within the subglacial lake reached a critical threshold, floating the ice off its bed and allowing the stored meltwaters to flow 50 km beneath Skeiðarárjökull to the margin. Flood waters progressively emerged from east to west along the ice margin as the flood progressed. The first flood waters were witnessed issuing from the Skeiðará outlets on the far east of the glacier at 7:30am on the 5th November, reaching a peak discharge of 45,000 m^3s^{-1} within 14 hours (Russell and Knudsen 2002). Later, flows began to emerge within the Gígjukvísl river channel at approximately 10:15, which are believed to have reached a peak discharge of 34,000 m^3s^{-1} by 03:00 on the morning of 6th November (Russell et al. 1999). By approximately 15:40, flood waters were spilling out from the entire length of the ice margin and the peak discharge in the Núpsvötn reached 2300 m^3s^{-1} at approximately 19:00 (Snorrason et al. 2002).

The aftermath of the jökulhlaup left Skeiðarársandur and the ice margin of Skeiðarárjökull severely altered. Several bridges along Iceland's main ring road (Route One) were destroyed and much of the road its self was severally damaged (Snorrason et al. 1997). Ice blocks up to 45 m in diameter, littered the ice marginal zone (Fay 2002), whilst 38 × 10^6m^3 of sediment was deposited within the ice marginal zone and on the sandur plain (Smith et al. 2000). The flood altered the appearance of the ice margin, filling in small lake basins with sediment and eroding large areas proximal to the glaciers main outlets (Russell et al. 1999).

Such detailed observations of processes that occurred during the November 1996 Jökulhlaup are essential in aiding our understanding of the

proglacial landscape of Skeiðarárjökull. Such observations allow direct process – form relationships to be established and greatly aid in our interpretation of the geomorphological forms that are developed in such proglacial environments. This very detailed understanding makes Skeiðarárjökull an excellent case study for the investigation of glaciers that are to be used as analogues for Quaternary and earlier glacier margins.

3.1.5 SKEIÐARÁRJÖKULL SURGE HISTORY

Not only is Skeiðarárjökull subject to high magnitude catastrophic Jökulhlaups, it is also subject to large scale, cyclic surge events (Pálsson et al. 1992). As with recent jökulhlaups, these surges have also played a significant role in sculpting the morphology and sedimentology of this highly dynamic landscape.

Skeiðarárjökull is known to have surged in 1787, 1812, 1857, 1873, 1929, 1965, 1985, and most recently in 1991 (Wisniewski et al. 1997; Björnsson et al. 2003). Jóhannesson (1985) provides a record of Skeiðarárjökull's advance and retreat history, presented in Figure 3-7.

Figure 3-7

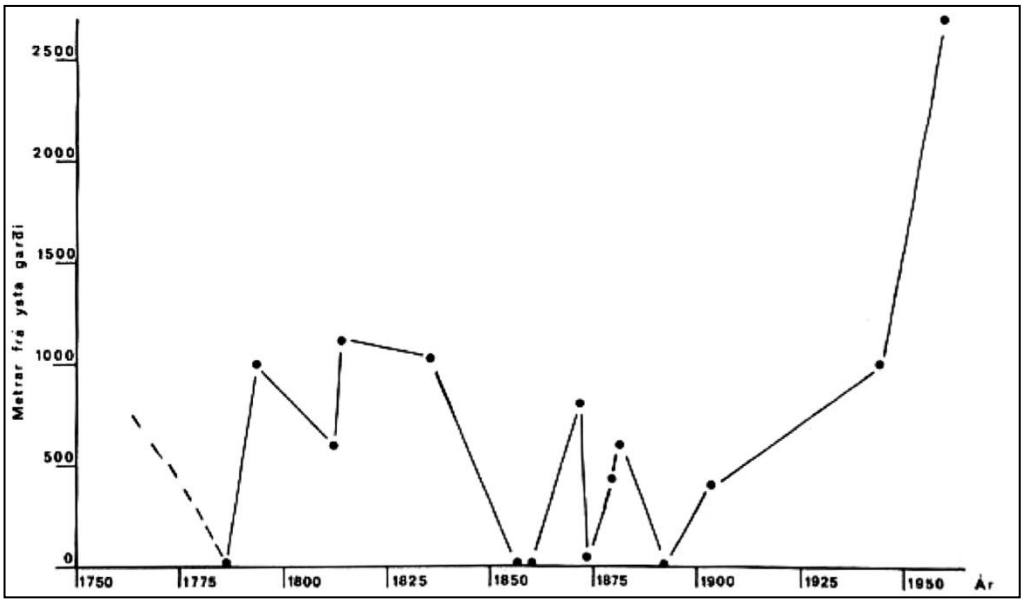

Graphic representation of the distance of Skeiðarárjökull's margin from the outermost terminal moraines between 1750 and 1985. Jóhannesson (1985)

Although at is probable that surges at Skeiðarárjökull always modified the ice marginal landscape, evidence of these modifications is only documented since the 1960's. In 1965, glacier advance in the middle portion of the ice-margin resulted in the overriding of a 210,000 m^2 ice marginal lake (Wisniewski et al. 1997). Advance of the ice margin into another lake caused large-scale glaciotectonic deformation of saturated glaciolacustrine sediments, and the production of large, ice margin parallel surface undulations. These ridges, comprising deformed glaciolacustrine sediments, were elevated to a height of 12 m above the level of the lake, and were formed as a result of sediments being squeezed out from under the glacier due to the weight of the advancing ice mass (Wisniewski et al. 1997).

Numerous authors (Thorarinsson 1943; Wisniewski et al. 1997; Russell et al. 2001; van Dijk 2001) have demonstrated the importance of surging in the development of the proglacial landscape in relation to the formation of large push moraine sequences and surge related fans formed as a result of ice advance

during the 1991 surge, and the release of large amounts of stored water following the end of the surge consecutively. Waller et al., (2008) also demonstrated the importance of surging at Skeiðarárjökull with the identification of a suite of drumlinized features that formed during the 1991 surge. Thus, surging has played a great part in the evolution of Skeiðarárjökull's ice marginal geomorphology in recent history.

3.1.6 JUSTIFICATION SUMMARY

Section 3.1 has demonstrated that Skeiðarárjökull is a highly dynamic piedmont glacier lobe, which drains a large portion of Europe's largest ice cap. It is subject to high discharge catastrophic outburst floods and has shown rapid fluctuations in its flow velocity as a result of periodic surge events. These characteristics make it a very strong contender for use as an analogue for Quaternary ice masses, as evidence for the former behaviour of many large Quaternary ice sheet and outlet lobes has shown that these former ice masses were also subject to such phenomenon (Prest 1969, Wright 1971, Clayton et al., 1985, Dyke and Prest 1987, Evans et al., 1999, Stokes and Clark 2001).

3.2 INTRODUCTION TO FIELD TECHNIQUES

To test the numerous hypotheses proposed in Chapter 2 (Table 2-1), many critical geomorphological and sedimentological tests must be carried out. All hypotheses pose some kind of geomorphological question, and to address those, accurate geomorphological maps of the field sites must be produced. Two kinds of geomorphological information have been used throughout this research:

1. Remotely sensed data acquired from aerial photography:
2. Primary data was collected through fieldwork expeditions carried out between June 2005 and April 2007.

Detailed descriptions of the methods utilising both of these data sources are provided in the following sections.

3.2.1 GEOMORPHOLOGICAL MAPPING USING AERIAL PHOTOGRAPHS

To assess the spatial pattern and distribution of landforms in the proglacial zone of Skeiðarárjökull it is essential that accurate and detailed geomorphological maps be produced. A large number of maps have been produced for this thesis based on available aerial photography. A series of geo-rectified aerial photographs of the field area for the years 1945, 1965, 1975, 1997, 2003, & 2007 were available within the School of Geography at the University of Newcastle. For each field area of interest, the aerial photograph was exported from the Geographical Information System (GIS) programme (Arc GIS), and imported into the CAD (Computer Aided Design) software, CorelDraw X3. Each of the photographs was then traced within this programme, aided by field observations in a similar method to that described at other Icelandic Glaciers by Evans and Twigg (2002) to produce highly accurate maps.

3.2.2 GEOMORPHOLOGICAL MAPPING USING DIFFERENTIAL GPS

Differential GPS is capable of collecting spatial data at a very high level of accuracy, especially in the Z, or elevation vector, and thus is an excellent tool for use in large scale topographic surveys. The dGPS system used was the Thales Promark 3, which comprises two identical units. One of the units is used as a 'base station' which is tripod mounted and collects data continuously every second at a fixed position for the duration of the survey. The second unit is attached to a 'detail pole', which is used to accurately pinpoint the features to be surveyed. The time taken to collect each data point is variable depending on the level of accuracy required. The manufactures instructions recommend that for accuracy of less than one centimetre, fifteen seconds worth of data collection is

required at each point. With this in mind, all points collected with this system were collected using a data collection time of 20 – 25 seconds to ensure the increased accuracy of the data.

Once set up, the sampling strategy required the measurement of point locations at key features, such as breaks of slope (concave and convex), channel banks (top and bottom), ridge crests, kettle hole edges, spot heights. All of the surveyed co-ordinates were saved within the systems internal memory and exported onto a laptop at the end of each day.

Following the completion of a survey, the data has to be 'post processed' with the data collected by the 'base station'. This process is carried out using the software package GNSS Solutions that is supplied with the dGPS.

Once the data is post processed, the spatial data is exported as a .txt file with the following attributes: Feature Code, X, Y, Z, (**Figure 3-8**). The co-ordinates are exported as UTM (Universal Transverse Mercator) Zone 28 north, which is the appropriate UTM zone for this area of Iceland. Once the data is exported from GNSS Solutions, it is imported into ESRI ARCGIS in the same way as above, before being transferred into Corel Draw for the production of plan form maps.

Figure 3-8

Feature Code	X	Y	Z
Moraine Crest	394995.3919	7099022.318	92.5595
Moraine Crest	394992.1012	7099019.415	93.1644
Moraine Crest	394988.6199	7099014.569	94.2804
Moraine Crest	394984.3361	7099010.158	94.8697
Moraine Crest	394978.2202	7099008.716	94.3466

Example of exported data table from GNSS Solutions, showing mapped feature codes and UTM co-ordinates in metres.

Due to the highly accurate vertical information acquired with the DGPS, it is not only possible to produce plan form geomorphological maps, but also

very detailed digital elevation models (DEM's). Using the collected GPS data, DEM's have been produced for different areas along the ice margin of Skeiðarárjökull using the ESRI's ARC Scene.

3.2.3 SEDIMENTARY SECTION LOGGING

To test many of the hypotheses set out in Chapter 1, very detailed sedimentological investigations of the walls of overdeepenings have to be carried out. Where possible, sedimentological investigations took advantage of natural exposures through sediments, such as sections cut by rivers or flooding events, however, many other exposures had to be excavated manually. In most cases, this meant to excavation of tiered pits or staircase exposures being dug into the sides of the topographic depressions.

Once exposures are cleaned, standard sedimentary logging procedures were employed to record sedimentological data shown in the section. This includes the production of a field sketch (with scale) to capture an image of the sedimentary architecture, making note of the size and relative position of individual facies within a section. For each individual lithofacies within a section, the following important characteristics were noted: a) grain size, b) depositional structures, c) deformational / faulting structures, d) presence of inclusions / intra-clasts, e) bed thickness and geometry and f) the nature of the contacts in between lithofacies (Evans and Benn 2004). In addition to the above, a large number of digital photographs of many sections were taken to produce detailed 'panel traces' by using the photographs as a base to draw each section, and then add the additional data discussed above (**Figure 3-9**).

Figure 3-9

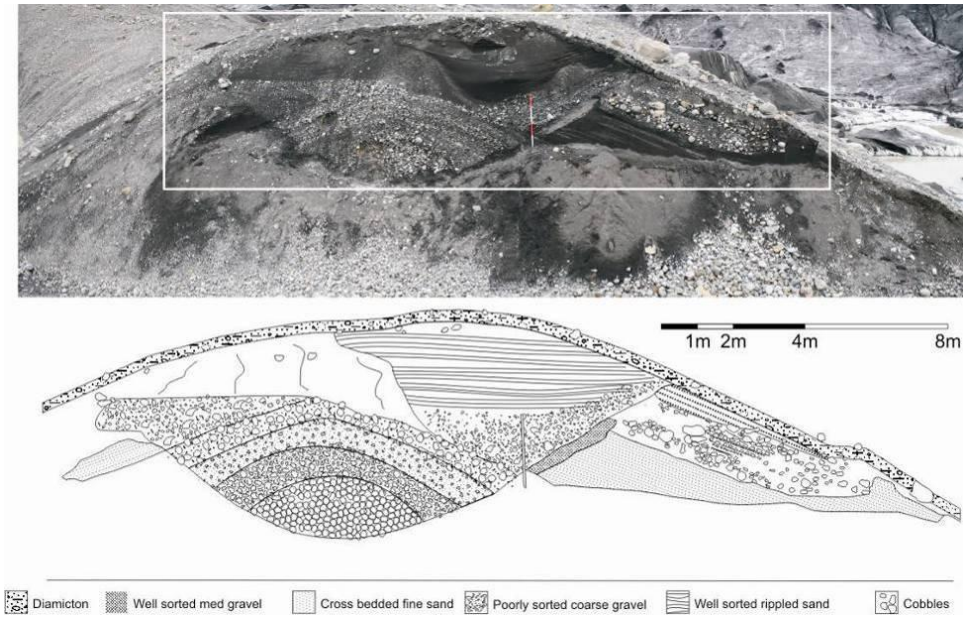

Photo mosaic and panel trace of a section cut through an esker in the Sæluhúsavatn area of the Skeiðarárjökull ice margin.

3.2.4 CLAST FABRIC ANALYSIS

The number of works dealing with clast fabric analysis within a glacial environment are abundant (Dowdeswell and Sharp 1986; Benn 1994; Benn 1995; Hooke and Iverson 1995; Bennett et al. 1999), as well as many more within the fluvial, mass flow and debris flow literature . The main reason for the collection of clast fabric data is to obtain an understanding of the local palaeo flow direction and the likely rheology or flow characteristics of the flow by which the materials in question were deposited. This information is essential if any attempt is to made to understand the origin landforms and the processes that resulted in their formation. To reconstruct flow directions within fluvial sediments or directions of strain within glacial sediments, a large number of clast fabric measurements were carried out at each location where possible. Clast fabric analysis requires the use of a compass clinometer to measure the orientation (compass bearing) and dip of the longest (a-axis) of a number of clasts that are protruding from, but remain in-situ within, a sedimentary exposure.

The methodology associated with clast fabric analysis can vary depending on what types of material are under investigation. For example, in many studies involving fluvial deposits researchers measured the dip of the a - b plane to calculate the direction of clast imbrication, whereas investigations of fabrics in glacial diamictons often, measure the dip of the a-axis.

Throughout this investigation, measurement of the a-axis was considered most appropriate, and is in keeping with a large volume of glacial sedimentology.

The size and shape of clasts measured for clast fabric studies vary from case to case, although the general consensus is that the greater the a-axis to b-axis ratio, the more reliable the palaeo flow interpretation, and for this reason most studies suggest an a:b length ratio of 2:1 or greater however ratios of 1.2:1 have been carried out (Tucker 1988; Hubbard and Glasser 2005). Due to the high abundance of compact clasts making up the vast majority of sediments at Skeiðarárjökull and the difficulty of finding elongated clasts, the acceptance ratio for clast fabric studies carried out during this research was lowered to the aforementioned 1.2:1.

Clast fabric analysis was carried out on a number of individual units or beds within sedimentary sections where the nature of the sediments would allow i.e., suitably cohesive to prevent collapse. Within each sample from these units, up to 50 of the largest clasts were measured to attain a representative sample (Hubbard and Glasser 2005). In each case, the clast fabric data are plotted as lower hemisphere 3D stereo plots using GeoPlot 2.1 (**Figure 3-10**).

Figure 3-10

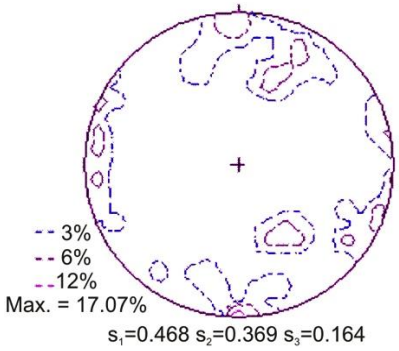

Clast fabric data presented as a 3 dimensional stereo plot.

3.2.5 CLAST SIZE, SHAPE AND SURFACE TEXTURE ANALYSIS

The size, shape, and surface texture of clasts within a sedimentary package make up an important data set for the interpretation of the transport history and depositional environment of sediments (Powers 1953; Boulton 1978). By measuring the size of the largest clasts within a unit, it is possible to come to some conclusion about the power of the transporting medium the clast passed though. In addition, measurements of a clasts shape and surface texture can be used to reconstruct the transport pathway through which a clast travelled prior to deposition (Boulton 1978; Benn and Ballantyne 1994). Such information is essential for the interpretation of the processes that result in the formation of landforms within the proglacial zone.

The collection of this data was carried out at the same time as the clast fabric data collection above. Following the collection of a-axis dip and orientation data, each clast was removed from the face and each of its axes (a, b and c) were measured and recorded as well as a visual description of their roundness based on Powers (1953).

Clast size, shape and surface texture data are presented in a number of different ways. Clast size data are averaged and presented as a single figure shown on the associated sedimentary log or panel. Clast shape data are plotted

onto triangular shape diagrams generated by inserting clast axis data into a TRI-PLOT spread sheet (Graham and Midgley 2000). These triangular shape diagrams show the proportion of clasts that fall into each of the descriptive shape classes of (Sneed and Folk 1958) (**Figure 3-11 - A**). Roundness data are plotted as roundness class percentage frequency histograms (**Figure 3-11 - B**).

Figure 3-11

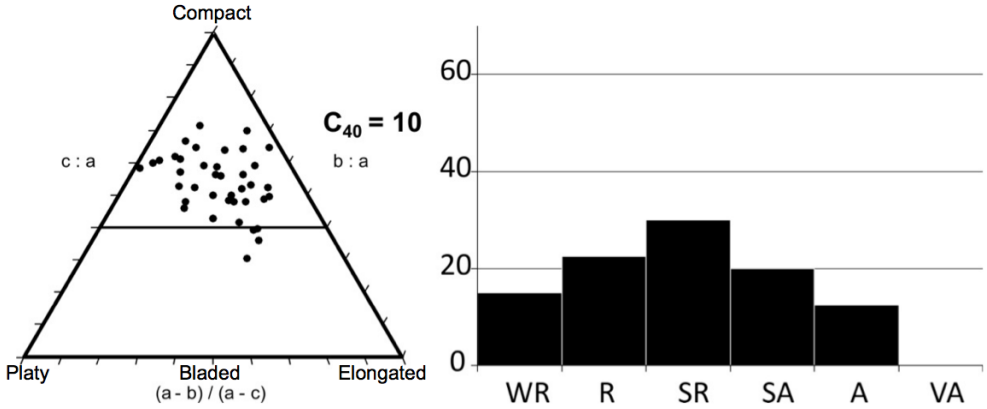

Clast shape and roundness data from esker sediments at the margin of Skeiðarárjökull, Southeast Iceland. A) shows a triangular shape diagram, displaying the proportion of clasts that fall into each of the descriptive shape classes of Sneed and Folk (1958) whilst B) shows a roundness class, against percentage frequency histogram based on the roundness classes of Powers(1953). Note: VA = Very Angular, A = Angular, SA = Sub-angular, SR = Sub Rounded, R = Rounded, WR = Well Rounded.

3.2.6 BULK SEDIMENT SAMPLING FOR LABORATORY ANALYSIS

In order to compliment and refine descriptions of grainsize distribution made in the field, a large number of bulk sediment samples were taken for further analysis in the laboratory. The procedure for this sampling was based on that proposed by Hubbard and Glasser (2005), who suggest that a bulk sample of approximately 2 kg is appropriate for grainsize analysis by dry sieving. Sediment samples were collected from most sedimentary facies identified at each excavation / section, except when the maximum grainsize exceeded approximately 70 mm, or where logistical or health and safety dangers made collection impossible. In which case samples were not taken and instead, visual

descriptions were made including approximations of proportion of fines, sand, gravel, etc.

Within particularly large exposures of massive materials (in most cases well sorted fine sands) numerous samples were taken at regular intervals horizontally and vertically across the exposed face in order to identify subtle changes within these larger sediment bodies.

3.2.7 LABORATORY TECHNIQUES – DRY SIEVING GRAINSIZE ANALYSIS

Grainsize analysis has long been used as a standard tool to aid in the interpretation of the processes that have been involved in the erosion, transport, and deposition of sedimentary partials (Tucker 1988; Evans and Benn 2004). It is rarely possible to find a direct relationship between particle size, or size distributions and process, due to variations in lithology, and erosion history (Evans and Benn 2004). However, when used in combination with other evidence such as sequence stratigraphy, clast texture, and fabric, grainsize analysis can be very useful in the development of interpretations of sediments (Evans and Benn 2004).

Boulton (1978) provided an excellent example of the use of grainsize distributions as well as other evidence to aid in the interpretation of transport pathways of sediments at the margin of Breiðamerkurjökull, in Southern Iceland a well as other glaciers (**Figure 3-12**). This research showed that sediments transported in a supraglacial position tend to have a far greater concentration of larger particles then those transported in the zone of traction at the glacier bed. This is due to continual abrasion at the glacier bed resulting in the fracturing of rock and formation of smaller partials.

Figure 3-12

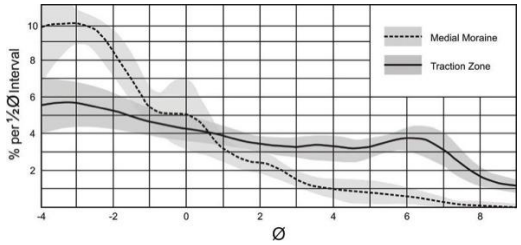

Grainsize distributions from sediments collected at Breiðamerkurjökull, Southeast Iceland. Modified from Boulton (1978).

In order to compliment and refine descriptions of grainsize distribution, many sample collected in the field were returned to the laboratory for detailed analysis. Each of these samples was oven dried over night at a temperature of 105°C. The drying procedure consisted of removing the sample from the plastic sample bags and placing them in broad open topped steel trays. Following the drying procedure, each sample was weighed using an electronic scale and the weight if the tray was deducted. Coarser or very sandy samples that were not prone to aggregation were immediately placed in an 11 piece sieve stack a sieved using an automated sieve shaker for 20 – 30 minutes. Samples which contained a large proportion of silt and clay sized particles are much more prone to aggregation, and so were disaggregated using a pestle and mortar prior to sieving. During this process, extra care was taken to ensure that individual grains were not fractured resulting in a fining of the grainsize distribution.

The sieves used were divided by whole phi units (Ø); 31.5 mm, 16 mm, 8 mm, 4 mm, 2 mm, 1 mm, 500µm, 250µm, 125µm, 63µm and ‹63µm (pan fraction).

3.3 CHAPTER SUMMARY

This chapter has identified and justified the use of Skeiðarárjökull, Southeast Iceland as the specific field site as which this research is to be carried out. Based on the nature of the site, it is considered a suitable analogue for the outlet glaciers of the large North American and European Quaternary Ice Sheets. Therefore, this satisfies part of Objective 2, which is the identification of an *appropriate* field site.

This chapter has also outlined the methods which will be used to critically assess the sediment landform assemblages associated with the formation of overdeepenings at the margin of Skeiðarárjökull. It has provided justification for the choice of these techniques and given examples of where they have been successfully been used previously.

4 RESULTS – EASTERN SÆLUHÚSAVATN OVERDEEPENING

4.1 INTRODUCTION – EASTERN SÆLUHÚSAVATN OVERDEEPENINGS

The aim of this chapter is to present field and laboratory data collected at Skeiðarárjökull to test the hypothesis described in Chapter Two. Due to the nature of the data collected and the variation of landforms and processes along the margin of Skeiðarárjökull, the results presented in this thesis are divided into three individual chapters, each presenting findings from specific geographical areas of Skeiðarárjökull's ice margin where sediments and landforms are regionally distinct. Chapter Four (this chapter) presents' data from the Eastern Sæluhúsavatn overdeepening, Chapter Five presents data from the Western Sæluhúsavatn overdeepening and Chapter Six presents data from the Háöldukvísl ice contact site.

To critically test the hypothesis described at the end of Chapter 2 and to satisfy Objective 2, an understanding of the sedimentological and geomorphological nature of the site must be achieved. The site is located approximately 2 km west of the western Skeiðará river outlet in the ice marginal area known as Sæluhúsavatn (**Figure 4-1**). This area consists of four topographic overdeepenings set into the ice proximal sandur surface, with dimensions up to 380 m × 250 m in plan form and approximately 15 m in depth, with undulating long profiles. These characteristics allow the features to be referred to as topographic overdeepening as defined in chapter one, and thus investigation of their form and sedimentology are highly appropriate for this study.

Figure 4-1

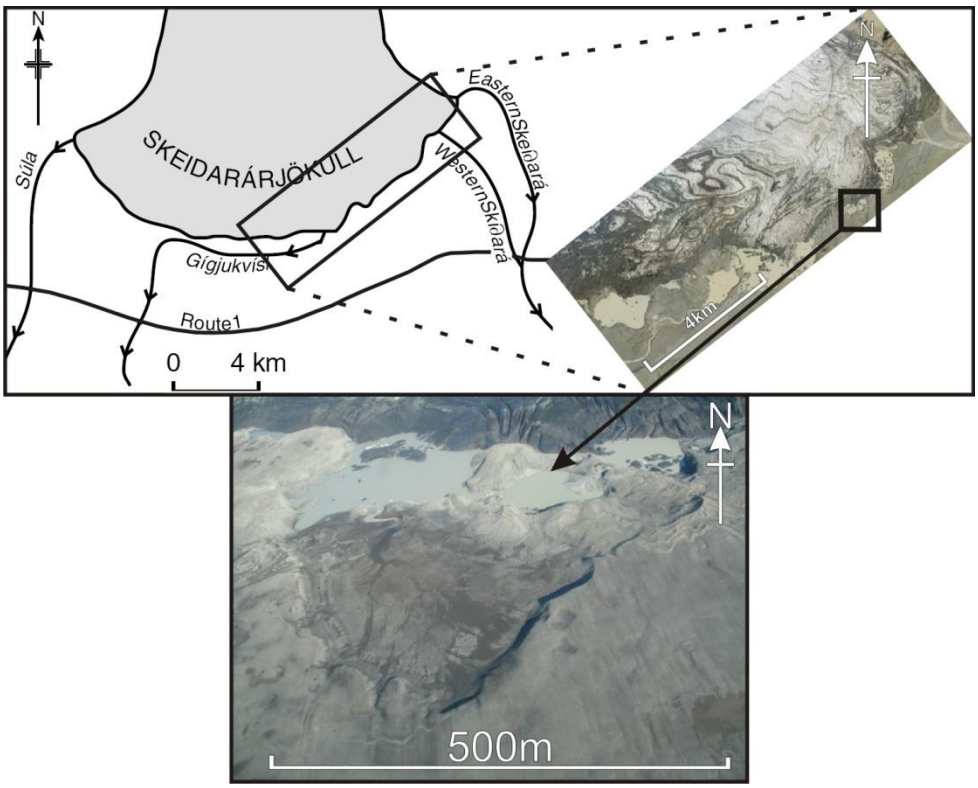

Map and aerial photograph showing the location of the Eastern Sæluhúsavatn overdeepening along the margin of Skeiðarárjökull and oblique air photograph showing the morphology of the four hollows as described above. Map modified from Roberts et al.,

4.2 GEOMORPHOLOGY OF THE EASTERN SÆLUHÚSAVATN AREA

To gain an understanding of the geomorphological evolution of the Eastern Sæluhúsavatn overdeepening, time sequence geomorphological maps were produced from aerial photographs taken between 1945 and 2003 (**Figure 4-2**). These five maps illustrate the morphological changes that have occurred in this area since the 1940's (**Figure 4-3**). These maps have been complimented with the construction of very detailed Digital Elevation Models, produced with the use of detailed topographic data. This data was collected using Differential GPS (dGPS) and gives a far greater understanding of the range of elevation than can be achieved from geomorphological maps alone (**Figure 4-4**).

4.2.1 TIME SEQUENCE GEOMORPHOLOGICAL MAPS

The 1945 geomorphological map shows the glacier margin at its most advanced position of all the maps produced for this site. There is very little detail visible in this area of the glacier margin due to the low quality aerial photography produced during the 1940's. A slightly streamlined sandur surface and a small mound in contact with the ice, adjacent to a small ice contact pond can be identified.

In the twenty years between 1945 and 1965, Skeiðarárjökull's ice margin retreated 315 m, revealing a large topographic overdeepening containing a lake. This lake was subsequently named Sæluhúsavatn (Vatn in Icelandic meaning lake), thus giving the area its name. Immediately north of the lake there is a large ridge parallel to the ice margin. The ice proximal ground north of this ridge is at a lower elevation to that of the sandur surface on the distal side of the lake. Therefore the ridge is formed within the topographic basin containing the lake. West of the lake, an ephemeral meltwater outlet has developed a wide braided stream network which flows into another large lake southwest of the Sæluhúsavatn. Although inflow to this lake appears to be ephemeral, this lake fed the former Sæluhúsakvísl river channel which was active at this time. To the east and west of the Sæluhúsavatn basin, numerous small discontinuous sub-parallel ridges are present in front of the ice. There is no evidence remaining of the ice contact mound visible on the 1945 map.

The 1975 geomorphological map shows that there has been very little change in the marginal landscape of Skeiðarárjökull between 1965 and 1975. The ice margin has retreated only a few, metres with little effect on any pre-existing landforms. The greatest change in this time period is the widening of the Sæluhúsakvísl braided river channel west of the Sæluhúsavatn lake basin, and

the formation of a pronounced linear ridge on the western side of the channel, which trends parallel to the glacier margin. There was no significant change in the morphology of the Sæluhúsavatn overdeepening.

Changes in the morphology of the Sæluhúsavatn lake basin between 1975 and 1997 are considerable. The 1997 geomorphological map shows that on the lake's north-eastern shore, a large fan shaped wedge of sediments has been deposited, partially burying a large portion of the ice parallel ridge. In addition, two channels and a mound in-between these channels have been formed on the south-western shore. Approximately 100 m southwest of the channels, a number of 'embayments' have formed within the Sæluhúsakvísl riverbank. The Sæluhúsakvísl channel has widened by approximately 150 m at the most distal extent shown on the map; however, as in 1975, the channel does not appear to be active. Northeast of the lake, a series of discontinuous, sinuous ridges have formed on the upper sandur surface and the small meltwater channels and ponds in that region appear to have been in-filled.

The six years between 1997 and 2003 appear to have produced the greatest amount of change in the Sæluhúsavatn area over the last sixty years. Since 1997, the ice margin has retreated approximately 200 m along the majority of the mapped area. This ice retreat has revealed a series of topographic 'hollows' along the ice margin in the location of the Sæluhúsavatn lake basin. The original lake basin seen between 1965 and 1997 is no longer water filled and stands as an empty hollow with lacustrine sediments filling its base. An ice marginal lake now exists at a lower elevation north of the original lake which is bound on its western and southern shores by the edges of the hollow which contained the original lake. The lake's eastern shore is bound by a gravel ridge which protrudes from the ice in a southerly direction. This ridge appears to

bifurcate at its ice proximal end and run parallel with ice margin towards the east before curving southeast and joining the area north of the original lake basin. To the east of the new ice contact lake basin lays a smaller hollow which is divided from the ice by the gravel ridge. This basin is only partially water-filled and has a large, well developed delta emerging from a gap in the gravel ridge on its eastern side. There is also a large gap in the ridge on the western side of this hollow, connecting it to the ice contact lake on the west. On the western side of the ice contact lake, a 160 m long, 20 m wide gully or trench extends from the western lakeshore to the apex of the braided outwash fan seen in 1997. To the north and west of the Sæluhúsakvísl channel, discontinuous sinuous ridges have formed and been dissected close to the river channel, where, as north of this location, truncated ridges exist juxtaposed to areas of low, flat, streamlined topography.

Figure 4-2

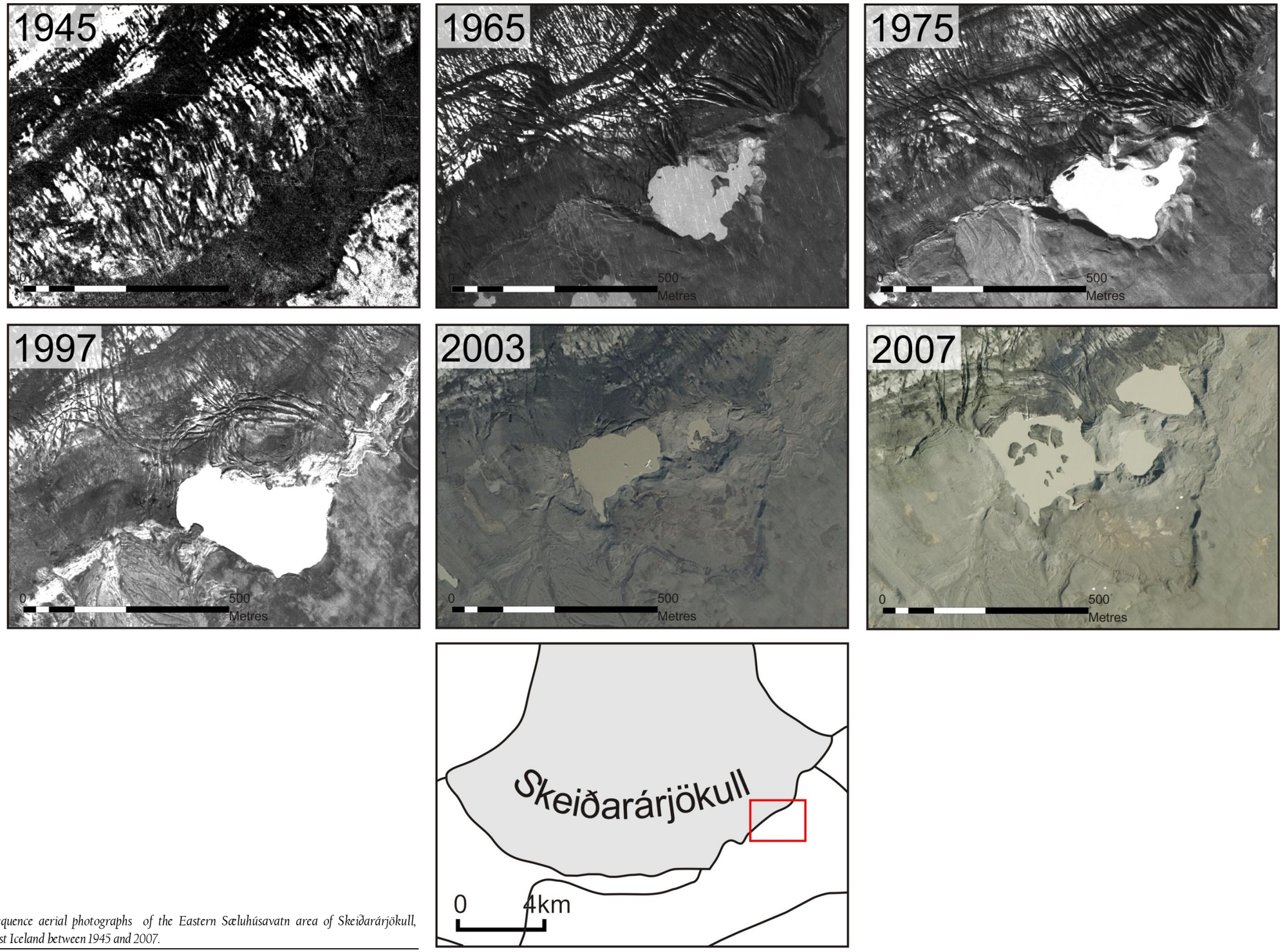

Time sequence aerial photographs of the Eastern Sæluhúsavatn area of Skeiðarárjökull, southeast Iceland between 1945 and 2007.

Figure 4-3

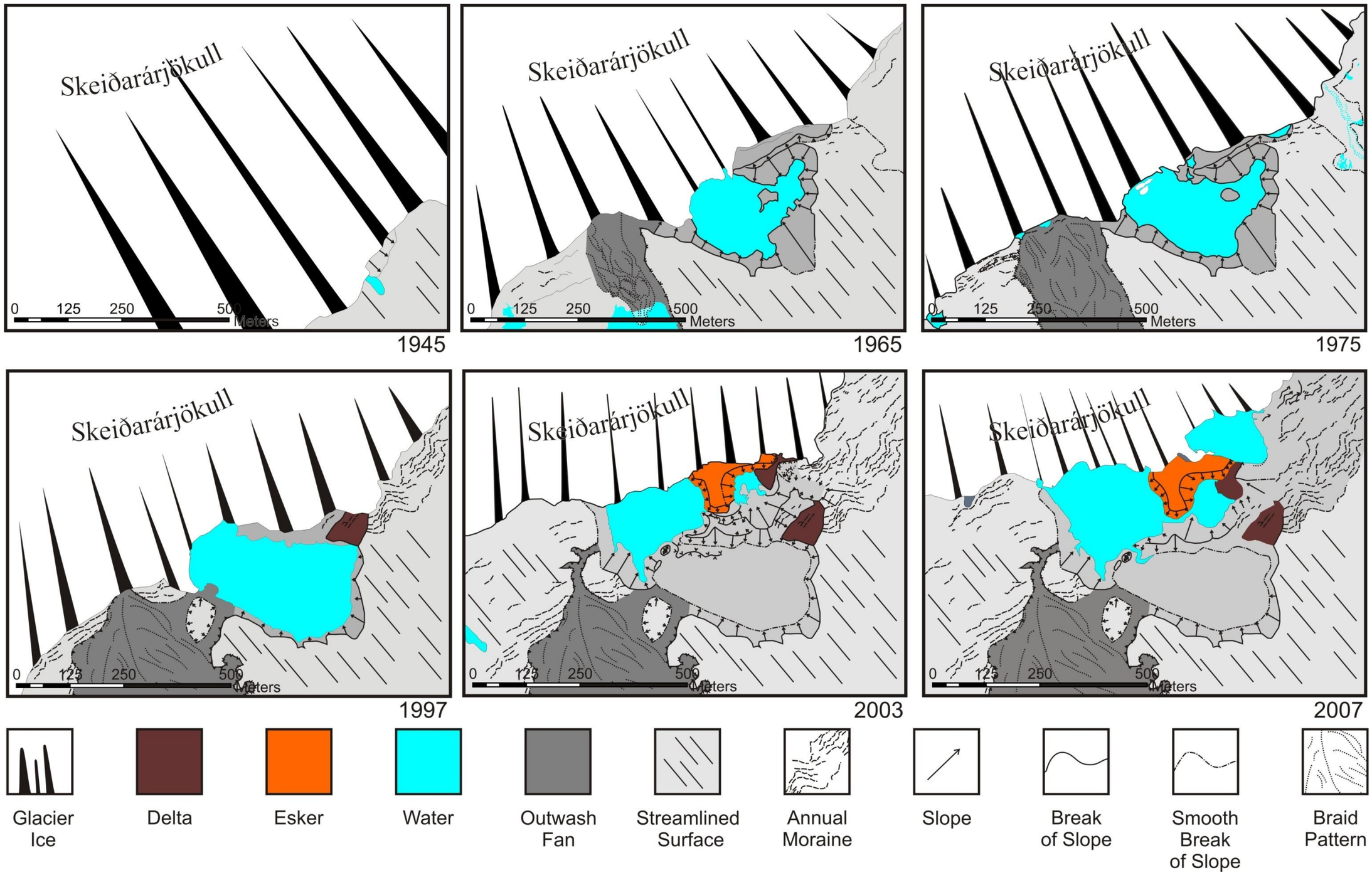

Time sequence geomorphological maps of the Eastern Sæluhúsavatn area of Skeiðarárjökull, southeast Iceland. These maps illustrate the morphological changes that have occurred in between 1945 and 2007.

4.2.2 2006 / 2007 DIGITAL TERRAIN MODEL

Although geomorphological maps produced from air photographs are excellent tools which aid in the understanding of plan form morphology and evolution of the ice margin, they do not give accurate insight into the three dimensional topography under investigation. High resolution differential GPS surveys of the Sæluhúsavatn area were carried out in 2006 to alleviate this problem and the resulting data were used to construct a digital terrain model (DTM) (**Figure 4-4**). Differential GPS data provides a higher level of detail than the previous maps, although the model only depicts the Sæluhúsavatn basins and not the surrounding topography. Since 2003, it is clear that the ice has retreated only slightly, and the dimensions of the ice contact lake on the west have not changed. Immediately east of the 'ridge enclosed basin', ice retreat has revealed a second water-filled ice contact basin to the east of the site. This terrain model allows a greater understanding of the relative elevation variations between different geomorphological features at this site. From the terrain model, it is clear that the top edge of the ridge which encloses the central hollow, grades to an elevation slightly below that of the main sandur surface. The DTM also shows the stepped transition between the upper sandur surface, the upper Sæluhúsavatn basin, and the lower Sæluhúsavatn ice contact lake.

Figure 4-4

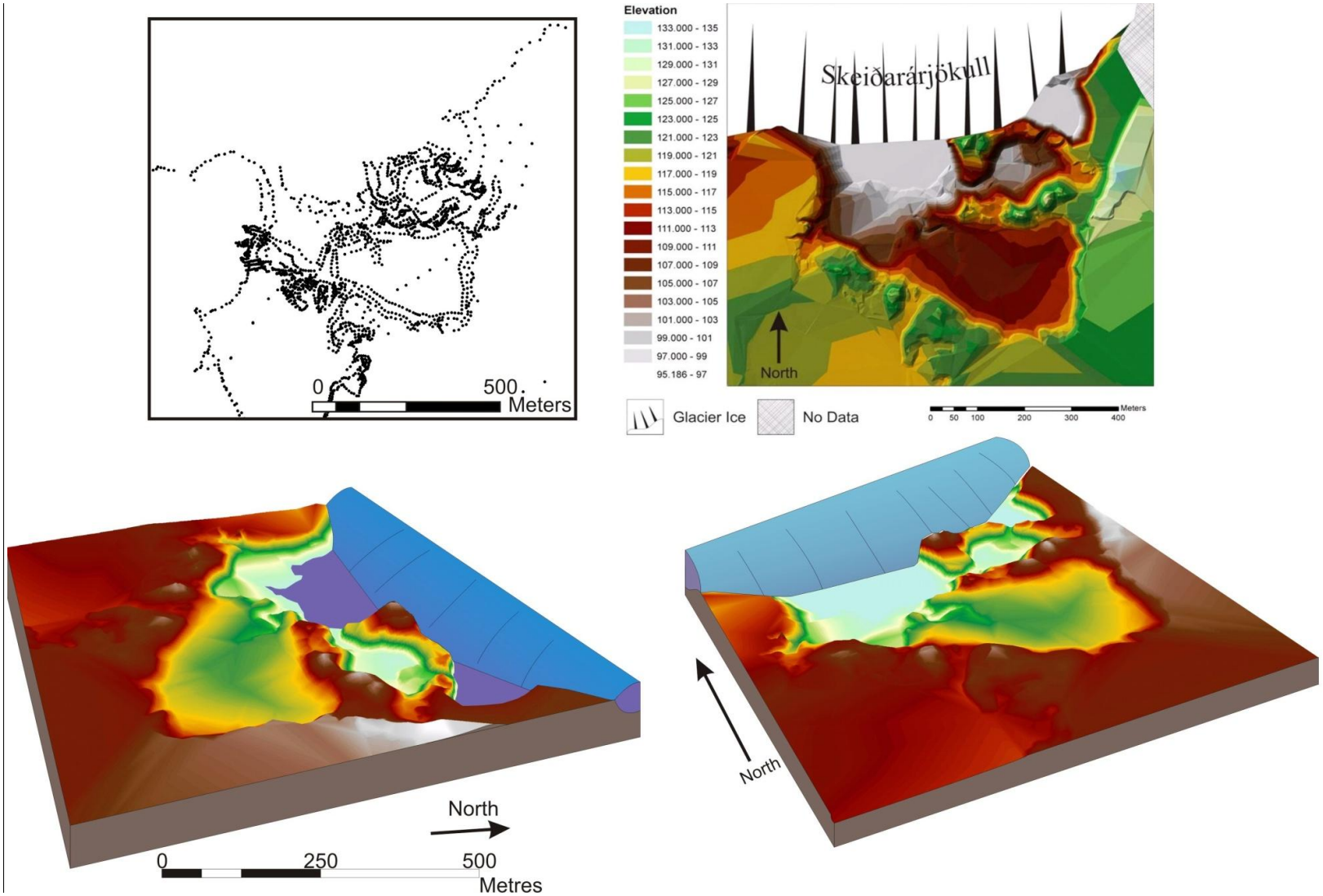

Raw dGPS data plot and digital terrain models (Triangulated Irregular Network - TIN) of the eastern Sæluhúsavatn basins. Differential GPS surveys conducted during 2006 – 2007.

4.2.3 GROUND BASED EASTERN SÆLUHÚSAVATN GEOMORPHOLOGICAL OBSERVATIONS

The Eastern Sæluhúsavatn Overdeepening is defined by a number of interconnected topographic hollows or basins at the margin of Skeiðarárjökull. These are associated with a number of other geomorphological features including gravel ridges, river channel and outwash fans. Each of these features of interest are highlighted on **Figure 4-5** and described in detail in the following pages.

Figure 4-5

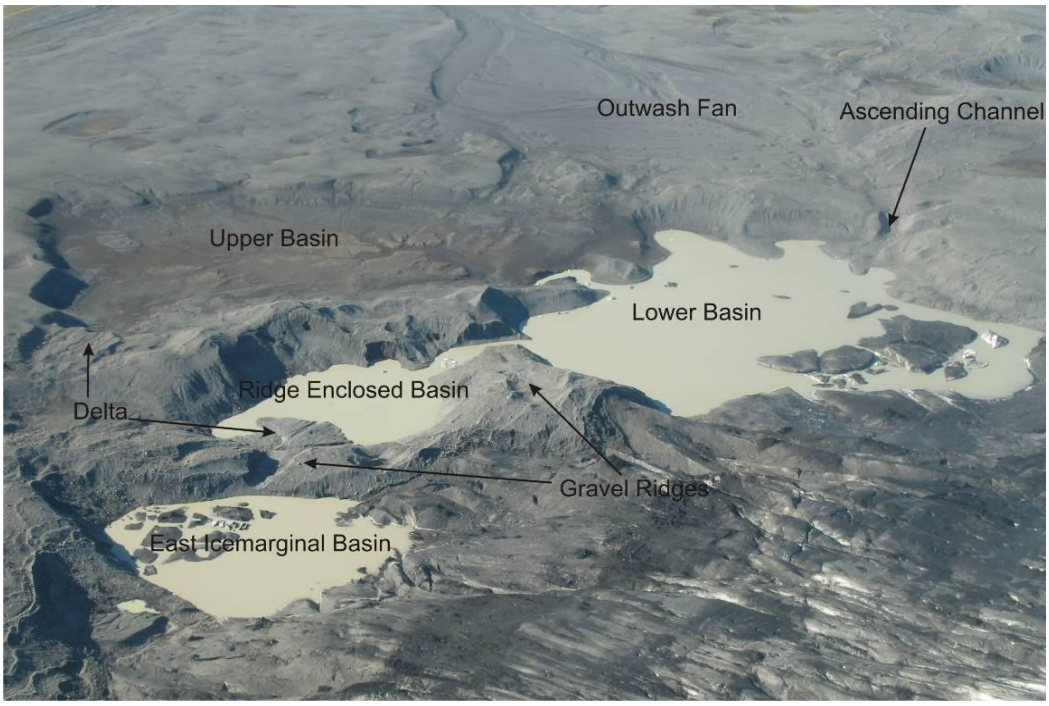

Oblique aerial photograph providing an overview of the Geomorphology of the Eastern Sæluhúsavatn Overdeepening.

4.2.3.1 Upper Sæluhúsavatn basin

The upper Sæluhúsavatn Basin is the largest of the four over-deepened basins located within the Sæluhúsavatn Area and is located at a higher elevation than the ice proximal basins. This feature is approximately 400 × 270 m wide and up to 15 m deep (**Figure 4-4**). The western and eastern edges of the overdeepening are defined by relatively sharp breaks of slope that mark the top

of the concave walls. To the south, the walls are less steep, grading smoothly to the outwash surface above. The northern wall of the overdeepening is defined by an undulating, moraine-like ridge that separates this basin from the Lower Sæluhúsavatn basin to the north. The upper basin is connected to the lower Sæluhúsavatn Basin by a shallow, convex slope along the northwest edge of the basin.

The floor of the overdeepening is composed of well sorted, fine sands and silts. Towards the north, these have been incised by water flow towards the ice margin and reveal thick sequences of bedded sands and silts.

On the east side of this upper basin there is an approximately 50 - 70 m wide, fan shaped wedge of sediment, which encroaches into the basin at an elevation approximately 2 m lower than the basin rim (**Figure 4-6**).

On the west side of the Upper Basin, there are two, narrow channels which are at a lower elevation than the basin rim. These channels connect with the large channel and outwash fan which is located to the west of the upper basin.

Figure 4-6

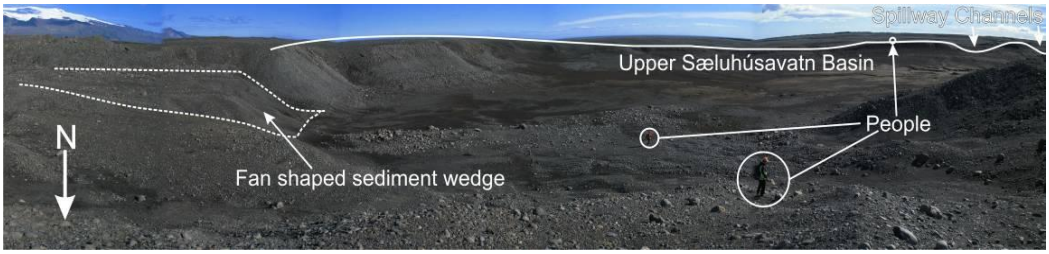

Photo-mosaic of the Upper Sæluhúsavatn Basin, highlighting the fan shaped sediment wedge on the east of the basin and the spillway channel on the west.

4.2.3.2 Lower Sæluhúsavatn basin

The Lower Sæluhúsavatn basin is located at the north of the Sæluhúsavatn site and is in direct contact with the glacier margin. The southern edge of the lower basin is defined by the ridge which makes up the northern

edge of the upper basin. Its eastern edge is defined by a tall ridge composed of sand and gravel deposits which is approximately 30 m higher than the bottom of the basin. There is a breach in this ridge running east to west, and from this breach, a large fan shaped wedge has been deposited within the lower basin. The walls of this lower basin are covered with numerous perfectly horizontal lines, etched into the unconsolidated sediments. The western edge of the lower basin rises steeply to the flat, outwash surface to the west, except where there is a large channel rising from the southwest corner of the basin.

Figure 4-7

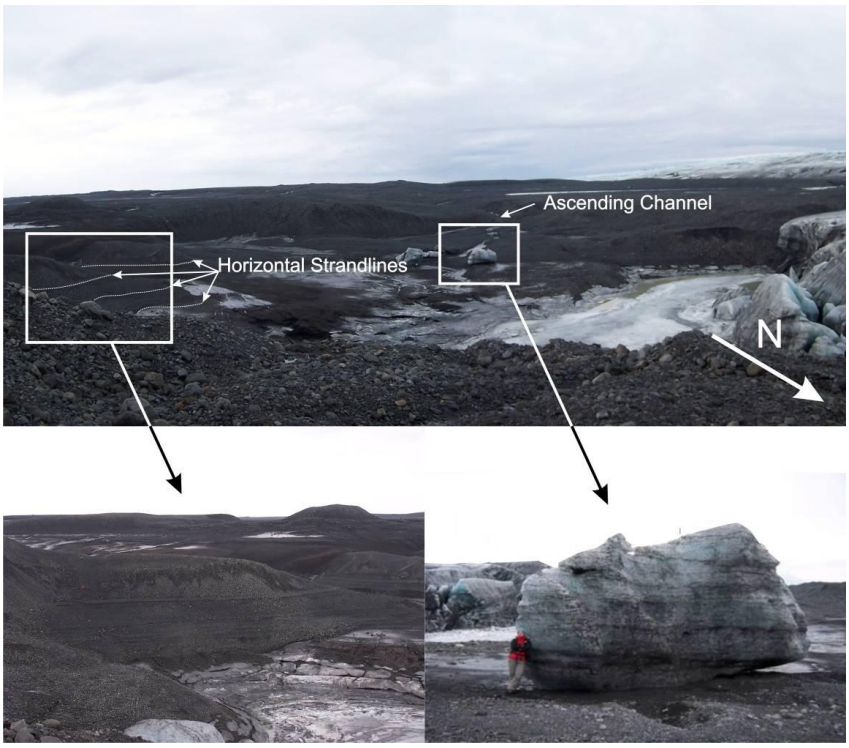

Photo-mosaic of the Lower Sæluhúsavatn Basin. Note the location of an ascending channel rising from the southwest and the presence of horizontal strandlines on the southern rim. Stranded ice block and person for scale. Photographs: A. R. Gregory and Prof A. J. Russell.

4.2.3.3 Lower 'ridge enclosed' basin

The lower, 'ridge enclosed basin' is located to the east of the lower Sæluhúsavatn basin, through the breach in the tall gravel ridge. This basin is enclosed on all sides by tall gravel ridges, except where breaching of the ridges has taken place. The breach in the eastern basin wall in associated with a large,

fan shaped wedge of sediment, which radiated outwards from the breach towards the centre of the basin (**Figure 4-8 - I**). The southern basin edge is composed of loose, slumped sand and gravel that contains numerous kettle holes (**Figure 4-8 - II**). These kettle holes were not visible during the early stages of fieldwork, but formed over night during the summer of 2006 when the water level in the basins began to rise.

The basin bottom is very uneven, and is composed of very well sorted, fine sand and silt. These sediments had be deposited on top of stagnating glacier ice (**Figure 4-8 - III**).

Figure 4-8

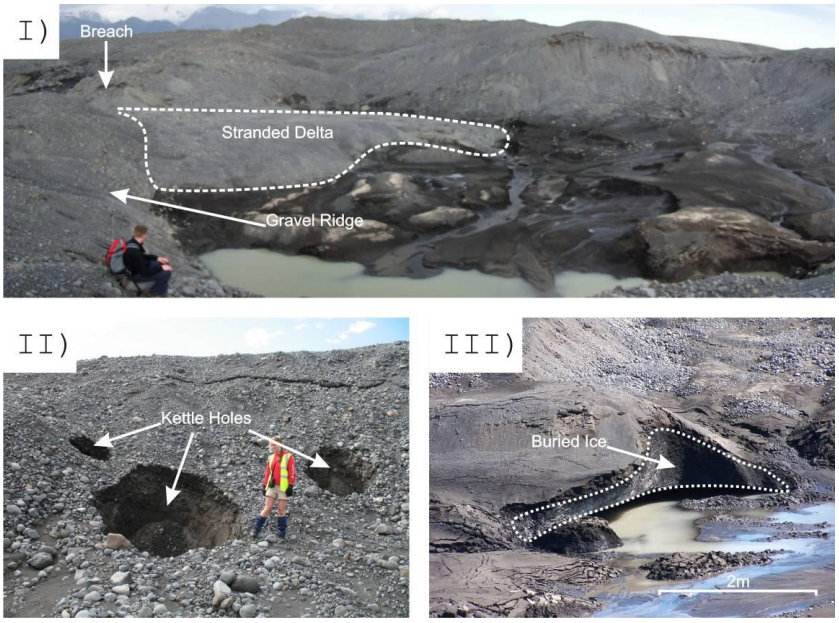

I) Photo-mosaic of the 'ridge enclosed basin'. Note the location of the breach in the ridge wall and the perched delta emerging from the gap. Also note the accumulation of fine silty sand in the bottom of the basin II) Kettle holes formed in the southern wall of the basin. III) Buried ice beneath silty sand in the bottom of the 'ridge enclosed basin'.

4.2.3.4 Deep proglacial channel and alluvial fan

As briefly mentioned above, in the southwest corner of the Lower Sæluhúsavatn Basin, there is a large, 30 m wide channel that transects the basin wall joining with the proglacial surface above (**Figure 4-9 - I**). This channel rises approximately 11 m, over a distance of 160 m, terminating at the head of a

proglacial outwash fan. This outwash fan radiates from the head of this ascending channel. The head of the outwash fan has been incised to a depth of approximately 4 m, to an older surface below, indicating that the fan is approximately 4 m deep at its head. The fan itself is composed from coarse sand and gravel material and the surface is covered with numerous rip-up clasts of unconsolidated sands, gravels, and diamictons (**Figure 4-9 - II**).

Figure 4-9

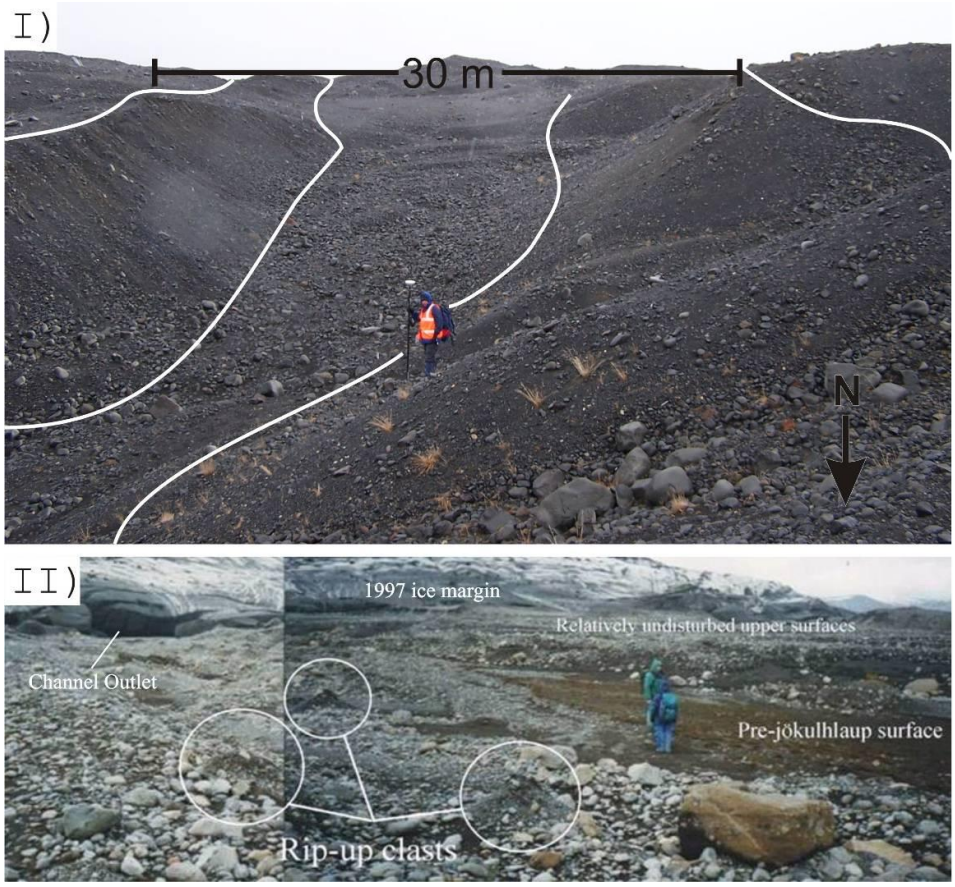

I) Photograph of the ascending channel rising out of the lower Sæluhúsavatn Basin. II) Photograph of the outwash fan surface take shortly after the 1996 jökulhlaup; note the numerous rip-up clasts on the fan surface. Photograph: Prof A. J. Russell.

4.3 SEDIMENTOLOGY OF THE EASTERN SÆLUHÚSAVATN AREA

Interpret sediment landform assemblages in the Eastern Sæluhúsavatn Overdeepening, a number of sedimentary excavations and sections were investigated. The locations of these exposures are shown in **Figure** 4-10.

4.3.1 SÆLUHÚSAVATN SANDUR SURFACE EXCAVATIONS

Two 1.5 m deep pits were excavated into the sandur surface, south of the Sæluhúsavatn Overdeepening. Excavation 1 pit was located approximately 100 m south of the upper Sæluhúsavatn basin edge at UTM coordinate 396295E 7099211N. Excavation 2 was located approximately 220 m south of the upper Sæluhúsavatn basin edge at UTM coordinate 396388E 7099085N (**Figure** 4-10). Descriptions and graphic logs of each of these excavations are presented below. By investigating the sediments that make up this part of the glacier foreland, it is possible to gain an understanding of the nature of sediments in which the over deepenings were formed and test hypothesise associated with flow expansion. In such cases, it would be expected to see a fining of sediments away from the overdeepening.

Figure 4-10

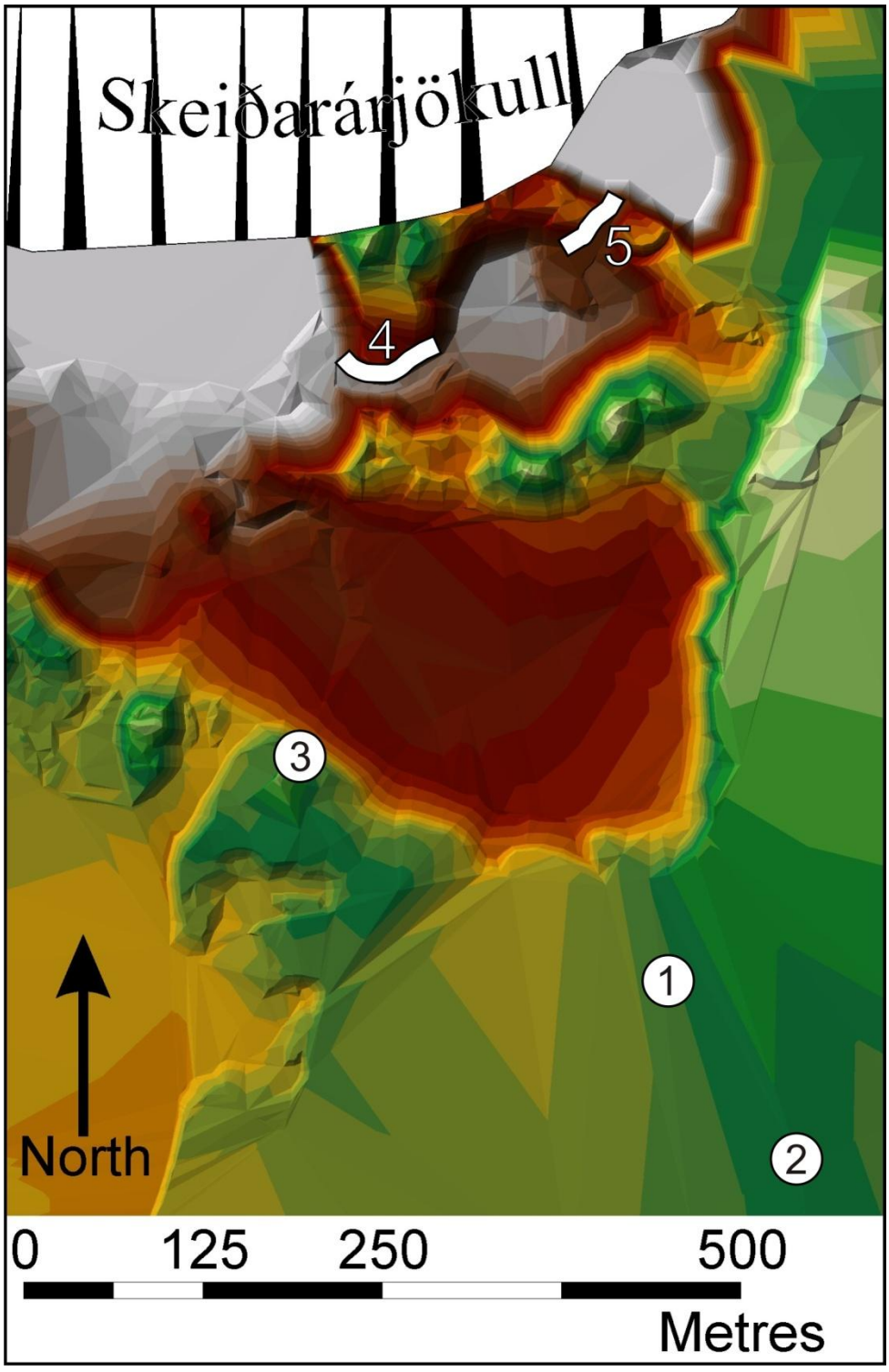

Terrain model showing the locations of sedimentary excavations and sections at the Eastern Sæluhúsavatn field site.

4.3.2 SECTION I

This 1.5 m deep excavation into the sandur surface shows four distinctive sedimentary units. The lowest unit in this excavation (Unit D), from 1.50 m to 1.25 m, consists of moderately sorted massive course sand to granules with 2 – 5% well rounded pebbles, up to 80 mm a-axis. The lack of fines within this unit is evident from the loose nature of the material and its tendency to collapse. Laboratory analysis of samples taken from this unit show that it is a bimodal, very poorly sorted, sandy coarse gravel, with a platykurtic kurtosis. This unit gradually grades into unit C above.

Unit C consists of moderately sorted beds of fine to course sand, inter bedded with seven beds of silt sized material (**Figure 4-13 - III**) from 1.25m to 0.6m. These sand and silt beds are 20 mm thick at maximum, however all silt beds have multiple lamina finer than 1 mm. Grading within sand beds (where visible) appears to be inverse. Laboratory analyses of samples taken from this sand show that they are unimodal, poorly sorted, slightly gravelly sand, with a mesokurtic kurtosis. All beds within this unit appear heavily deformed (**Figure 4-13 - III**). At 0.6m, the sands rapidly grade into the coarse sand matrix of unit B above (**Figure 4-13 - II**).

Unit B (0.6 – 0.36m) consists of massive, poorly sorted predominantly clast supported, rounded to sub-rounded cobble clasts up to 140 mm a-axis (**Figure *4-14***). The clasts are surrounded, but not supported by a poorly sorted, coarse sand matrix (**Figure 4-13 I and II**). Laboratory grainsize analysis shows that it is a unimodal, very poorly sorted, sandy, very coarse gravel, with a platykurtic kurtosis (**Figure 4-12**). Clast shape analysis presented in (**Figure *4-14*),** shows a significant cluster of clasts around the compact platy/bladed/elongated categories, with a small number of clasts falling into the bladed category. These two upper units could be considered as a single unit

showing coarse tail grading; however the abrupt change in clast size at 360 mm depth and the massive nature of the units above and below this threshold demonstrate that this is not the case. Clast fabric analysis of clasts held within unit B show a statistical A-axis preferential alignment through the plane 350°-170°; however, as can be seen from **Figure 4-11,** there is a wide degree of variance (51°). Eigen vales are presented on **Figure 4-11,** have been plotted on a fabric shape tri-plot and are shown to be slightly isotropic. Thus this fabric is considered weak. The contact between units B and A at 0.36m has an amalgamated nature, showing a sudden reduction in the size and concentration of clasts in unit B while the nature of the matrix remains constant (**Figure 4-13 - I**).

Unit A from 0.36m to 0.05m is a massive unit contains 5 – 10% well rounded to sub-angular small cobbles, supported by a moderately well sorted sandy matrix (**Figure 4-11**). Laboratory grainsize analysis shows that it is a very poorly sorted, bimodal, medium gravelly fine sand with a mesokurtic kurtosis (**Figure 4-12**).

The upper 50 mm consists of a poorly sorted unit predominantly composed of well-rounded large pebbles (30 – 40 mm b-axis). The unit is clast supported and has a matrix of well-sorted fine sand.

Figure 4-11

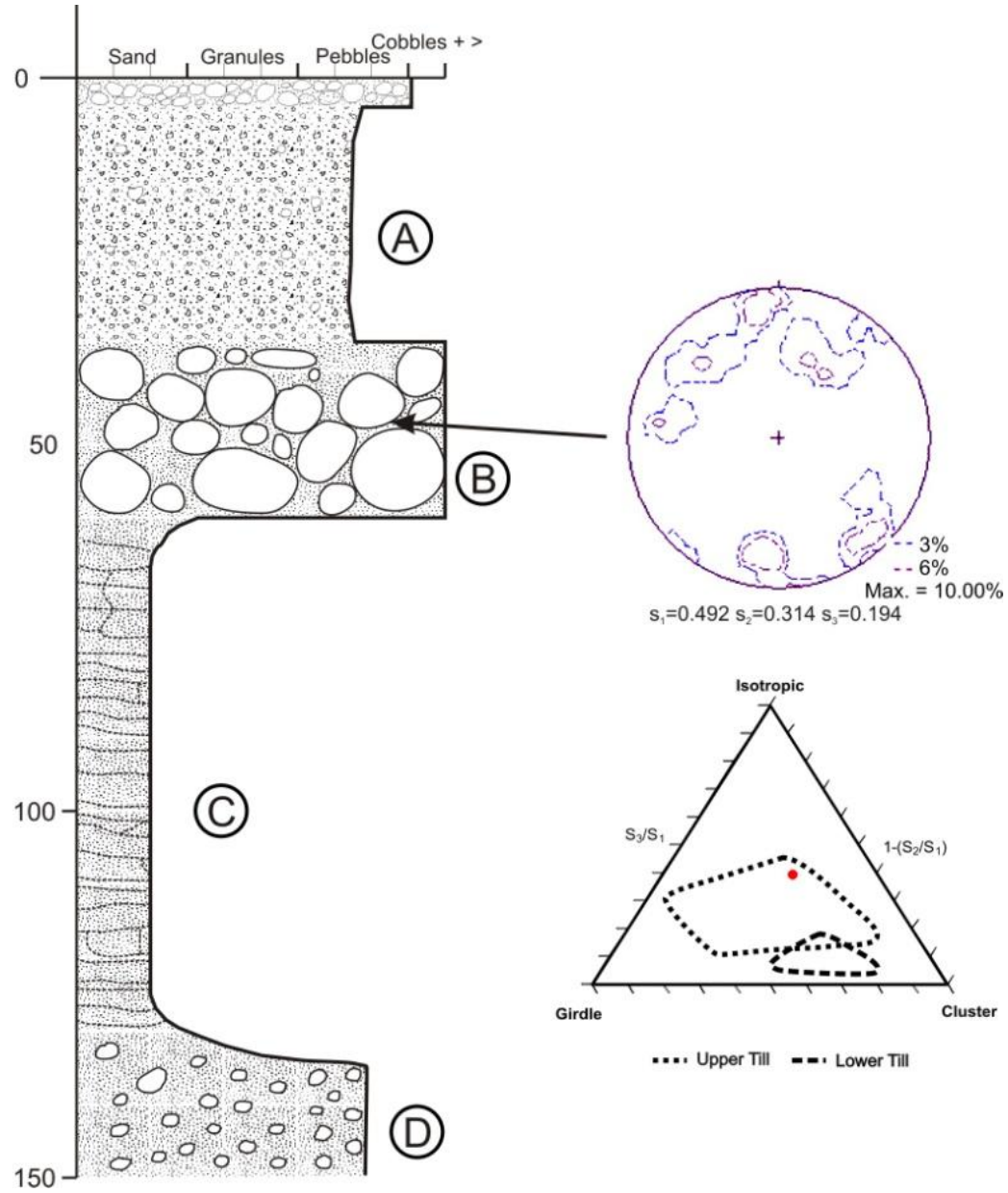

Graphic log of sedimentary sequence found at the Sæluhúsavatn sandur surface, north excavation showing four primary units consisting of (A) Massive poorly sorted sand, (B) Massive, clast supported cobbles, (C) Deformed, moderately sorted beds of fine to course sand, inter bedded with laminated silt beds and (D) Massive course sand with matrix supported well rounded pebbles. Lower Hemisphere Projection shows A-axis clast fabrics of clasts held within unit B.

Figure 4-12

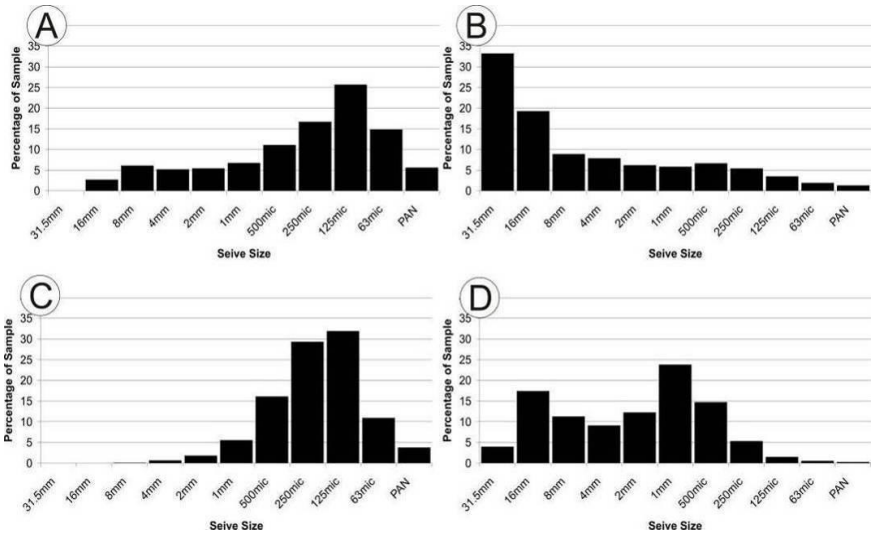

Grainsize distribution histograms of bulk sediment samples taken from the Sæluhúsavatn sandur surface north excavation.

Figure 4-13

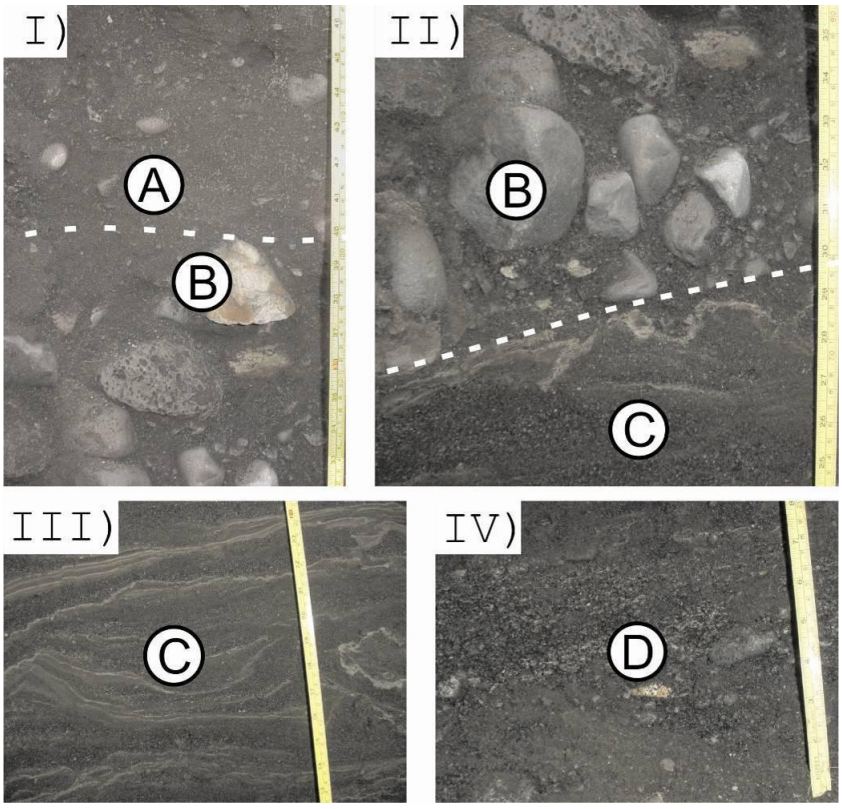

I) Photograph illustrating the nature of contact between units A and B. II) Photograph illustrating the nature of contact between units B and C. III) Photograph illustrating the nature of deformation within unit C. IV) Photograph illustrating the coarse granular texture of unit D.

Figure 4-14

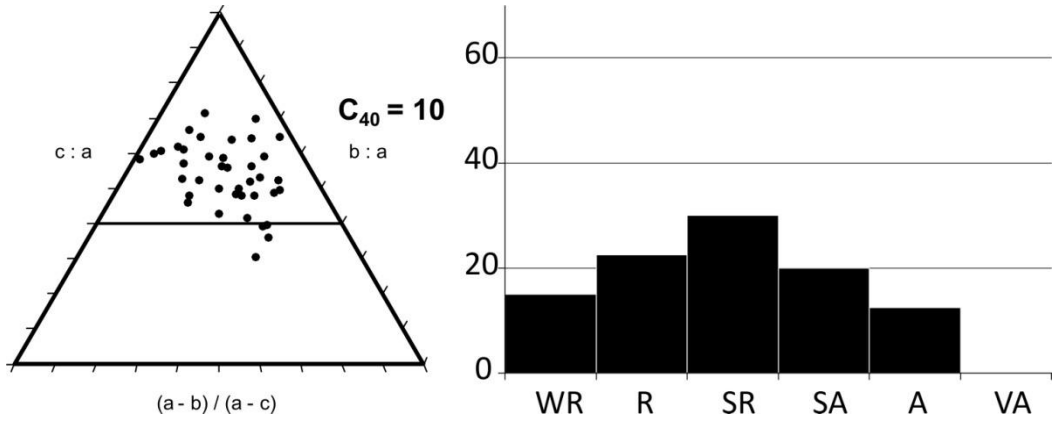

Clast shape tri-plot and clast roundness percentage frequency bar chart for clasts originating within unit B of the Sæluhúsavatn sandur surface north excavation.

4.3.3 SECTION I: INTERPRETATION

The rounded nature of clasts within Unit D is consistent with fluvial transport. However, the bimodal nature of the sediments may suggest a more complex process of deposition. Based on the grainsize distribution, sediment texture and clast size, this unit is interpreted as having been deposited in a relatively high energy, turbulent sub-aqueous environment where flow separation has resulted in the removal of fines in a similar manor to sub-aqueous debris flows.

The sediments that make up Unit C are considered typical of those deposited within a very low energy sub-aqueous environment (Smith 1978). It is considered likely that these materials were deposited within a relatively shallow lake which was likely fed by an ephemeral meltwater stream (Smith 1978). It is proposed that the coarser sand beds were deposited during a period or periods of active water input into the lake, and that the fine silty beds were deposited during times periods when water inputs had ceased or were at a minimum. It is possible that such low energy periods could coincide with winter cold periods where low flows and ice cover allow the settling of fine sediments. This

hypothesis cannot be confirmed or rejected based on the available data and thus the term *varve* has not been used to describe these bedded sediments.

The deformation of the bedded sediments described above is interesting. Due to the lack of deformation around individual cobbles, it is considered unlikely that this deformation occurred following the deposition of the large cobbles above. There are two possible scenarios that could have resulted in this deformation. First, it is possible that this deformation is a result of an advance in the position of the ice margin following deposition. Such an advance could result in significant loading to occur on top of the sediments from above, resulting in liquefaction of saturated sediments and deformation of the beds as has been seen at many glacier margins in Spitsbergen, Sweden and the UK (Boulton & Caban, 1995). Alternatively, the deformation could have resulted from variations in density between the upper and lower sediments, caused by variation in water content, resulting in a process referred to by Rijsdijk (2001) as '*density driven deformation*'. Considering the lack of any till formation, or evidence of glaciotectonic landforms, the deformation having formed as a result of ice margin overriding is considered unlikely.

The large proportion of rounded clasts (70%) and the predominantly compact shape of the cobbles within Unit B suggest deposition within a high energy turbulent fluvial environment. This is further supported by clast fabric analysis which presents a very weak pattern of alignment, indicative of a very rapid and chaotic period of deposition, where clasts have not been able to become arranged in any significant alignment (Collinson et al. 2006) and, like above, deposition has been en masse.

The bi-modal nature of the sediments that make up Unit A, with the presence of well rounded clasts, is typical of relatively high energy fluvial deposition, with the rounding of clasts typical of abrasion within a fluvial

setting. However, the lack of structure within the deposit suggests that these sediments were deposited en masse, which is typical of rapid deposition from turbulent, high energy flows (Carrivick et al. 2004). It is likely that these sediments are the product of turbulent flows during one of Skeiðarárjökull's historic jökulhlaups.

The upper 50 mm of this unit are typical of a winnowed rock armour surface. This is the result of aeolian removal of fines from the top part of the upper most sedimentary unit. This process results in the gradual increase in the average grainsize found on the sandur surface, until the grainsize increases to a point where further sediment removal by wind cannot occur *(Summerfield 1991)*.

A model for the formation of this sedimentary sequence is presented in **Figure 4-15**. This shows the transition from deep water deltaic deposition and removal of fine sediments within sub-aqueous debris flows to shallow water deposition and the formation of bedded sands and inter-bedded silts and clays. Following this low energy deposition, the rapid deposition of high energy fluvial deposits results in aggradation of the sandur surface and deformation of the underlying soft sediments. The final stage in the evolution of this upper sandur surface is the advance of the glacier margin, resulting in the streamlining of the upper surface. Considering the lack of any till or evidence of glacitectonics, it is considered likely that this ice advance was short lived.

Figure 4-15

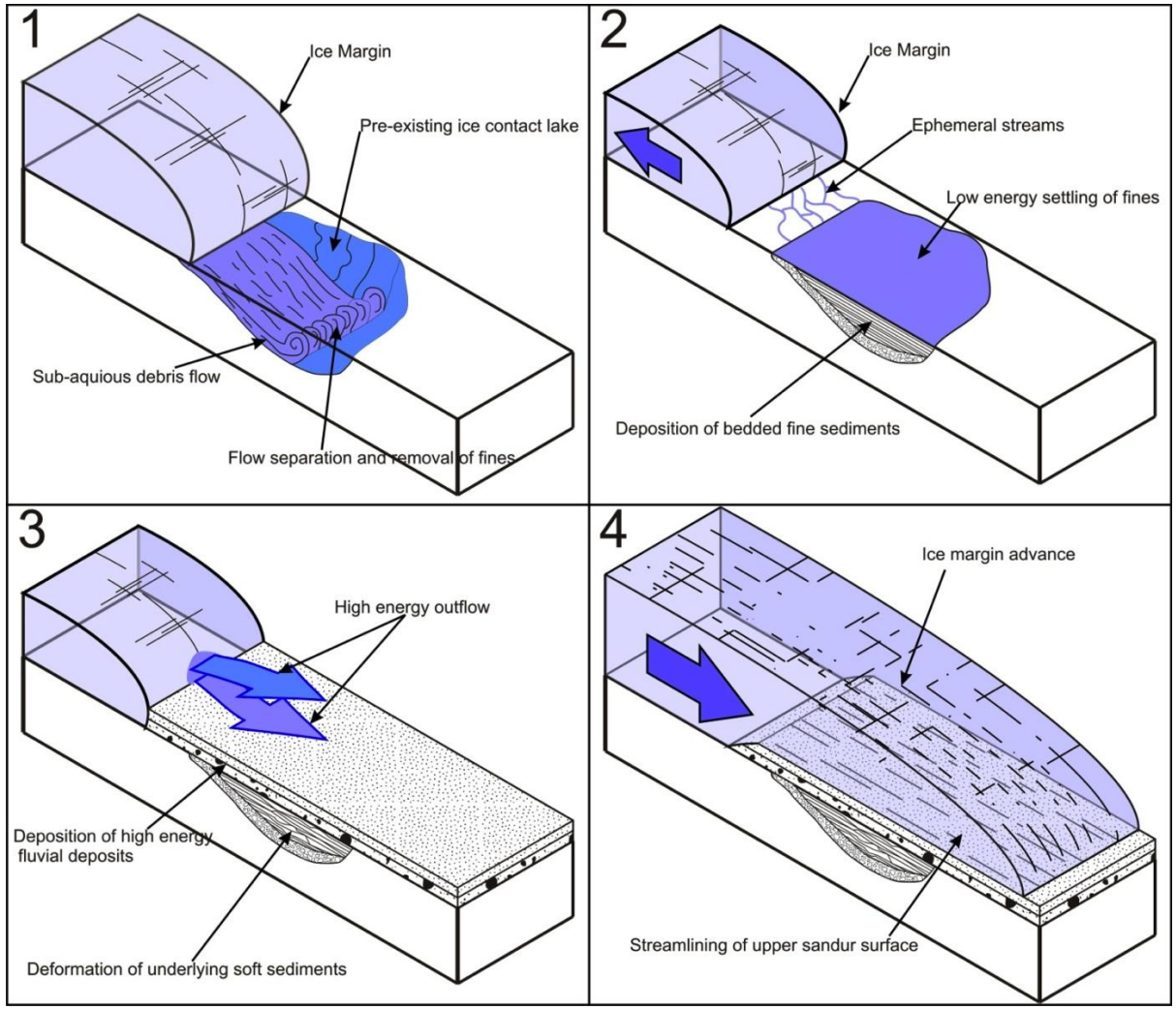

Conceptual model illustrating the processes and sequence of events leading to the deposition of sediments found within the Eastern Sæluhúsavatn northern sandur surface excavation.

4.3.4 SECTION 2

This 1.45m deep pit excavated in the upper surface of Skeiðarársandur to the South of the Sæluhúsavatn Upper Basin exhibits four primary stratagraphic units (Figure 4-16). Unit D at the bottom of the excavation, consists of well-rounded cobbles (>100 mm A-axis) within a well-sorted, open framework granule matrix, which itself is sub- to well-rounded (**Figure 4-17 and Figure 4-18 - III**). Laboratory grainsize analysis shows that unit D consists of unimodal, poorly sorted medium gravel with a leptokurtic kurtosis. The relative lack of sand and fines make this unit especially difficult to excavate due to the lack of cohesion between grains resulting in frequent collapse. At 1.2m depth, Unit D grades into unit C above, with a marked increase in clast size and increase in fines within the matrix.

Unit C consists of massive, clast supported, well rounded, cobbles and boulders, mostly 100 mm A-Axis but reaching 300 mm in places. The bottom of the unit has a well-sorted, medium sand matrix below 0.85 m which grades into an open framework in the upper 0.15m of the unit. In a number of places, unit C contains laminated silty intra-clasts containing woody splinters and small rounded pebbles (**Figure 4-18 - II**)

The open framework of Unit C is overlain at 0.85m depth by Unit B which consists of 40% massive sub- to well-rounded pebbles and cobbles (> 100 mm A-axis), supported by poorly sorted, coarse sand / fine gravel matrix with significant quantities of silt and clay. Due to the very large grainsizes incorporated within this sample, laboratory grainsize analysis was not attempted because of the logistical difficulties in collecting sufficiently large enough samples for representative analysis (Gale and Hoare 1991; Evans and Benn 2004) although the matrix of unit B has a visual texture similar to that of unit A above. At 0.58m depth, the contact between Unit B and Unit A below is

marked by a distinctive decrease in grainsize of both clasts and matrix (**Figure 4-18 - III**).

Unit A consists of very poorly sorted, muddy, sandy, gravel, containing sub- to well-rounded pebbles. The percentage of clasts (by area) does not exceed 10%, but decreases with elevation, showing evidence of coarse tail grading. Laboratory grainsize analysis of these sediments show that it is a trimodal, very poorly sorted, muddy, sandy, gravel, with a platykurtic kurtosis (**Figure 4-17 - A**).

Identical to the north excavation, the sequence revealed at this site is topped by a thin (20 – 50 mm) layer of clast supported rounded pebbles, approximately one to two clasts thick surrounded by a well sorted fine sandy matrix.

Figure 4-16

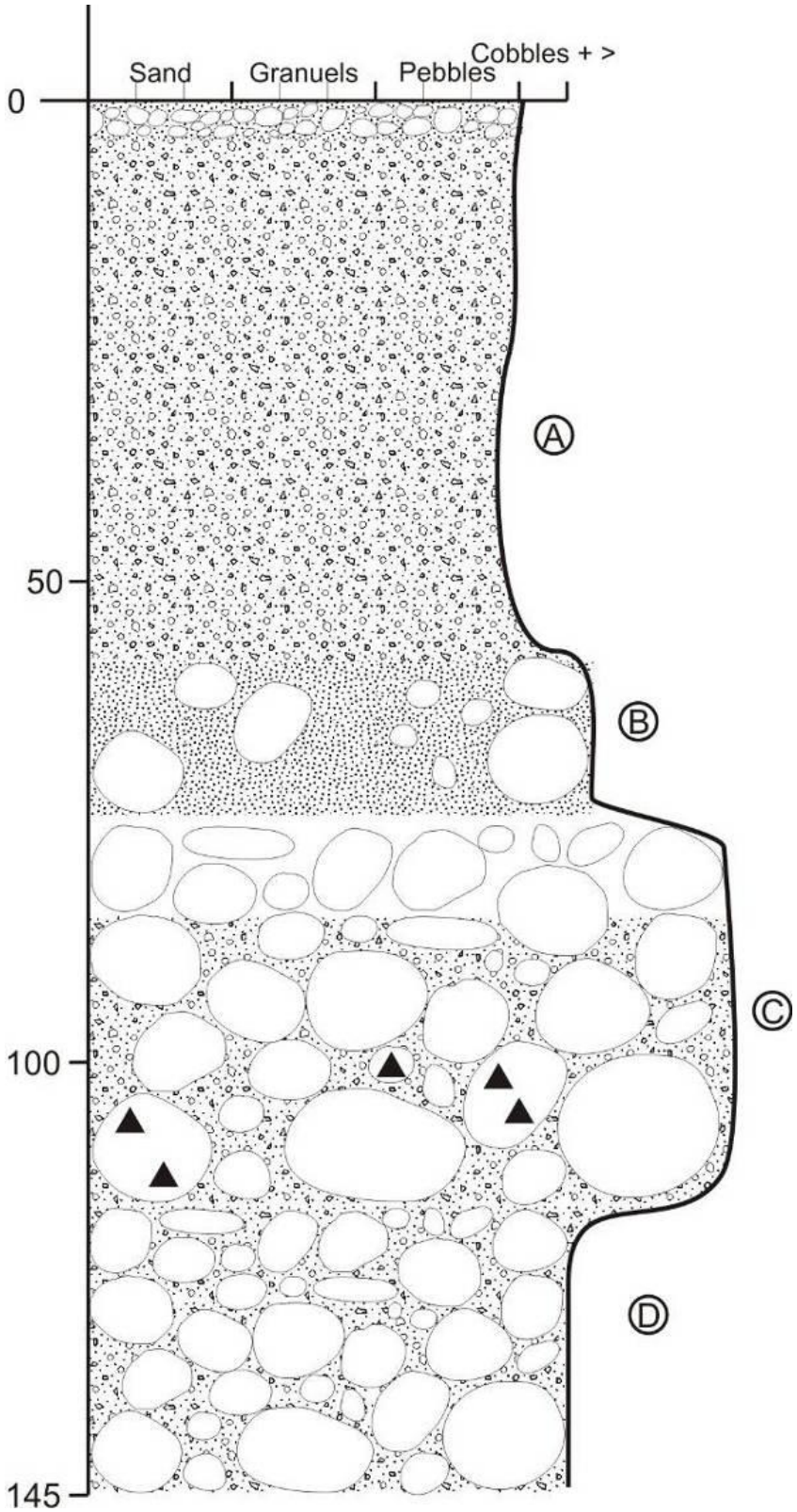

Graphic log of sedimentary sequence found at the Sæluhúsavatn sandur surface, south excavation showing four primary units consisting of (A) Massive very poorly sorted muddy sandy gravel (B) Massive, matrix supported cobbles, (C) Clast supported cobbled and boulders (D) Massive cobbles within an open framework granule matrix.

Figure 4-17

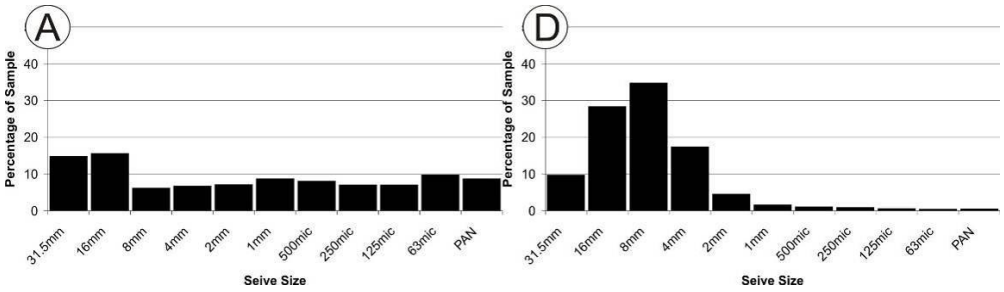

Grainsize distribution histograms of bulk sediment samples taken from the Sæluhúsavatn sandur surface south excavation. Sample 020806 – c is taken from unit a, sample 020806 – a is taken from unit D

Figure 4-18

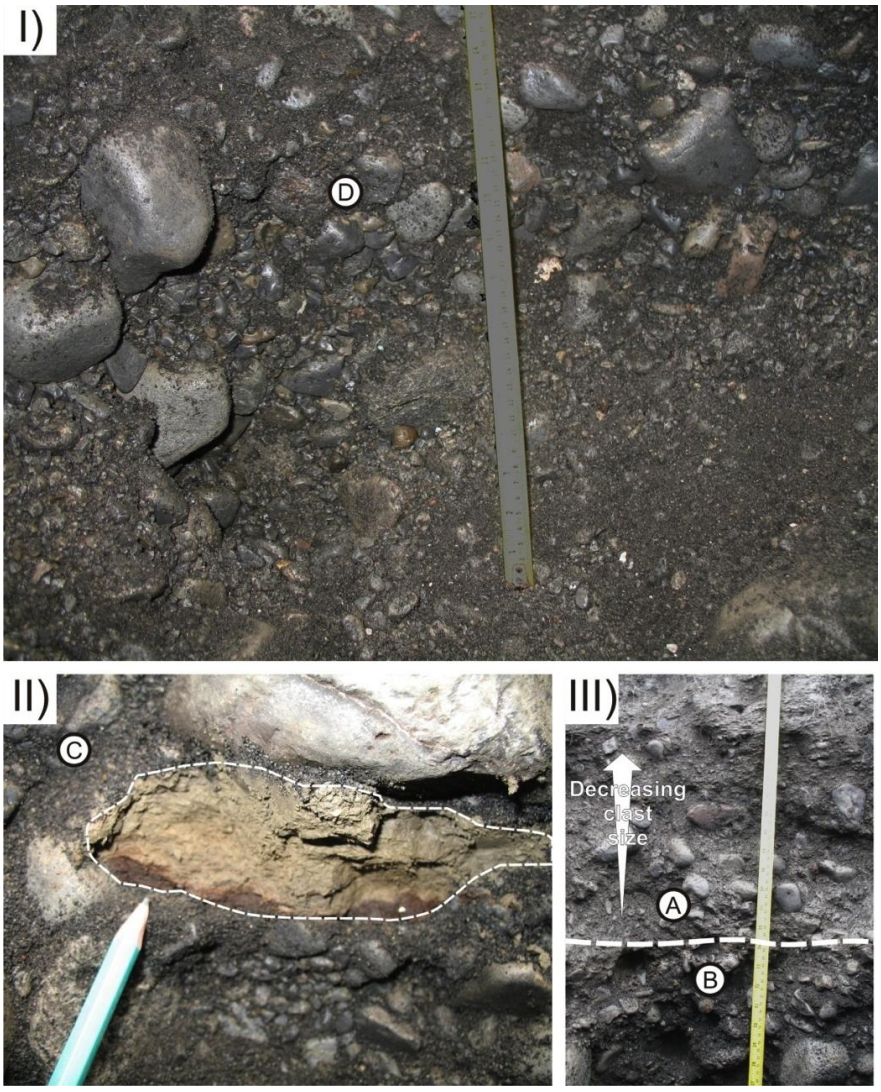

i) Photograph illustrating the incohesive, open framework texture of Unit D. ii) Photograph showing silty intra-clast within unit C. iii) Photograph illustrating the nature of contact between units A and B and decreasing clast size with elevation in unit A.

4.3.5 SECTION 2: INTERPRETATION

Units D and C at the bottom of this exposure are typical of high energy, possibly hyperconcentrated deposits, based on their open framework texture (Russell and Knudsen 1999), massive structure (Carrivick et al. 2004) and inclusion of intraclasts (Duller et al. 2008). Unit D is likely to be the product of high energy, upper flow regime, hyperconcentrated flows which has lead to the formation of open framework gravels with large cobble inclusions (Russell and Arnott 2003). As flow energies reduced, we see a rapid transition into Unit C above, with the deposition of very well rounded cobbles and finer matrix material. Based on this interpretation, these sediments are likely to have been deposited during one of Skeiðarárjökull's many historic outburst floods (jökulhlaups).

Unit B contains many large rounded clasts similar to those seen in Unit C below; however its matrix is more cohesive, containing a greater quantity of fine silts and clays, similar to the matrix of Unit A above. The amalgamation of these two units suggest that Unit B has formed in a similar manner to sediments at Skalafellsjökull described by Evans (2000). Evans (2000) concludes that tills overlying sands and gravels at Skalafellsjökull formed by the deformation of subglacial tills over outwash materials, resulted in the 'cannibalisation' of the underlying sediments into the overlying tills. This process resulted in characteristics of the underlying sediments becoming incorporated into the overlying till, including deformed sand and silt lenses, resulting in a continuum referred to as the 'shear amalgamation zone'. The absence of such structures at Skeiðarárjökull is likely a result of the nature of the massive, underlying fluvial deposits, which provides little structure to record the process of deformation. None the less, the clear continuum from Unit C to Unit A through Unit B allows this unit to be interpreted as an 'amalgamation zone'.

Unit B is therefore interpreted as a deformation till, formed by the amalgamation of the underlying fluvial sediments (Unit C) with the overriding subglacial tills.

The very poor sorting of Unit A, which contains almost equal portions of grainsizes from clay to cobbles (Figure 4-17) allows this unit to be described as a diamicton. Although clast fabric data is unavailable, observations of streamlining and fluting on the upper surface, visible on oblique aerial photography (Figure 4-1) provides evidence that the area has been over ridden by glacier ice (Shaw 1988; Benn 1994; Evans and Twigg 2002). Based on these simple observations, Unit A is interpreted as a sub-glacial till, which has been deposited atop of underlying glaciofluvial sediments, resulting in the entrainment of Unit C to form an amalgamation zone (Unit B) below the more uniform and massive Unit A. This is similar to the 'till melange' sequences described within the literature which can result in the formation of tills with distinct units of bedded sands or other intraclasts that have been entrained from the underlying sediments (Menzies, 1990, Hoffmanna & Piotrowski, 2001). In this case, the abundance of rounded clasts is interpreted as a consequence of the nature of the parent material from which the deposited materials were derived. Well rounded clast within diamictons are not uncommon in Iceland (Evans and Twigg 2002), and it is well documented that Skeiðarárjökull is likely to over lay a soft bed, comprising a large proportion of outburst flood deposits which are well rounded as a result of their former transport history. The fact that these clasts have retained their rounded exterior and have not been subject to any significant fracturing or faceting allows one to interpret this over riding as a relatively short duration and that these deposits have not been transported a significant distance. If the period of advance had been more sustained and the distance over which these sediments transported been greater, one would expect

abrasion and fracture to be more apparent and the number of sub-angular and angular clasts to have increased (Boulton 1978).

The upper 20 - 50 mm of this unit is interpreted as a rock armour lag that has been produced as a result of aeolian removal of fine grains at the sandur surface (Summerfield 1991). **Figure 4-19** presents a schematic model of the processes described above, designed to illustrate the sequence of processes, which lead to the formation of sediments found within the Sæluhúsavatn Sandur Surface South Excavation.

Figure 4-19

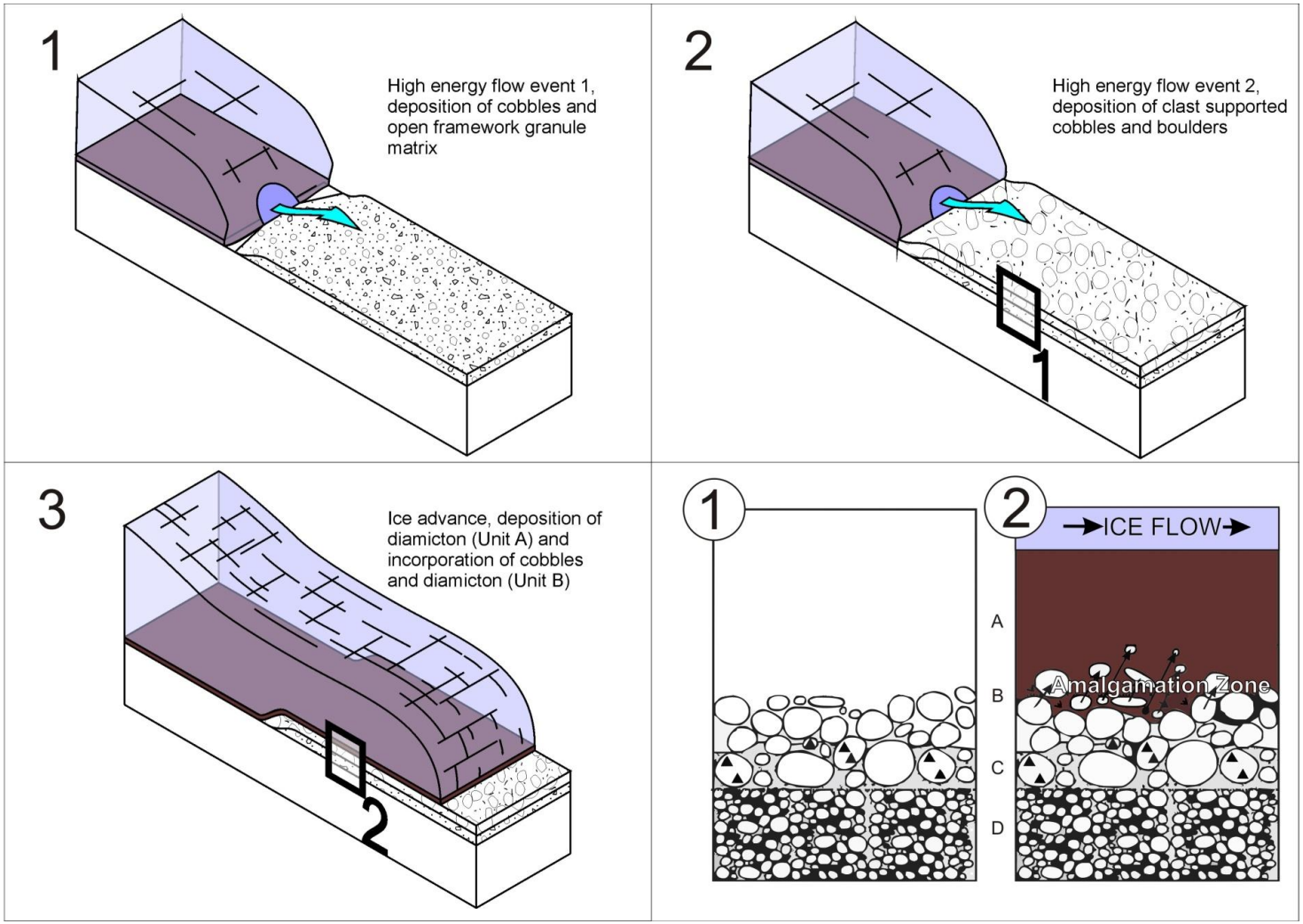

Conceptual model illustrating the processes and sequence of events leading to the deposition of sediments found within the Eastern Sæluhúsavatn southern sandur surface excavation.

4.3.6 SECTION 3

A 3.7 m deep, tiered section was excavated into the 4m high, concave, west wall of the upper Sæluhúsavatn basin, to investigate the nature of sediments in which this over deepening is formed. A scale 'panel' sketch of the excavation (Figure 4-20) was produced in order to accurately depict the sedimentary architecture, including a graphic log for the second unit. Clast fabric lower hemisphere stereo projections and a clast fabric shape tri-plot are also presented on Figure 4-20. Unit photographs are presented in Figure 4-21, grainsize distribution histograms are presented in Figure 4-22, while clast shape tri-plots and roundness histograms are presented in Figure 4-23.

The lowest exposed unit (Unit I) in the excavation is composed of inversely-graded matrix-supported, poorly sorted, sub- to well-rounded clasts. The matrix material grades from coarse sand at the bottom to granules at the upper contact, which has an arcuate form (Figure 4-21-I). This unit has a unimodal grainsize distribution, (Figure 4-22-I) with a fine skew and platykurtic kurtosis. Clast fabric is moderate, with a wide range in the orientation of clasts and Eigen values of S1=0.531, S2= 0.320, and S3= 0.149 (Figure 4-20). When these values are plotted on the clast fabric shape tri-plot of Benn (1994)they fall within the envelope for deformation tills at Breiðamerkurjökull (Benn 1994) (Figure 4-20). Clast shape data show a C40 index of 24%, with near even distribution of clasts within the middle of the Sneed and Folk Tri-plot. There are even quantities of sub-angular, sub- rounded and rounded clasts (Figure 4-23). The lower left hand side of this unit is dissected by a large silty-clay structure which forms a sand filled pipe, lined with clay at the bottom of the unit and which diverges into numerous silty tributaries towards the upper bounding surface of the unit (Figure 4-24).

Between 3.75 and 3.1m, above the arcuate contact, Unit H is composed of very poorly sorted pebbles and cobbles (150 – 200 mm a-axis) within a well sorted, fine sand matrix which exhibits some evidence of silty/clay lamina (**Figure *4-21*- I**). Both the lower arcuate contact and upper bounding surfaces are sharp, but not erosive. Grainsize analysis of a bulk sample taken from this unit (**Figure 4-22 - H**) show that this unit is bimodal, very poorly sorted, fine, silty, sandy, coarse gravel. Clast fabric analysis (**Figure 4-20**) from this unit shows the majority of clasts have A-axis dips towards the north, and Eigen values of S_1=0.549, S_2= 0.290, and S_3= 0.161. When these values are plotted on the clast fabric shape tri-plot they fall within the range of values seen for deformation tills at Breiðamerkurjökull (Benn 1994). Clast shape data show a C_{40} index of 25%, with near even distribution of clasts within the middle of the Sneed and Folk Tri-plot (**Figure 4-23-3**). Clast roundness is dominated by sub-angular to rounded clasts, with 10% well rounded clasts and a small portion of angular clasts.

Between 3.1 -2 m, the exposure displays a wide variation of sedimentary facies and structures. From 3.1 - 2.9m there is a massive unit consisting of 5% rounded clasts with a-axis approximately 20 – 30 mm, held within a coarse sand / granule matrix. The lower bounding surface of this unit is horizontal and sharp, but does not appear to be erosive. It is defined by clay, water escape structures. The upper bounding surface is again defined by a water escape structure, but in this case has an irregular, stepped form.

This unit is overlaid by an inversely graded unit of medium sand to gravel (D on **Figure 4-20**). Grainsize analysis from the middle of the unit shows a bi-modal grainsize distribution. Almost 70% of the unit consists of coarse sand, with an outlying 5% of silt and clay (**Figure 4-22 - D**). There is a small cluster of pebble sized clasts at 2.7 m depth on the left hand side of the exposure

(labelled F on **Figure 4-20** and **Figure 4-22 - F**). Unit D is dissected by, and its upper surface defined by, a number of silty-clay structures which appear to become confined towards the lower left hand side of the unit, and diverge upwards and towards the right.

Between 2.4 – 2m depth (labelled G on **Figure 4-20**), the unit consists of poorly sorted, sub-rounded to rounded cobbles up to 150 mm a-axis, within a moderately sorted, fine sand matrix (**Figure 4-22 - G** and **Figure *4-21* - IV**). Grainsize analysis (**Figure 4-22 - G**) revealed bimodal, very poorly sorted, sandy, coarse gravel. Cobbles within this unit make up approximately 50% by area. Analysis of clast fabric within this unit shows a cluster of a-axis dips orientated towards the northeast (**Figure 4-20**), with Eigen values of S_1=531, S_2= 397, and S_3= 072. When plotted on the fabric shape tri-plot, these fabrics lie close to the centre of the plot, within the area identified by Benn for Icelandic deformation tills. There is a wide range of clast shapes within the sample, although most are towards the compact corner of the tri-plot, and C40 = 34%. The sample is dominated by sub-angular to rounded clasts, with a small proportion of well rounded clasts (**Figure 4-23-2**). Above 2m lies a 1 m thick unit of bedded sand and fine gravel (**Figure 4-20**). Individual beds range from 1 mm (fine sand/silt) to 50 mm (fine gravel). The majority of this unit consists of sub-centimetre, planar beds of very fine sand, inter-bedded with thinner beds of very well sorted, open framework, fine gravel (approximately 1 mm). Occasionally, open framework fine gravel beds reach 25 - 30 mm thick, and fine sand beds up to 50 mm thick. Most beds of both fine sand and fine gravel in this lower most unit, are laterally discontinuous due to channel scour and fill structures (**Figure *4-21*- II**). Channel scour structures are filled primarily with well sorted, fine gravel, but in some instances, scours are filled with very fine sand or silt. Dimensions of these structures range from 10 – 30

mm deep and 50 – 150 mm wide. Laboratory analysis of sediments within the lower half of this bedded unit (**Figure 4-22 - C**) reveals unimodal, poorly sorted very fine gravelly coarse sand with a leptokurtic kurtosis. Above this lower unit, from 1 m – 1.25 m, there are a number of much thicker (>50 mm), well sorted, fine – medium gravel beds which are more laterally continuous. The thickest of these gravel beds is at 1.17 m, and contains a small number of outsized small pebble clasts with a unimodal, normal grainsize distribution (**Figure 4-22 - B**). Below the thickest gravel bed at 1.20 m, there is a 40 mm thick bed of inter-bedded very fine sand and silt, with beds approximately 1 – 2 mm thick. This is bound by a sharp lower contact to a bed of fine sand below. Its upper contact is gradational, grading up into a thin (10mm thick) bed of fine, open framework gravel. This unit contains no large or out-sized clasts. Laboratory grainsize analysis of the sandy beds shows that the sediments exhibit characteristics of leptokurtic, unimodal, poorly sorted, slightly gravelly, muddy sand.

Within this bedded sand unit, there is a very large silty clay-lined, clastic dyke or pipe structure. The structure has not been infilled with sediment and remains open as a vertical, cylindrical void in the exposure. This is visible on the surface as a thin (1 mm) thick vertical vein of silt. Upon excavation, this structure opens out into a vertical pipe at least 300 mm in diameter. The walls of this pipe are coated in a few millimetres of wet silt and clay. This dyke structure follows the plane of large normal fault which dissects this unit. This is evident from the large displacement of beds on either side of the structure (**Figure *4-21*- III**).

The uppermost one metre of this excavation is a massive, very poorly sorted sand and gravel, with a small proportion of finer particles (silts and clay). The matrix contains a large proportion of pebble sized (maximum a-axis 95 mm), sub-rounded to rounded, predominantly compact clasts many of which

showed evidence of facets or surface marks (**Figure 4-22 - A** and **Figure *4-21* –I, Figure 4-23-1**). Laboratory analysis shows this unit to be trimodal, very poorly sorted grainsize distribution, comprising sandy very coarse gravel, with a platykurtic kurtosis. Clast fabric analysis shows that a-axis orientations predominantly align along a north north/east – southwest orientation, Eigen values S_1=531, S_2= 397, and S_3=072 (**Figure 4-20**). The clast fabric shape is slightly girdled, although remains within the boundary for upper tills as defined by Dowdeswell and Sharp (1986).

Figure 4-20

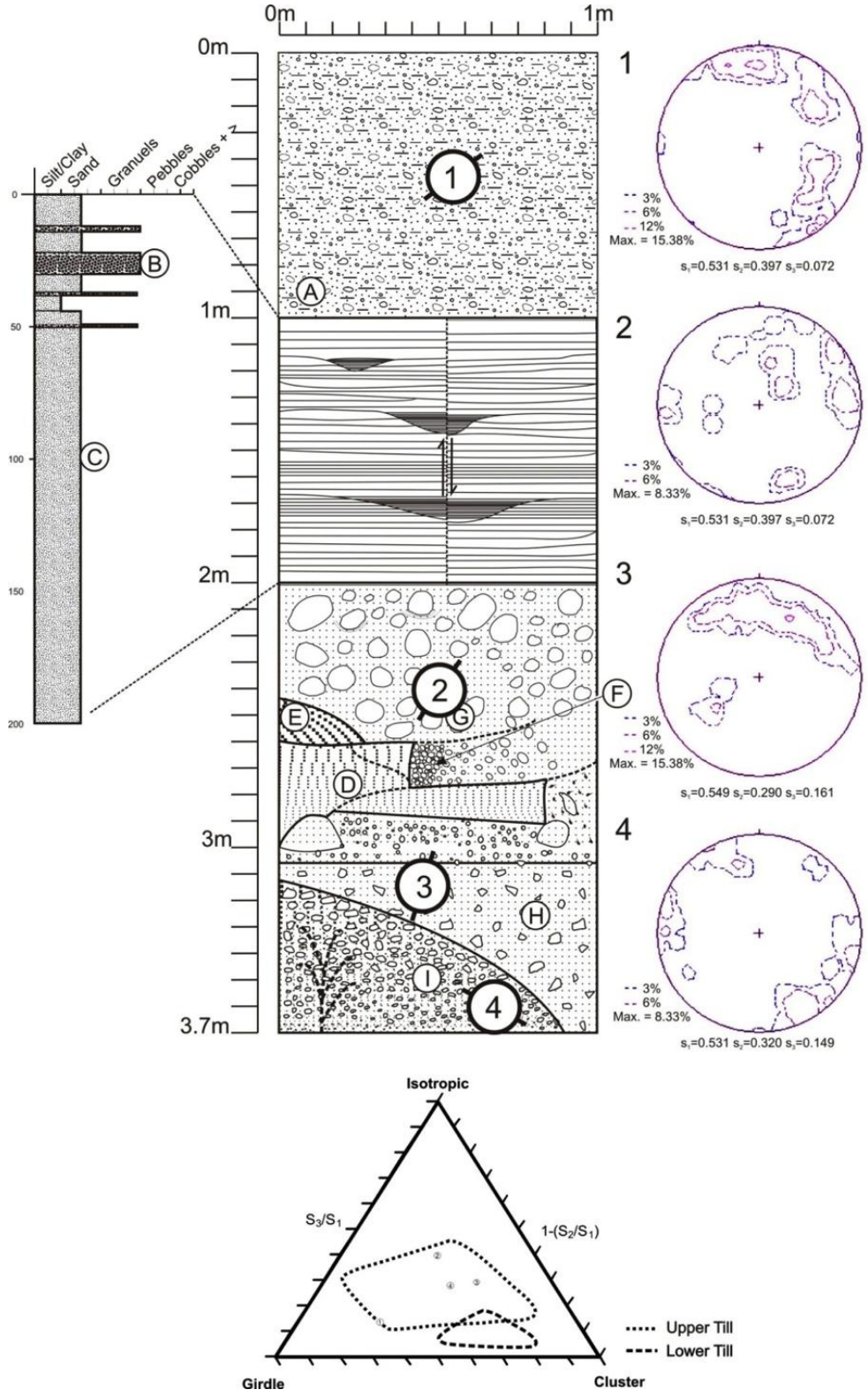

Panel sketch of the excavation into the Sæluhúsavatn upper basin west wall; including a graphic log for the second unit and clast fabric rose diagrams. Circled letters refer to bulk sediment samples taken for grainsize analysis. Black lines crossing the clast fabric lower hemisphere projections illustrate the orientation of the face of the exposure.

Figure 4-21

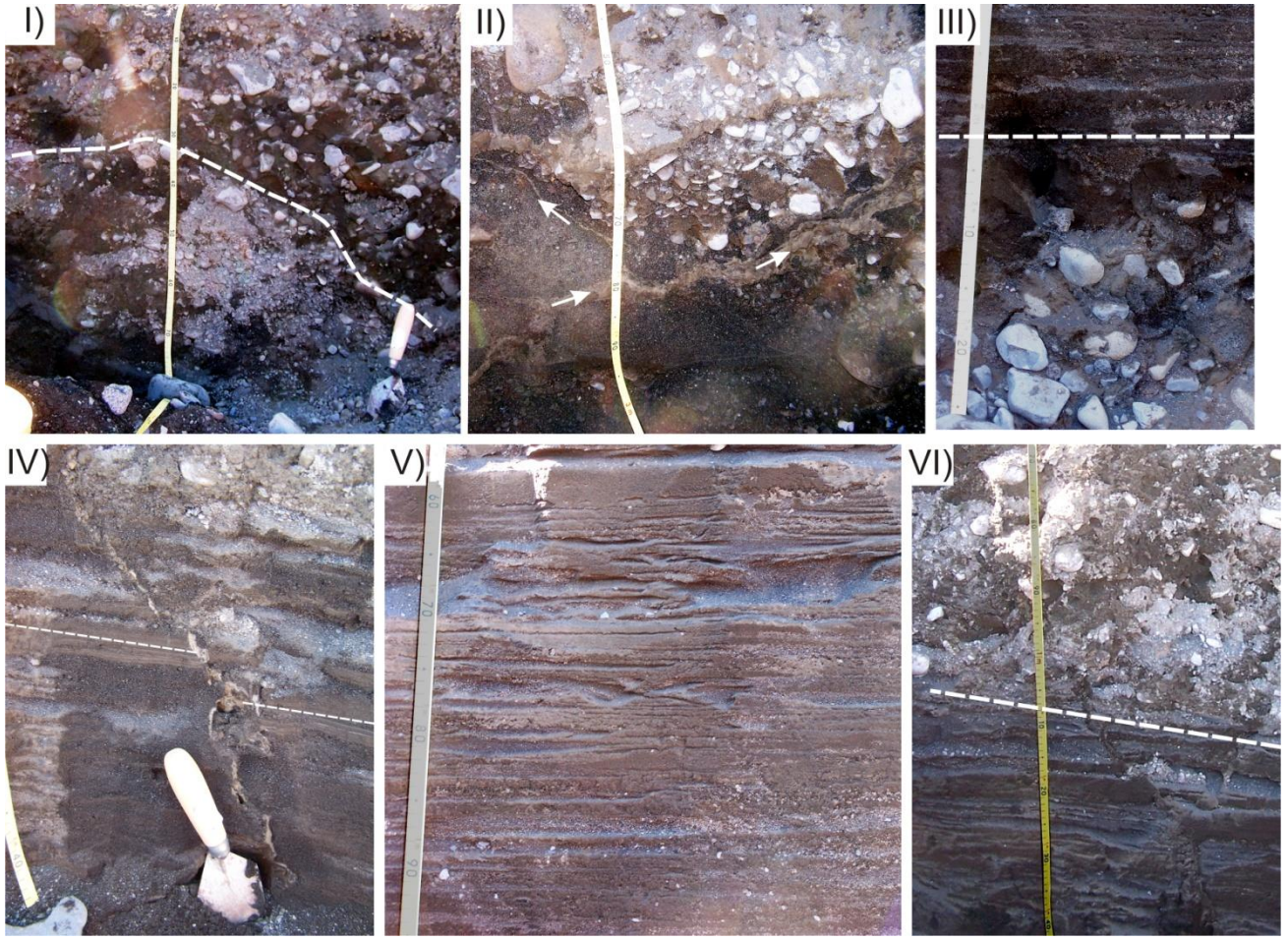

Photographs of sedimentary facies found at the Sæluhúsavatn upper basin west wall excavation. I) Contact between lower most two sand and gravel units, top right shows massive, poorly sorted pebbles – cobbles within well sorted fine sand matrix. Bottom right shows moderately sorted, inverse graded sand and gravel matrix with poorly sorted clasts throughout, II) Water escape structures within deformed sands and gravels; III) Lower contact of bedded sands with poorly sorted well rounded cobbles within fine sand matrix ; IV) Displaced beds either side of normal fault containing water escape structure within bedded sands ; V) Bedded fine sand with fine gravel scour and fill structures; VI) Sharp contact between upper diamicton unit and lower bedded fine sands.

Figure 4-22

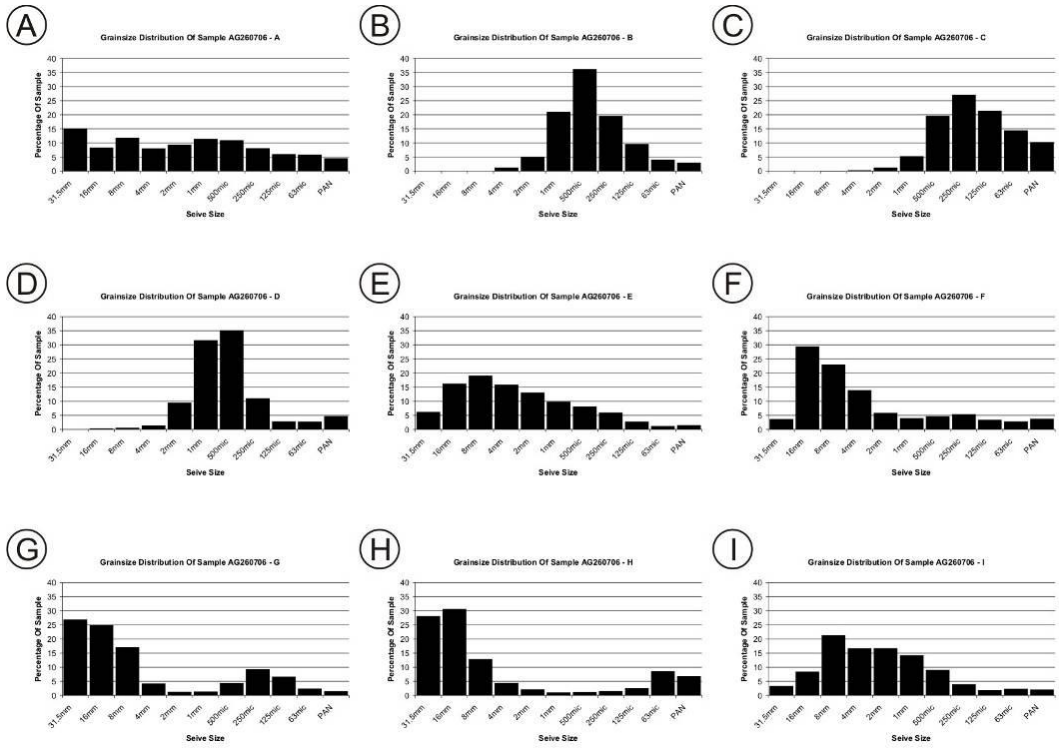

Grainsize distribution histograms of bulk sediment samples taken from the Sæluhúsavatn upper basin west wall excavation.

Figure 4-23

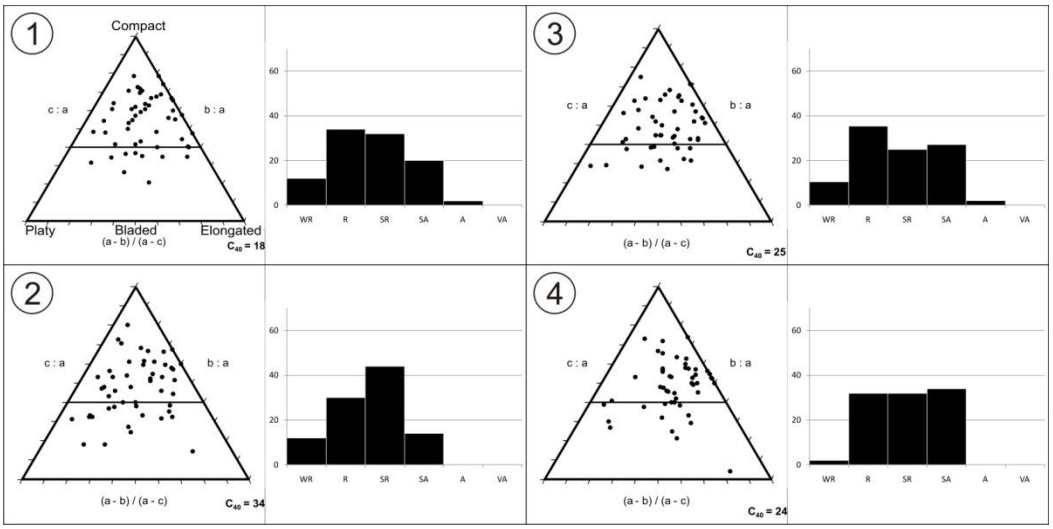

Sneed and folk clast shape Tri-Plots and percentage frequency roundness histograms for clast samples taken from the Sæluhúsavatn upper basin west wall excavation.

Figure 4-24

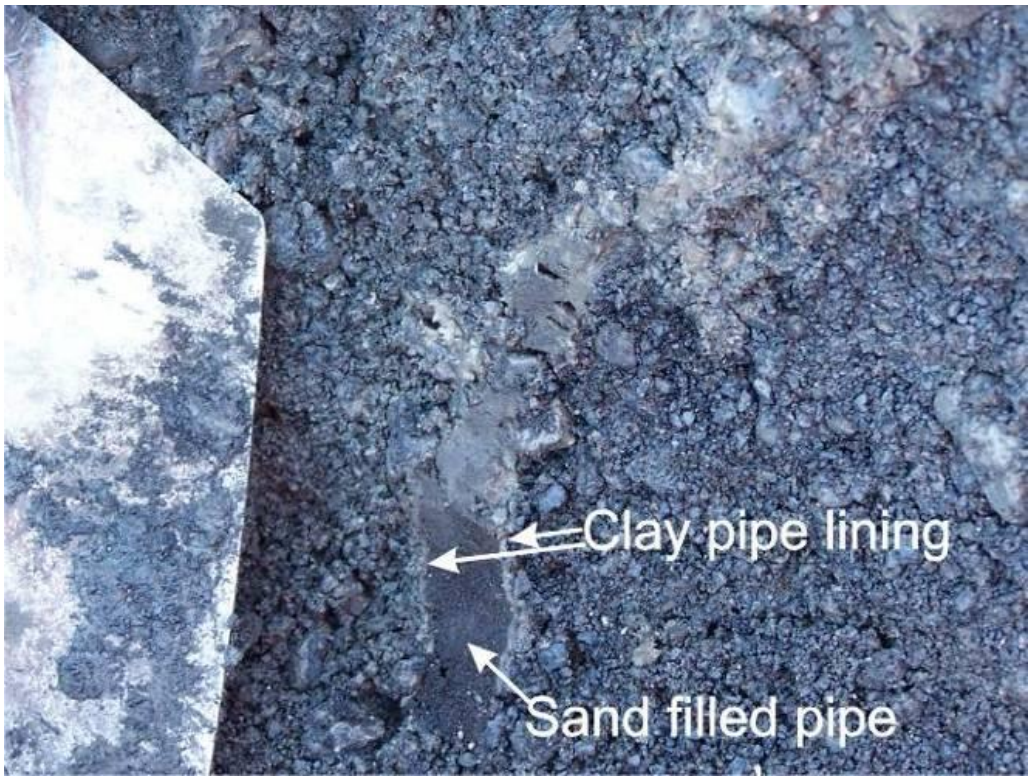

Photograph of a sand filled pipe in the bottom left of the upper basin, west wall exposure

4.3.7 SECTION 3: INTERPRETATION

This section provides a detailed interpretation of the sediments described in Section 4.3.6 above. The processes inferred from the interpretation are described and illustrated on the conceptual model presented in **Figure 4-25**.

The lowest sedimentary units in this excavation, from 3.7 m to 3 m are interpreted as relatively high-energy fluvial deposits. The inverse grading seen within this unit could be interpreted as a result of rising stage energy increase (Maizels 1993); however it is equally possible that this inverse grading is a result of deposition from hyperconcentrated flows (Duller et al. 2008). The relatively weak clast fabric at this location favours the interpretation of rapid deposition (Collinson et al. 2006).

From 3 – 2.4 m, the wide range of sedimentary facies located within such a limited space suggests that their deposition occurred as a result of slumping or

viscous flow. It is believed that higher energy processes such as fluvial activity or ice advance would have destroyed the subtle structures found within this unit of the exposure. This suit of facies are therefore interpreted as the result of low viscosity, saturated debris flow deposits, originating from the glacier margin (Dobracki and Krzyszkowski 1997). The saturated nature of the sediments also explains the formation of the numerous water escape structures that are observed within the units (Lowe 1975; Lowe 1976).

The poorly sorted, large, rounded cobbles with a sand matrix, found between 2.4 and 2m are typical of a number of depositional environments. Such bi-modal sediments have been observed in sub-aqueous environments, associated with delta forest and bottom set deposition. In such cases, bi-modality is a function of low energy setting of fine grained sands and the incorporation of larger cobbles which role down the delta foreset (Iseya and Ikeda 1987). However, the lack of bedding within the sand matrix, suggests that the sediments were deposited far more rapidly, as a result of turbulent flow (Russell et al. 2003). The lack of any significant clast fabric (**Figure 4-20**) also suggest rapid deposition from turbulent flow (Collinson et al. 2006). It is likely that this unit was deposited by a higher energy event that preceded the deposition of the low energy sands above.

Between 2.4 - 1m depth, the bedded sands and gravels are interpreted as low energy fluvial deposits, which have been emplaced as a result of small ice surface streams reworking ice proximal materials. The numerous channel scour and fill structures found within this unit are indicative of high rates of channel avulsion (Singh 1977). This is indicative of fluvial systems which experience rapid fluctuations in both discharge and sediment load over relatively short periods of time which is in contrast to the sediments that would be expected

from a well established glacier outlet portal, where discharges are much greater (Shaw 1988; Warburton 1990; Gurnell et al. 2000; Orwin and Smart 2004).

The large dyke or pipe structure which is devoid of a sedimentary infill, and runs through this bedded sand unit is interpreted as a water escape structure (Lowe 1975; van de Meer et al. 2009). The presence of a silty-clay contact between the pipe void and the host material in similar to other dykes found in Iceland such as those at Sólheimajökull (Le Heron and Etienne 2005). At Sólheimajökull, Le Heron and Etienne (2005) interpret a clastic dyke swarm as having formed by over pressurisation from the advancing glacier above, and deformation of sediments downwards into incipient fractures. However, in this case, the absence of any infilling sediments suggest that the period of increased pressure was minimal and short lived, resulting in dewatering of the underlying sediments. It is likely that this structure, and the smaller scale structures in the underlying sediments, formed during the glacier advance event which deposited the uppermost till unit (described below). Increased hydrostatic pressure resulting from the mass of ice above is believed to have forced this water out of the sediments immediately in front of the advancing ice margin (van de Meer et al. 2009). This hypothesis also explains why the propagation of water escape structures ends at the bounding surface between the bedded sand and the upper till. The presence of this structure provides confidence in the interpretation that the sediments below were deposited very rapidly, and remained saturated at the time when the overlying sands were deposited (Lowe 1976; Russell et al. 2003).

The uppermost 1m of the Sæluhúsavatn upper basin west wall excavation has a very poorly sorted, multi modal grainsize distribution, with almost equal quantities of clay, silt, sand and gravel, and clasts up to cobble size. Based on grainsize distribution alone, these sediments can be described as a diamicton, and shows clear similarities to other Icelandic multi-modal sediments described

from by Boulton (1978) from the 'tractional' zone of Breiðamerkurjökull. The high proportion of sub-angular to sub-rounded clasts within the unit is typical of sub-glacial diamictons, where continual abrasion results in the rounding of clasts, but crushing and fracturing increase angularity, preventing clasts from becoming well rounded (Boulton, 1978). This unit shows a higher proportion of rounded and well-rounded clasts than is commonly seen from most glacial tills. However, this is considered a consequence of the fluvially dominated nature of the parent material which is likely to have been well rounded due to the nature of the high energy fluvial environment which dominates the majority of processes across Skeiðarársandur (Russell et al. 2006) Further confidence in the interpretation of these sediments as a till is provided by clast fabric shape. When compared with till fabrics from other Icelandic proglacial environments, the fabrics at this location compare with examples of upper tills from Skalafellsjökull (Dowdeswell and Sharp 1986).

This rounded nature of clasts is attributed to a relatively short lived periods of glacier advance during the glaciers recent history which results in relatively short periods of subglacial sediment transportation, reducing the opportunity for clast to clast interactions and the fracturing of clasts to produce more angular clasts (Boulton 1978).

A schematic conceptual model to illustrate the processes described within this interpretation is provided in **Figure 4-25**. This shows the evolution of processes at this point in the Sæluhúsavatn area, beginning with high-energy outwash and progressing to ice contact slumping and viscous debris flows, to low energy fluvial reworking and deposition to eventual over riding by glacier ice.

Figure 4-25

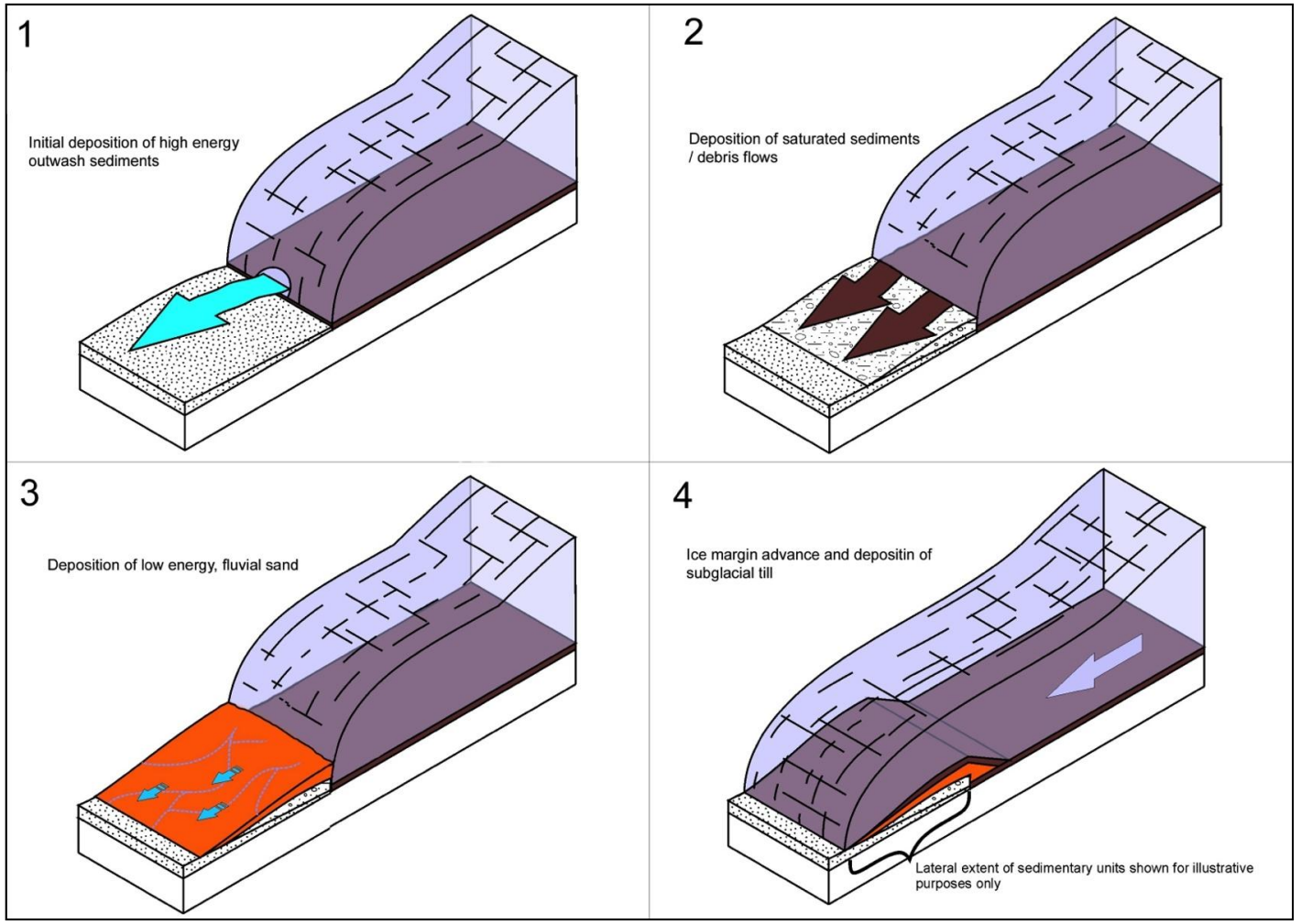

Conceptual model illustrating the processes and sequence of events leading to the deposition of sediments found within the Sæluhúsavatn upper basin west wall excavation.

4.3.8 SECTION 4

This section is located on the northern (south facing) side of the deeply incised spillway channel that connects the lower Sæluhúsavatn ice contact basin with the smaller basin immediately to the east (**Figure 4-10**). The erosion of this spillway has provided excellent exposure of the sediments that make up the ridge that partitions the ice contact portion of the East Sæluhúsavatn area into its constituent basins.

As can be seen from **Figure 4-26** below, the section in question is approximately 22 m wide, and 8 m high, with the lower 2 m obscured by talus. Well-rounded pebbles, cobbles, and boulders, held within sandy matrices of varying quantities, dominate the entire section. What follows is a detailed description of each unit and their bounding surfaces. The red lines on **Figure 4-26** show the locations of stratagraphic logs (**Figure 4-27**) drawn along the exposure in order to provide a better illustration of grainsize than is available from the panel sketch. Due to the subtle variations between each unit, facies codes have not been used, and instead each unit has been numbered from west to east (left to right).

Unit 1 comprises moderately well sorted, massive, sub-rounded to rounded large pebbles and cobbles, within a fine sand matrix. Grainsize analysis of these sediments reveals a very leptokurtic distribution, with 84% of the sample having a diameter greater than 2 mm (**Figure 4-28 - A**). Clast fabric analysis displays a weak fabric, with a very isotropic fabric shape and Eigen values of S_1= 0.425, S_2= 0.316 and S_3= 0.259 (**Figure 4-29 - 1**). The majority of clasts have a compact shape, with a low C40 index of 8% and are predominantly sub-rounded to rounded (**Figure 4-31**). The upper bounding surface of this unit is marked by a sharp increase in mean grainsize where it meets Unit 2 above.

Unit 2 exhibits large, predominantly sub-rounded cobbles to up 200 mm a-axis within a fine sand matrix. They display subtle normal grading, from cobbles at the lower bounding surface to large pebbles at the upper. Unit 2 comprises at least 80% clasts by area, thus it was too coarse to sample for grainsize analysis. However, analysis of the matrix from two separate locations reveals a moderately well sorted, leptokurtic to very leptokurtic distribution with a coarse skew and confirms the existence of fine tail coarsening from west to east (**Figure 4-28 - B and D**). Clast fabric analysis taken from two locations within the single unit both reveal clusters of clasts dipping at approximately 225° and 20° (**Figure 4-29 - 2 and 4**). Sample 2 to the left of the section shows a an overall weak fabric, with Eigen values of S_1= 0.487, S_2= 0.262 and S_3= 0.252, resulting in an isotropic fabric shape. Clast shapes are predominantly blocky (C_{40} = 20), and are dominated by sub-rounded clasts, although clast roundness ranges from angular to well rounded. However, Sample 4 shows a slightly stronger fabric, with Eigen values of S_1= 0.633, S_2= 0.209 and S_3= 0.159, resulting in slightly clustered fabric shape. Clast shapes are predominantly blocky (C_{40} = 12) and roundness ranges equally from sub-angular to sub-rounded, with small quantities of angular and well rounded clasts.

Unit 3 is predominantly massive, moderately sorted sandy gravel comprising small pebbles up to 15 mm within a fine-sand matrix. This matrix comprises approximately 25% of the unit. Towards the eastern edge of this unit (to the right of the ranging pole), the massive nature grades to coarse tail inverse grading. Grainsize analysis reveals a very leptokurtic distribution with a very fine skew (**Figure 4-28 - C**). Clast fabric analysis is slightly clustered, with Eigen values of S_1= 0.546, S_2= 0.248 and S_3= 0.206 however, overall the fabric is weak, with minor clusters through the plane 190 - 010° (**Figure 4-29 - 3**). Clast

shapes are predominantly blocky (C_{40} = 12) and roundness is dominated by sub-angular clasts, although clast roundness ranges from angular to well rounded

Like the contacts described above, the contact between Units 3 and 4 is sharp, but shows no evidence of erosion. It is marked by a distinct coarsening and reduction in the degree of sorting. Unit 4 is poorly sorted, sub-rounded to rounded pebbles and small cobbles within a moderately well sorted sand matrix.

Unit 5 lies directly above Unit 3 and is bound by a sharp increase in grainsize. Unit 5 comprises sub-rounded to rounded boulders, up to 400 mm in diameter, within a medium sorted, sandy matrix. The clasts within this unit appear to be, partially clast supported. On the west side of this unit, sediments appear to be slightly normally graded, however, this structures gives way to a more massive texture as the unit is traced to the east.

Unit 6 lies above Unit 5 on the western side of the section and has a bounding surface that is defined by a dramatic increase in grainsize. It is composed primarily of poorly sorted, medium cobbles, and small boulders, which are normally graded into coarse gravels. The unit is densely packed and clast supported, with none of the sand sized material that is found in many of the other units at this locality.

Unit 7, east of units 2, 3 and 5 is composed of a poorly sorted, bimodal unit of 80% well rounded cobble clasts. These clasts are up to 100 mm a-axis and held within a sandy matrix. There is a weak indication of inverse grading shown by clusters of large cobbles or small boulders at the top of the unit, below the contact with Units 8 and 9 above. At a number of locations within this unit, the sand matrix is finely bedded and deformed around overlying cobbles (**Figure 4-30 - I**). Clast fabric analysis taken from the far left (west) of this unit shows a slightly girdled fabric shape, with Eigen values of S_1= 0.521, S_2= 0.367 and S_3= 0.112(**Figure 4-29 - 5**). Clast shape is predominantly blocky (C_{40} = 22%) and

there is a wide range of roundness types, dominated by sub-rounded clasts, but with a normal distribution from angular to well rounded (**Figure 4-31**).

Unit 8 is located to the east of unit 6, above unit 7, and is by far the most extensive unit of the section. It is a normally graded, poorly sorted unit composed of large rounded cobbles and boulders held within a fine sand matrix. The boulders grade upwards into densely packed, partially clast supported, coarse gravel. The largest boulders (>200 mm a-axis) at the bottom of the unit show deformation of the bedded matrix, as seen in Unit 7. The contact between Units 7 and 8 is defuse, defined by distinct variations in clast size, while the matrix material in-between these two units show very little variation. Instability of the face prevented clast fabric analysis from being carried out.

Unit 9 is found immediately above Unit 8 and is defined by a sharp erosive undulating contact. It is composed of 10 - 15% well rounded clasts (>100 mm a-axis) held within a dark, sandy matrix.

Unit 10 above is defined by an undulating contact, itself defined by an increase in the density of clasts (30%) and reduction in clast size (20 - 50 mm). The lower bounding surface of Unit 10 undulates in phase with the undulations of unit 9 below. The matrix material of Unit 10 is composed of sands with a high proportion of fines identical to that of Unit 9.

Unit 11 lies directly above Unit 10. Its lower bounding surface undulates similarly to those of Units 9 and 10. The bounding surface is defined by a huge reduction in the proportion and size of clasts. Unit 11 consists of a sandy matrix with a large proportion of fines, identical to that of Units 9 and 10. Within this matrix are a small number (2 - 5% by area) of small sub-angular to sub-rounded clasts up to 20 mm a-axis.

Unit 12 is located to the east of the section, above the eastern end of Unit 8. It is a small exposure approximately 3 m wide and 0.5 m high, obscured on its

eastern side by talus. The unit consists of inverse to normal graded gravels, bound on its upper and lower surfaces by thin silty clay beds. These gravels are approximately 20 - 30 mm a-axis in the middle of the unit, grading to fine granules (2 - 4 mm) at the top and bottom of the unit. Grainsize analysis of bulk samples taken from the middle (**Figure 4-28 - E**) and bottom (**Figure 4-28 - F**) of this unit show two unimodal, very poorly sorted gravel units. **Figure 4-28 - E**, taken from the middle of the unit, the coarsest section, reveals very leptokurtic, coarse gravel, while **Figure 4-28 - F**, taken from the finer, bottom of the unit, shows mesokurtic, sandy medium gravel. Clast fabric analysis of this unit (**Figure 4-29 - 6**) shows a concentration of clasts with shallow a-axis dips trending north and south south-east. The fabric shape is mildly girdled, with Eigen values of S_1= 0.546, S_2= 0.355 and S_3= 0.099. Clast shapes are dominated by blocks (C_{40} = 16%), and there is a wide range of roundness types, dominated by sub-angular clasts.

Unit 13 lies directly above Unit 12 and, like Unit 12 is bound top and bottom by thin silty clay beds. The upper and lower bounding surfaces undulate and appear to link to the upper surface of Unit 10 and lower surface of Unit 9 respectively. However, the internal sedimentology of Unit 13 is not linked in any way to those of units 9 and 10. Unit 13 consists of densely packed, clast supported rounded cobbles 50 - 100 mm a-axis. There is a small amount of sandy matrix material.

Unit 14 is located directly east of Unit 13. Its upper bounding surface leads from that of Unit 13. Unit 14 is composed of a single, moderately sorted, normally graded unit of coarse gravels and sand. Two bulk samples were taken from this unit for grainsize analysis. The upper sample (**Figure 4-28 - G**), taken from the top 50 mm of the unit, shows a bimodal, very poorly sorted, sandy medium gravel, with a large proportion of sands and fines, and a platykurtic

kurtosis. Analysis of the lower 50 mm (**Figure 4-28 - H**) shows a unimodal, poorly sorted unit of very coarse gravel, with larger pebbles and cobbles, and minimal proportion of sands. Analysis of kurtosis shows that this unit is very leptokurtic. Unit 14 is dissected by a vertical silty clay pipe structure which terminates at the silty clay bed on the upper bounding surface of unit 14 (**Figure 4-30 - II**).

Unit 15 is composed of approximately 60% well rounded cobble clasts (>200 mm a-axis) within a silty sand matrix. The lower bounding surface of this unit is defined by a 20 - 30 mm thick silty clay bed which quickly dissipates into the matrix above. The upper bounding surface appears to have been eroded by the unit above.

Unit 16 is a massive sandy unit with medium sized pebble clasts and a distinctive beige colouring. The upper 10 - 20 mm of this unit exhibits a greater number of clasts (40%); however this number greatly reduces to approximately 10% below this upper zone. Despite this variation in clast concentration, the unit is not considered to be graded as the transition is sharp and distinctive. Bulk sediment samples from two locations in this unit were taken for grainsize analysis. The first (**Figure 4-28 - I**) was taken from the finer portion of the unit that exhibits only a smaller proportion of clasts. The analysis revealed a unimodal, very poorly sorted, sandy medium gravel, with a fine skew, and mesokurtic kurtosis. The second sample was taken from the coarser material in the top 10 - 20 mm of the unit (**Figure 4-28 - J**). This analysis showed a unimodal, very poorly sorted, very coarse silty sandy medium gravel, with a very fine skew, and leptokurtic kurtosis. Clast fabric analysis from this unit reveals a strong cluster in the bottom right of the lower hemispheric projection (**Figure 4-29 - 7**). Eigen values of S_1= 0.618, S_2= 0.346 and S_3= 0.037 result in a slightly girdled fabric shape and very low isotropy. Clast shapes are dominated by

blocky clasts with a range of roundness types from angular to well rounded, predominantly sub-rounded.

The entire section is overlain by Unit 17, a very poorly sorted silty, sandy, gravelly diamicton, which contains a large number of sub-angular to rounded clasts. Clast fabric analysis and sediment samples could not be taken from this unit due to its height and instability of the exposure face. However, the unit forms a thin, even carapace approximately 0.1 – 0.3m thick and is similar in character to Sample O from Section 5. Grainsize analysis from that location, approximately 100m to the east, consists of tri-modal very poorly sorted muddy, sandy gravel (**Figure 4-36 – O**).

Figure 4-26

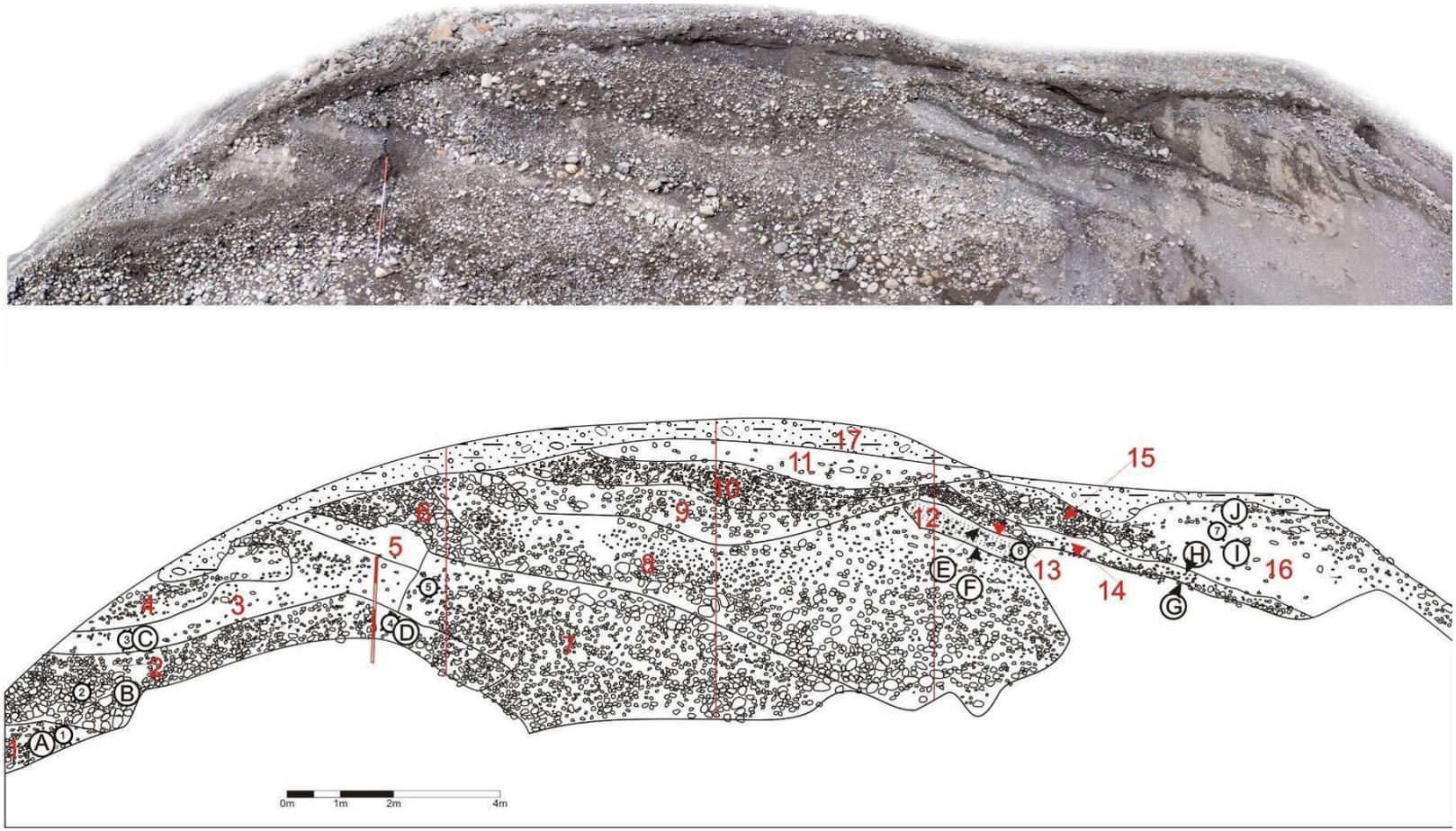

Photo mosaic and panel sketch of section in the north spillway wall in-between the lower Sæluhúsavatn ice-contact lake basin and the smaller basin to the east. Numbered circles show the plane of a-axis dip directions (50 clasts per sample) and the location of clast fabrics sampled for ***Figure 4-29****. Circled letters show locations of samples taken for grainsize analysis, shown in* ***Figure 4-28****. Red numbers refer to units described in the text and red lines show the locations of stratagraphic logs shown In* ***Figure 4-27****.*

Figure 4-27

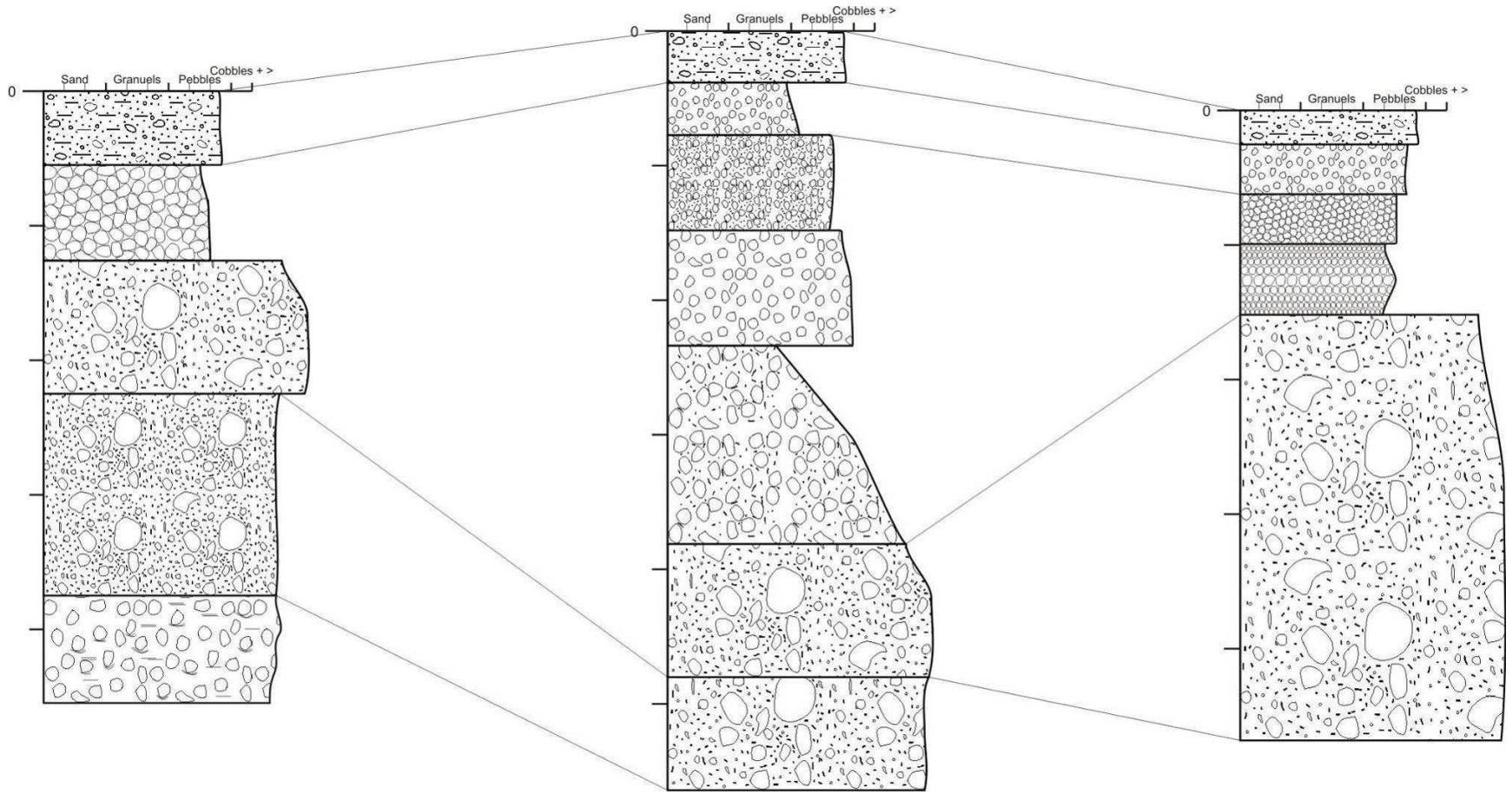

Stratagraphic logs showing variations in grainsize vertically and horizontally along the Sæluhúsavatn lower basin, north spillway wall exposure. Logs relate to A, B and C on ***Figure 4-26*** *and dashed lines show continuations of the same stratagraphic unit along the exposure.*

Figure 4-28

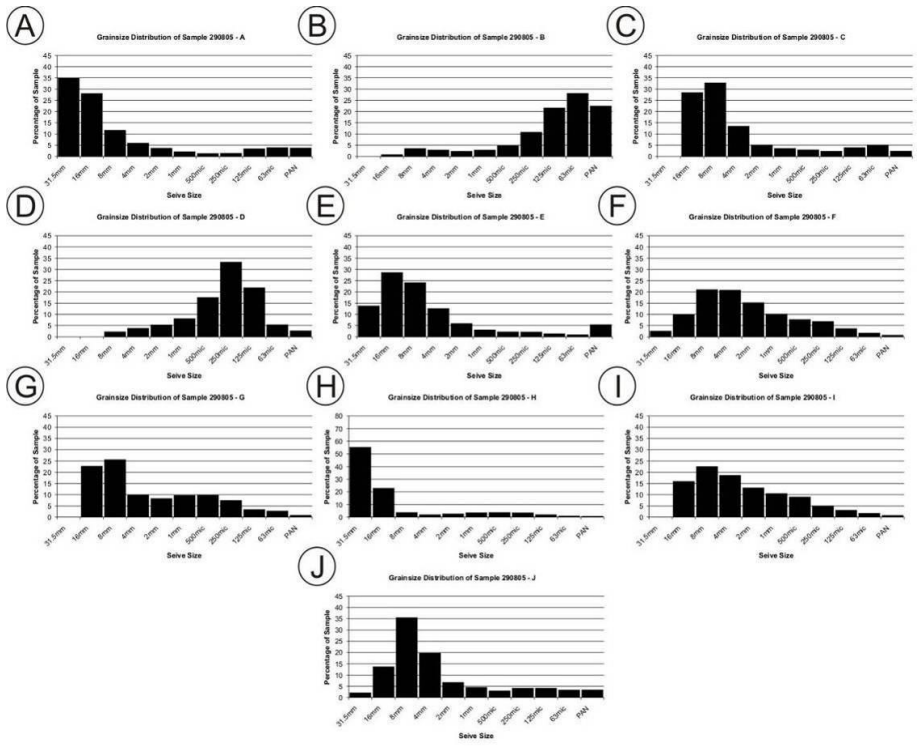

Grainsize distribution histograms of bulk sediment samples taken from the north spillway wall in-between the lower Sæluhúsavatn ice-contact lake basin and the smaller basin to the east

Figure 4-29

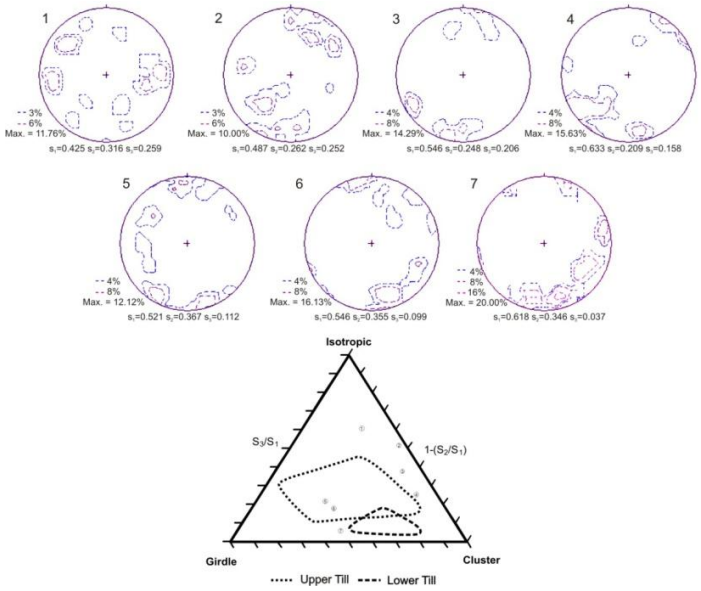

Lower hemisphere equal area projections of clast fabric data from the Sæluhúsavatn north spillway wall. Corresponding fabric shapes are plotted on the fabric shape tri-plot of (Benn 1994)

Figure 4-30

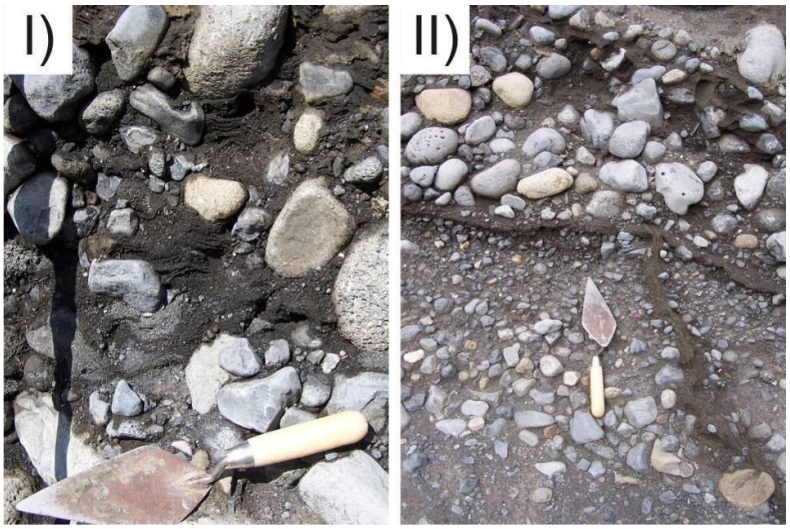

Close-up photographs of structures within the Sæluhúsavatn north spillway wall. I) Deformed bedding within well sorted sand matrix. II) Well sorted, silty sand pipe fill structures within a normally graded pebble conglomerate.

Figure 4-31

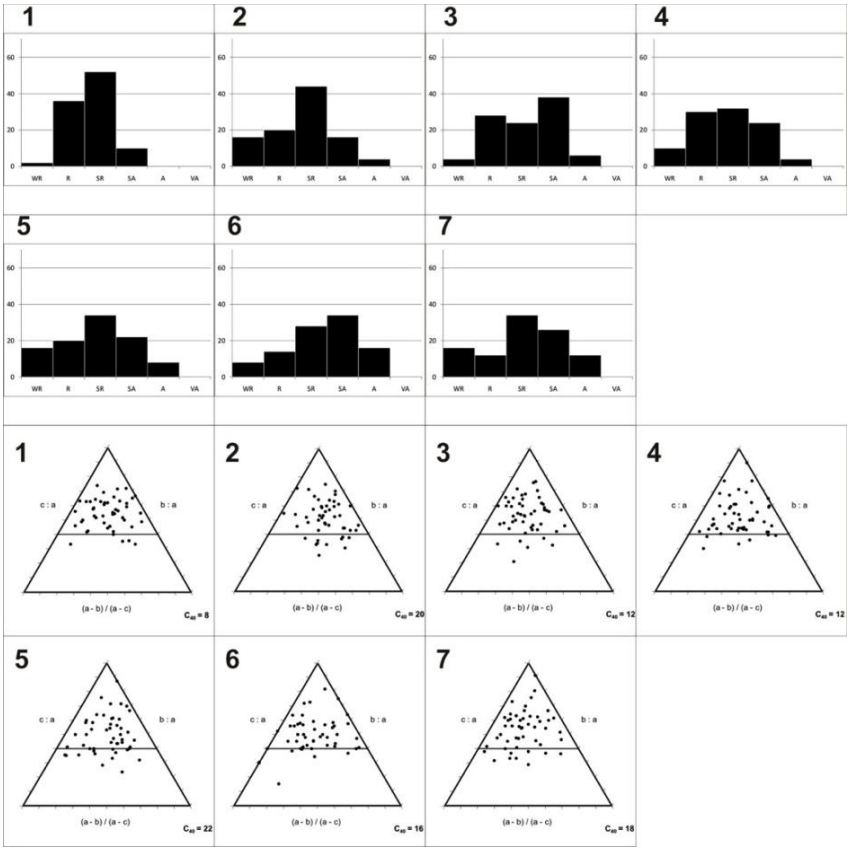

Sneed and Fork Clast Shape Tri-plots and Percentage frequency clast roundness histograms for clast samples from the Sæluhúsavatn Lower Basins north Spillway Wall exposure. Numbers referee to numbered circle locations shown on figure 4.17.

4.3.9 SECTION 4 INTERPRETATION

All of the sedimentary units that are displayed within this large exposure are consistent with deposition from a fluvial environment. Low C_{40} values are indicative of active transport processes (Benn and Ballantyne 1994), while the wide range of sedimentary facies suggests that these sediments have been laid down by a number of different fluvial processes, potentially over a prolonged period of time. Many of the massive and inversely graded units are interpreted as having been deposited very rapidly from highly turbulent, possibly hyperconcentrated flows (Maizels 1993; Duller et al. 2008).

Similar deposits to the bimodal units located towards the bottom of this exposure (**Figure 4-32**) have been interpreted to have formed in a wide range of sub-, en-, and proglacial settings, by numerous authors (Saunderson 1977; Proudfoot et al. 1982; Veillette 1986) referenced in Shaw and Gorrell (1991). These authors suggest that such bimodal deposits are typical of fluvial and / or sub-aqueous deposition, associated with delta or bedform foreset and bottom set deposition. In such cases, bi-modality is a function of low energy settling of fine grained sands and the incorporation of larger cobbles which role down the delta foreset. Support for such deposition is provided by the deformation of sand beds within the unit's matrix, around large cobble clasts. However, such bimodal deposits have also been interpreted as products of high energy, hyperconcentrated flows (Russell and Arnott 2003). In this instance, due to the presence of the deformed, bedded sand matrix, the interpretation presented by Shaw and Gorrell (1991) is considered the most appropriate. These sediments are believed to be dune foresets, where flow separation over the dune crest has resulted in the co-deposition of cobble bed load and sandy suspended load.

Figure 4-32

Bimodal, rounded cobble gravel, with graded bedding within the sand matrix. From Shaw and Gorrell,(1991), Figure 9.

Figure 4-33

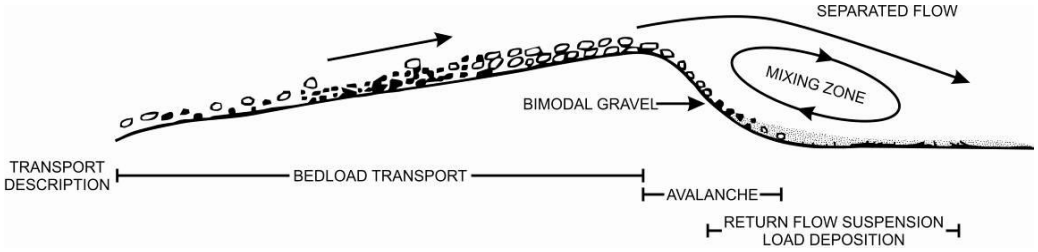

Formation of Bimodal gravel by bed load avalanching down foreset and mixing with suspended sands in the lee of the bedform. After Iseya and Ikeda,(1987)

The upper most units (9, 10, and 11) are interpreted as channel cut and fill deposits associated with incision and aggradation within a highly active, fluvial channel. Each unit is interpreted as the result of an individual flow event, or pulse, which results in initial erosion, and then deposition during its waning stage. The timing of each of these units is not possible to ascertain from the available data. It is possible that each unit was deposited by an individual flow

event over a sustained period of time. However, erosion and aggradation has been noted as a product of pulsed flows within high energy jökulhlaup flows at Skeiðarárjökull (Russell and Knudsen 1999), and thus it is likely that this sequence could have been deposited within a matter of minutes within the same flood event.

The sandy pipe structure which is seen penetrating through this exposure is interpreted as a water escape structure (Lowe 1975; van de Meer et al. 2009). The presence of such structures can be used to support the interpretation that these sediments were laid down rapidly, resulting in the trapping of water between loosely packed grains(Lowe 1976).

Based on the very poorly sorted grainsizes incorporating grainsizes from clay to cobbles, the overlying poorly sorted diamicton is interpreted as a subglacial, basal till, deposited at the ice contact as the glacier over road the underlying glaciofluvial deposits. This example is similar to those presented by Lundqvist et al, (1993) where subglacial till were found to drape the upper surface of subglacially formed eskers in South-Central Wisconsin.

Based on the morphology of the ridge, these deposits are believed to have been deposited within an ice contact conduit and record the aggradation and progradation of a fluvial bedform or macroform (Brennand 1994; Burke et al. 2008), and it is therefore interpreted as an esker. The exact position of this macroform within the glacier cannot be determined precisely. The pristine nature of each sedimentary unit, without the presence of any faulting or major slumping could suggest that the esker is not underlain my ice and thus it could be interpreted as subglacial. However, the lack of such features cannot be taken as absence of buried ice. Additionally, it cannot be determined whether this feature was formed within a subaerial or ice roofed conduit. Flow within ice roofed conduits often results in high water pressures which can result in the

formation of secondary flow circulations within the conduit and the formation of pseudo-anticlinal bedding (Brennand 1994). However, the lack of such bedding cannot be used to favour a subaerial interpretation. Burke et al., (2008) found no evidence of pseudo-anticlinal bedding within a proto-esker that was known to have formed within an ice roofed conduit at the margin of Skeiðarárjökull.

4.3.10 SECTION 5

Section 5 is located in a cut through a 11 m high gravel ridge which runs in-between the far eastern and middle Sæluhúsavatn basins as shown in **Figure 4-4**. The primary feature of this section is the large pseudo-anticlinally bedded core of cobbles and boulders in the centre of the exposure (**Figure 4-34**). The central core is flanked on both sides by beds of well sorted, medium to fine sands that dip away from the central core. The top of the central core and the sand beds is intersected by a sharp erosive contact which can be traced up the left side of the sand beds, over the cobble core and back down the sand beds on the right. Overlaying the dipping sand beds on the right lays a poorly sorted unit of sand, gravel, cobbles and boulders. In some places this unit exhibits lenses of well sorted or graded material with well defined beds; however, overall the unit is considered poorly sorted and somewhat chaotic. Above the erosive contact, the sediments grade in a single unit from gravel and small pebbles to fine, rippled sands. Each of these individual sedimentary units will now be discussed in detail beginning on the western (left) of the exposure.

The far western unit on the left side of this section is a finely laminated unit of moderately sorted, medium to fine sand with a few inclusions of gravel sized clasts. The laminations in this unit dip towards the western (left) edge of the section (**Figure 4-35 - I**). Further investigations of this lamination indicate a wide variation within the dip and strike of these beds, varying from 180° - 247°

(strike) and 6° - 20° (dip). Detailed grainsize analysis of these sediments reveals very fine, gravelly medium sand, with a very fine skew and leptokurtic kurtosis. The contrast in colour between beds and laminations shown in **Figure 4-36 - I** highlights the well sorted nature of each individual lamination. This unit also incorporates numerous beige pumice fragments within pods or bands which dip in the same orientations as the main laminations.

The upper contact between this unit and the unit above is defined by a very thin (1 - 3 mm) pseudo-lamination of fine brown-orange clay. This is an inter-granular lamination which can be traced along the top of the laminated sands, trending down and then over the top of the 'pseudo-anticlinal core' (**Figure 4-35- I**).

Above this clay layer is a poorly sorted, semi clast supported unit of sands and coarse gravel, up to 150 mm a-axis. This unit is presents a series of beds or aligned clasts that result in the resemblance of beds (**Figure 4-35 - II**). To the left of the unit, the 'beds' consist of large sub-rounded clasts up to 150 mm axis. Towards the top of the unit, the sediments grade into finer fractions and become better sorted with more of the sand matrix present. This grades to the right into sub-angular clasts with up to 100 mm a-axes. Where matrix is present, it comprises medium black sand. Grainsize analysis was carried out on two samples from this unit (**Figure 4-36 -B** and **C**). This analysis reveals a slight reduction in the maximum grainsize from left to right. Both samples from this unit reveal poorly sorted, sandy medium gravel, with a mesokurtic kurtosis. Sample B on **Figure 4-36** is bimodal, while sample C on the right, has a unimodal grainsize distribution. Clast fabric analyses from the three locations within this unit show a predominantly weak fabric at all location (**Figure 4-37- 1, 2, and 3**). CFA1 taken from the left of the section shows a small cluster of points at the top of the lower hemisphere projection, indicating a shallow

preferential dip toward the north. A similar cluster is notable at the bottom of the projection. The overall fabric shape is girdled / isotropic, and has Eigen values of S_1= 0.468, S_2= 0.369 and S_3= 0.164. CFA2 displays a similar pattern to CFA1; however the alignment of the clusters is rotated approximately 10° anticlockwise and has a much stronger fabric which has a more clustered shape and Eigen values of S_1= 0.626, S_2= 0.245 and S_3= 0.130. CFA3 shows a weaker fabric shape located in-between the points of CFA1 and CFA2 on the fabric shape tri-plot **(Figure 4-38)**. CFA3 has Eigen values of S_1= 0.532, S_2= 0.323 and S_3= 0.145.

Clast shape within this unit shows little variation, dominated predominantly by blocky clasts with C_{40} indices of 18%, 10% and 4% **(Figure 4-39 - 1, 2, and 3)**. Clast roundness on the other hand does show some variation across the unit, with samples 1 and 3 dominated by sub-angular to sub-rounded clasts, while sample 2 shows a higher proportion of angular clasts **(Figure 4-40)**.

The upper and western contacts of this unit are obscured by talus although it is considered likely that they reflect those on the opposite side of the exposure. The lower contact of this unit, where it meets the outermost unit of the 'pseudo-anticlinal core' is diffuse, probably a result of fine surface talus which was inaccessible when cleaning.

The 'pseudo-anticlinal core' below is defined by at least 4 primary 'beds'. The inner most of these beds is defined by large, open framework, well rounded cobbles between 300 - 400 mm a-axis **(Figure 4-35 - III)**. These cobbles normally grade towards the top and sides of the unit, towards a diffuse contact with the unit above. Clast fabric analysis from two locations within this section shows a preferential dip orientation along a northwest - southeast plane. **Figure 4-37 - 6** presents a lower hemisphere projection of the clast fabrics taken from

the top left of the section. It presents a relatively strong fabric with Eigen values of S_1= 0.571, S_2= 0.223 and S_3= 0.203, resulting in a mildly clustered fabric shape (**Figure 4-38**). **Figure 4-37 - 7** presents clast fabric analysis data from the eastern side of this unit. This lower hemisphere projection shows similar clustering around the same poles as above, but with a greater degree of scatter. Eigen values of S_1= 0.501, S_2= 0.289 and S_3= 0.209 which suggests a weaker fabric with a more isotropic fabric shape (**Figure 4-38**). **Figure 4-39 - 6 and 7** shows that there is no variation of clast shape within the inner core unit. Both Sneed and Fold tri-plots show a dominance of clasts with a 'compact' shape and C_{40} indices of 8% and 6%. Clast roundness data show dominance by sub-rounded clasts, with a significant number of rounded clasts. Only 10% of the sample falls into the sub-angular category (**Figure 4-40**). Grainsize analysis has not been carried out on this unit due to the logistical problems associated with collecting a large enough sample to be representative.

Above this inner unit, the following unit consists of poorly sorted rounded pebbles within a medium black sand matrix. This unit shows some evidence of inverse grading; however this is not continuous throughout the whole unit. Grainsize analysis from the left side of this unit shows a unimodal, poorly sorted, sandy gravel, with a fine skew and platykurtic kurtosis (**Figure 4-36 - D**). Grainsize analysis of the right side of the unit reveals bimodal, very poorly sorted, sandy, course gravel. This sample has a very fine skew and platykurtic kurtosis (**Figure 4-36 - E**). Clast fabric analysis from these same locations show two very different, very strong clast fabrics. **Figure 4-37 - 5** presents clast fabric data from the left of this unit. The lower hemisphere projection shows a significant cluster in the top left quarter of the projection showing the majority of clasts have a shallow dip towards the northwest. The strong fabric is illustrated by Eigen values of S_1= 0.751, S_2= 0.201 and S_3= 0.047 and

a clustered fabric shape (**Figure 4-38**). **Figure 4-37 - 8** presents clast fabrics from the right of the unit. It shows a cluster of points in the top right quarter showing the majority of clasts have a shallow dip towards the northeast. Eigen values of S_1= 0.703, S_2= 0.215 and S_3= 0.028 illustrate the strong clustered fabric (**Figure 4-38**). Clasts shapes from both samples are dominated by blocky clasts, although there is some variation in C40 from left to right (18% - 2%) (**Figure 4-39 - 5 and 8**). Clast roundness data from this unit shows some subtle variation from left to right with sub-angular and sub-rounded clast dominating o the left and a much greater proportion of rounded and well rounded clasts to the right (**Figure 4-40**). The upper contact of this unit is defined by a sharp reduction in grainsize, into the following unit.

The unit above is defined by inverse grading of poorly sorted, course gravels, containing rounded pebbles up to 150 mm a-axis, within a black medium sand matrix. Clast fabrics from the left of this section show a very strong clustered fabric (Eigen values of S_1= 0.783, S_2= 0.183 and S_3= 0.034), with all clasts within the sample clustered in the top left of the southern hemisphere projection (**Figure 4-37 - 4**). This shows that, similar to the unit below, clasts in this location have a shallow dip towards the northwest. Clast fabrics on the right side of this unit exhibit a different pattern with a much weaker girdled fabric (Figure 4-38) and Eigen values of S_1= 0.467, S_2= 0.201 and S_3= 0.047 (**Figure 4-37-9**). Grainsize analysis of the sediments from this unit show a unimodal, poorly sorted coarse gravel with a very fine skew, and a mesokurtic kurtosis (**Figure 4-36 - F**). Clast shapes are predominantly blocky with a C_{40} indices of 22% **(Figure 4-39 – 9).**

In the upper most unit of the pseudo-anticlinal core, the degree of sorting reduces and the whole unit is defined by poorly sorted large rounded cobbles within medium black sand. The size of cobbles within this unit also greatly

increases towards the apex of the anticline. The upper contact of this unit is obscured by talus along its middle section, but is defined by a sharp erosive contact on the anticline flanks, which is highlighted by the aforementioned clay intra-granular lamination. Grainsize analysis of this upper most anticlinal unit reveals a unimodal, poorly sorted, very coarse gravel, with a very fine skew and very leptokurtic kurtosis (**Figure 4-36 - G**). Clast fabrics from the east side of this unit (**Figure 4-37 - 10**) presents Eigen values of S_1= 0.598, S_2= 0.229 and S_3= 0.143 and has a slightly clustered fabric shape, with dips clustered towards the south. Overall, this unit is considered as having a moderate fabric.

Clast roundness within this upper unit is defined by sub-angular, sub-rounded and rounded clasts in near equal measure (**Figure 4-40 - 10**), while clast shape is dominated by blocky clasts with a C_{40} index of 18% (**Figure 4-39 - 10**).

Above the erosive contact described above, to the right of the 'pseudo-anticlinal core', lies a single, normally graded unit that is up to 4 m thick. The lower 1.75 m of this unit comprises coarse gravel and sand with large, sub-rounded to rounded cobbles and boulders up to 500 mm a-axis (**Figure 4-35 - IV**). These coarse gravels grade into medium sands with few inclusions of small clasts up to 30 mm a-axis (**Figure 4-35 - V**). These sands appear to be perfectly laminar towards the top of the unit. Although poorly sorted, the gravels and cobbles at the bottom of this unit exhibit some degree of bedding, with the beds intersected by the face and apparently dipping towards the west (no formal measures could be taken due to the difficulty of the identifying beds up close). Two bulk samples have been taken from this section for detailed grainsize analysis. The first sample was taken in the lower coarse gravel unit and showed bimodal, very poorly sorted, sandy coarse gravel, with a very fine skew and mesokurtic kurtosis (**Figure 4-36 - K**). Grainsize analysis from the upper sandy

unit reveals unimodal, poorly sorted, very fine, gravelly medium sand, with a coarse skew and leptokurtic kurtosis (**Figure 4-36 - L**). Five separate clast fabric analysis samples have been taken from the bottom, coarse section of this unit (samples 11, 12, 13, 15 and 16 on **Figure 4-37**), Fabric strength ranges from weak to moderate (S_1=0.462 – 0.667) and shapes are distributed with in middle of the shape tri-plot from moderately girdled to moderately clustered (**Figure 4-38**).

As with most of the units from this exposure, clast shape analysis for all 5 samples show very little variation from the other units (**Figure 4-39 - 11, 12, 13, 15 and 16**), dominated by blocky clasts and with C_{40} indices ranging from 8% - 18%.. The above samples are also dominated by sub-angular and sub-rounded clasts, with only minor variations of rounded and angular clasts (**Figure 4-40 - 11, 12, 13, 15 and 16).**

The lower contact of this gravel unit is also defined by a sharp erosive contact. To the left of this lower contact lies a single unit of poorly sorted gravels that is outlined by erosive contacts. This unit has a maximum thickness of approximately 500 mm and length of 2 m, although the unit is orientated at an angle of approximately 45°. The unit is composed of coarse granules and gravel clasts, supported by a very small amount of grey coloured sand (**Figure 4-35 - VI**). The sediments appear to fine upwards from approximately 4 mm, at the lower contact, to 1 mm at the upper contact. The lower contact is defined by the intra-granular clay lamination that is described above, which is in some places deformed around pebbles and pressed into the sands below. Grainsize analysis reveals bimodal, poorly sorted, medium gravel, with a fine skew and leptokurtic kurtosis (**Figure 4-36-J**). Clast fabric analysis from the lower portion of the unit reveals a weak to moderate fabric orientated along a plane between north-northwest and south-southeast. This shows Eigen values of S_1= 0.562, S_2= 0.299

and S_3= 0.149 and a moderately clustered fabric shape (**Figure 4-37 – 14** and **Figure 4-38**).

As with most units, the majority of clasts within this unit have blocky shapes and a C40 index of 14% (**Figure 4-39 - 14**). Similarly to the units described above, this unit is dominated by sub-angular and sub-rounded clasts, with a smaller proportion of angular and rounded clasts (**Figure 4-40 - 14**).

Below this gravel unit lays a second unit of well-sorted bedded sands (**Figure 4-35 - VII**). This unit stretches across almost the entire eastern side of the section for approximately 12 m, with a maximum height of 1.5 m at its apex. At first sight, this unit is exactly the same as the bedded sand unit located on the west side of the exposure which is described above, except that the bedding dips in the exact opposite direction. This unit differs slightly to that on the west side of the section as it contains a number of coarser sand granule beds towards the apex. These beds are defined by erosive contacts and comprise coarser materials that have a dip in the opposite direction to the dips of the main unit (**Figure 4-35 - VIII**). Grainsize analysis of these gravel units reveals a unimodal, poorly sorted, gravelly sand, which is coarsely skewed and has a leptokurtic kurtosis (**Figure 4-36 - H and I**).

Directly above this sand unit lies a massive, poorly sorted unit of rounded to well rounded cobbles and boulders, up to 700 mm a-axis. These large clasts are primarily clast supported, with many forming boulder clusters or stacks. Some areas containing larger clasts have an open framework texture (**Figure 4-35 - IX**), however where matrix is present, it is composed of very fine sand and silt. At a number of locations, silty laminar are found within the matrix sands and these have been deformed around the largest boulders. Towards the bottom of the unit, the proportion of silty clay increases with a discontinuous bed of laminated silty clay up to 40 mm thick, emerging intermittently along the

exposure (**Figure 4-35 - X**). This clay 'lens' is deformed by boulders above. Within this boulder dominated unit is a single channel fill structure located in the middle of the unit. This channel shaped 'lens' is approximately 1.2 m wide by 300 mm deep, and comprises two distinct units (**Figure 4-35 - XI**). The lower unit comprises poorly sorted, clast supported, rounded cobbles and pebbles, with a small proportion of granular matrix. There is a sharp contact with the unit above, which is composed of moderately sorted, medium gravel, with a few well rounded pebble clasts (**Figure 4-35 - XI**). Grainsize analysis of the upper unit of this channel fill reveals a unimodal, poorly sorted, medium gravel, with a very fine skew and very leptokurtic kurtosis.

The upper left of the boulder unit presents a second channel fill structure. This is approximately 500 mm high at the apex of the unit and pinches out to the east over a distance of 2.5 m. The channel fill is composed of poorly sorted gravel with large matrix supported boulders and cobbles. Where the sediments are finer (gravel and granules), they appear bedded, dipping east in the same inclination as the top surface of the ridge. The matrix is composed of fine sands with a small proportion of silt unevenly distributed throughout the unit.

The surface of the ridge is draped with a thick carapace of diamicton (**Figure 4-35 - XII**). This unit makes up the uppermost unit of the section and is composed of tri-modal, very poorly sorted, muddy, sandy gravel (**Figure 4-36 - O**).

Figure 4-34

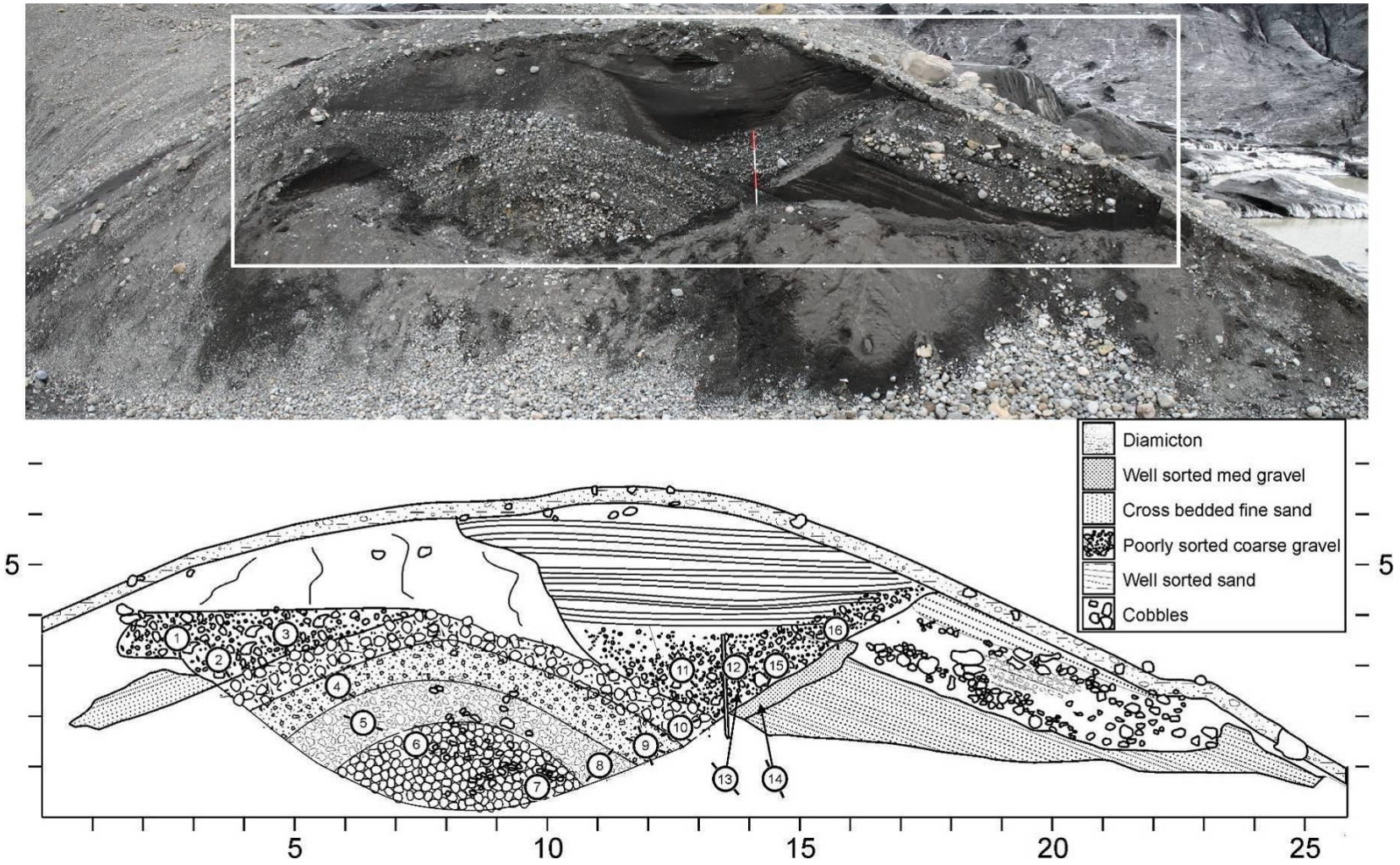

Photo mosaic and panel sketch of Section 5 in the Sæluhúsavatn east basin spillway wall in-between the lower Sæluhúsavatn eastern ice-contact lake basin and the smaller central basin. Numbered circles show the plane of A-axis dip directions (50 clasts per sample) and the location of clast fabrics sampled for figure 5.21

Figure 4-35

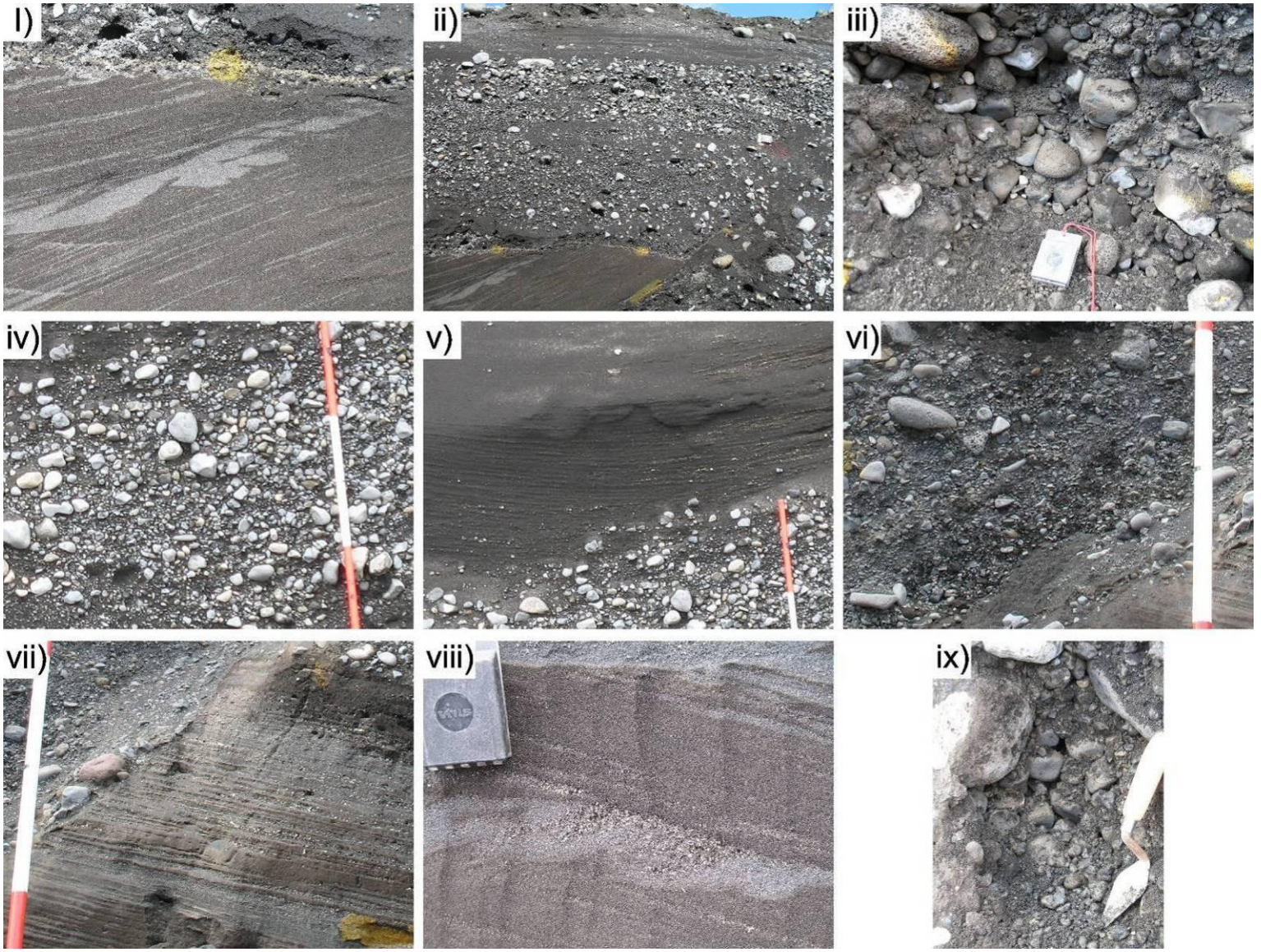

Photographs illustrating the variety of sedimentary facies found at Section 5. i) Cross bedded fine sands on the western flank of the 'anticline'. ii) Poorly sorted course gravels. iii) Open framework cobbles and boulders in the centre of the pseudo-anticlinal 'core'. iv) Poorly sorted coarse gravel and sand at the bottom of a graded unit on the upper right of the exposure. v) Course gravels grading into bedded sands at the top of the exposure. vi) Poorly sorted cobbles and gravels on east (right) side of exposure. vii) Cross bedded sands and fine gravels located on east (right) side of the pseudo-anticlinal 'core'. viii) Close up of vii, showing gravelly scour structures with cross bedding in the opposite direction to the main unit. xi) Semi-open framework cobbles and boulders in upper right portion of exposure. x) Think silty clay lamination up to 50 mm think between cross bedded sands below and poorly sorted cobbles and boulders above. xi) Large channel shaped infill structure containing two distinct coarse gravel bed units. xii) Diamicton drape atop well-sorted sands located at the far right (east) of the exposure.

Figure 4-36

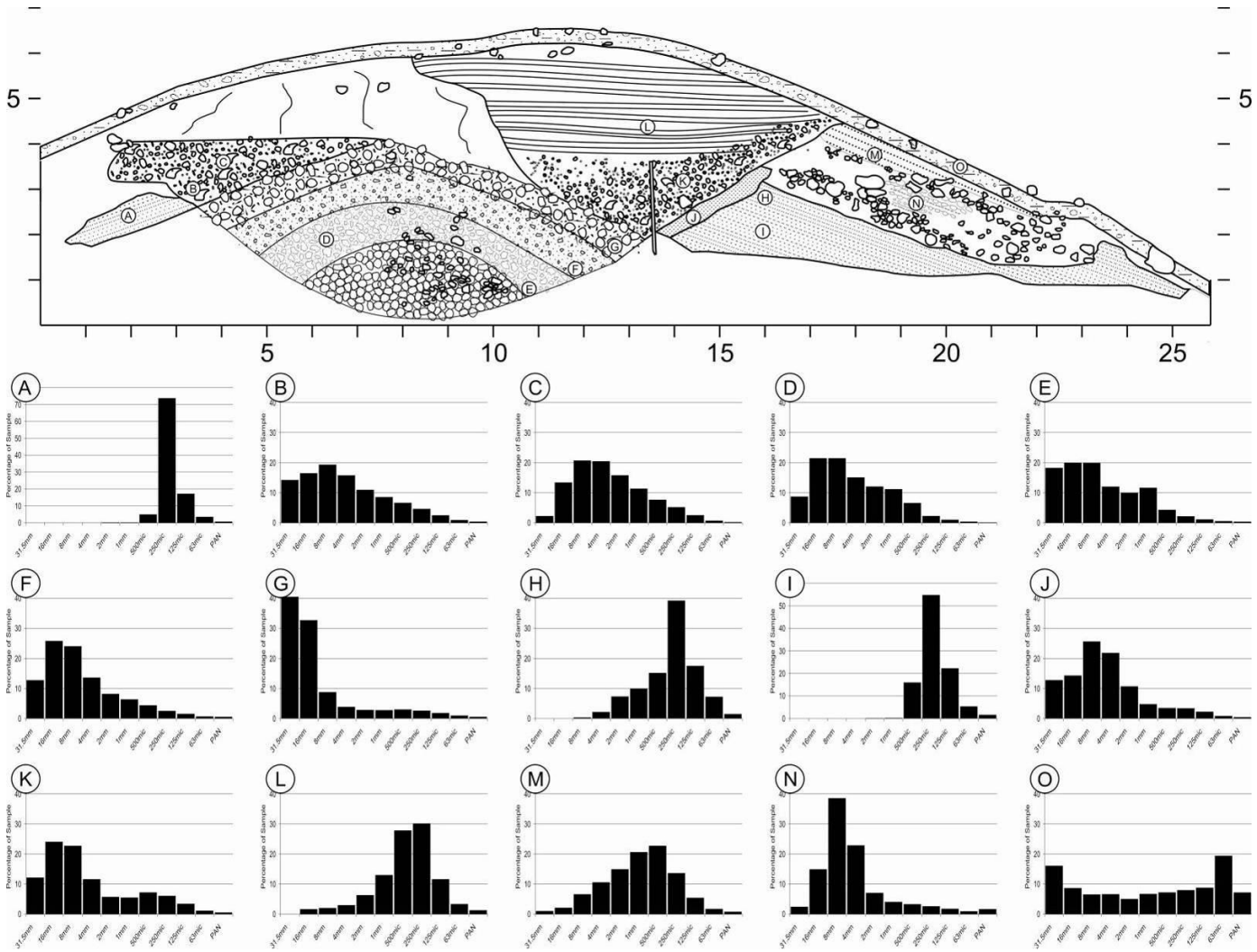

Grainsize distribution histograms of bulk sediment samples taken from Section 5

Figure 4-37

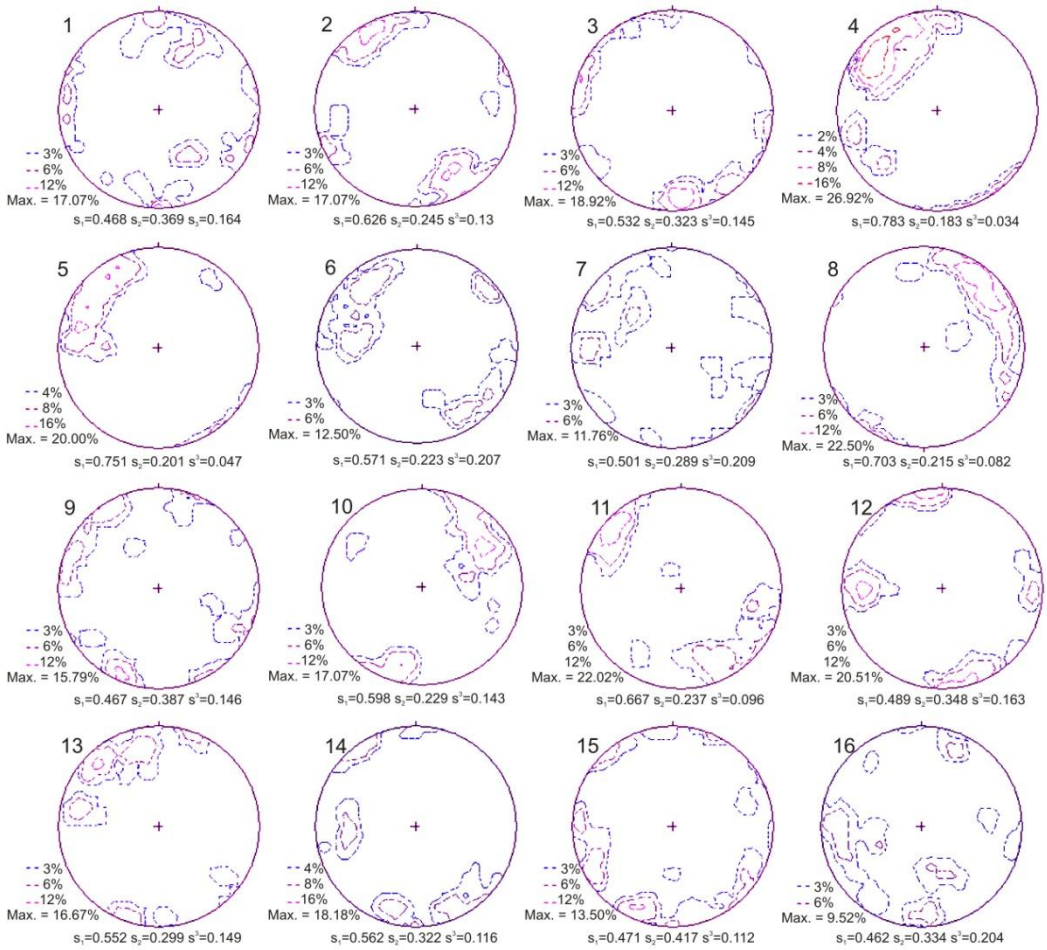

Lower hemisphere equal area projections of clast fabric data from Section 5.

Figure 4-38

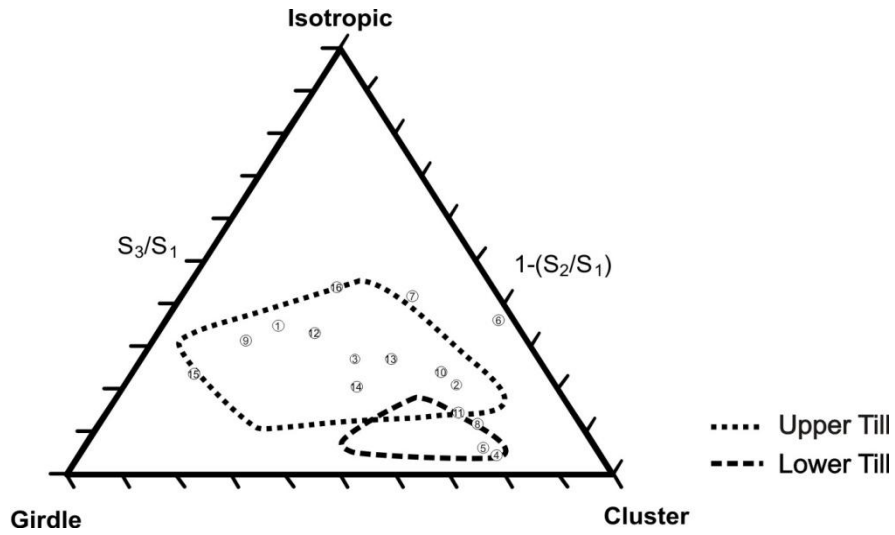

Fabric shape tri-plot from Section 5. Sample numbers are indicated by numbered circles. Dashed lines illustrate fabric shape clusters from sub-glacial tills at Skalafellsjökull (Dowdeswell and Sharp, 1986).

Figure 4-39

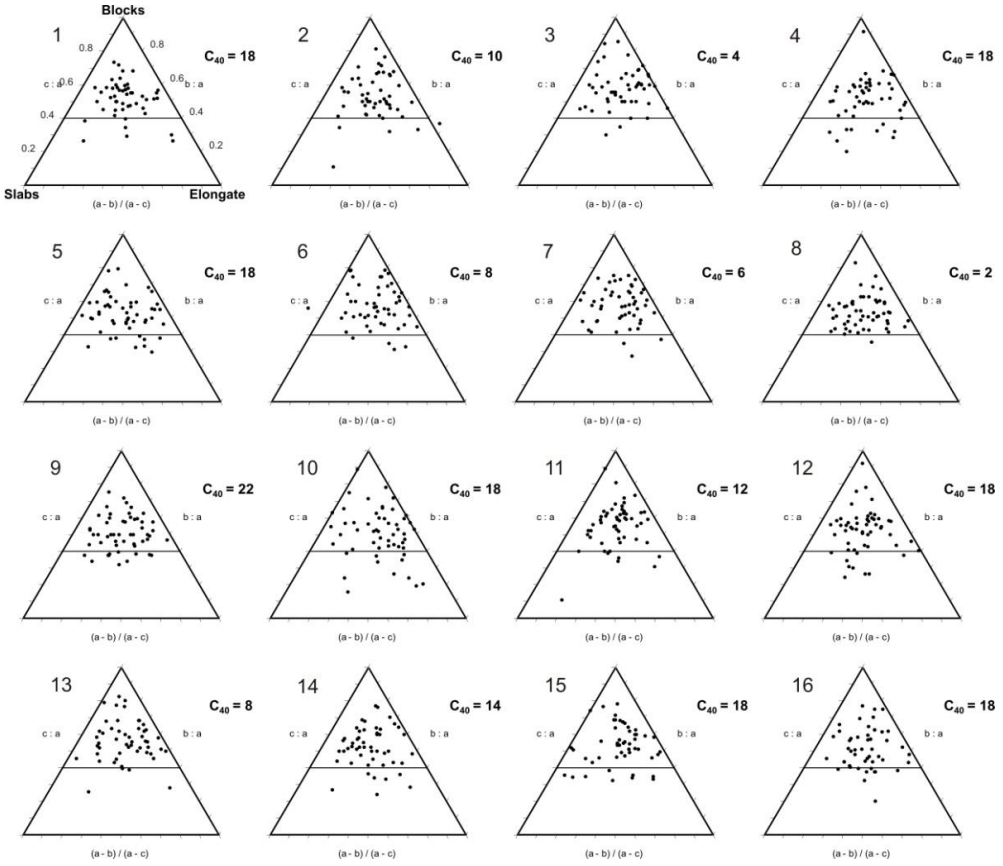

Clast shape tri-plots based on a-b-c axis length ratios for clasts from Section 5.

Figure 4-40

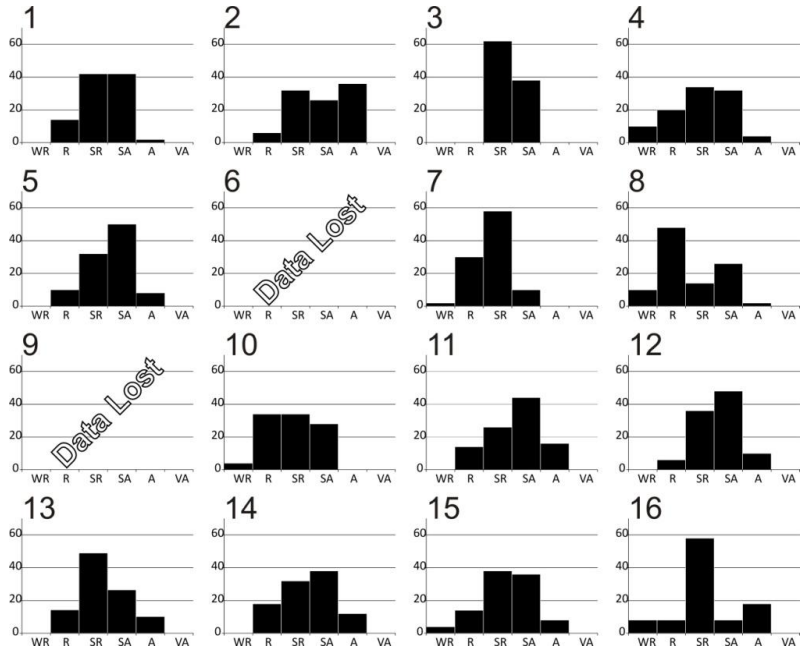

Clast roundness histograms showing data from Section 5. The location of these samples can be seen on Figure 4-26.

4.3.11 SECTION 5 INTERPRETATION

The sedimentary units exposed at Section 5, in the Sæluhúsavatn East Basin Spillway Wall, give an excellent insight into the internal make up of this 25 m wide, greater than 8 m high gravel ridge. The well rounded, open framework cobbles found at the centre of the 'pseudo-anticlinal core' are indicative of very high energy fluvial transportation within an ice walled conduit (Brennand 1994). The very weak clast fabric from this unit suggests that deposition was extremely rapid. Moving outwards from the centre of the core, the reduction in clast size and the presence of matrix material suggests a possible reduction of flow strength. The strong clast fabrics shown in samples 4, 5 and 8, with axis orientations dipping away from the centre of the ridge, is typical of what would be expected as a result of sediments deposited from a meltwater vortex flow through a sub- or englacial conduit as described by Brennand (1994). However, the alignment of a-axis parallel to flow, rather than perpendicular, is unusual under normal fluidal flows. This alignment of clast fabrics could suggest that flows were, in fact, hyperconcentrated, and that increased viscosity of the material resulted in realignment of clasts parallel to flow. In such a case, it is possible that the reduction in grainsize is a result of a switch from fluidal to hyperconcentrated flow, rather than a drop in energy. As flows continued, variations in discharge or upstream flow path resulted in the deposition of various grades of sediment, firstly resulting in an increase in grainsize as seen in the large cobbles, which make up the apex of the anticline core. There is then a sudden switch to the deposition of the bedded sands and fine gravels that are now found only along the flanks either side of this core. It is envisioned that at the time of deposition, these sand arched over the top of the whole structure, resulting in a single, normally grading unit from open

framework cobbles in the centre of the core, to well sorted sands and fine gravels at the periphery.

Following the termination of flow within this meltwater vortex, a second flow event has resulted in erosion into the bedded sands along the eastern flank of the ridge (right hand side of the exposure). This flow is believed to have fluctuated significantly, resulting in the deposition of open framework cobble and boulder stacks as well as individually incised channel structures infilled with relatively well-sorted gravels. This period of deposition was followed by a final period of erosion, which removed much of the sands from the top of the ridge and a large proportion of the aforementioned gravels and cobbles. This event resulted in the deposition of a single unit which grades from coarse gravels to well sorted laminar sands. Such a normally graded unit is an indication of reducing flow energies, likely to have occurred during the waning stage of a flood event.

Figure 4-41 presents a schematic model that illustrates the numerous flow events that are believed to have resulted in the deposition of sediments exposed at the Sæluhúsavatn East Basin spillway wall exposure.

The presence of the clay bed which lies in-between this cobble unit and the well-sorted sands below is an enigma. Such a unit, suggests a sustained period of tranquil conditions, and the fact that the clay can be traced across the anticlinal structure to the cross bedded sands on the west of the exposure suggest that the erosion event described above may not have been isolated to the eastern flank. However, the difficulty in hypothesising the processes that would result in the formation of such an un-uniform erosive contact, and allow tranquil conditions to persist long enough to allow the deposition of fines over such an irregular surface provide confidence in the hypothesis that this erosive event was isolated to the eastern flank. With the absence of contrary evidence, it is

envisaged that a short period of tranquil conditions immediately following the erosion of the eastern flank resulted in the deposition of the thick sequence of silty clay found atop of the erosive contact on the eastern side of the exposure. It is envisaged that the reminder of the silty lamina that is seen to traverse the 'pseudo-anticlinal core' and persist on the western side of the exposure, is a 'groundwater trace '. The nature of the intra-granular lamina support the hypothesis that the silts were deposited after the deposition of the gravels above by inter-granular deposition by groundwater flow through the highly permeable sediments (van de Meer et al. 2009). It is believed to be purely coincidental that the thinker silty clay unit on the eastern side of the exposure coincides with the inter-granular lamination.

Finally, based on the grainsize distribution of the diamicton which forms a thick carapace encasing the entire gravel ridge, this unit is interpreted as sub-glacial till (Boulton 1978). The thickness of this unit, and the absence of faults within the face of the exposure support sub, rather than englacial deposition, as subsequent melt out of an englacial esker would likely result in faulting and slumping. Therefore the interpretation is that the structure has been preserved subglacially for some time.

Figure 4-41

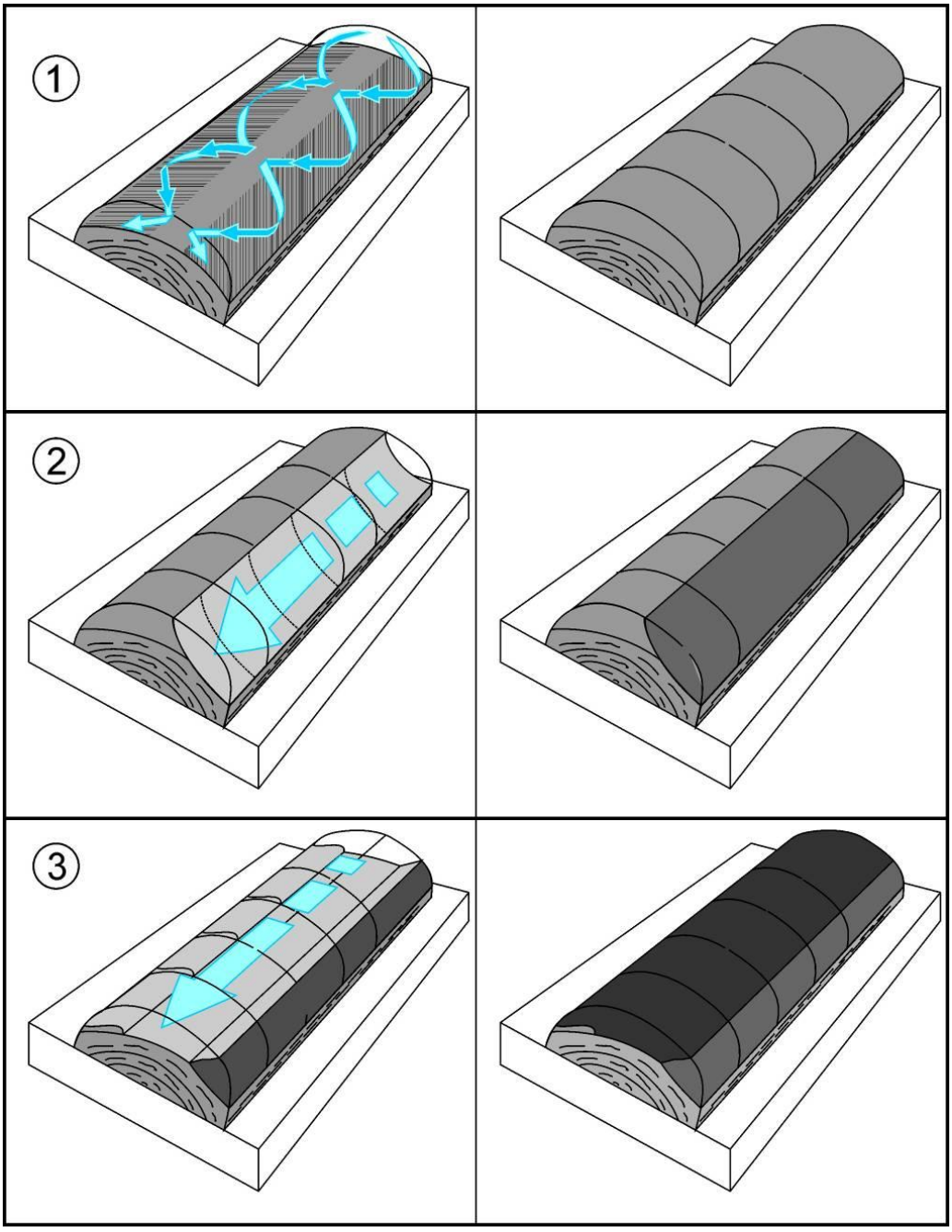

Three stage process of esker formation at Sæluhúsavatn. 1 - Hyperconcentrated vortex flow results in the deposition of a 'pseudo-anticlinal core', grading from cobbles to sand. 2 - Erosion along the eastern flank and deposition of poorly sorted cobbles and gravels. 3 - Final erosion event and deposition of normally graded gravels to sand. Formation of final subglacial diamicton not illustrated.

Based on the morphology of the above ridge and the sedimentary structures found within it, this ridge is interpreted as an esker (Price 1969; Brennand 1994; Burke et al. 2008). In recent years, it has become increasingly important to identify the exact position of deposition of eskers, with numerous authors providing great debate about the origin of sub-glacial or englacial eskers

(Price 1969; Russell et al. 2005; Burke et al. 2008). This esker is interpreted as a sub-glacial esker and is based on the pristine condition of each sedimentary unit. If this were an englacial esker, ice melt below would likely result in uneven melt out below, resulting in settling of the above sediments and the formation of numerous faults through the exposure.

Therefore, this ridge is interpreted as a subglacial esker ridge, formed within an entirely ice enclosed conduit by high-energy meltwater flows. It is likely that this esker could be interpreted as a 'multi-event' esker, having formed during multiple flood events over a long period of time. However, it cannot be ruled out that this esker formed following a numerous fluctuations of flow within the same flood event (Russell and Knudsen 1999).

4.4 SEDIMENT - LANDFORM ASSEMBLAGES WITHIN THE EASTERN SÆLUHÚSAVATN

The models presented throughout this chapter share a number of common themes, including sandur aggradation, high magnitude flood events and ice margin fluctuations. Although many of the sediments that have been interpreted through the development of these models do not show lateral connectivity, when considered together, these ideas provide significant input to the development of a conceptual model for the formation of this landscape.

4.4.1 IMPACTS OF THE NOVEMBER 1996 JÖKULHLAUP - EASTERN SÆLUHÚSAVATN

Based on detailed topographic data, geomorphological observations, and the surface sedimentology of the large proglacial fan to the west of the site, the large, ascending, channel which rises from the Lower Sæluhúsavatn Basin is interpreted as a Tunnel Channel (Ó Cofaigh 1996; Clayton et al. 1999; Beaney 2002; Sjogren et al. 2002).

The interpretation of this channel as a tunnel channel is supported by the following key observations.

A. The association of the freshly cut channel ascending from the lower Sæluhúsavatn basin and the proglacial outwash fan (**Figure 4-5** and **Figure 4-7**).
B. The lack of any major meltwater outlet or proglacial outwash fan in the Sæluhúsavatn area prior to the 1996 Jökulhlaup, as shown on pre 1996 aerial photographs (**Figure 4-2** and **Figure 4-3**), and ground based observations by others. Suggesting that that the channel can only have been eroded sub-glacially during the 1996 jökulhlaup event.
C. The presence of numerous rip-up clasts on the proglacial fan surface which were not present prior to the event confirms that major subglacial excavation took place at this location during the 1996 jökulhlaup (**Figure 4-7**).

This interpretation provides evidence of the first contemporary example of Tunnel Channel formation, and supports the findings of many researchers of Quaternary Tunnel Channels, who have hypothesized that such features are formed by high magnitude, subglacial meltwater flow (Brennand 1994; Brennand and Shaw 1994; Clayton et al. 1999; Beaney and Shaw 2000; Beaney 2002; Sjogren et al. 2002; Russell et al. 2003; Kozlowski et al. 2005; Brennand et al. 2007).

4.4.2 Formation of the eastern Sæluhúsavatn overdeepenings

The interpretation of the ridges that make up the ice proximal basin walls as eskers is considered key to the understanding of these landforms. It is believed that the presence of these eskers provides the initial conditions that are required for the formation of these over-deepened landforms.

The formation of closely spaced eskers as is seen in the Sæluhúsavatn, along with significant sandur aggradation which has been documented in the sedimentary record of the basin walls, has resulted in the partial infilling of inter ester areas and development of overdeepenings within areas of non-deposition which were still occupied by ice during the period of deposition and sandur

aggradation. **Figure 4-42** below present a conceptual model for the evolution of this landscape.

Figure 4-42

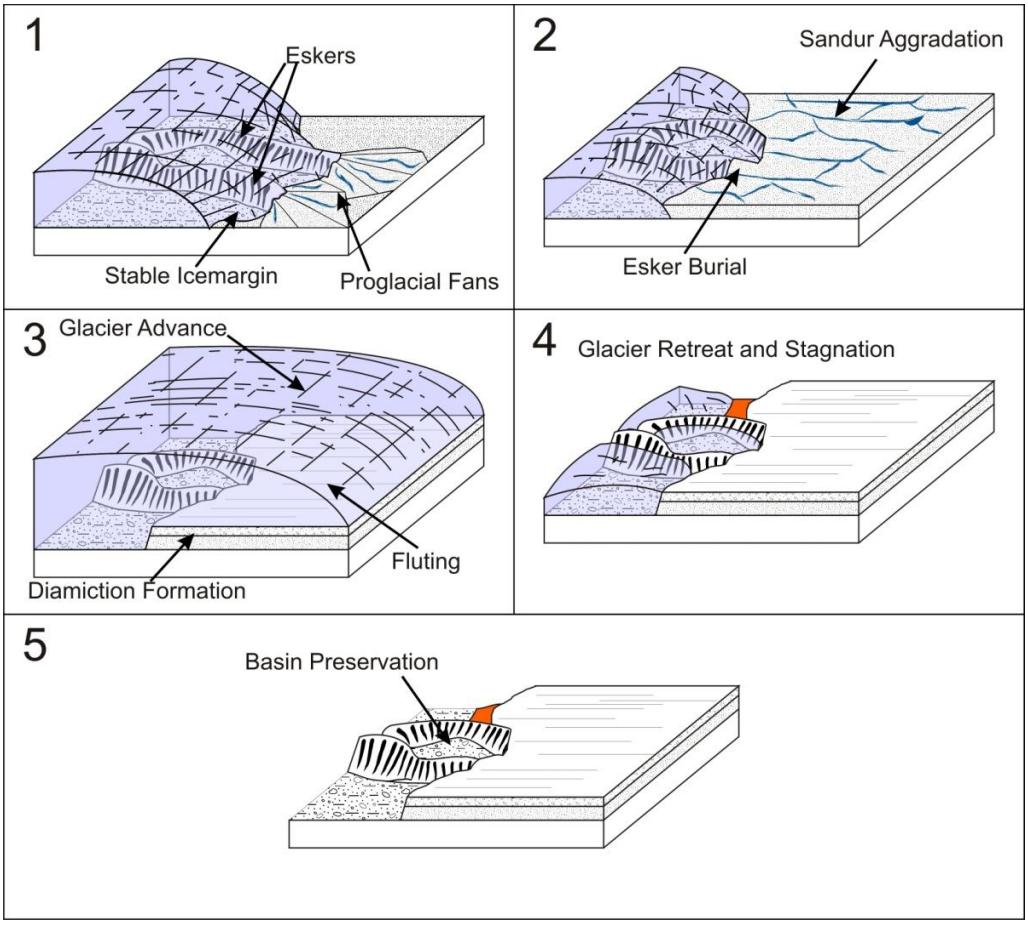

Schematic model illustrating the formation of the Eastern Sæluhúsavatn Basins. 1) Formation of eskers. 2) Sandur aggradation in front of stable ice margin. 3) Ice advance, diamicton formation and fluting of sandur surface. 4) Ice retreat and burial of stagnant ice, adjacent areas become infilled by ice marginal sedimentation processes. 5 Ice retreat and melt out of stagnant ice leading to preservation of over deepened topography.

4.5 CHAPTER SUMMARY

This chapter has presented and interpreted a number of geomorphological and sedimentological observations made within the Eastern Sæluhúsavatn site. These interpretations suggest that the formation of landforms in this area is dominated by high energy, subglacial fluvial erosion, esker formation and sandur aggradation. It has become apparent that the ice proximal basins within this area have formed as a result of eskers transecting the proglacial zone and partial sedimentation within inter esker areas has resulted in basin formation in areas of non-deposition.

The processes responsible for the formation of the ice distal, Upper Sæluhúsavatn Basin, are not as clearly understood. Sedimentary evidence provides a clear story of sandur aggradation and ice margin oscillations. However, the processes responsible for the lack of deposition within the basin cannot be determined outright. It is recommended that further work be carried out on the upper sandur surface, utilising geophysical techniques, in order to assess whether the eskers seen at the ice margin protrude further beneath the sandur to form the walls of the upper basin.

5 RESULTS - WESTERN SÆLUHÚSAVATN OVERDEEPENING

5.1 INTRODUCTION – WESTERN SÆLUHÚSAVATN OVERDEEPENING

This chapter presents geomorphic and sedimentological data collected from the western Sæluhúsavatn overdeepening. This site is located approximately 4 km west of the western Skeiðará river outlet in the ice marginal area known as Sæluhúsavatn (Figure 5 – 1). It consists of a steeply sloping area of the ice marginal trench, which can be sub-divided into a number of smaller topographic overdeepenings at lower - ice marginal, and higher - ice distal elevations. The area meets the criteria for overdeepenings set out in Chapter 1, and thus an investigation of the area's form and sedimentology are highly appropriate for this research. One of the most distinct features of this area is the presence of a number of streamlined, asymmetrical hills that are orientated in line with the ice flow direction.

Figure 5-1

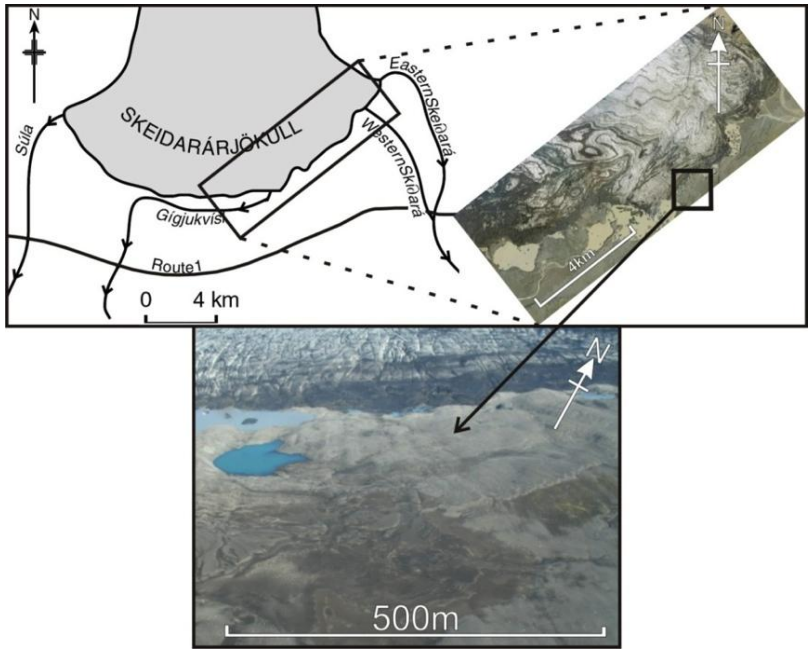

Map and aerial photograph showing the location of the western Sæluhúsavatn basins area along the margin of Skeiðarárjökull, and oblique air photograph showing the areas. Map modified from Roberts et al.,

5.2 GEOMORPHOLOGY OF THE WESTERN SÆLUHÚSAVATN

To gain an understanding of the geomorphological evolution of the western Sæluhúsavatn, time sequence geomorphological maps were produced from aerial photographs taken between 1945 and 2007 (**Figure 5-2**). Nine maps were produced in total, presented in **Figure 5-3**. These were complimented by a collection of detailed topographic data in the field which has allowed the production of a detailed digital elevation model (DEM) of the site. Detailed descriptions of the surface features have also been made from field observations.

5.2.1 TIME SEQUENCE GEOMORPHOLOGICAL MAPS

The 1945 geomorphological map (**Figure 5.3 - A**) shows the glacier margin at its most advanced position for the last 60 years. The ice margin is in contact with the surface of Skeiðarársandur, which appears to have a streamlined surface texture. There is a small proglacial lake located in contact with the central part of the glaciers margin and to the north of the lake there is a sharp, sinuous break of slope which falls towards the ice margin and grades into the sandur surface on its eastern side.

The 1965 map (**Figure 5.3 - B**) shows little evidence of the features previously visible on the 1945 proglacial surface. However, there is no evidence of any significant changes in the south east corner of the map. A number of changes are apparent in the north east corner, and the southern portion of the ice margin. In the north east there are two, near parallel, smooth breaks of slope which trend north-northwest to south-southeast. The western break is convex, resulting in a shallow sloping surface which dips towards the east-northeast. The bottom of the slope is defined by a concave break of slope, where the gradient shallows to the level ground beyond.

The greatest geomorphological change is seen in the middle / bottom of this map where a very large (500 x 400 m) lake basin has formed. It is clear that this basin is not entirely filled with water and that the southern flanks of the lake basin are considerably steeper than those to the northeast. These north-eastern slopes gradually rise to the sandur surface over a distance of approximately 250 m. A narrow ridge approximately 75 m wide with a sharp crested apex runs through the centre of this proglacial lake. The centre of the ridge appears to have collapsed, resulting in the formation of a small delta.

Figure 5.3 - C shows no evidence of change in the distal area of the ice margin between 1965 and 1968. Immediately adjacent to the ice in the northern part of the map, a number of small proglacial streams have formed as well as a small alluvial fan which is in contact with the ice margin. Meltwater flowing southwards from this fan has entered the proglacial lake at its northern limit, and a small delta has formed at this location. The ridge in the centre of the lake is now in contact with the lake basin rim at its southern end. The small flat area in the centre of the gravel ridge has expanded significantly.

By 1975 **(Figure 5.3 - d)** the primary change in the geomorphology of the western Sæluhúsavatn area is the change in the plan form of deposits within the proglacial lake. It is clear from the map that a significant proportion of the western side of the delta is no longer visible, and a number of small islands have formed, as well as a larger gravel expanse which is in contact with the ice margin in the far south of the lake. The southern end of the gravel ridge is no longer in contact with the southern edge of the lake basin.

The 1986 map shows little change in the distal area of the ice margin. Within the lake basin, the southern half of the gravel ridge has entirely disappeared, and the delta has significantly increased in area.

Aerial photographic data is extremely limited for this area of the ice margin during 1992. From the limited data that is available, it is clear that the ice margin has advanced considerably into the proglacial lake. An alluvial fan has formed at the southern end of the site and the water level in the lake has risen, and plan-form area increased to occupy a new lake basin at a higher elevation (**Figure 5.3 - f**).

By 1997 the ice margin had retreated back to a position similar to that seen in the 1986 photograph. The surface slope of the alluvial fan seen in 1992 appears to have reduced in gradient, but the overall area of the fan has increased. This fan also became disconnected from the ice margin. The large proglacial lake which was located to the east and north of this fan has drained, and appears to have been entirely infilled. To the west of this alluvial fan, there is an area of freshly exposed glacier bed and ice stagnation topography, which makes the transition between ice margin and proglacial area difficult to identify. There is no evidence remaining of the ice contact proglacial lake that occupied this area in 1986 and earlier. In the north east corner of the map, a deeply incised braided river channel has formed and there is no longer any evidence of the gentle break of slope that appeared in this location in previous years.

Glacier margin retreat of 250 m between 1997 and 2003 was accompanied by a number of significant changes in the geomorphology of the western Sæluhúsavatn area. At the northern edge of the ice margin, a number of elongated drumlins have emerged from the retreating ice margin. These are orientated approximately northwest to southeast, perpendicular to the orientation of the ice margin and parallel to the direction of ice flow. To the south of this streamlined area, an enclosed ice contact lake has formed to the north of a broad, relatively tall ridge. This ridge is approximately 100 m wide and 300 m long, with a broad crested apex. It also occupies the same position of

the northern (englacial) section of the ridge which was exposed in 1965 and last seen in 1986. To the south of this ridge, a large expanse of ice contact proglacial lake has developed.

Between 2003 and 2007 (**Figure 5-3- i**), ice margin retreat has further exposed the subglacial surface at the margin of the Western Sæluhúsavatn area. Although there is no change in the higher elevation ice distal area, the streamlined and drumlinized area in the centre of the map shows some evidence of change. The drumlins within this area appear to be better defined and the small, enclosed lake basin has been transected at its south eastern end by the formation of an alluvial fan. This alluvial fan appears to have prograded into the basin from the east. Ice retreat has resulted in the ridge feature becoming disconnected from the glacier margin and the expansion of the large proglacial lake to the south.

.

Figure 5-2

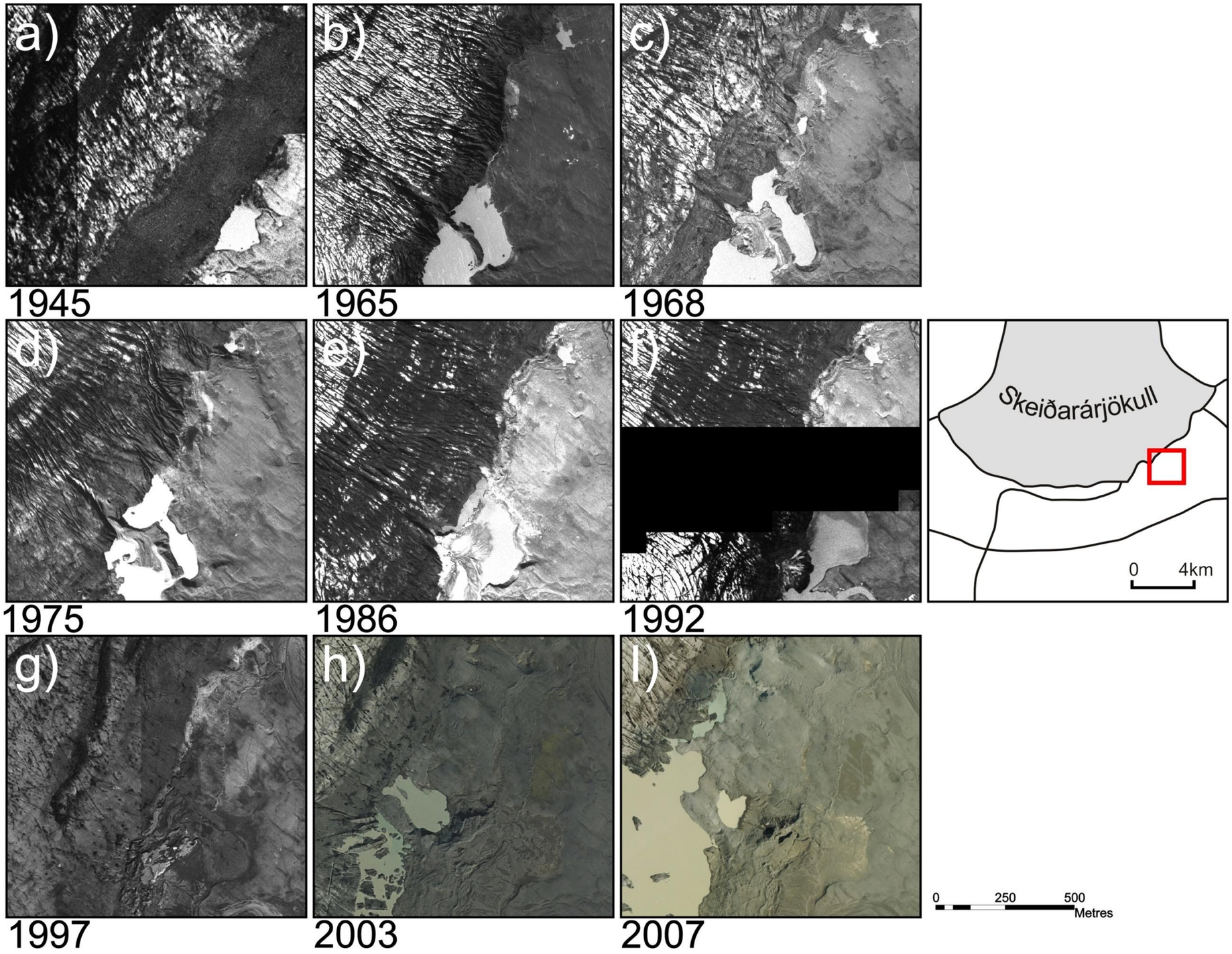

Time sequence aerial photographs of the western Sæluhúsavatn area between 1945 and 2007. These photographs form the basis of the geomorphological maps presented in ***Figure 5-3*** *below.*

Figure 5-3

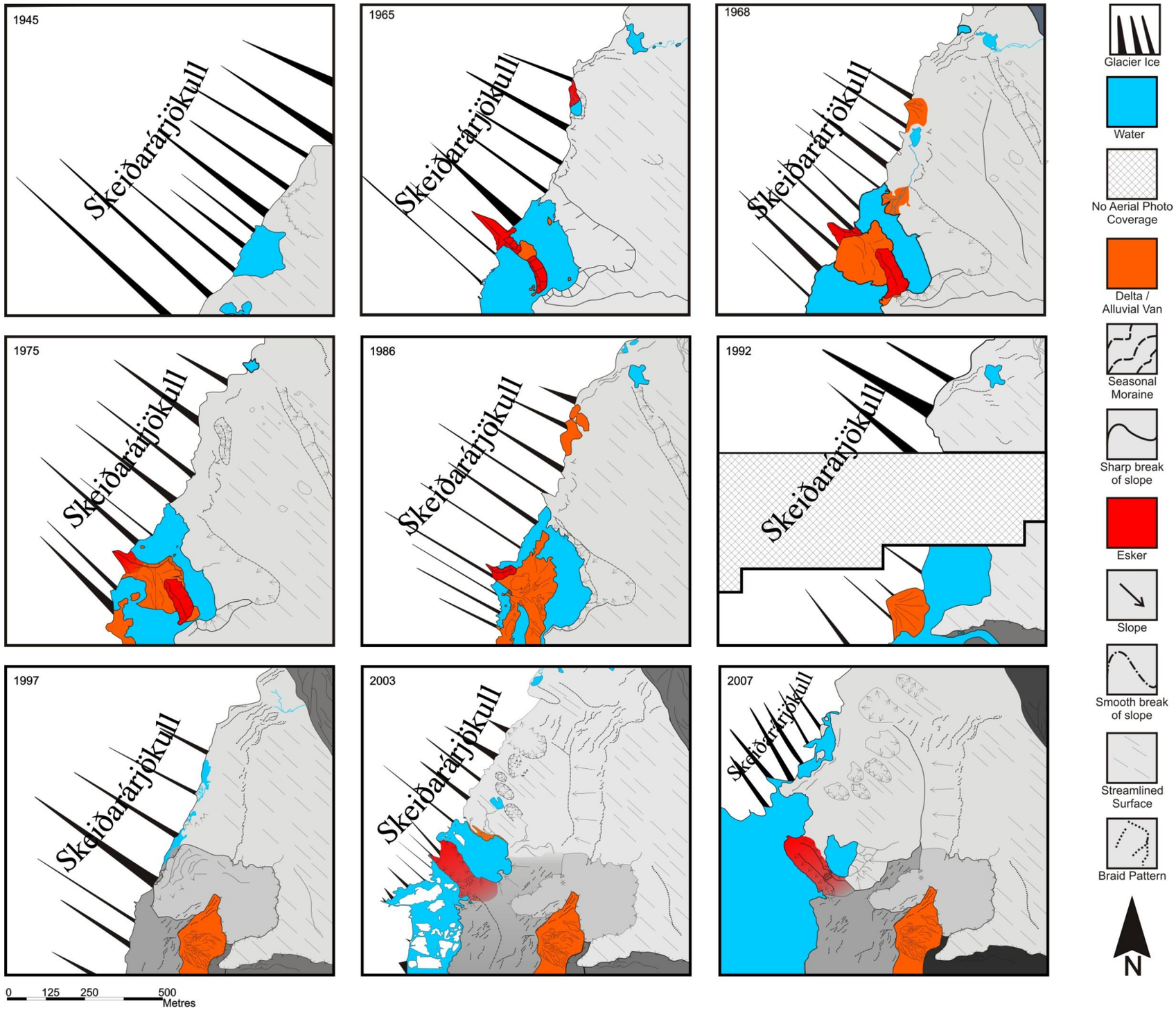

Time sequence geomorphological maps of the Western Sæluhúsavatn area of Skeiðarárjökull, southeast Iceland. These maps illustrate the morphological changes that have occurred in between 1945 and 2003.

5.2.2 WESTERN SÆLUHÚSAVATN 2006 / 2007 DIGITAL TERRAIN MODEL

High resolution differential GPS surveys of the Western Sæluhúsavatn Area were carried out in order to gain accurate three dimensional topographic data of the area under investigation (**Figure 5-4**). The resulting data were used to construct a Triangulated Irregular Network (TIN) and Digital Elevation Models (DEM) (**Figure 5-5**). Differential GPS data provides a higher level of detail than the previous maps, although the model only depicts the ice proximal area between the gravel ridge and streamlined area shown in the centre of the 2003 geomorphological map. This section of the thesis describes the geomorphology of the Western Sæluhúsavatn area based on detailed field observations, with reverence to the TIN and DEM oblique scenes shown in **Figure 5-5.**

Since 2003 it is clear that the ice has retreated significantly, further exposing the area of streamlined glacier bed, and resulting in the small proglacial lake becoming detached from the ice margin by a narrow strip of recently exposed glacier bed. The gravel ridge has also become detached from the ice margin, and ice retreat has allowed the proglacial lake located to the south, to develop north around the ridge. The gravel ridge is approximately 19 m high, with an elevation of 109 m ASL. To the north of the gravel ridge, the streamlined, drumlinized landscape is clearly visible in the plan form TIN and DEM oblique scenes, which highlight the asymmetric oval plan form and rounded surfaces of these features.

This detailed topographic data also highlights the steeply reversed slope down which the glacier has retreated over the last 18 years. Over a distance of 450 m, between the glacier margin and the highest point of the outwash plain, the land surface rises approximately 40 m out of the ice proximal trench. The

smaller basin features are formed by ridges and drumlinized topography that divides the ice proximal trench into individual overdeepenings.

Figure 5-4

Raw differential GPS data of the Western Sæluhúsavatn Area

Figure 5-5

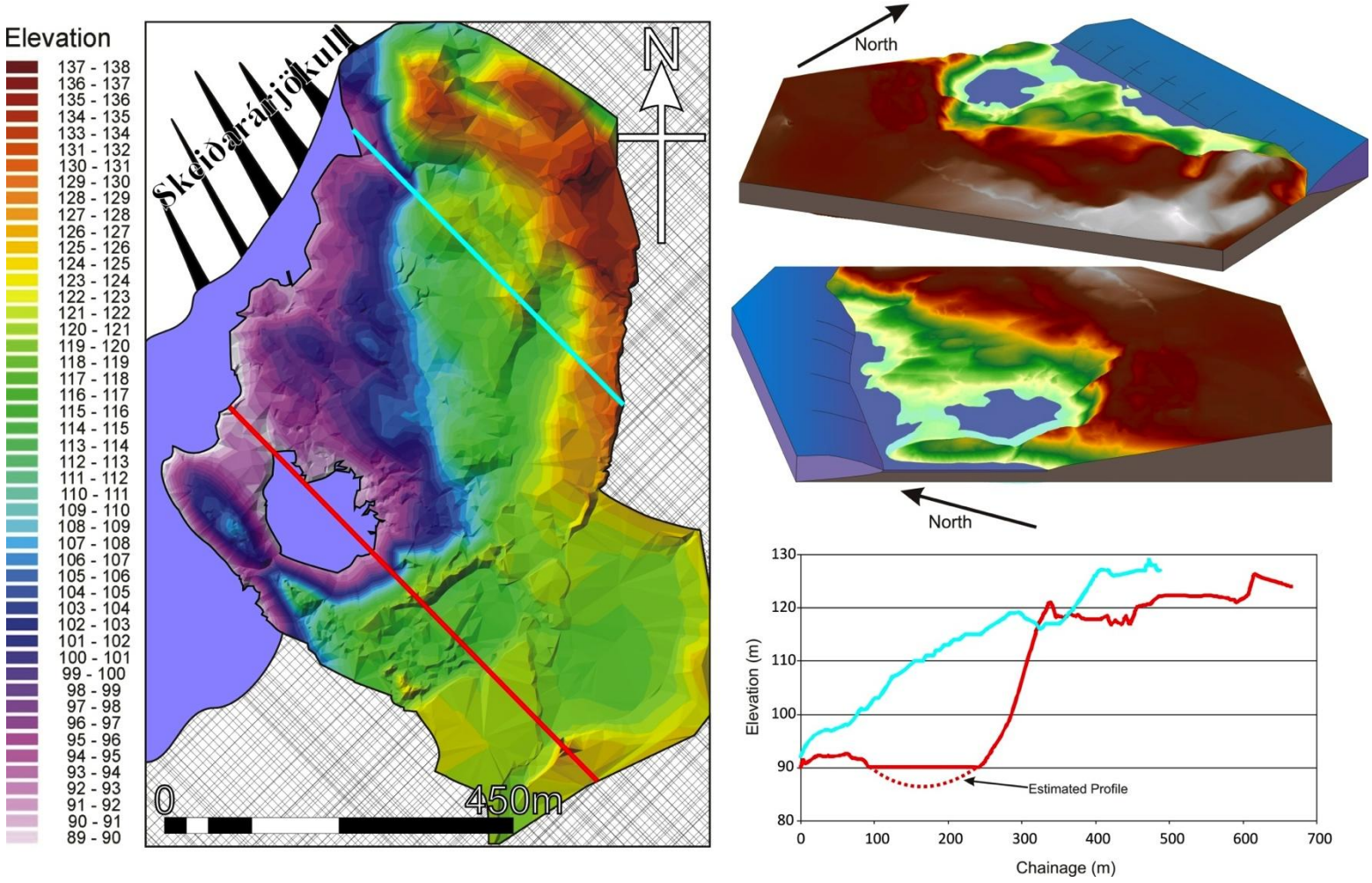

Triangular Irregular Network (TIN) with oblique angle DEM's of the Western Sæluhúsavatn area. TIN is approximately 500 m across . Red and Blue lines make the positions of longitudinal cross sections across the north and south of the site. Cross section profiles presented with approximate 10x vertical exaggeration.

5.2.3 WESTERN SÆLUHÚSAVATN GEOMORPHOLOGY

The western Sæluhúsavatn area can be divided into three geomorphologically distinct regions labelled 1, 2 and 3 on **Figure 5-6**. The northern ice proximal zone comprises the area to the north of a small, lake basin while the southern zone incorporates the lake and ridge described previously to the south. The ice distal area comprises the area east of the lake and ridge, which is at a higher elevation and can be generally characterised by the ice margin parallel ridges in the north and the steep break of slope which defines the top of the lake basin in the south.

Figure 5-6

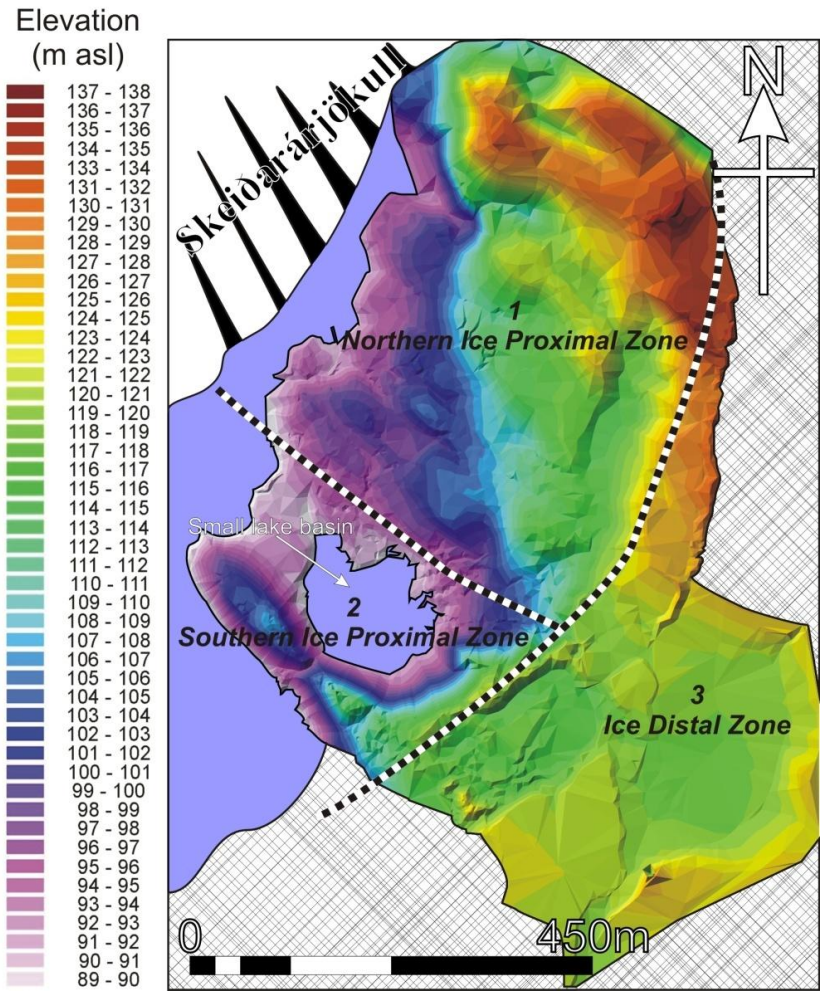

Triangular Irregular Network (TIN) of the Western Sæluhúsavatn indicating the locations of the Northern and Southern Ice Proximal Zones and the Ice Distal Zone.

5.2.3.1 Northern ice proximal features

The northern ice proximal area can be easily distinguished by its convex long profile and abundant drumlinoid topographic features (**Figure 5-7 and Figure 5-12**). These features are commonly 10's of metres wide, up to 100 m long and 1 - 3 m high. Each is orientated with its long axis aligned towards the south east. These features are much more apparent on the flatter surface closest to the ice margin below an elevation of approximately 109 m A.S.L. Above this elevation, streamlining of the ground surface is still apparent, however it is less easily identified on the DTM, and the lee sides of these features tend to be merged with the ascending ground surface, making them less easily identifiable. In a number of places, small, cylindrical, vertical walled shafts have formed in the surface of this drumlinoid topography.

Where linear features are located on the stoss side of larger topographic features, their orientation is slightly diverted around the sides of the feature where as linear features located on the top or at the lee of larger features have an orientation parallel with the main lineated topography (**Figure 5-8**).

The surface of this recently deglacierized terrain is composed primarily of poorly sorted gravels and cobbles. In a number of randomly distributed locations across this recently deglacierized surface, the surface grain size increases significantly, and comprises large, well rounded, cobbles and boulders.

The largest drumlin located in the northern part of this area has a very distinctive, near vertical, south facing flank. This flank is perfectly aligned with what appears to be a narrow, ice flow parallel gully, which rises up in-between the flank of this drumlin and the adjacent drumlin to the south (**Figure 5-9**)

Figure 5-7

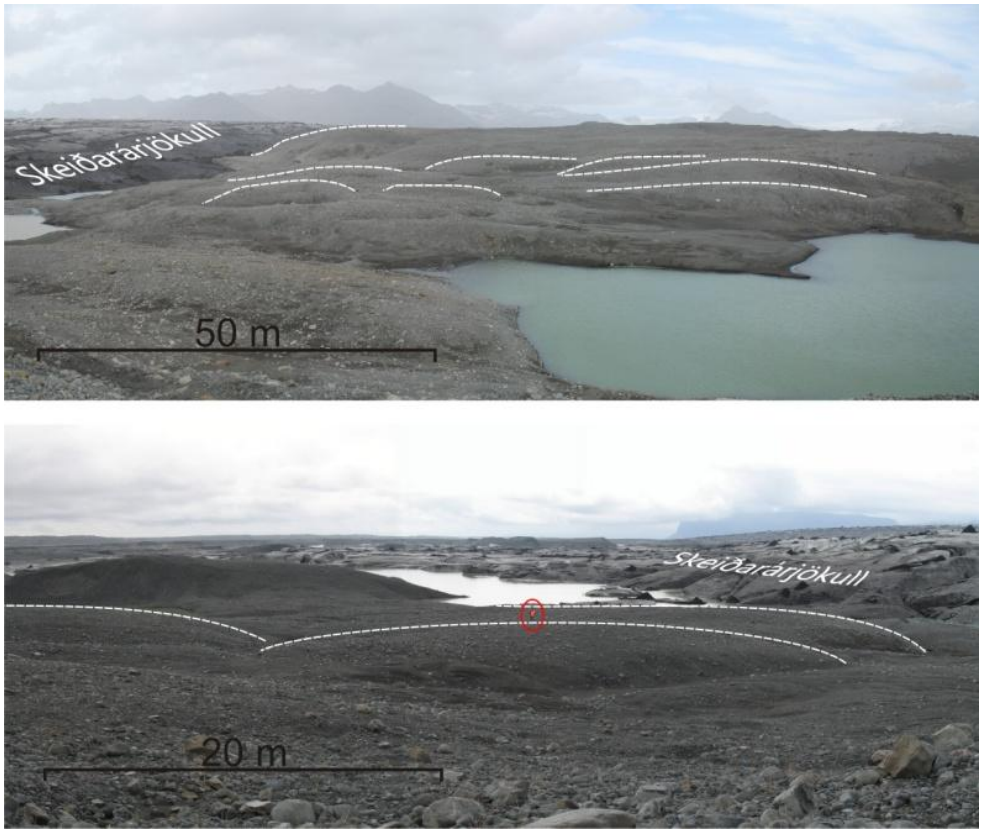

Photographs of the western Sæluhúsavatn drumlinoid features looking northeast (top) and west (bottom). Dotted lines depict the streamlined apex of the features upper surface. Person circled for scale in middle distance.

Figure 5-8

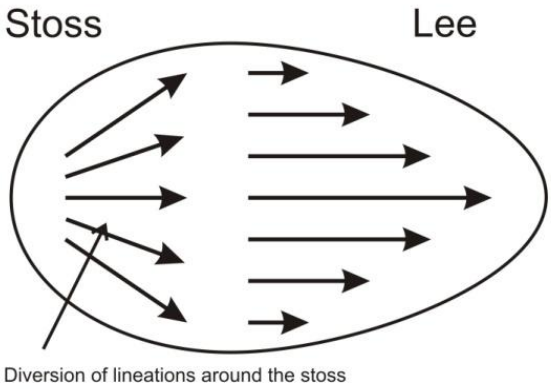

00Schematic illustration of the diversion of lineations around the stoss of larger streamlined topography.

Figure 5-9

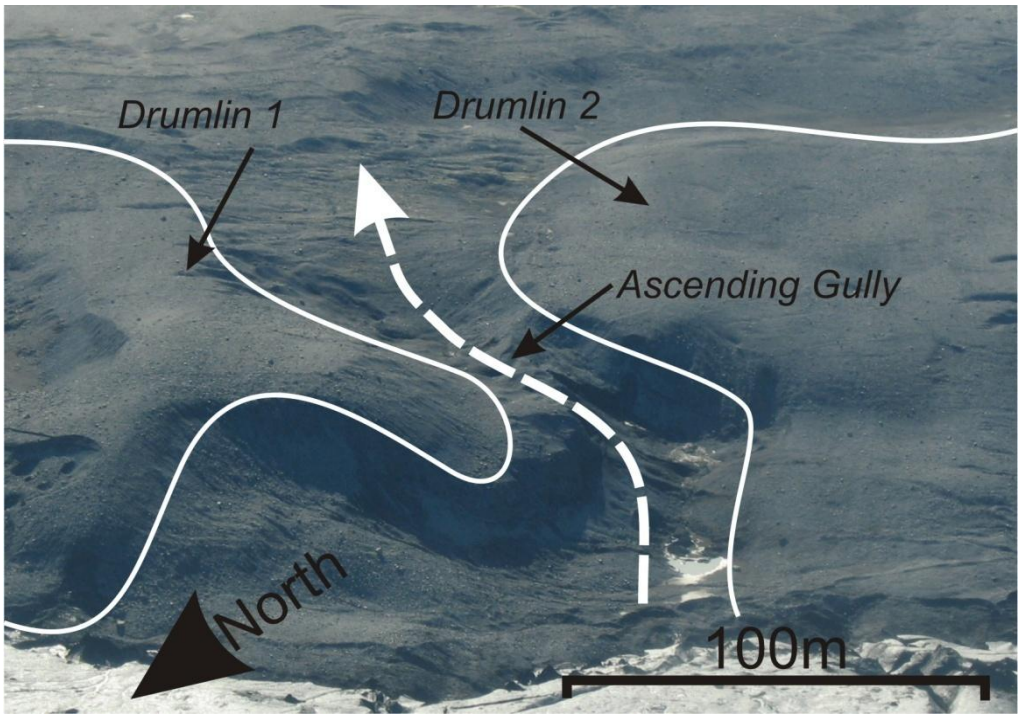

Oblique aerial photograph of the most northern drumlinoid landform in the Western Sæluhúsavatn Area. Illustrating the presence of an ascending gully along its southern flank.

5.2.3.2 Southern ice proximal features

The southern ice proximal zone covers a much smaller area than that to the north and is clearly identified by the switch in the nature of the cross section. If a cross section were drawn north west to south east (ice proximal to distal) across the northern zone, this would depict a clear convex topography, where as in the southern zone, a proximal to distal cross section would be concave. The most morphologically distinct feature of this zone is the large gravel ridge at the areas southern boundary. This ridge is approximately 300 m long and is orientated in a northwest - southeast direction. The highest point, in the middle of the ridge, has an elevation of 109 m ASL, resulting in a relief amplitude of 19 m. The height of the ridge increases an additional 10 m where its southern end grades up into the sandur surface to the south. A deep and narrow gully up to 10 m in depth cuts across the southern end of the ridge approximately 200 m from the ridge's northern tip.

The upper surface of the ridge is very similar to the surfaces seen in the area to the north, composed of striated, lodged, and bulldozed boulders and flutes, which are all orientated parallel with the orientation of the ridge, and small seasonal advance moraines on the stoss, ice proximal end of the ridge. **Figure 5-12** shows the location and orientation of linear features in this area. The rose diagram illustrates that the majority of these features are orientated towards the southeast, which is consistent with the local ice flow direction.

5.2.3.3 Western Sæluhúsavatn ice distal geomorphology

The upper surface of the western Sæluhúsavatn ice distal area has a morphology that is distinct from the ice proximal zone. The area is defined by a series of shallow, enclosed basins, interconnected by narrow spillways and broad areas of flat, unconsolidated, gravelly topography (**Figure 5-10**). Basin 1 is located immediately to the south of the of the steep water filled lake basin described in **Section 5.2.3.2**. The northern edge of this basin comprises a tall, steep ridge composed of relatively fine sands and gravels. It is clear that this ridge contains a significant amount of buried ice, seen in exposures at the surface. The bed, or inner surface of the basin, is flat towards is north eastern edge, however it becomes increasingly undulating towards the south where the topography is composed of a series of long, rectilinear ridges up to 10 m long and 1 m high (**Figure 5-11**).

Figure 5-10

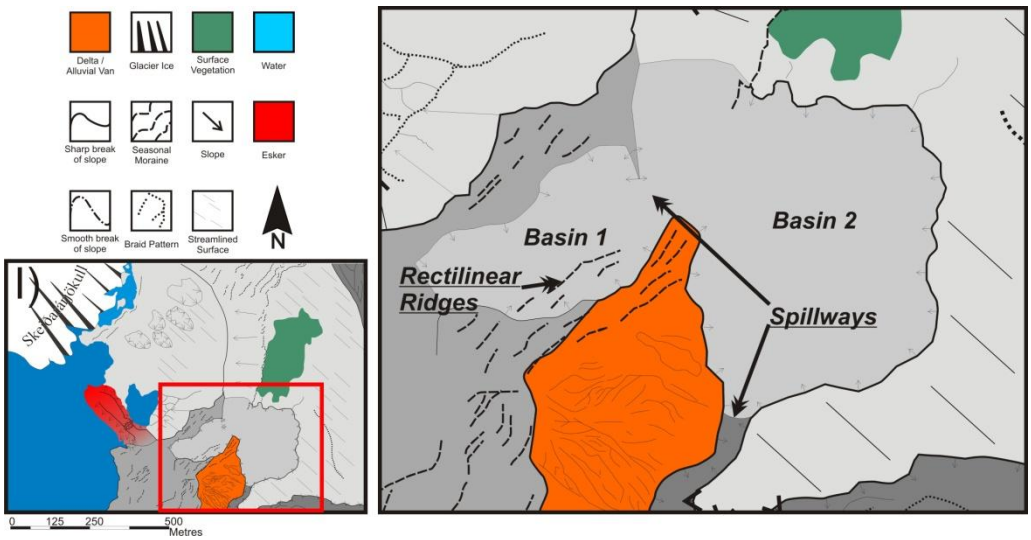

Close up geomorphological map of the Western Sæluhúsavatn ice distal area highlighting the location of basins and ridges.

Figure 5-11

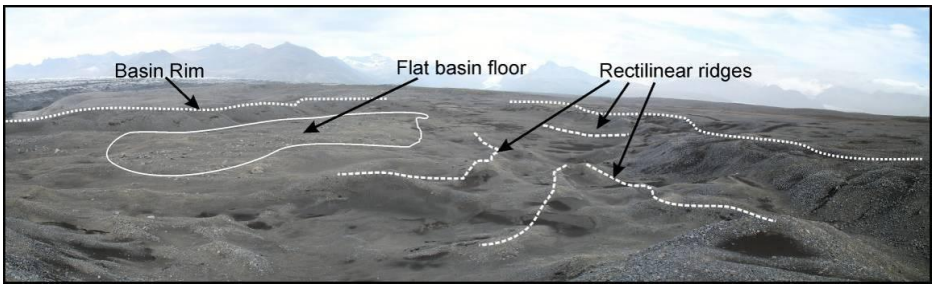

Photo-mosaic illustrating the main features of basin 1 found at the Western Sæluhúsavatn site.

The southern edge of this basin is defined by a steep break of slope, which rises 1-2 m up to a very flat, broad, surface with a fan shaped plan form. The upper surface of this fan is composed of relatively fine grained, gravelly deposits with occasional cobbles and boulders. The eastern edge of basin 1 is defined by another sharp break of slope that drops down 1 m to a second large enclosed basin to the east (Basin 2 - **Figure 5-10**).

Basin 2 is enclosed on all sides except for a shallow and narrow gully which forms a link to basin 1, and a larger breach in its southern edge where a spillway intersects the dry fluvial channel to the south (**Figure 5-10**). This

channel is orientated initially south from the basin before it turns east, around an area of raised topography, and leads towards the coast across Skeiðarársandur. The bed of this second upper level basin is composed entirely of silty sands with occasional gravel clasts. This has given rise to the formation of small scale aeolian sand ripples on the surface of the basin floor.

To the north and east of basin 2, the character of the sandur surface changes distinctly. There is an increase in the amount, and maturity of vegetation and the surface has better developed rock armour which suggests that this is an older surface which has not been modified by glacial action or outburst flood in recent years. To the north, large moraines 2 - 3 m high mark the edge of this more mature surface.

Figure 5-12

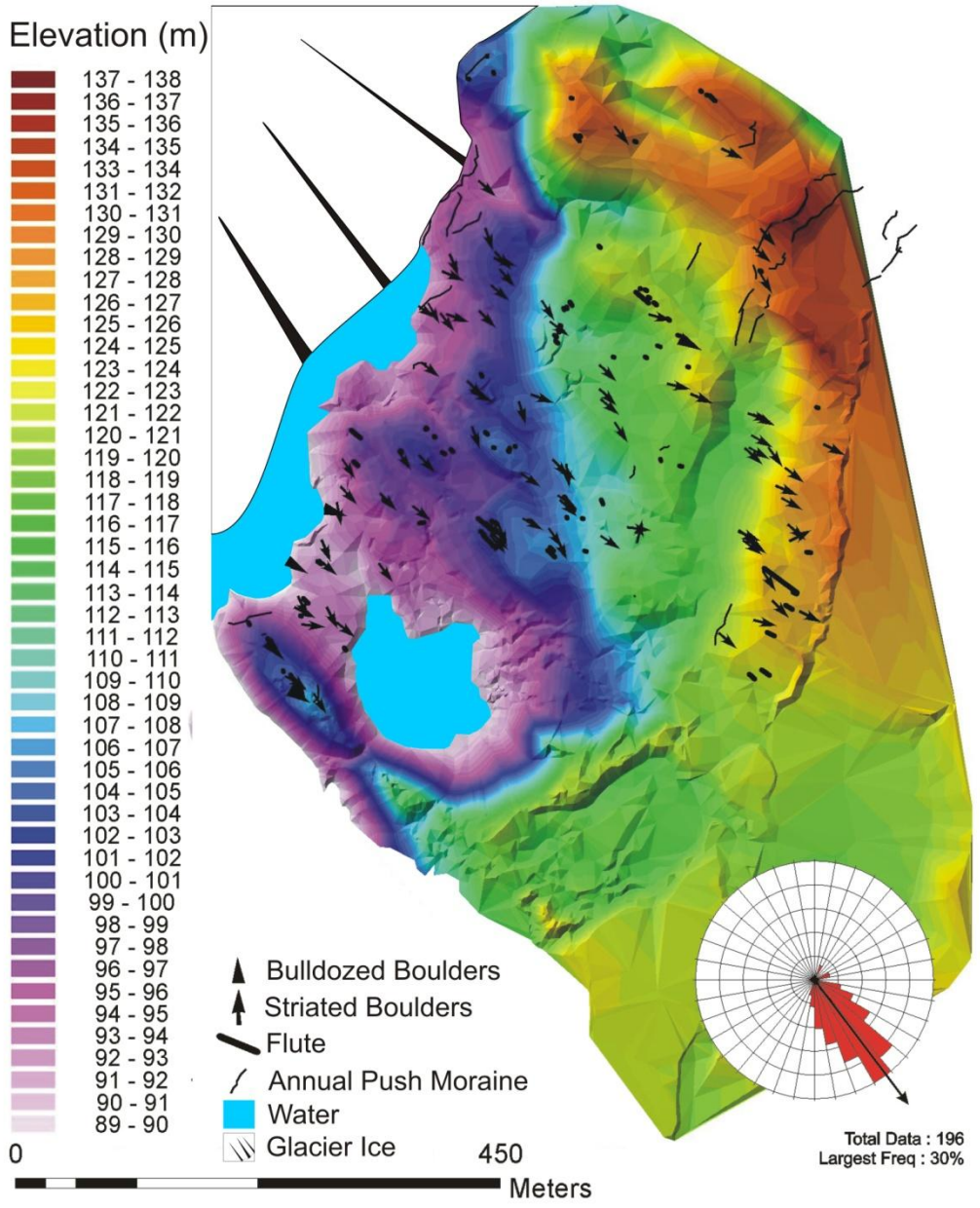

Triangular Irregular Network (TIN) of the western Sæluhúsavatn area produced from differential GPS data. The TIN shows the topography of the western Sæluhúsavatn and the locations of flutes and striates / bulldozed boulders on the proglacial surface. Rose diagram illustrates the orientation of liner features within the western Sæluhúsavatn.

5.3 SEDIMENTOLOGY OF THE WESTERN SÆLUHÚSAVATN

Three sedimentary exposures have been investigated within the Western Sæluhúsavatn. The first at the southern edge of drumlin 1, the second at the north edge of drumlin 1, and the third was excavated through an ice-margin-parallel lineation composed of cobbles and boulders located to the south of drumlin 1 (**Figure 5-13**).

Figure 5-13

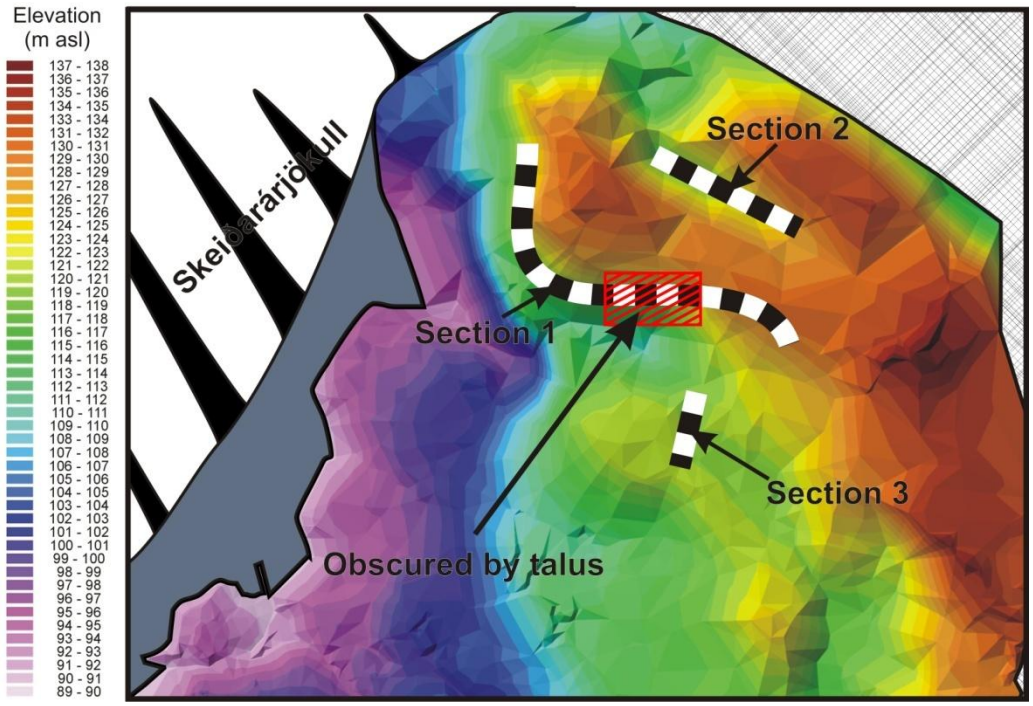

Map showing the locations of sedimentary exposures and excavations in the Western Sæluhúsavatn.

5.3.1 SECTION 1

This exposure comprises a 200 m long, 5 - 10 m high, face on the south and west facing edges of a large drumlin at the north of the area (**Figure 5-13** & **Figure 5-14**).

The western, ice proximal end of the exposure reveals a distinct, very poorly sorted unit of very well rounded, clast supported cobbles and boulders.

The matrix material makes up approximately 10% of the unit and comprises relatively poorly sorted silty sand.

Grain size and clast fabric analysis were not carried out at this location due to the large size of clasts involved and the difficulty associated with collecting a large enough sample to be representative. A high degree of clast fracturing is seen within the cobbles and boulders within this unit (**Figure 5-14 – A**).

To the south and east of this cobble unit, the exposed face exhibits a distinct change in character as the single unit becomes three distinct bedded units (1 - 3 **Figure 5-14 - B**). The bounding surfaces towards the west of the lower two units is obscured by talus, however it is evident that the upper bedded unit is a continuation of the cobble unit to the west (**Figure 5-14 - B**).

Unit 1 comprises a matrix of massive, poorly sorted sand and gravel, which supports rounded to well-rounded clasts. These clasts range from pebble to boulder size. Through the middle of this lowest unit there is a 0.1 - 0.15 m wide, vertical silty sand vein or dyke. This feature diverges horizontally along the length of what is considered to be the bounding surface between the units above (**Figure 5-14 - B and C**). There is no evidence of preferential alignment of clasts within this unit.

The lower contact unit 2 (**Figure 5-14**) is defined by the sandy silt structure, which has penetrated up from the unit below. Thus structure has obscured the true nature of the bounding surface between these two units. The main body of this unit is composed of a single, normally-graded unit of sand, cobbles, and boulders. This normal grading is occasionally interrupted by outsized cobbles. Where the upper unit is dominated by fine sand and gravel, these sediments have a distinctive, pseudo-bedded texture which is revealed by subtle, sub-horizontal alignment of pebble clusters. Like the clasts that make up

other sedimentary units in this area, these have a very well rounded surface texture and high degree of sphereicity.

The upper bounding surface of unit 2 is defined by a thin (1 - 2 cm) unit of silty sand (**Figure 5-14 - D**). Like the unit below, this silty unit is connected to the silty unit at the lower bounding surface by a second silty, vertical vein or dyke located to the east of the lower vertical structure. This upper structure defines the uppermost limit of these dyke features.

Unit 3 of this exposure is composed of massive, very poorly sorted, well rounded cobbles and boulders, similar to those seen closer to the ice margin. There are a number of 'areas' within this unit where subtle changes in the sedimentary nature of the exposure can be seen. However, there is no spatial pattern to these variations and no apparent bounding surfaces.

The upper and lower section of this unit contains higher concentrations of large cobbles and boulders while the central portion is composed of subtly more uniformly sorted coarse gravels, pebbles, and cobbles. The upper portion of this unit also exhibits a large number of cobble and boulder clusters that appear to be aligned horizontally.

Unit 3 also exhibits slight variations in the colour of the matrix material. The lower left (west) and upper middle portions of this unit are distinctly darker in colour (dark brown) than the remainder of the unit that is pale beige in colour. The most likely explanation for this variation in colour is due to the retention of moisture as a result of a subtle variation in grainsize, with the darker colour most prominent where the matrix material is finer (Tucker 1988; Collinson et al. 2006).

A large section of the middle part of this exposure, from approximately 100 - 150m, is obscured by talus (**Figure 5-13**). At the far eastern end of the face

the height of the exposure reduces significantly and the sedimentary beds are pinched out to just two visible units (**Figure 5-14 - E**).

Unit 4 is composed of the poorly sorted, well rounded cobbles and boulders seen elsewhere in the exposure. This unit is overlain by Unit 5, a thick (>1 m) unit of poorly sorted, silty diamicton. Unit 5 represents the uppermost sedimentary unit and is topped by a thin cobble lag that comprises the upper surface of the landform.

The clastic dyke located in the centre of the exposure, is composed of a silty clay pipe approximately 3 – 5 cm in diameter (**Figure 5-14 C**). The walls of this pipe are up to 5 mm thick and there is evidence that these clays have diffusely penetrated into the surrounding sands and gravels.

The pipe structure itself is infilled with clearly bedded very well sorted fine to medium sand. These sands are occasionally inter-bedded with 2-3 mm thick units of sandy silt and clay. The angle of bedding relative to the pipe walls is also seen to vary along its length. These variations in angle occasionally occur within the vicinity of the silt and clay beds (**Figure 5-14 C**).

Figure 5-14

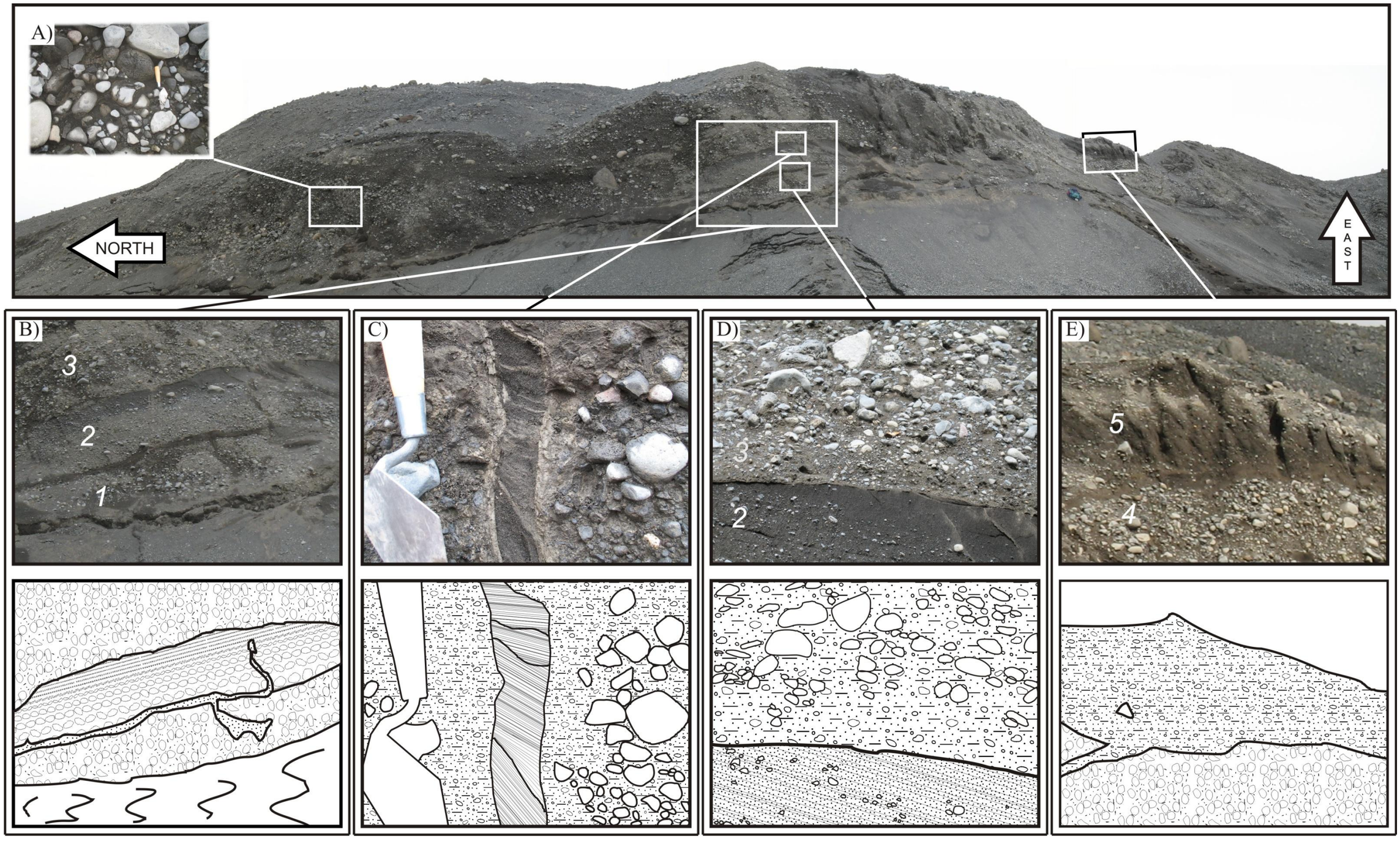

Photo mosaic and sketches of sedimentary structures at the Western Sæluhúsavatn Section 1 . A) Numerous rounded and fractured cobbles and boulders. B) Massive and normally graded sands and gravels with horizontal and vertical clastic dyke, C) Close detail of the clastic dyke, showing clay lining and bedded sand infill, D) Well sorted pseudo-bedded fine sands overlaid by poorly sorted cobble conglomerate, and E) Poorly sorted cobbles and boulders overlaid by poorly sorted diamicton. .

5.3.2 SECTION I: INTERPRETATION

The large clast size and well rounded nature of the cobble and boulder unit found at the ice proximal end of this exposure are indicative of very high energy fluvial transportation. The very poor sorting may suggest very rapid deposition from turbulent flow leading to on-mass deposition and the formation of structure less deposits (Costa 1988; Russell et al. 2003). This interpretation of very rapid deposition is supported by the abundant fractured clasts found within this unit. Such fractured clasts have been interpreted as the result of high energy clast impacts when rapidly transported cobbles come to an abrupt halt. It is inevitable that clasts fracture through percussion whilst they are in transport; however the fact that all the fragments of these fractured clasts remain in contact suggest that this fracturing did not occur whilst the clast was in motion. An alternative hypothesis suggests that such fracturing could be a consequence of post depositional fracture caused by earthquakes or faulting (Riggs and Lindemann 2008). However, considering the unconsolidated nature of the sediments, and the relative rarity of high magnitude earthquakes in this area of Iceland, which are likely to result in fracturing of these clasts, this hypothesis can be rejected.

The central portion of this exposure is clearly composed of alternating beds of massive and normally graded deposits. These massive, poorly sorted units are consistent with rapid deposition from highly turbulent flows (Costa 1988; Russell et al. 2003) while the better sorted, normally graded deposits are indicative of reducing energy, waning stage deposits (Maizels 1989; Collinson et al. 2006). The texture of these finer deposits is similar to those described by Russell et al., (2001) from the ice proximal end of the major 1996 jökulhlaup, waning stage outlet known as the 'double embayment'. Those deposits were interpreted as having been deposited by sub-critical flow immediately

downstream of a hydraulic jump formed by flow expansion at the mouth of a primary meltwater outlet. The alternating nature of was interpreted as a result pulsating flows which had been witnessed during that single event. A similar interpretation is favoured for the alternating beds of massive and normally graded fluvial deposits found within this section. However, the timing of individual depositional events is not possible to ascertain.

The clastic dykes present within with this exposure are interpreted as water escape structures based on their morphology, geometry, and sedimentary infill (Lowe 1975; Lowe 1976; van de Meer et al. 2009). The absence of an erosive surface between units 2 and 3 where these structures terminate provides evidence that these features did not penetrate downwards through the sediments as a result of overriding ice and thus it is more likely that the water flow direction was upwards through the sediments. Once this escaping water reached the bounding surface between units 2 and 3, a change in the porosity of the sediments it likely to have allowed this water to dissipate with the unit, leading to the termination of the structure.

The presence of water escape structures suggests that these sediments were deposited very rapidly, on top of highly saturated sediments (Russell et al. 2003). Considering the well developed, pipe structures that are present, it is clear that these features were formed by liquidised flow as a result of an external force producing increased porewater pressure, rather than fluidization caused by settling of the parent material (Lowe 1976).

The presence of these clastic dyke structures at the surface of this exposure provides evidence that this scarp has been actively eroded and that the morphology of the feature has been modified since its initial deposition. Such structures form as a result of highly pressurised groundwater that is forced towards the surface through the sediment body (Lowe 1975). As always, this

water follows the most hydraulically efficient pathway. Such structures could not have been formed at the surface / ice contact, as flow along the ice contact would undoubtedly be a more hydraulically efficient pathway than through the substrate and the clastic dyke would not have formed.

5.3.3 SECTION 2

Section 2 comprises a 50 - 60 m long exposure located on the north facing slope of drumlin 1, orientated parallel to the drumlin's long axis. This unit is composed of a single unit of steeply dipping beds of poorly sorted coarse gravel with a large proportion of rounded to well rounded clasts ranging from pebble to boulder in size. The beds in this unit have a dip orientation which is up ice, towards the ice margin. The unit is capped by a thin, < 0.5 m, carapace of poorly sorted diamicton.

These up ice dipping beds are very subtle, and individual bedding plains are highlighted by the steep alignments of clasts within the face and the continuity of grainsize along each bed. The angle of dip reduces away from the ice margin, with an up ice dip of approximately 35° at the ice proximal end of the exposure, reducing to approximately 15° distally **(Figure 5-15)**

Figure 5-15

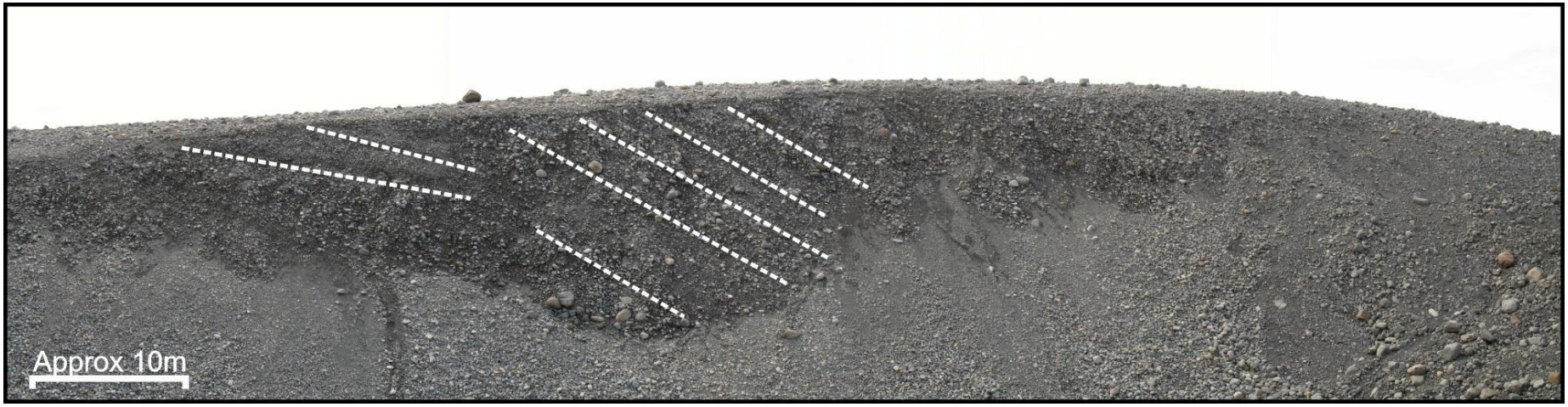

Photograph mosaic of the Western Sæluhúsavatn north facing exposure. Illustrating the up ice dipping coarse gravel beds and the smooth convex shape of the upper surface.

5.3.4 SECTION 2: INTERPRETATION

The large clast size and well rounded nature of the materials which make up this exposure are indicative of very high energy fluvial transportation (Baker 1984; Costa 1988), while the very poor sorting may suggest very rapid deposition from turbulent flows (Costa 1988; Russell et al. 2003). Although the nature of the exposure was insufficient to allow detailed analysis of individual structures, the position of these up ice dipping beds leads to the interpretation of these units as back set beds. The position of this drumlin, and the lack of any significant source of water flowing from the south to the north, provides adequate justification that these are not foreset structures. The presence of such back set bedding within this exposure is indicative of stoss side, bedform aggradation (Brennand 1994; Burke et al. 2008). Such sediments have been interpreted previously, associated with the formation of large scale microform formation within enlarged sub and englacial conduits, associated with deep flow depths (Brennand 1994; Burke et al. 2008). Back set bedding has also been associated with deposition downstream of a hydraulic jump, caused by flow expansion at a glacier outlet (Russell and Knudsen 1999).

The presence of coarse grained, back set bedding provides significant evidence of a interpretation associated with high energy fluvial transport and deposition at an area of flow expansion (Baker 1984) such as would be seen at a melt water outlet. As such it would be acceptable to interpret these sediments to be the remnants of coarse grained alluvial fans. However, detailed records of the ice marginal position of Skeiðarárjökull over the last 100 years or so (Wisniewski et al. 1997) suggest that this area of Skeiðarárjökull's ice margin has not been exposed since before the glacier reached its Little Ice Age maximum, as a result it is unlikely that these deposits were laid down within a subaerial environment. As such, it is considered more likely that the sediments

which make up this exposure were deposited sub or englacially, within a cavity, and the resultant flow expansion resulted in the upstream aggradation of sediments on the stoss of a macroform. It is known that there were no 'major' meltwater portals in this area of the ice margin during the 1996 jökulhlaup and it is therefore likely that these sediments were deposited during one of Skeiðarárjökull's historic jökulhlaups.

5.3.5 SECTION 3

At the northern end of the site, just south of drumlin 1 (**Figure 5-9**), there are a number of long, ice margin parallel, gravelly cobble, linear ridges on the deglaciated surface. These linear ridges are typically 10s of meters long, 0.25 - 0.5 m wide and approximately 0.1 m in height. They are defined by a convex, rounded apex and are composed of material similar to the surrounding area, but with a higher concentration of pebbles and cobbles (**Figure 5-16**).

The aim of excavating through this linear ridge was to investigate any potential link between the surface lineations and the formation of the surrounding topography. Previous authors (Boulton and Caban 1995; Boulton et al. 1995; Piotrowski 1997; van de Meer et al. 2009) have hypothesised that erosion of a glacier substrate could be linked to ground water flow through the substrate, below the ice / sediment interface. It is considered possible that this linear ridge represents a point at which pressurised ground water may have breached the surface of the glacier substrate from below.

Figure 5-16

Photograph of the Linear Surface Ridge prior to excavation. This cobbles ridge is perfectly aligned with the sandy ridge in the background that remains in place due to buried glacier ice.

To test this hypothesis, three excavations were made along the length of a single lineation. Each of the excavations showed exactly the same sedimentology except for one minor variation. Each pit was excavated to a depth of 0.5 - 0.75 m and each was composed primarily of a single unit of poorly sorted sandy diamicton that was consistent with the surrounding surface. There was no variation in the sediments that composed the ridge, and those adjacent or below.

However, in two of the three excavations, narrow 'lenses' of well sorted sand were present. These 'lenses' were orientated near vertically and have an apparent wedge shape, with the widest end of the wedge at the ridges upper surface and tapering to a point at a depth 0.1 - 0.25 m. **Figure 5-17** shows a photograph and sketch of one of the excavations through this ridge.

Figure 5-17

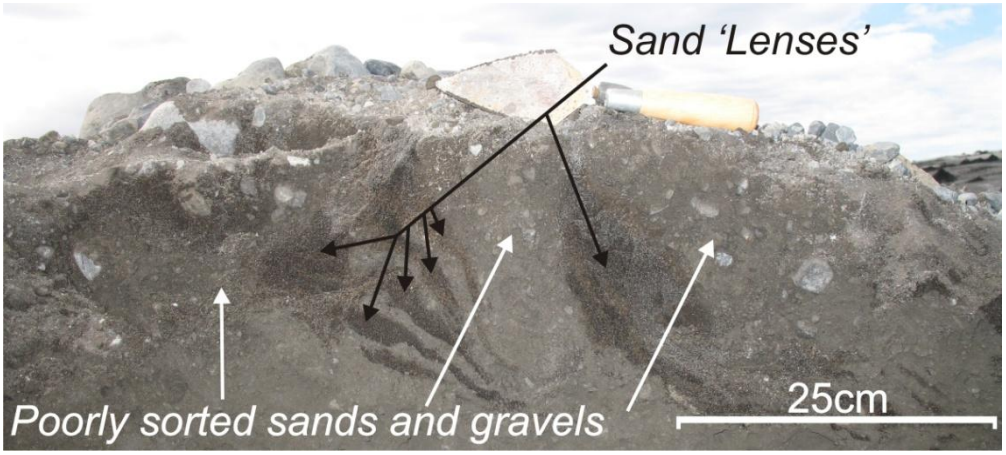

Photograph of an excavation through the Western Sæluhúsavatn linear surface ridge. The feature is composed of massive, very poorly sorted sands and gravels with vertical 'lenses' of well sorted sand.

5.3.6 SECTION 3: INTERPRETATION

Based on the above sedimentological descriptions and observations of similar features located at and within the glaciers ice margin, these lineations are interpreted as a linear 'pressure bulge', formed at the base of a former hydro-fracture. This area of the Skeiðarárjökull ice margin is well documented to have been subject to significant hydrofracturing during the November 1996 Jökulhlaup (Roberts et al. 2000). During jökulhlaups, subglacial water pressures are able to exceed the shear strength of ice and exploit weaknesses, such as closed crevasse traces, or establish new flow paths through the glacier (Roberts et al. 2000; 2002; 2002). This process allows water to flow vertically through the englacial system, under pressure, and onto the glacier surface. It is hypothesised that during jökulhlaups, water pressures within the glacier bed immediately below the hydro-fracture would be greater than the pressure within the hydro-fracture, due to the vertical movement of water through the hydro-fracture in a similar manner to that described by Boulton and Hindmarsh (1987) for flow through subglacial conduits. This variation in pressure between the area below the hydrofracture, and within the hydrofracture, is believed to result

in the glacier bed deforming upward towards the zone of low pressure similarly to that described by Boulton and Hindmarsh (1987). Such deformation is believed to cause the surface of the lineation to crack along the top of its length as the surface bulges and dilates. Following the flood, a large proportion of these hydrofractures were infilled with well sorted sands (Roberts et al. 2001; Russell et al. 2006). It is believed that upon melt out of the hydrofracture, this englacially deposited sand would fall vertically into these cracks and fill the voids produced by this dilation.

This hypothesis is supported by observations made at the ice margin, where traces of similar lineations can be seen melting out of the glacier ice. As seen in **Figure 5-18,** well sorted sand which has been deposited in an englacial position within the hydro-fracture, has melted out, leaving a linear trace of the hydro-fracture on the proglacial surface.

Figure 5-18

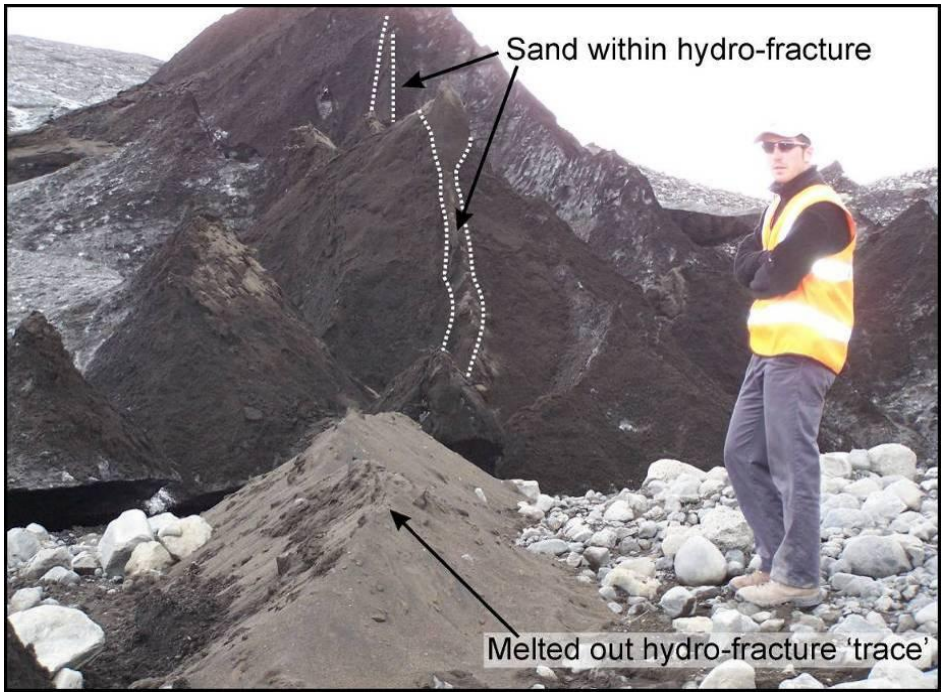

Photograph illustrating the melt out process of hydro-fractures at the Western Sæluhúsavatn ice margin, Skeiðarárjökull. Photograph P. Bailey

If these lineations had been formed by subglacial meltwater flow beneath the glacier substrate, the lenses of sand would have originated from some point up glacier and would have been deposited *in-situ*. If this were the case it is likely that such sand lenses would be seen along the entire length of the linear ridge and, over much greater depths. However, this is not the case and it is considered that these sand lenses are more likely to be a secondary infill, deposited following melt out from above. **Figure 5-19** presents an idealised conceptual model of the formation of these linear features.

Figure 5-19

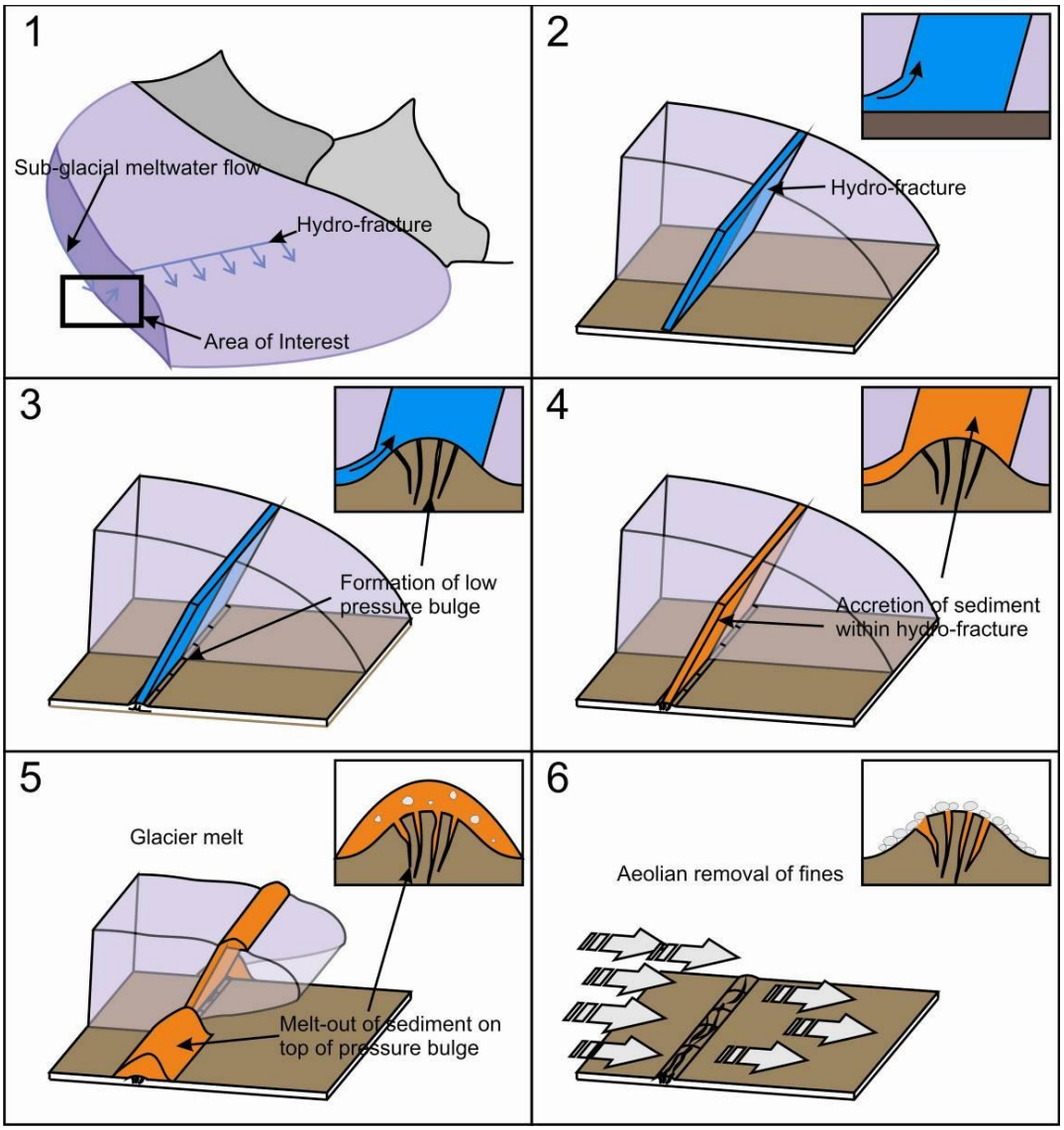

Conceptual model of the formation of linear surface ridge in the Western Sæluhúsavatn basins Area. 1 and 2) Jökulhlaup subglacial meltwater flow and formation of hydro-fractures. 3) Low pressure within hydro-fracture cause formation of "pressure bulge" within subglacial sediments. 4) Accretion of sediments within hydro-fracture. 5) Glacier melt, melt out of sediments on top of pressure bulge and infilling of dilation cracks. 6) Aeolian removal of fines results in remnant 'pressure bulge' lineation with infilled dilation cracks and surface lag of larger pebbles and cobbles.

5.3.7 SEDIMENTS WITHIN THE WESTERN SÆLUHÚSAVATN GRAVEL RIDGE

During fieldwork conducted for this project, exposures of the sediments which composed the western Sæluhúsavatn gravel ridge were not available and attempted manual excavation proved unsuccessful. However, prior to this project a number of photographs of a sedimentary exposure located at the south of this ridge were taken by Prof A J. Russell (**Figure 5-20**). This exposure was located within the gully that has been eroded across the width of the structure as seen in **Figure 5-5**.

Detailed sedimentological analysis of this exposure has not been carried out, however it is clear from these photographs that the internal composition of this ridge comprises very poorly sorted sands and gravels, with a high concentration of rounded cobbles and boulders. Unit 1 is composed of matrix supported sands and gravels with a high degree of packing and some cohesiveness. Units 2 and 3 show an increase in the level of sorting and become increasingly clast supported (Personal Communication: Prof A. J. Russell). These photographs also reveal a very slight pseudo-anticlinal bedding structure within these units. The top of the unit is overlain by a very thin veneer of very poorly sorted, silty diamicton.

Figure 5-20

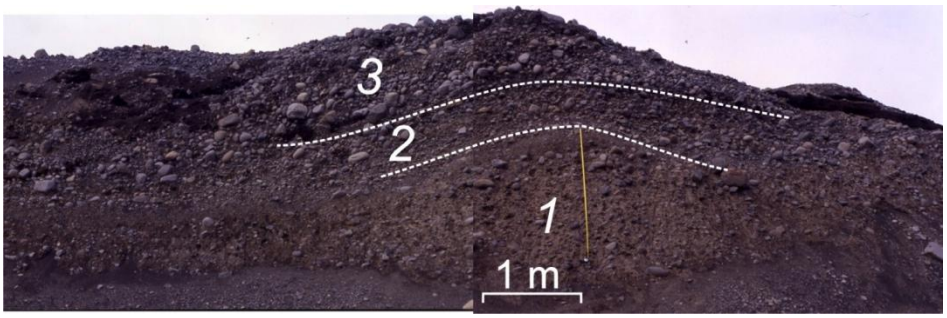

Partial cross section through the upper 4 m of the gravel ridge found at the southern end of the Western Sæluhúsavatn area. Dashed lines indicate the position of subtle bounding surfaces between units with the exposure. Photographs: Prof A. J. Russell, 2004.

5.3.8 INTERPRETATION OF SEDIMENTS WITHIN THE WESTERN SÆLUHÚSAVATN GRAVEL RIDGE

The poorly sorted nature of the sediments exposed through this gravel ridge is consistent with high energy, turbulent, fluvial sedimentation. The pseudo-anticlinal bedding is common within esker sediments (Brennand 1994; Delaney 2002), and is interpreted as being formed by water flowing, within a narrowly constrained conduit, where interactions with the channel bed and walls cause the formation of a vortex (Brennand 1994). The tight packing of sediments towards the centre of the ridge and increase in both sorting and clast support through the units towards the apex may be consistent with sediment exhaustion during a single, high magnitude jökulhlaup (Personal Communication: Prof A. J. Russell).

5.3.9 SEDIMENTS WITHIN CYLINDRICAL HOLES

A number of brief observations have been made of the sediments that comprise the walls of vertical sided, cylindrical holes found within the surface of the western Sæluhúsavatn area. The walls of these holes are composed primarily of poorly sorted sands and gravels, often with a very granular, in-cohesive texture, overlaid by a thin 0.2 - 0.5 m think carapace of silty diamicton. These observations provided a brief glimpse at the nature of the underlying sedimentology of the Western Sæluhúsavatn. Additional information about the underlying sedimentology was been provided over a wider area, following the recent erosion of the ice marginal area by a switch in the route of the River Skeiðará, which has revealed the sediments underlying this drumlinized landscape. These observations are described in section 5.3.10 below.

5.3.10 RECENT CHANGES IN THE WESTERN SÆLUHÚSAVATN AREA

Recent changes in the field area and observations made by others (Prof A Russell) since the completion of field work for this thesis have shed further light on the origin of landforms and sedimentary deposits found within the Western Sæluhúsavatn area. As a result of continuing glacier margin retreat into Skeiðarárjökull's over deepened basin, detachment of the glacier from the proglacial sandur east of Sæluhúsavatn has resulted in the drainage capture of the Skeiðará river. This drainage capture along the margin of Skeiðarárjökull has resulted in large qualities of meltwater from the Skeiðará River being redirected along the ice margin, resulting in significant erosion of the ice proximal landscape, and the creation of vertical cliff faces up to 20 m in height adjacent to the ice margin (**Figure 5-21**).

Observations of this vertical cliff face show that the sediments which make up the drumlinoid features overlie buried glacier ice and that they are primarily composed of coarse grained sand and gravel deposits. A table of the primary observations is presented in **Table 5-1**, and the implications of these observations are discussed in greater detail at the end of this chapter.

Figure 5-21

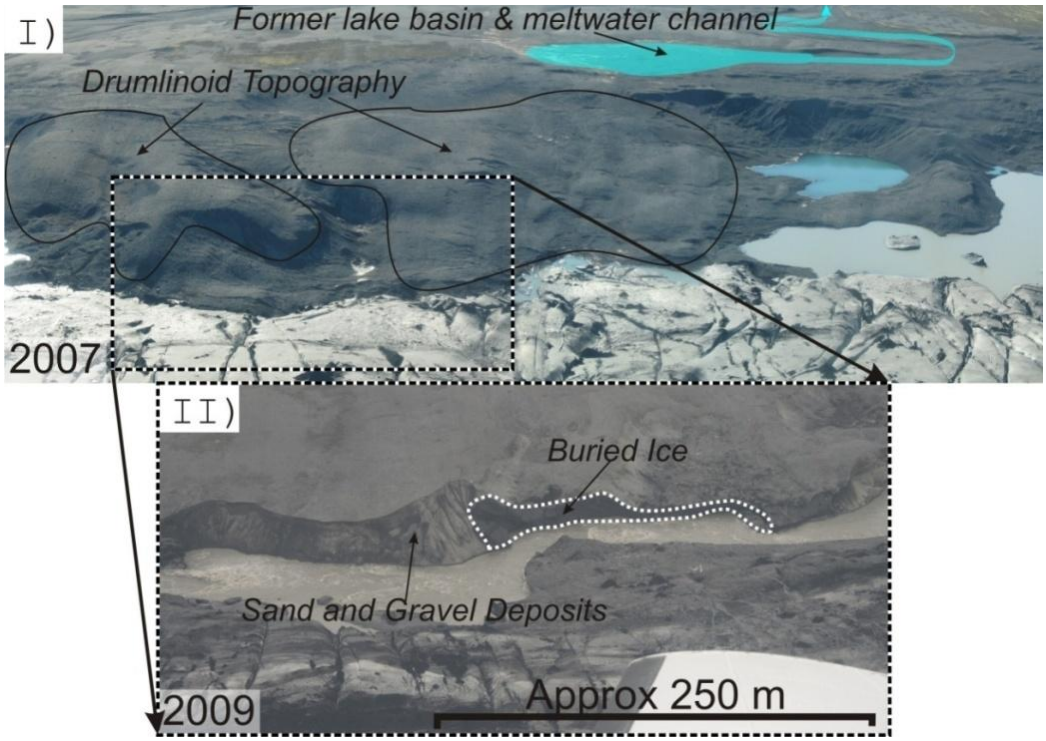

Oblique aerial photographs looking south, illustrating recent changes in the Western Sæluhúsavatn Area. I) Highlighting the main geomorphological features taken in 2007. II) Drainage capture during 2009 has resulting in large scale fluvial erosion of the ice proximal zone, revealing buried ice and sand and gravel deposits (Photograph Prof A. J. Russell).

Table 5-1

Key observations of the River Skeiðará Drainage Capture	
Length of exposure	~500m
Depth of sediments	>25m
Depth to surface of buried ice	2 - 25m
Thickness of buried ice	2 - 20m

5.4 DISCUSSION OF SEDIMENT - LANDFORM ASSOCIATIONS WITHIN THE WESTERN SÆLUHÚSAVATN

The interpretations of the Sediment - Landform Associations within the Western Sæluhúsavatn are now presented in three sections dealing with the northern and southern ice proximal areas, and the ice distal area.

5.4.1 NORTHERN ICE PROXIMAL SEDIMENT - LANDFORM ASSOCIATIONS

The northern ice proximal landscape of the Western Sæluhúsavatn Basins is dominated by streamlined, drumlinoid topography that produces a convex slope that ascends from the ice margin to Skeiðarársandur. This area saw relatively little change following the 1960's, with only slight variations associated with the deposition of small ice contact alluvial fans. By 2003, the formation of the numerous drumlinoid features has become apparent.

Based on the distinct streamlined surface morphology and poorly sorted, coarse gravel internal sedimentology, with a surface drape of diamicton, these landforms are interpreted as gravel-cored drumlins (Boulton 1987; Newman and Mickelson 1994). The presence of a thin veneer of diamicton overlying predominantly coarse gravels suggests that this landscape was produced by deformation of the glacier bed around 'plastically stiff' sediments, which are more resistant to shear deformation than the overlying glacial till (Boulton 1987; Boulton and Hindmarsh 1987; Boyce and Eyles 1991; Waller et al. 2008). The formation of such drumlinoid features elsewhere along the Skeiðarárjökull ice margin has been recently attributed to fast ice flow during the 1991 surge (Waller et al. 2008). However in this case, 2003 was the first time that this area of the ice margin has been exposed in recent history; and therefore comparison of the surge landforms before and after was not possible (Waller et al. 2008). Although it is possible that the 1991 surge of Skeiðarárjökull could have

influenced the formation of the drumlins in the Western Sæluhúsavatn, it is not possible to directly relate their formation to the 1991 surge event.

Erosion of the southern flank of drumlin 1 is considered unlikely to have occurred as a result of direct glacier erosion during an ice advance. This is supported by Waller et al. (Waller et al. 2008) who demonstrated that till deposition at Skeiðarárjökull was associated with the cessation of subglacial abrasion. Direct sub-glacial erosion would mean a switch from erosion to deposition back to erosion, only on the flanks of the drumlin. Furthermore, the lack of any evidence for meltwater flow towards the ice margin along the southern flank, such as a stream channel, delta or alluvial fan at the lowest end of the gully, suggest that this feature did not form subaerially, following glacier retreat. Based on this scarp's alignment with a gully, which ascends to the outwash surface (**Figure 5-9**), the erosion of this drumlin is interpreted as a result of subglacial melt water flow during the peak and waning stage of the 1996 jökulhlaup. The erosion of this scarp, along the flank of this drumlin suggests that meltwater routing along the glacier bed was controlled by subglacial topography, with conduits forming in the lower areas of the bed which have the lowest hydraulic potential.

The presence of remnant hydrofracture sediments which abut the eroded scarp (**Figure 5-16**), within the gully and adjacent to it, allow an approximate reconstruction of the processes that led to the formation of this landform during the jökulhlaups rising limb.

The presence of the hydrofracture sediments within the gully does not necessarily suggest that the hydrofracture was formed following the erosion of the gully. The alignment of the 'pressure bulge' and hydrofracture sediments is evidence that the hydrofracture was present in this location during and immediately following the 1996 jökulhlaup. The presence of the linear 'pressure

bulge' ridge to the south of the gully, and the absence of such a ridge within the gully, suggest that the pressure bulge was eroded away following its formation. It is hypothesised that low effective pressures caused by a rapid increase in subglacial porewater pressure during the rising stage of the jökulhlaup, led to the formation of the hydrofracture across the whole length of the northern ice proximal area (Roberts 2005). As discharge increased, effective pressure increased and subglacial meltwater flow became topographically controlled, following the flanks of drumlin 1 and eroding the gully through the bottom of the hydrofracture, removing any evidence of the 'pressure bulge' (Roberts 2005; Burke et al. 2008). Upon glacier retreat, englacial sediments within the hydrofracture dropped from the ice into the gully where they were relatively protected (**Figure 5-22**), allowing their preservation.

Figure 5-22

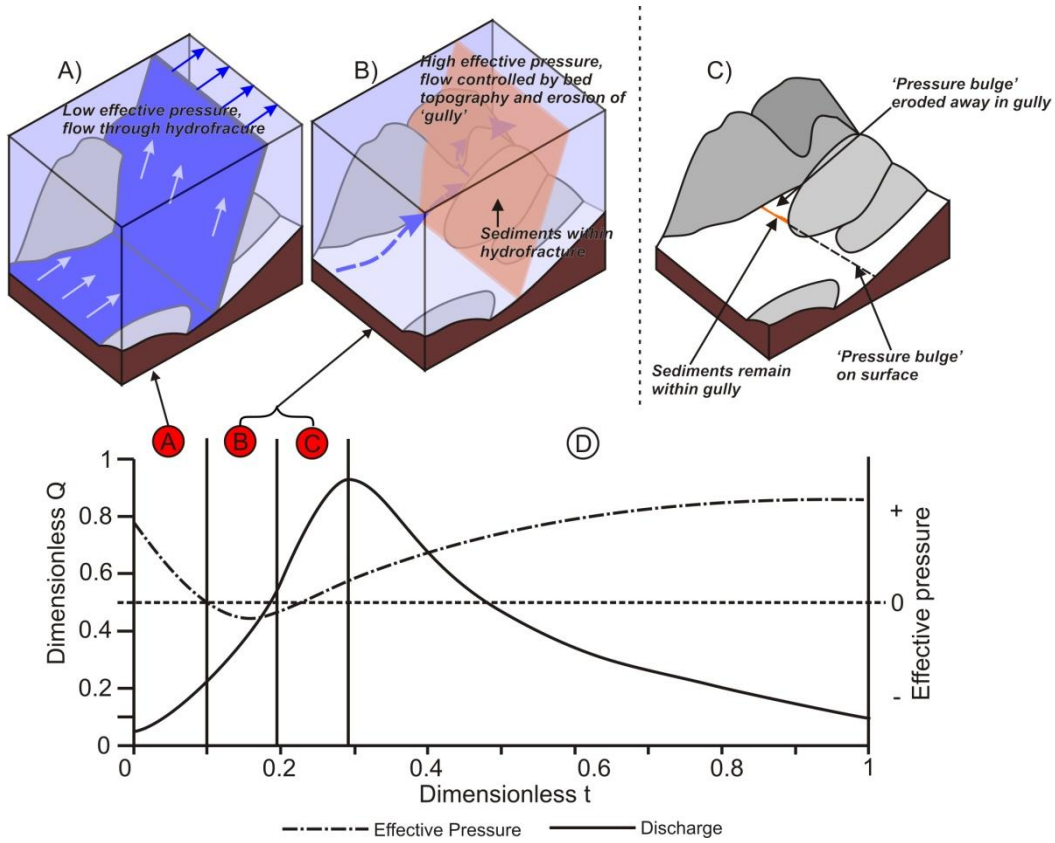

Conceptual models illustrating the impact of discharge and effective pressure at the Western Sæluhúsavatn on sub and englacial meltwater routing during the 1996 Jökulhlaup. A) Low effective pressure allows the formation of hydrofractures and flow vertically through the ice to the surface. B) as discharge increases, effective pressure increases, flow through hydrofracture ceases, leading to deposition of englacial deposits and fluvial erosion of glacier bed. C) Following ice retreat and lowering, englacial sediments melt out of the ice and occupy the gully floor. Conceptual hydrograph modified from Roberts (2005) Discharge (solid line) and concomitant effective pressure (dashed line)

The deep, cylindrical shafts that were noted on the surface of drumlins in the western Sæluhúsavatn have a morphology similar to Type (A), steep walled kettle holes as describe by Fay (2002). As such, these features are interpreted as kettle holes. The kettle holes identified in the western Sæluhúsavatn are also similar to those discussed by (Waller et al. 2008), which are interpreted to have been formed as a result of ice blocks falling from the front of the ice margin during the 1991 surge and subsequently being over ridden and incorporated into the substrate. Based on the recent observations of large quantities of glacial ice

buried at depth beneath this area of the ice margin, the interpretation provided by Waller et al.,(2008) may not be applicable in this area. It is possible that the kettle holes observed in the western Sæluhúsavatn may have formed as a result of melting of the large quantities of buried ice that has recently been identified, rather than small (1m) sized blocks that became detached and over-ridden by the surging glacier front. However, the melt out of such large quantities of ice would be expected to form larger scale ice melt out topography such as that identified at Breiðamerkurjokull by Price (1969), and such features as sinks and moats (Fleisher 1986) . That said, the observations made by Fleisher, (1986) were within Quaternary landscapes, following the complete melting of entire dead ice zones. Therefore, it is possible that the formation of discrete, cylindrical kettle holes may be part of the early stages of larger scale ice melt out.

5.4.2 SOUTHERN, ICE PROXIMAL TO DISTAL SEDIMENT - LANDFORM ASSOCIATIONS

The distinct changes in the southern ice proximal zone, and enlargement of the ice marginal basin that appeared between 1945 and 1965, is interpreted as a result of enhanced erosional processes that were active during the 1960 -1965 advance of Skeiðarárjökull (Wisniewski et al. 1997). The most striking aspect of this change is the formation of the enlarged lake basin at the south end of the ice margin, which suggests that this 400 - 500 m wide area was excavated to a depth in excess of approximately 20 m during this event. However, there is no direct evidence to suggest what specific processes were responsible for excavation of this area, whether it be direct glacial abrasion or meltwater. There is also no evidence of the re-deposition of this eroded material on the outwash plain, which could aid in the identification of the erosive processes responsible (Benn and Evans 1998). Based on seismic soundings of Breiðamerkurjökull, Björnsson (1996) estimated that a 300m deep, 20km long trench was excavated

below the glacier over a 158 year period during the glacier's Little Ice Age advance. This was averaged at a rate of approximately 0.7 m depth of erosion per year and was attributed to a combination of subglacial abrasion, subglacial sediment deformation, and high subglacial melt water discharge, with the majority of the erosion attributed to subglacial meltwater erosion. This average rate of 0.7 m is considerably less than that which would be required to erode an approximately 20 m deep basin at Skeiðarárjökull over a 5 year period, assuming an average erosion rate of approximately 4 m a^{-1}. Notwithstanding the enhanced glacier motion resulting from the 1960 - 1965 advance of Skeiðarárjökull, it is considered unlikely that such erosion rates could be achieved as a result of abrasion and deformation caused by enhanced glacier motion alone. It is increasingly probable that meltwater played a significant role in the formation of this basin, which is supported by the occurrence of 5 individual Jökulhlaups between the period of formation (1945 – 1965). It has already been demonstrated within this thesis that the 1996 jökulhlaup was capable of eroding the proglacial glacier bed over very short time scales. The lack of evidence of the re-deposition of eroded sediment may be a result of subsequent burial by successive Jökulhlaups. Alternatively, these sediments may have been transported away from the site, laterally along the ice margin, as was seen at the recent surge related outburst of the Bering Glacier, Alaska (Fleisher et al. 1998).

Having identified the presence of buried glacial ice beneath this region of the ice margin following the lateral diversion of meltwaters in the summer of 2009, it could be argued that the lowering to the proglacial area and formation of this basin between 1945 – 1965 could have been a consequence of the melt out of this buried ice. The meltout of ice and its contribution to landform development have been widley noted in Iceland (Price, 1967; Evans and Twigg, 2002). However, these studies do not provide specific, calculated melt rates against

which comparisons can be made. Following investigations into the melt out of buried ice within a collapsing kame terrace, McKenzie (1969) concluded a melt rate of between 0.6 – 1mm per day. Over a twenty-year period this would result in the melting of between 4.38 m and 7.3 m, far short of the observed 20m. In addition, following geophysical investigations on the proglacial area of Skeiðarárjökull, Everest and Bradwell (2003) found that a ›30m thickness of buried ice had survived for approximately 200 years, and it was concluded that it is likely to remain for at least a further 200 years. As such, although it is possible that ice melt out may have contributed to the formation of this basin; it is considered unlikely that it was the sole forming agent.

The long ridge that is formed through the centre of the proglacial lake in the western Sæluhúsavatn is interpreted as an esker. This interpretation is based on its distinct geomorphology, including its prominent aspect above the surrounding landscape, longitudinal morphology, and broad apex (Price 1969; Saunderson 1977; Brennand 2000; Evans and Twigg 2002; Burke et al. 2008). The presence of flutes and striated boulder on its upper surface provide evidence that it has been over ridden by ice (Rose 1989; Benn 1994; Evans and Twigg 2002), whilst the basic sedimentological observations of well rounded cobbles and boulder and pseudoanticlinal bedding suggest that it has formed as a result of sediment deposition from high energy flow flowing within a confined conduit (Brennand 1994; Delaney 2001). The lack of faulting or post melt out deformation in the esker sediments suggest that the landform was bedded on the glacier bed, rather than glacier ice, which would melt from below resulting in deformation and faulting in the sediments. Subsequently, this esker is interpreted as having been formed sub-glacially, rather than englacially.

The formation of the large esker ridge through this area does provide some evidence for high energy meltwater flow (Price 1967; Brennand 2000;

Delaney 2001; Burke et al. 2008), however it is not possible to ascertain whether this esker was formed during the waning stage of the high energy release of melt water which eroded the basin or as a result of a subsequent high energy release of meltwater. The synchronous erosion of glacier substrates and deposition of eskers has been proposed in the literature (Moores 1989; Ó Cofaigh 1996). However, the formation of a 'low point' within the glacier bed is likely to act as an area of low hydraulic potential, resulting in increased meltwater flow through that region (Shreve 1972; Shreve 1985; Jørgensen and Sandersen 2006). Therefore, such increased flow could contribute to esker formation after the initial period of erosion.

The discontinuous collapsed section in the middle of the esker that is evident between 1965 and 1986 is likely to have formed as a result of the melt out of buried ice blocks within the esker ridge. Numerous authors have discussed the process of englacial ice blocks being excavated during jökulhlaups and becoming incorporated within re-deposited englacial and proglacial deposits (Cassidy et al. 2003; Russell et al. 2006; Burke et al. 2008). The melt out of these ice blocks subsequently leads to the instability and collapse of the surrounding sediments (Price 1969; Russell et al. 2001; Fay 2002). Alternatively, it is possible that this esker is formed englacially, and that the collapse of this section of the ridge is a result of the melting of ice below the esker ridge (Howarth, 1971). However, this is considered unlikely in this case, as it would be expected to observe overall lowering of the ridge along its length in addition to areas of collapse. However, show no such evidence of lowering has been observed.

Lowering of the lake level in this photograph appears to have resulting in exposing more of the esker than was previously visible. The shortening of the esker ridge seen on the 1975 map could be a consequence of subsequent rising water levels, which would also explain the disappearance of a section of the

delta. However, the formation of the other small gravel islands suggests that the lake level has lowered. It is likely that the gravel ridge was ice cored in some places, resulting in the collapse of the southern end and centre, and that the delta and islands have formed by subsequent lowering, suggesting frequent fluctuations in lake water level.

Between 1975 and 1986, the entire southern end of the esker ridge appears to have degraded and all that remains is the broad, low lying deltaic feature. With the lack of evidence of large-scale erosive processes, it is unlikely that this sedimentary mass has been actively removed by any large scale, high energy processes such as a jökulhlaup. With the lack of evidence of erosion, it is considered more likely that this feature was significantly ice-cored (Menzies 2002; Burke et al. 2008) and that its degradation can be attributed to ice melt out, assisted by seasonal fluctuations in lake level. This is a process that has been witnessed in the Eastern Sæluhúsavatn area over recent years.

The lack of data from 1992 makes clear interpretations of the landform changes in this area during this time difficult. However, it is clear that the 1992 ice margin has significantly advanced since 1986, causing water to pond within a hollow at a higher elevation than the lake seen in 1986. The advance in the glacier margin is attributed to the 1991 surge event (Russell et al. 2001; Björnsson et al. 2003; Waller et al. 2008). In addition to a newly formed ice contact lake, a previously formed alluvial fan and delta have formed within the lake, indicating the existence of a new meltwater outlet.

By 1997 the alluvial fan which developed during the 1991 surge of Skeiðarárjökull increased in plan area and still remains as a prominent feature of the landscape, detached from the ice margin. It is possible that the meltwater portal from which the sediments that constitute this fan were deposited, may have been utilised during the 1996 jökulhlaup and that the jökulhlaup

contributed to its growth. Alternatively this alluvial fan may have expanded as a result of lower energy seasonal flows prior to and following the jökulhlaup.

Despite the energetic nature of the 1996 jökulhlaup, which resulted in significant morphological changes along numerous sections of Skeiðarárjökull's ice margin as a result of both erosion and deposition (Russell et al. 1999; Russell et al. 2001; Russell 2005; Russell et al. 2005), there has been very little evidence of morphological change as a result of this event within the western Sæluhúsavatn. The gravel ridges located at the glacier margin and extending up to the upper, ice distal area of the Western Sæluhúsavatn remains unchanged from the 1975 and 1986 maps to the present (**Figure 5-3**).

Prior to the 1960 - 1965 advance (Wisniewski et al. 1997), the ice distal zone was relatively lacking in any significant topographic relief and was composed of a streamlined outwash surface. The origin of this outwash surface is possibly associated with the surge event of 1929 and overall glacier advance up to the early 1930's, as this was the glaciers most advanced position throughout the 20th Century (Wisniewski et al. 1997). Following the 1960 - 1965 advance, erosion of the glacier bed is interpreted to have resulted in the formation of the large hollow by either; direct glacial erosion, meltwater flow, or a combination of the two. This hollow would subsequently become inundated with ice during the 1991 surge event. Following the 1991 surge, the surge-related alluvial fan was deposited on top of this ice and was later added to by deposition during the 1996 jökulhlaup. These sediments provide significant thermal insulation to protect the ice from melting during the subsequent retreat seen since 1991. Therefore, the detachment and burial of this ice is considered the primary process that has lead to the formation of this, undulating, and concave long profile (**Figure 5-23**).

Furthermore, the burial of this ice mass has effectively prevented the infilling of this basin by reducing the accommodation space within the

overdeepening. Therefore, further contributing to the future development of negative topography in this area.

Figure 5-23

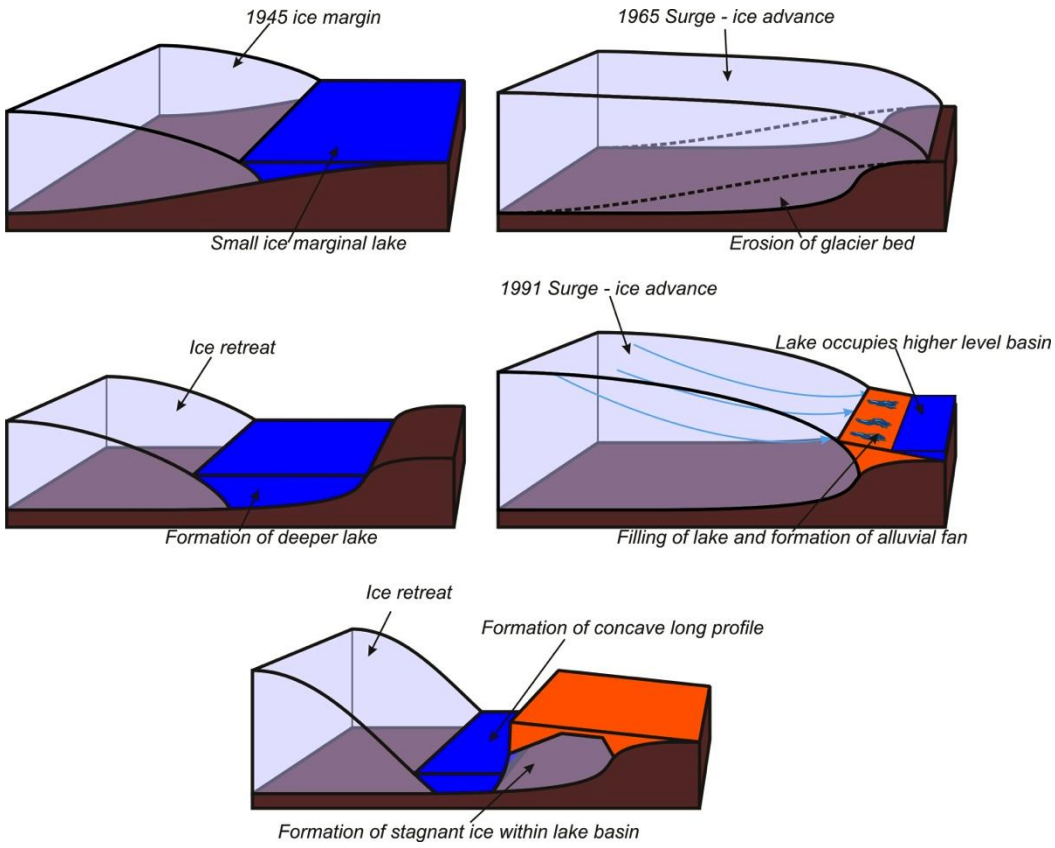

Conceptual model illustrating the processes responsible for the formation of the concave long profile present within the southern end of the Western Sæluhúsavatn Basins Area.

5.5 CHAPTER SUMMARY

This chapter has presented geomorphological and sedimentological observations made within the western Sæluhúsavatn basins area, and has developed a number of process based models for the evolution of this landscape over the last century. The main process themes that are considered are associated with numerous periods of glacier advance and retreat, englacial and subglacial meltwater routing and the development of buried, stagnant ice. It appears that ice advance into areas of pre-existing negative topography can result in a positive feedback mechanism, further enhancing the preservation of these areas by preventing the subsequent deposition of material within topographic lows, displacing material around the periphery of the feature are further enhancing its negative relief. Hooke,(1991), proposed a similar hypothesis for the formation of negative topography at the glacier bed, associated with similar positive feedback mechanisms associated with subglacial meltwater erosion. However, in the case of the Western Sæluhúsavatn this feedback is associated with the burial and stagnation of ice, which prevents the infilling of this negative topography from subsequent floods or ice advances, rather than the enhancement of active erosive processes.

These themes are considered further in Chapter 7, where they are brought together with findings from elsewhere along the margin to highlight the importance of the interaction of these processes and landforms in the development of ice marginal overdeepenings.

6 RESULTS - HÁÖLDUKVÍSL ICE CONTACT AREA

6.1 INTRODUCTION – HÁÖLDUKVÍSL ICE CONTACT AREA

This chapter presents geomorphic and sedimentological data collected from the western Háöldukvísl ice contact area of the Skeiðarárjökull ice margin. In order to critically test the hypothesis described at the end of Chapter 2 and to satisfy Objective 2, an understanding of the sedimentological and geomorphological nature of the site must be achieved. The site is an area approximately 2 km due north of the area of Skeiðarársandur known as Háöldukvísl in the centre of the Skeiðarárjökull's ice margin (**Figure 6-1**). It is approximately 1 km west of the 1996 supraglacial jökulhlaup outlet known as the 'double embayment' and consists of an 800 m long elongated overdeepening which trends northwest – southeast. The feature emerges from beneath the glacier margin and terminates at the edge of a large proglacial lake, which has formed following the retreat of the glacier margin. As this feature emerges from the glacier margin with an orientation that is oblique to both the ice and the general ice marginal over-deepening, it is clearly an overdeepened landform in its own right. Thus investigation of its form and sedimentology are highly appropriate for this study. Further detailed descriptions of the area's geomorphology are presented in **Section 6.2**.

Figure 6-1

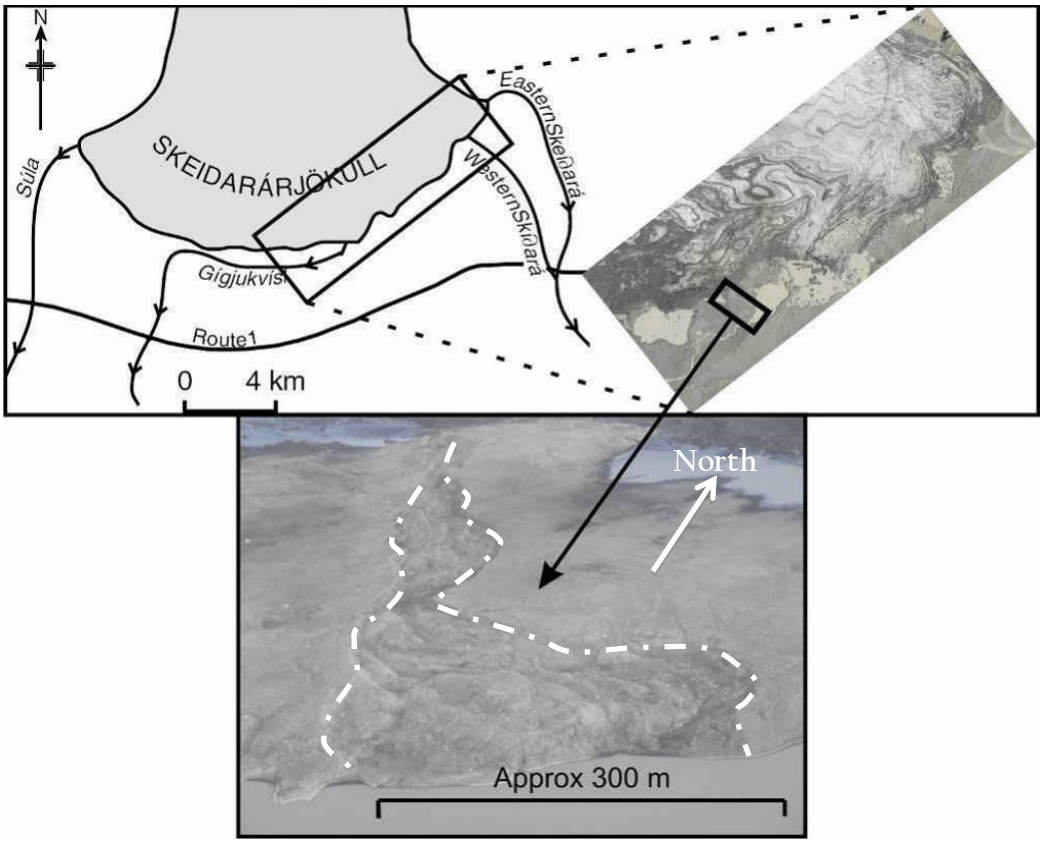

Location Map and aerial photograph showing the position of the Háöldukvísl ice contact area in relation to the rest of Skeiðarárjökull. White dashed lines define the edges of the linear overdeepening.

6.2 GEOMORPHOLOGY OF THE HÁÖLDUKVÍSL ICE CONTACT AREA

6.2.1 LARGE SCALE GEOMORPHOLOGICAL OBSERVATIONS

To gain an understanding of the geomorphological evolution of the Háöldukvísl ice contact area, a series of time sequence geomorphological maps have been produced from aerial photographs taken between 1992 and 2007 (**Figure 6-2**). These four maps illustrate the significant changes in morphology that have occurred during the last 20 years (**Figure 6-3**). Aerial photographs of this area are not available prior to 1992, as this area was previously overlain by the glacier and has only recently been exposed as a result of glacier retreat. Retreat of the glacier margin only began revealing this feature in the late 1990's and therefore only aerial photography from 2003 and 2007 is available for use in

geomorphological analysis of the feature itself. Photographs from 1991and 1997 provide excellent illustrations of the nature of the ice margin and ice marginal geomorphology prior to glacier retreat and provide details of the geomorphology of the wider Háöldukvísl.

The 1992 geomorphological map shows two large, well developed, alluvial fans emanating from the margin of Skeiðarárjökull. These fans are superimposed with numerous, small braided river channels which discharge from the fans apex. The large variation between active and passive channels shows how the streams have actively avulsed over the surface of the fan over a short period of time. The outer edges of both fans are clearly defined by a sharp break of slope between the edge of the fan and outwash plain to the south. From the edge of the fans, meltwater continues to flow in numerous braided channels, in a south-westerly direction away from the ice margin. To the southwest of the western most fan, there is a lake basin into which much of this meltwater is flowing.

By 1997, the entire landscape of the Háöldukvísl ice contact area has changed dramatically. A large canyon has been excavated into the eastern edge of the ice margin and the entire outwash plain is littered with kettle holes. The area shows numerous braided channels although none are active. There is no indication of flowing meltwater over any part of the proglacial area, with just a small number of small ice contact lakes providing the only evidence of meltwater. There is also no remaining evidence of the large alluvial fans that were present five years earlier.

By 2003, the ice margin in this area has retreated by approximately 700 m since 1997, resulting in further dramatic changes in the ice marginal landscape. The canyon excavated into the ice margin has melted out, leaving behind an inverted mould of the former ice margin. To the north, a large proglacial lake has

formed, draining west through a single, meandering river channel. To the north of the lake and river channel, an area of former glacier bed has been exposed. This area appears to be relatively flat overall; however there does appear to be significant portions of raised, plateau areas that are slightly higher than areas around them. These can be identified by their distinct lineated or streamlined surface texture. This streamlining appears to be orientated in a north-northeast to south-southwest direction. In the centre of this glacier bed topography, there is an area of distinctly undulating topography resembling a linear overdeepening, which is in distinct contrast to the surrounding topography. This is the area of greatest interest for this chapter.

By 2007, the ice margin has retreated a further 500 m, revealing more of the streamlined glacier bed. To the west a large ice contact lake has formed, into which numerous small meltwater channels drain towards the west. The large meltwater channel that drains from the west side of the largest lake has changed significantly, with the large meander loop visible in 2003 having been cut off. This resulted in flows being diverted further to the south, eroding a new steep scarp in the higher-level outwash plain.

The linear overdeepening in the centre of the map has further developed, its edges have become more defined and easily identifiable from the surrounding streamlined surface, and it is seen to be approximately 1 km in length.

To the north and south of this feature, the streamlined surfaces are more well defined as flat or lobate lineated surfaces, intersected by topographically lower ephemeral meltwater channels.

Figure 6-2

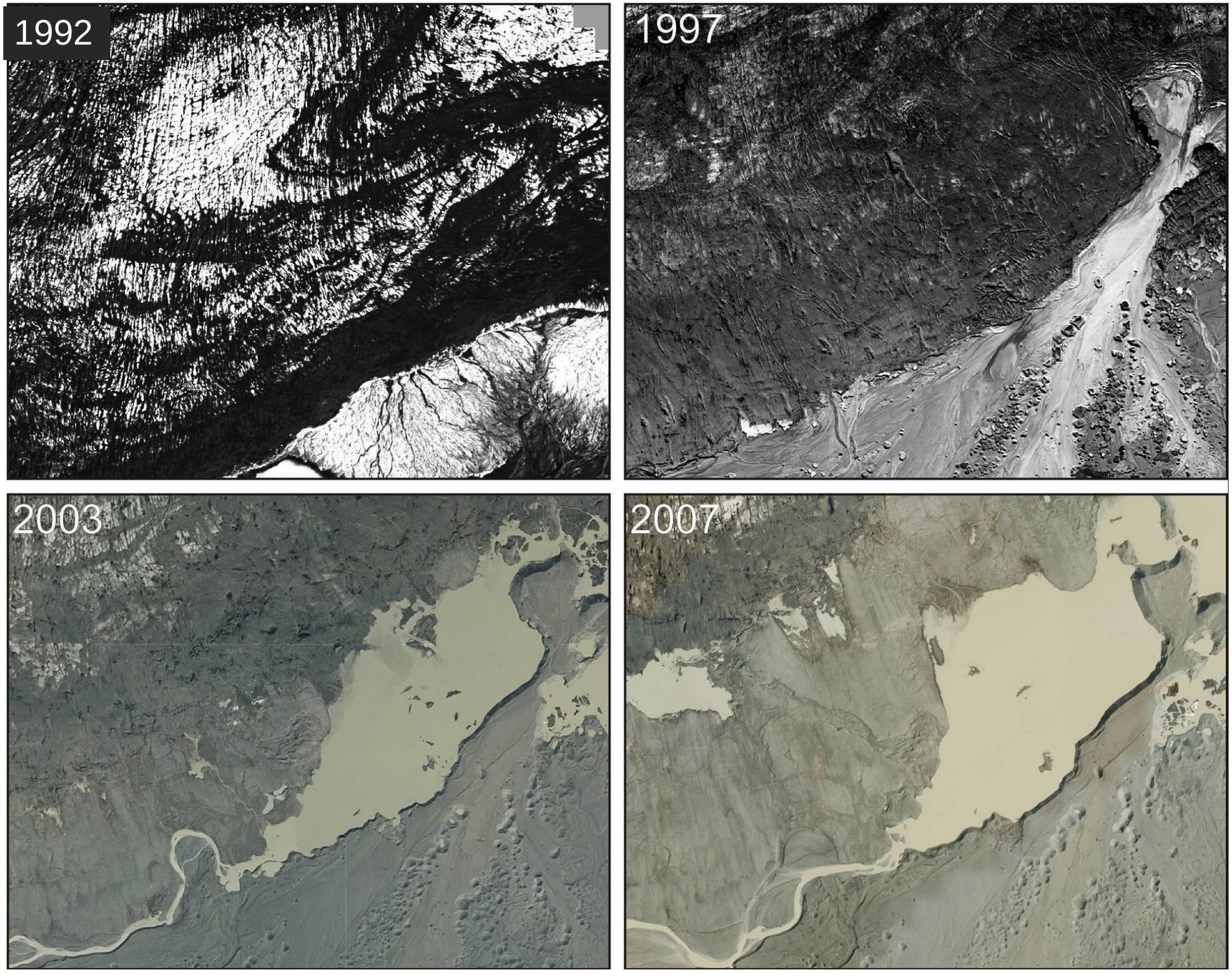

Time Sequence Aerial Photographs of the Háöldukvísl ice contact area and wider Ice margin taken between 1991 and 2007. Each photograph is 2 km across (Landmælinger Ísland)

Figure 6-3

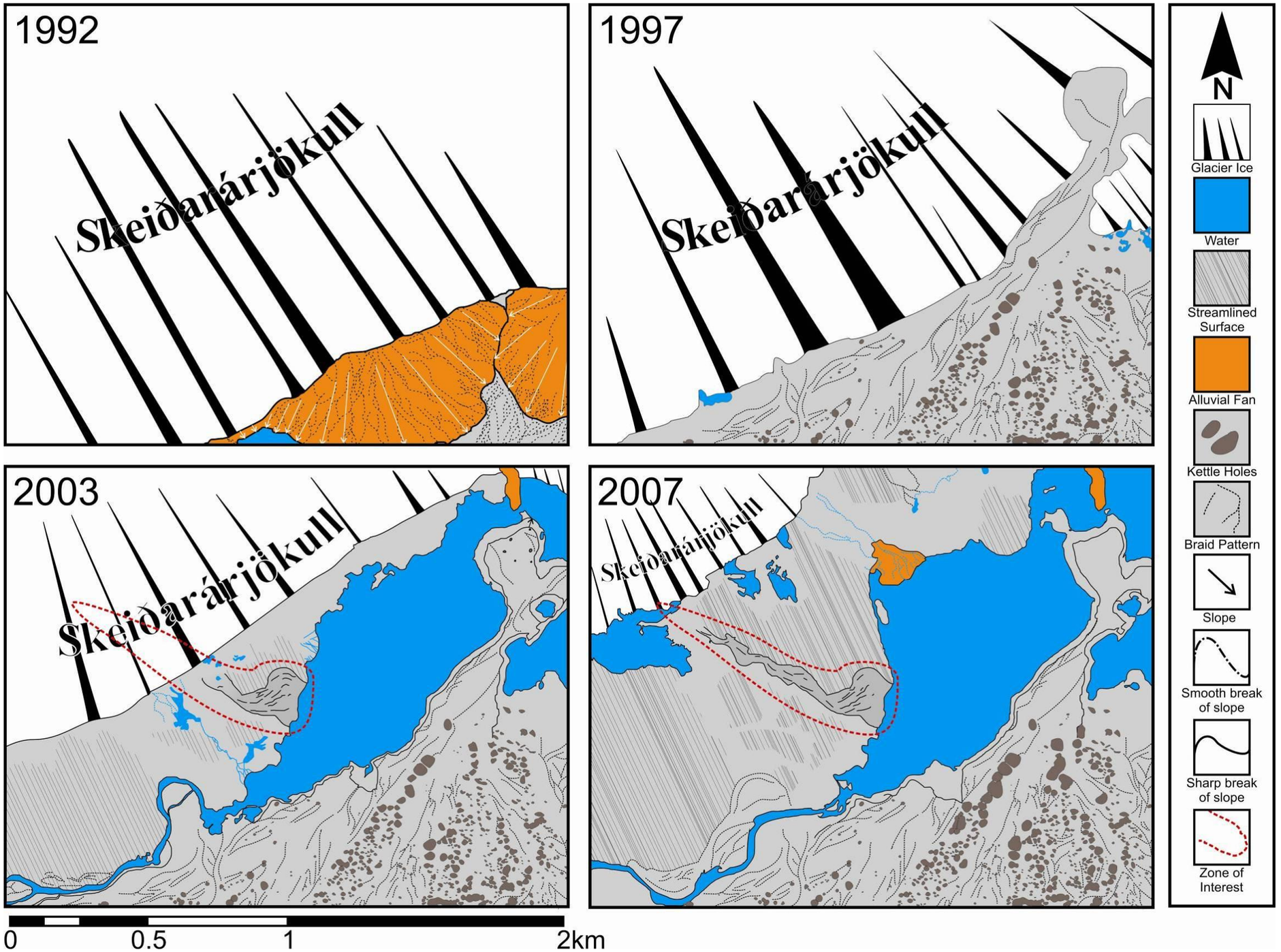

Time Sequence Geomorphological Maps of the Háöldukvísl ice contact area and wider Ice margin including the 1996 Jökulhlaup 'Double Embayment'. The area of interest is defined by the long, darker grey feature which trends from northwest to southeast, located in the centre of the 2003 - 2007 maps.

6.2.2 SMALL SCALE GEOMORPHOLOGICAL OBSERVATIONS

The Háöldukvísl ice contact area can be divided into three geomorphologically distinct areas (**Figure 6-4**). The area to the north of the linear overdeepening is a low, broad hill that is elevated by a few meters above the surrounding landscape at its most central point. Along the northern and eastern fringes of the hill the land surface grades smoothly into the surrounding topography. The northwest edge of the hill slopes gently downwards towards the glacier margin while the southern edge of the hill is truncated by the overdeepening.

Figure 6-4

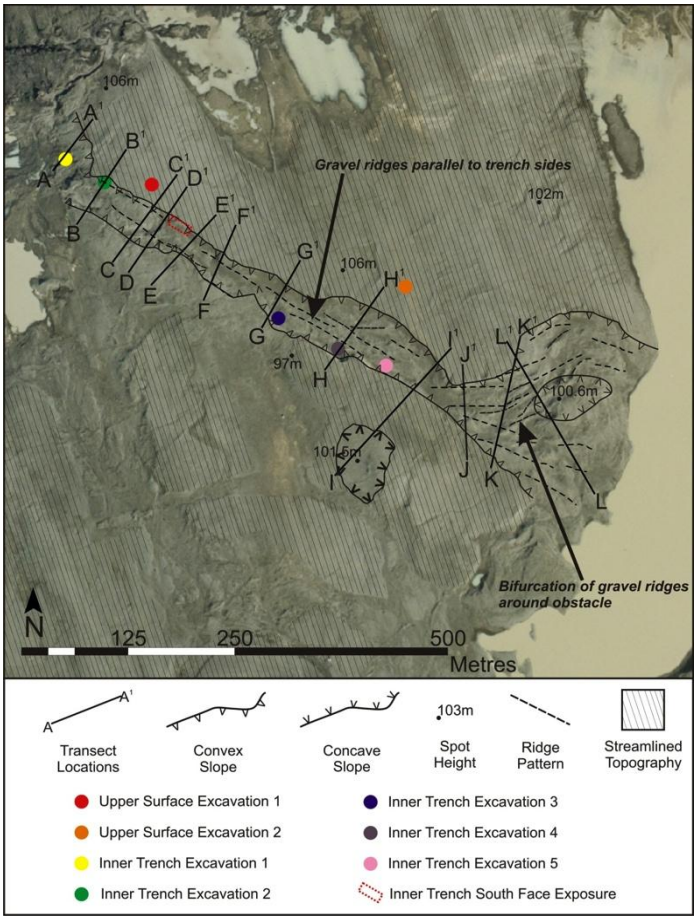

Photo-geomorphological map of the Háöldukvísl overdeepening, illustrating the streamlined nature of the upper surface to the north and south, the bifurcating nature of ridges occupying the overdeepening and the locations of topographic cross sections. Coloured circles indicate the positions of excavations made for sedimentological analysis

The upper surface of the hill is characterised by numerous linear features which are orientated both parallel and oblique to the ice margin (**Figure 6-5**). These lineations can be characterised further depending on their location and morphology. Those located closest to the ice margin, on the stoss side of the hill are better defined than those in the lee and can be described as low (up to 0.2 m) curvilinear assemblages of poorly sorted diamicton. In some places, these features appear to be underlain by thin slabs of glacier ice that dip at a low angle up glacier (**Figure 6-5 - III**). In the lee of the hill, these ice margin parallel lineations are less well defined, possibly as a result of degradation due to their relative age, or due to their underlying topography.

The upper surface also shows evidence of another type of ice margin parallel lineation. These vary distinctly from those described above as they appear to be composed of moderately sorted sand and gravelly sediments.

This upper surface is also covered with numerous ice flow parallel linear features of which there are two types. The most common type is usually associated with lodged and striated boulders, and give the entire upper surface of the hill a distinctly streamlined surface texture that is clearly demonstrated by oblique aerial photography (**Figure 6-5 - I, IV**). The second type of ice flow parallel lineations have a rectilinear morphology and appear to be superimposed on top of the streamlined surface (**Figure 6-5 - II**). These features are far less common, and do not have the continuous nature of the features making up the streamlined surface. Their orientation varies along their length, with sharp, angular changes in orientation.

Figure 6-5

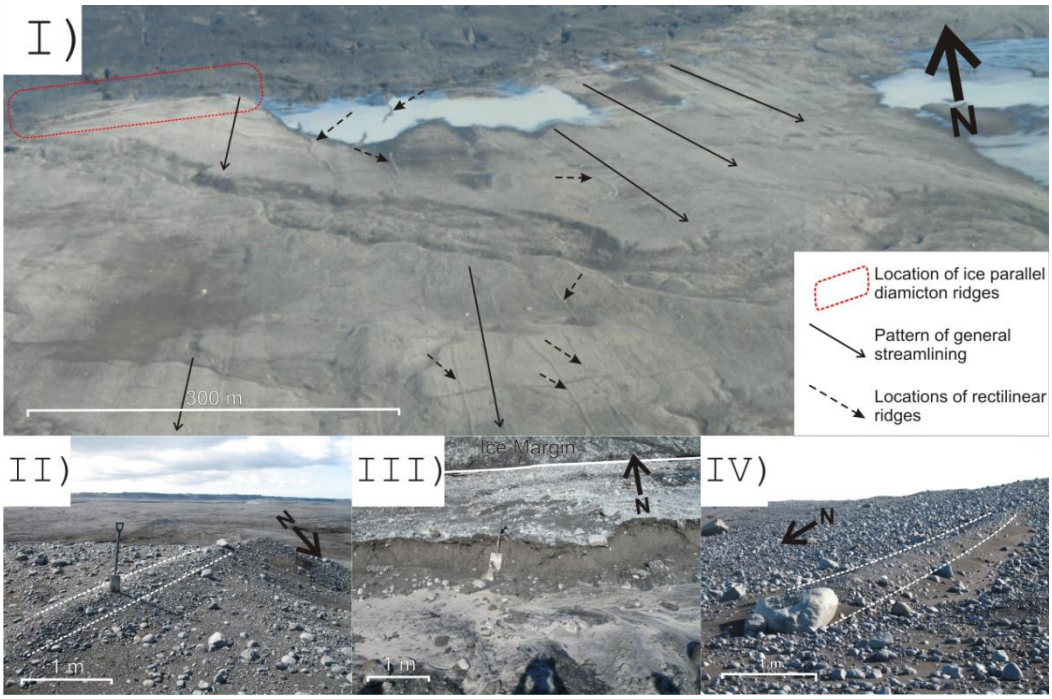

Aerial and ground based photographs illustrating the various types of linear landforms found at the Háöldukvísl ice contact site. I) Oblique aerial photograph illustrating the linear overdeepening, streamlined / fluted topography and super-imposed, ice flow parallel rectilinear ridges. II) Ice flow parallel rectilinear ridge; III) Ice margin parallel diamicton ridge (controlled moraine); IV) Streamlined surface with striated boulder and flute.

To the south of the linear overdeepening, the area is much flatter, lower lying topography. The area shows some evidence of both types of ice flow parallel lineations that have been observed to the north; however these are less common than on the upper hill surface. The overall surface texture of this southern area is much finer grained, and there are far fewer large boulders distributed across the surface than there are to the north. The only topography of note in this area is an anomalously high hill that stands proud of the surrounding landscape by seven meters, which is shown in Transect I on **Figure 6-6**.

The linear overdeepening itself defines the transition between the area of higher topography on the north and the area of relatively lower topography to the south. The feature is set into the lee of the broad, low hill that makes up the

northern portion of the area and in plan form the feature is relatively narrow at its northerly, ice contact limit where it emerges from the ice margin (**Figure 6-5 - I** and **Figure 6-4**). Its western edge trends approximately northwest – southeast in a near continuous straight line to the edge of the large proglacial lake that has developed along the central ice margin. The position of the feature's north-eastern edge varies along its length and does not follow a straight path, in contrast to the morphology of its western edge. At its ice proximal extent, the feature is only 90 m wide with its north and south edges running parallel to the southeast. Distally, the feature initially narrows to approximately 75 m as its north-eastern edge migrates slightly to the south before extending outwards to the east where the whole feature widens to a maximum width over 250 m (**Figure 6-4**). A series of tall, bifurcating, gravel ridges are found along the floor of the feature. These ridges are orientated approximately in the same direction as the main (Figure 6-7).

The plan form of this linear overdeepening feature is shown in the photo-geomorphic map presented in **Figure 6-4**. This clearly illustrates the northeast to southwest trend of the feature and the orientation of lineations on the sandur surfaces to the north and south. The linear overdeepening feature itself is defined along its northern and southern edges by sharp breaks in slope which dip inwards into a network of bifurcating gravel ridges. In plan form it is clear to see that the ridges at the northern end of the feature are all orientated parallel to each other, and the breaks of slope. To the south and east, the ridges bifurcate around a 100 m × 50 m hill located towards the centre of the bifurcating ridges, where the feature splays out towards its southern end. At a number of places along the length of the linear overdeepening, these ridges converge from two

individual features into one single ridge (**Figure 6-4**). Elsewhere the opposite is true, where single ridges often split and diverge into two.

Survey cross sections presented in Figure 6-6 clearly demonstrate how the morphology of the inner gravel ridges changes along the linear overdeepening from its northern to southern ends. At the northern end of the linear overdeepening, the ridges that run parallel along its length are primarily tall and thin, with concave sloping sides leading to a point at a very well defined ridge crest. Further south along the linear overdeepening, the gravel ridges become increasingly undulating, with convex slopes and broader, less pronounced crests.

Figure 6-6

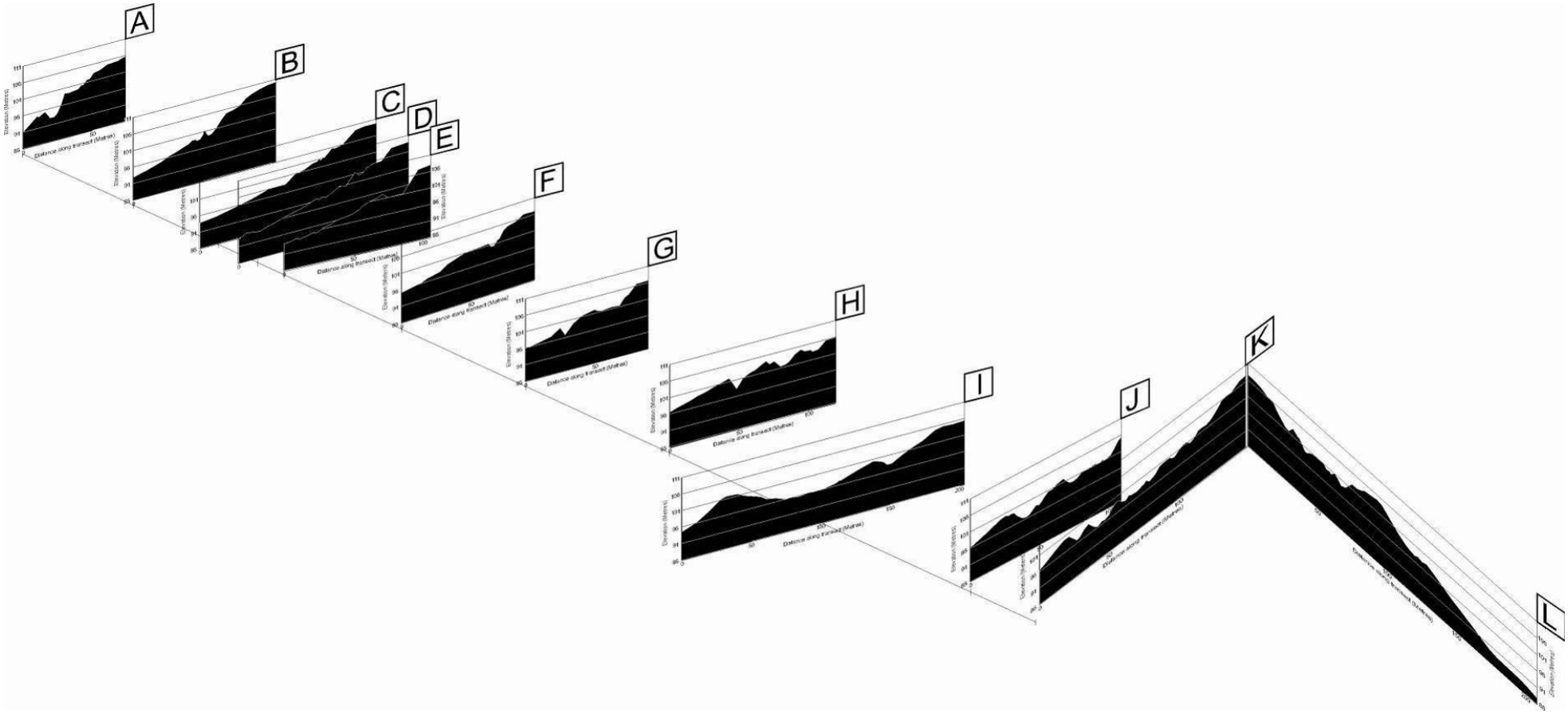

Geographically orientated topographic cross sections of the Háöldukvísl linear overdeepening, illustrating the changing nature of the ridges from northwest to southeast.

Figure 6-7

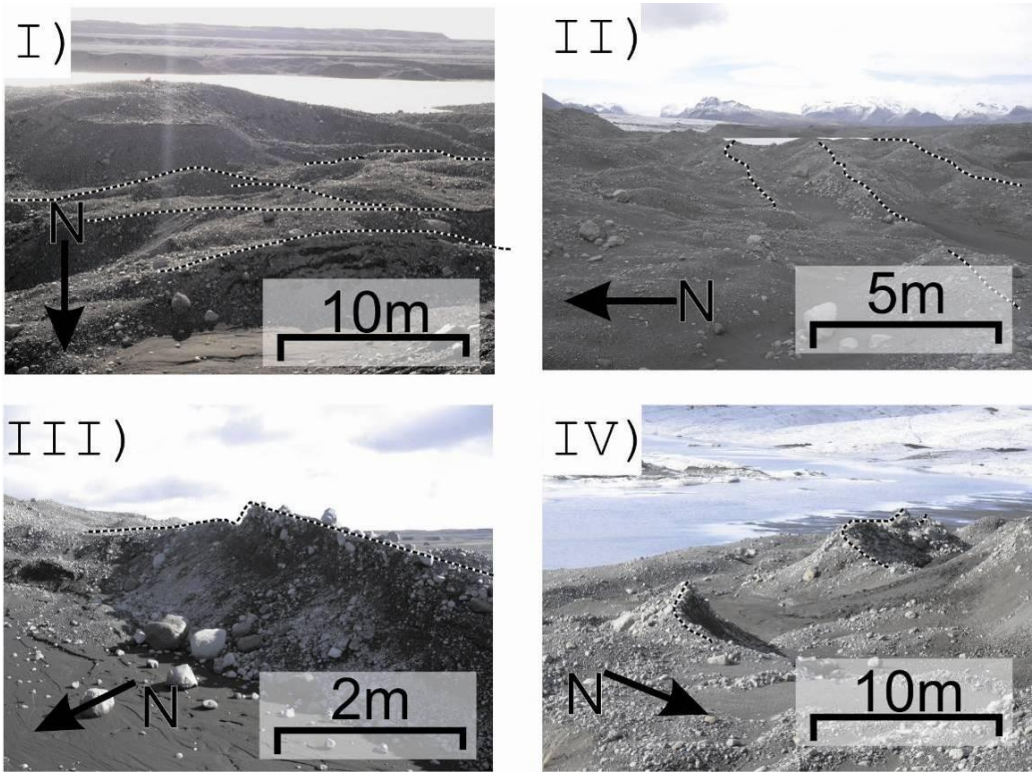

Photographs of the internal geomorphology of the Háöldukvísl linear overdeepening. The linear overdeepening is composed of numerous rectilinear gravel ridges that are orientated parallel to the orientation of the main feature.

6.3 SEDIMENTOLOGY OF THE HÁÖLDUKVÍSL ICE CONTACT AREA

To interpret sediment landform assemblages in the Háöldukvísl ice contact area, a number of sedimentary sections were investigated. Each of these sections was excavated manually between the June of 2006 and April 2007. The methodology for sampling and recording these excavations followed that laid out in Chapter 3. Two pits were excavated into the lineated surface located to the north of the Háöldukvísl linear overdeepening, while an additional five sections were investigated within gravel ridges at various locations along the length of the feature. The locations of these exposures are shown in **Figure 6-4**.

6.3.1 UPPER SURFACE SEDIMENTARY SECTIONS

Two sections were excavated into the upper surface of the low hill to the north of the Háöldukvísl linear overdeepening as indicated on **Figure 6-4**. Pit 1 was located at the northern end of the feature at UTM 28 0391664E, 7098005N. This was a 1 m wide, 0.5 m deep excavation, which transacted a 23 m long ice margin parallel lineation in the upper surface north of the linear overdeepening. This lineation was chosen due to its close proximity to the linear overdeepening and because it was truncated by the it at its northern end. Due to the potential for erosion as a result of pressurised groundwater flow (Kjaer et al. 2006; van de Meer et al. 2009), and the previous evidence of hydro-fracturing (through ice) at Skeiðarárjökull (Roberts et al. 2000; Roberts et al. 2002; Russell et al. 2006), the aim of excavating a pit through this surface lineation was to look for evidence of hydro-fracturing through the glacier substrate. Such evidence would indicate evidence of high pressure ground water and support a pressurised ground water hypothesis for the formation of the Háöldukvísl linear overdeepening (Kjaer et al. 2006).

Pit 2 was excavated at UTM 28 0391937E, 7097850N to the south of Pit 1. This excavation was located approximately 40 m from the northern edge of the linear overdeepening with a depth of 1.3 m.

6.3.1.1 Upper surface excavation 1

This shallow excavation revealed three primary sedimentary units. Between 0.5 (the bottom) and 0.17 m, the sediments are dominated by poorly sorted diamictons. There are two distinct diamicton units; the lower unit below 0.4 m and the upper unit between 0.4 m and 0.17.

The lower unit at 0.4 m depth shows a rapid grading in the colour of the diamicton, which grades from grey at the bottom to orange brown at the top. This grey diamicton is defined by a large proportion of silt and clay, with only

minimal quantities of sand. As above, this silty clay matrix provides support to a large proportion of rounded to sub-angular clasts that are up to 40 mm a-axis. The upper unit is dominated by a high proportion of sand and provides support to a large proportion of rounded to sub-angular clasts, which are up to 40 mm a-axis.

At 0.1 m depth there is a sharp contact with the unit below, which is primarily composed of medium to coarse gravel. Clast contacts are common, however overall they are supported by a matrix composed of coarse sand and granules. These gravels remain for a shallow depth of 0.07 m before another sharp contact with the unit below.

The upper 0.1 m, which makes up the portion of the ridge which is elevated above the surrounding ground surface, is composed of a massive, moderately well sorted sand unit, containing a small proportion of small to medium sized clasts, ranging from 8 – 60 mm a-axis. **Figure 6-8** provides an idealised drawing of the ridge and cross section sedimentology, as well as a graphic log illustrating variations in grainsize vertically within this exposure.

Figure 6-8

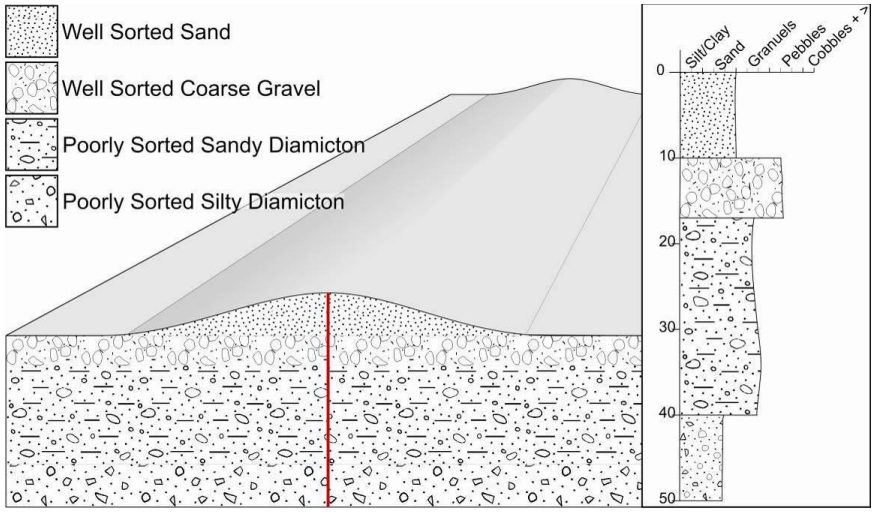

Idealised cross section of the upper surface ridge excavation and graphic log. Red line indicates position of the log

6.3.1.2 Interpretation of upper surface excavation 1

Pit 1 through this ice margin parallel surface lineation clearly demonstrates that the materials that make up this ridge are entirely superimposed upon the Háöldukvísl's upper surface.

The lower diamictons which contain a considerable proportion of rounded to sub-angular clasts could be considered typical of tills formed by the over-riding of proglacial outwash fans such as those described by Boulton (1978; 1987) and Evans and Twigg (2002). The coarse sands and granules that are present at a shallow depth are likely to be the result of winnowing of finer materials from the till below. Such winnowing is likely to have occurred as a result of low energy meltwater flow at the glacier bed and through the upper surface of the glacier substrate. Winnowing by wind is rejected as this area of glacier bed is known to have not been exposed prior to the deposition of the sand unit above, as shown on the aerial photographs presented in **Figure 6-2**. Sub-aerial fluvial winnowing has also been rejected upon the same grounds, due to the lack of surface water channels on this recently exposed glacier bed surface, and due to the interpretation of the overlying sediments having an englacial origin as is concluded below.

The well sorted nature of the upper sand unit could suggest a wide range of depositional processes; such as low energy, steady state fluvial settings (Collinson et al. 2006), very high energy outburst floods (jökulhlaups) (Duller et al. 2008) or sub-aqueous efflux (Russell and Arnott 2003). However, its deposition within a single, linear ridge allows the number of potential processes to be reduced significantly. Such well sorted sands have been observed elsewhere along the margin of Skeiðarárjökull, deposited englacially within rectilinear hydro-fractures (Roberts et al. 2000; Roberts et al. 2001; Roberts et al. 2002; 2002; Russell 2005). In these cases, well sorted sands are deposited by

accretion to the ice walls as a result of glaciohydraulic supercooling (Alley et al. 1998; Alley et al. 2003). Such features are also still visible within the ice, up glacier from this location (**Figure 6-9**). Thus, this lineation is interpreted as the superimposed trace of a former hydro-fracture. It is suggested that upon deglaciation, well sorted sands deposited within the hydro-fracture fell vertically out of the ice and were deposited in a linear 'trace' upon the freshly deglaciated surface. It is likely that winnowing by the wind removed a large proportion of the finest materials, resulting in the formation of a pebble armoured, slightly elevated linear feature. Thus, the superimposed, ice flow parallel lineations found at the Háöldukvísl ice contact site are not considered to be associated with the formation of the Háöldukvísl linear overdeepening.

Figure 6-9

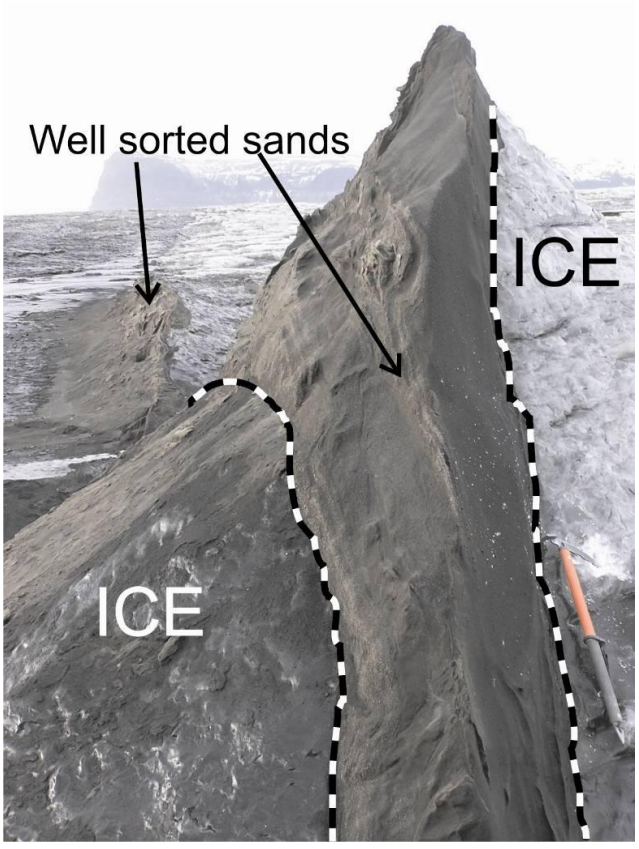

In-situ hydrofracture containing very well sorted fine-medium sand located up ice from the Háöldukvísl linear overdeepening.

The lack of a 'bulge' within the lower surface sediments suggests that the flood waters which initiated the hydrofracture did not produce low enough pressures to cause the underlying sediments to deform up into the ice as has been seen elsewhere along the Skeiðarárjökull ice margin (i.e. **Section 5.3.5**). This would be expected, as the lineation, and thus the hydrofracture, are orientated parallel with the direction of flow, and therefore high water pressures within the underlying sediments are unlikely to build up.

Overall the materials that are found beneath this ridge are interpreted as a sub-glacial till, comprising poorly sorted sands and gravels typical of subglacial basal transportation (Boulton 1978) and are consistent with what would be expected within a recently deglaciated glacier bed such as this (Waller et al. 2008).

6.3.1.3 Upper surface pit 2

Pit 2 was excavated to a depth of 1.3 m into the upper surface of the low hill to the north of the Háöldukvísl linear overdeepening. As can be seen in **Figure 6-10**, the upper 1.3 m of the sediments at this location are composed of four distinct units. The very bottom of this unit excavation 1.3m is composed of highly saturated grey clay - silt for an unknown depth. The saturated nature of the sediments resulted in significant slumping and under mining of the excavation walls meaning that only the upper surface of this unit was visible.

Unit 1, the lowest 'whole unit' at the bottom of the pit is composed of massive, poorly sorted, grey diamicton with is characterised by a number of vertical sandy structures running through the entire bed (**Figure 6-11-II**). The upper contact of this unit is equally as sharp as the lower contact below. The upper bounding surface of Unit 4 is defined by a very sharp lateral contact with a narrow 0.05 m thick bed of very well sorted silty clay. This unit was difficult

to excavate as it had the consistency and appearance of wet cement (**Figure 6-11**). Upon drying, this unit was a very well sorted silty clay.

Unit 2 above is composed entirely of massive, poorly sorted, grey, diamicton. This diamicton has very high silt content, with equal amounts of sand and fine gravel, and few (2%) clasts up to 40 mm a-axis. However, at the lower contact of this unit, a single, large well-rounded cobble, 120 mm a-axis was noted.

Unit 3 represents a transition layer between Unit 1 above and Unit 3 below. The brown sands of Unit 1, with small inclusions or lenses of grey diamicton, dominate the upper portion of unit 2. The lower portion of Unit 2 is composed primarily of grey diamicton, with small inclusions or lenses of sand from Unit 4.

Unit 4 comprises the upper 0.2 m of the excavation, and is composed of well sorted, fine brown sand with occasional rounded cobbles ≈70 mm a-axis. Below 0.2 m the sands begin to grade into poorly sorted, coarse, grey, diamicton, with clusters or lenses of diamicton incorporated within the sands.

Figure 6-10

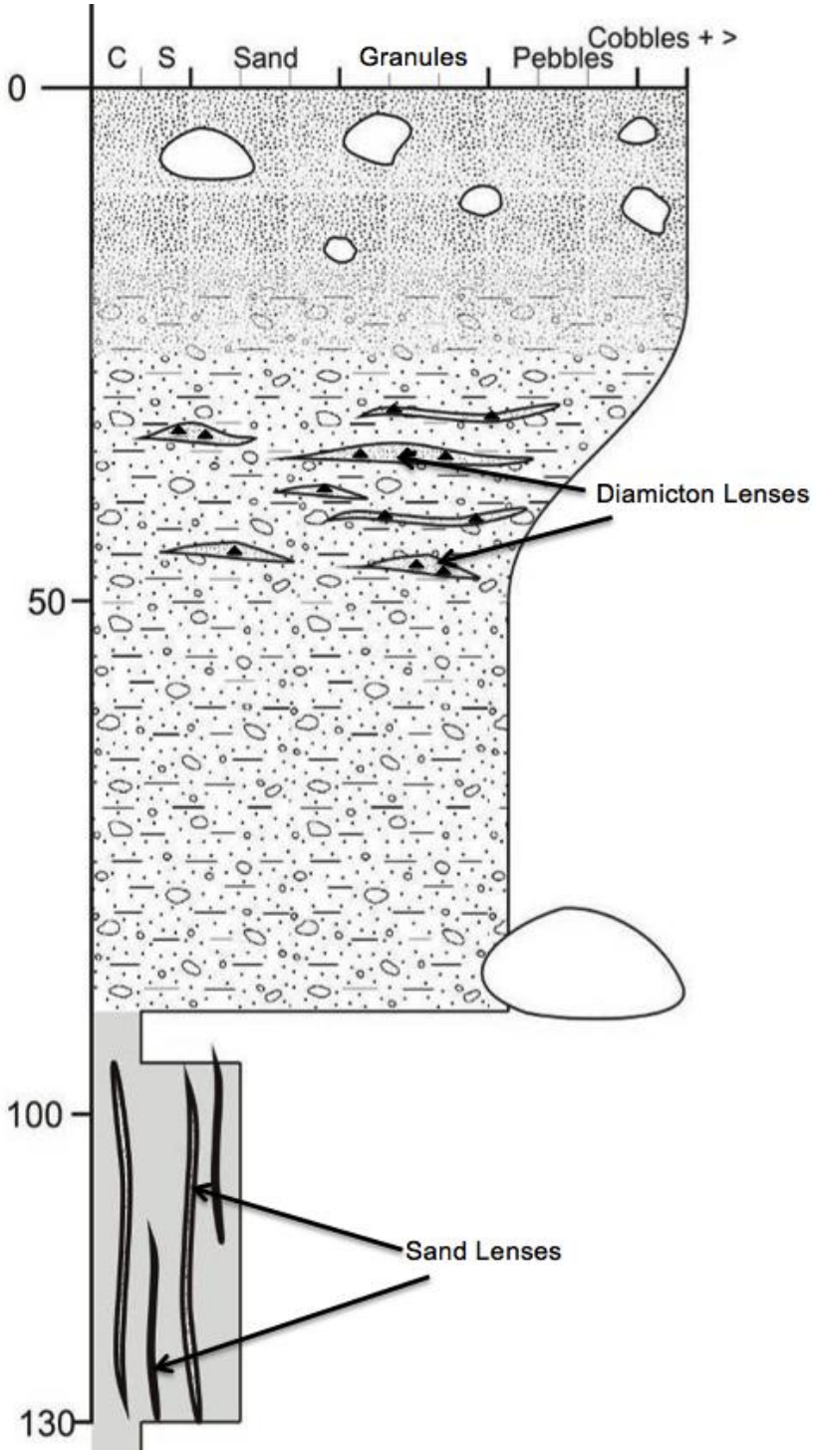

Graphic log depicting the sedimentary sequence exposed at the Háöldukvísl southern upper surface excavation.

Figure 6-11

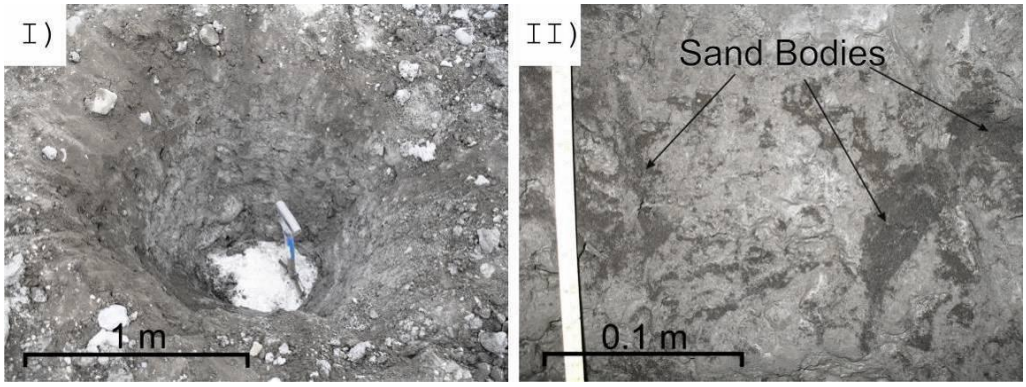

I) Saturated 'Cement like' silty clay in the bottom of the Upper Surface Pit 2 during excavation. II) 'Bodies' of sand within grey diamicton at the bottom of the Háöldukvísl southern upper surface excavation.

6.3.1.4 Upper surface pit 2: interpretation

All of the sediments within this excavation are interpreted as being composed of numerous forms of subglacial diamicton that have been deposited over at least two phases of glacier advance and retreat.

The vertical sand inclusions found within the lowest diamicton unit are interpreted as intraclasts of sand that have been re-worked and incorporated into the diamicton from an unexposed unit at depth. Similar units of diamicton, with smeared sand inclusions, have been described by Evans and Twigg (2002) from the streamlined proglacial surface of Breiðamerkurjökull. In that case, sands are described as 'ingestions' of underlying sand, which are believed to have been incorporated from below as a result of shear deformation within the subglacial sediments (Boulton 1987; Benn and Evans 1996).

The upper sandy diamictons which incorporate rounded cobbles, suggest that the parent material is likely to have had an initial fluvial origin (Boulton 1987; Philips et al. 2002). The diamictons found within the upper units of this section appear to represent a zone of transition between the lower silty diamicton and the upper, sandy diamicton. This transition is likely to be the result of deposition of glaciofluvial outwash on top of the diamicton, followed by subsequent over riding. Such overriding would deform the overridden fluvial

sediments, producing a melange of sandy subglacial diamicton with characteristic rounded pebbles from the parent fluvial deposits (Benn and Evans 1996).

The upper 1.3 m of sediments within the Háöldukvísl hill show that the hill has undergone at least two phases of ice advance and retreat. The latest phase of advance has clearly resulted in the overriding and deformation of glaciofluvial sediments, leading to the formation of a sandy diamicton melange with sand intraclasts. While a previous advance has resulted in the deposition of subglacial till and resulted in the deformation and incorporation of sand 'ingestions'.

6.3.2 HÁÖLDUKVÍSL OVERDEEPENING SEDIMENTARY SECTIONS

To gain an understanding of the sediment landform assemblages found within the Háöldukvísl linear overdeepening, sedimentary logs from a number of the ridge structures running parallel along the feature were made. Five sections were logged with the position of each highlighted on **Figure 6-4.** All of the excavations within the overdeepening were located on the east-facing slope of the ridges in question. This is due to the east facing slopes having a much steeper slope making them easier to clean, with the west facing slopes covered in significant quantities of talus and being considerably more degraded.

6.3.3 HÁÖLDUKVÍSL OVERDEEPENING SOUTH FACE EXPOSURE

Figure 6-12 presents a single photograph taken of an exposure on the south-facing slope located at the ice marginal end of the landform (**Figure 6-4**). This face became severely degraded and it was not possible, or safe to produce a detailed log or make additional observations. The photograph does show the nature of the sediments that make up the large streamlined hill area to the north

of the overdeepening. Descriptions of the section are presented below, along with a panel sketch.

The panel sketch below clearly shows that the exposure is composed of three distinct stratagraphic units. The lowest unit exposed at this section is composed of very poorly sorted, massive sand and gravel that contains a high proportion of much larger, boulder sized material. This is characterised by numerous boulder clusters that are interspersed by zones of finer sands and gravel. Toward the left (west) side of the exposure, in the upper portion of this unit there is a large cluster of boulder sized material that is supported within a sandy matrix. This is overlain by a subtly bedded, coarse sand and gravel unit that displays a high concentration of rounded to well rounded clasts. The upper 1.5 – 2 m of the unit is composed of very poorly sorted diamicton that is composed of a sandy-silt matrix containing numerous cobble and boulder sized clasts. The unit shows a subtle increase in the concentration of rounded clasts from top to bottom. In a number of places, clasts within this unit appear to be aligned horizontally, indicating horizontal bedding within the unit.

Figure 6-12

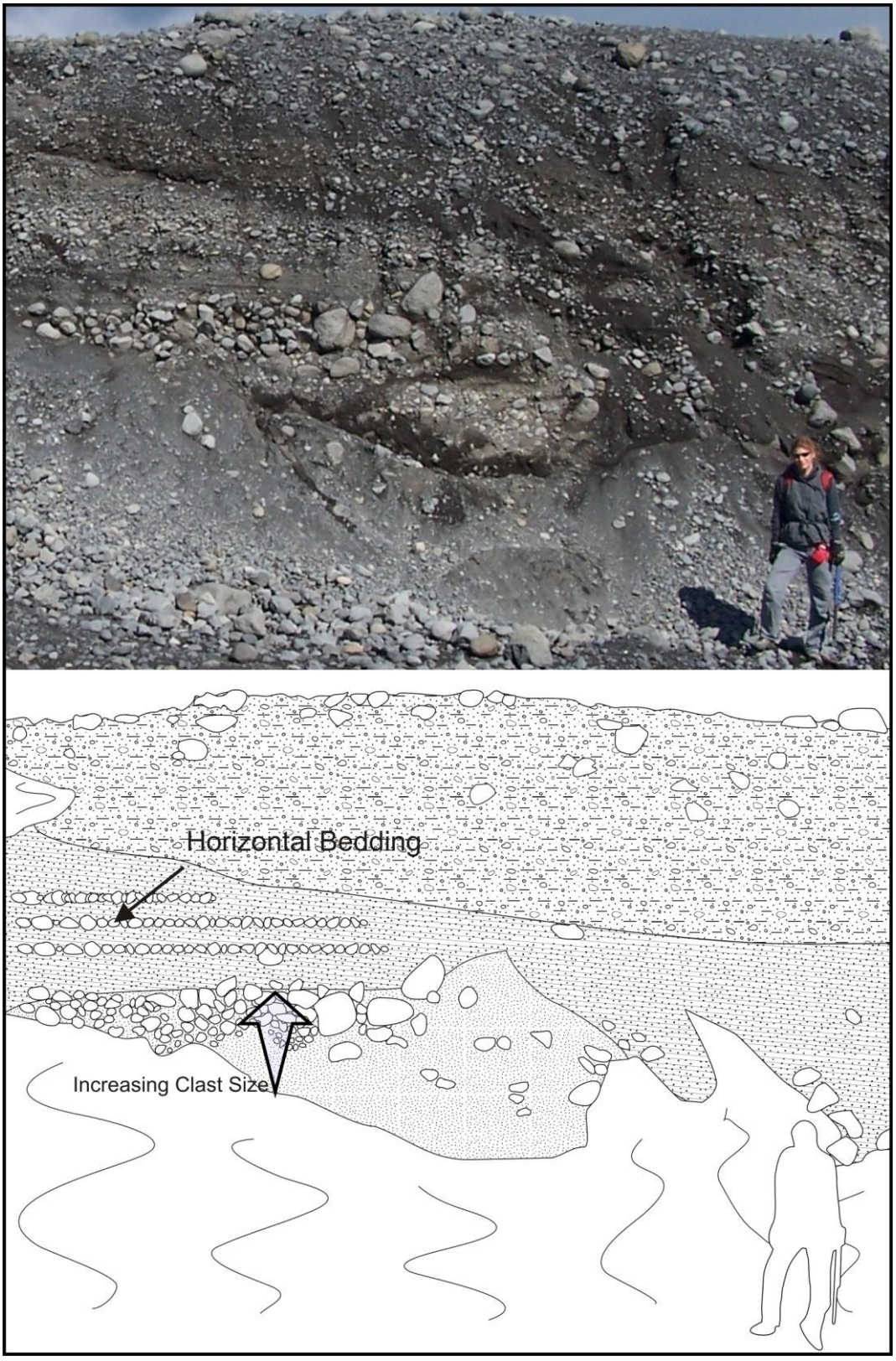

Panel sketch of the sediments exposed in the southwest facing exposure of the Háöldukvísl overdeepening. Three distinct units are visible; an upper diamicton unit and two lower fluvial units

6.3.4 HÁÖLDUKVÍSL OVERDEEPENING SOUTH FACE EXPOSURE INTERPRETATION

From the brief descriptions that can be made from **Figure 6-12**, it is believed that the internal sediments of the Háöldukvísl 'hill' have a high-energy fluvial origin. It is likely that the lower units are derived from rapid deposition from very turbulent flows, leading to the deposition of a structure less, poorly sorted mass (Carrivick et al. 2004). The deposition of better sorted; bedded sediments above suggest a reduction in turbulence and deposition associated with bed load traction. These bedded sediments share similar characteristics with those described by Brennand (1994), which are interpreted as traction deposits from fluidal flows. The overlying diamictons then suggest that the whole area was overridden by glacier ice which has deposited a thick carapace of diamicton over these fluvial gravel deposits and resulted in the streamlining of the upper surface. There is clear evidence of interaction between the fluvial and glacial sediments, as indicated by the high proportion of rounded cobbles and boulders present within the diamicton unit which suggest a degree of mixing between the two units, as rounded cobles from the underlying gravels have become entrained within the overlying diamictons (Boulton 1978; Benn and Evans 1996).

6.3.5 SECTION 1

The first Háöldukvísl overdeepening excavation is located at the very northern extent of the Háöldukvísl overdeepening, approximately 100 m south of the 2007 ice margin position (**Figure 6.3**). The exposure was located on the east face of a 2.5 m high, very narrow, gravel ridge that is orientated northwest to southeast. The exposure is located at the northern end of the ridge. **Figure 6-13** provides a detailed log of the sediments that make up this exposure and each unit is described in detail below.

Between 0 - 0.4 m depth, the exposure is composed of medium to large, sub-angular to sub-rounded cobble clasts, up to 100 mm a-axis supported within a poorly sorted sandy matrix. At 0.4 m, the overall grainsize increases with large cobbles to small boulders held within a moderately sorted fine to coarse sand matrix. Cobbles and boulders have a sub-angular to sub-rounded surface texture and many clasts show numerous facets that are consistent with a glacial origin. In a number of places, the matrix material exhibits discrete bedding which is locally deformed around the undersides of the largest cobbles. There is a very small amount of silt and clay present within the matrix (<1%), however overall, the matrix has a distinctive granular texture.

At 0.8 m there is a 40 mm thick bed of inter-bedded, very well sorted, silty clay lamina. Each individual lamina is less than 1 mm think. However, this unit is not laterally continuous like the other units in the section and does not have well defined upper and lower contacts (**Figure 6-14 - I**).

Between 0.84 - 1.45 m there is a thick unit of bimodal, poorly sorted well rounded pebbles (45%) within a coarse sand / granular matrix. There are a few intra-granular clay bands and small (< 1cm diameter) dykes orientated from bottom left to top right across the unit. The unit becomes clast supported in the top 50 mm before contact with clay bed above.

From 1.45 to 1.70 m depth there is a bed of well sorted, planar bedded, very fine sand. This unit has no out-sized clasts or other internal structures (**Figure 6-14 -II**). The lower bounding surface of these sands grades normally into the coarse gravel unit below.

The lowest 0.9 m of the exposure are composed of a moderately well sorted, open frame textured, granular, medium sized gravelly matrix which ranges from coarse sand to small pebbles (>5 mm). Clasts within this matrix are up to 50 mm a-axis and are rounded to well rounded. Clasts make up

approximately 20% of the unit and can be described as predominantly massive, except for a 30 mm thick bed of silty sand lamina found at 2.4 m depth.

Figure 6-13

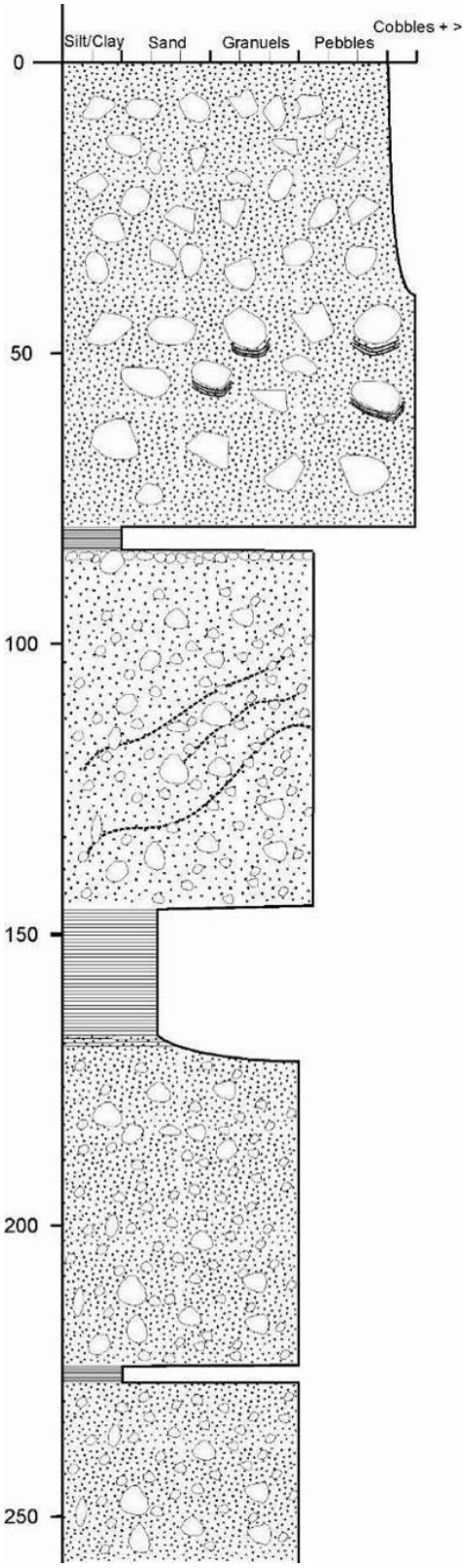

Graphic log illustrating the sequence of sediments found at the Háöldukvísl overdeepening excavation 1.

Figure 6-14

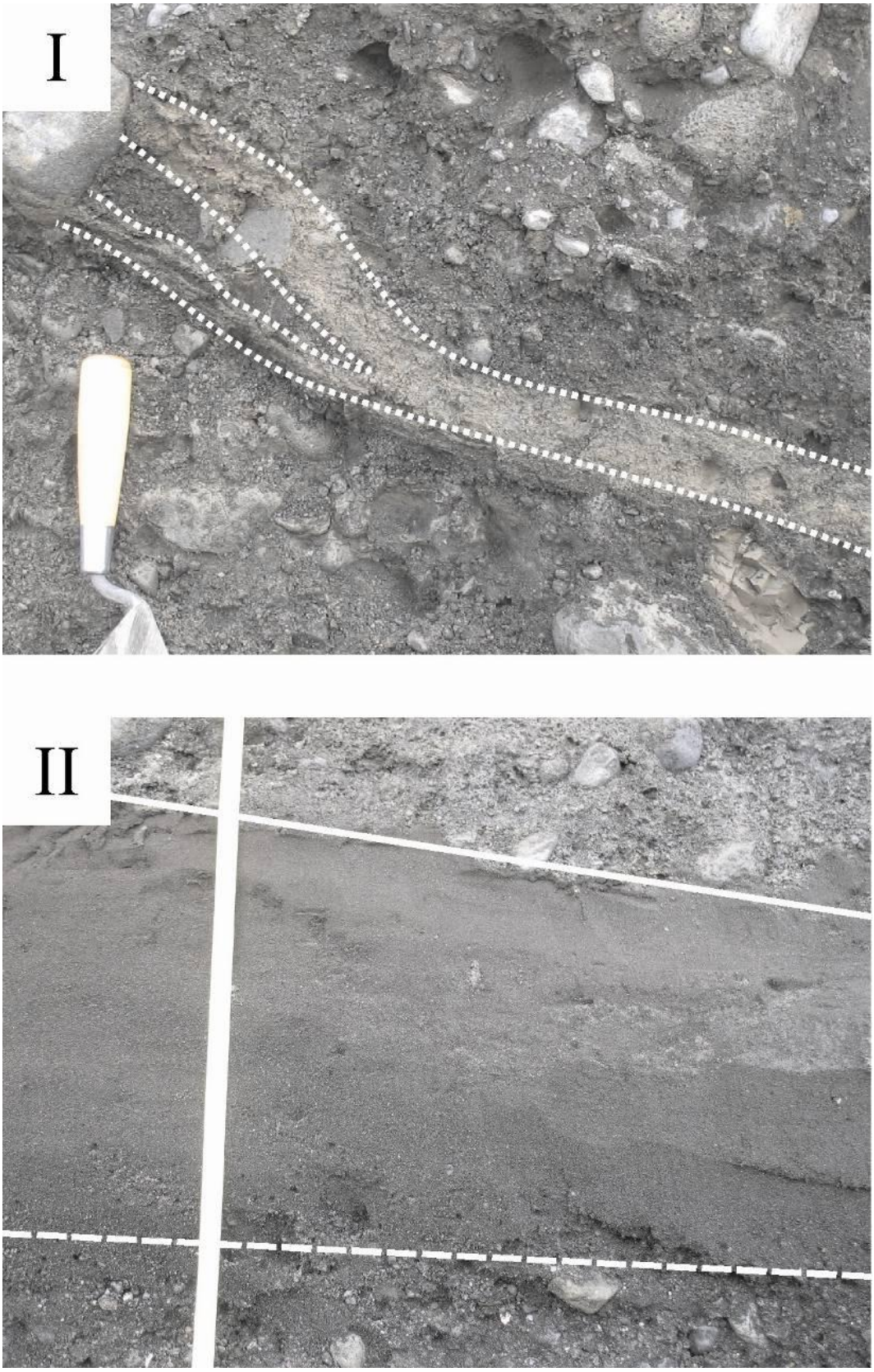

Photographs of sedimentary facies found at Háöldukvísl overdeepening excavation 1. I) laterally diffuse silty-clay lamina at 0.8 m depth. II) Sharp (upper) contact between poorly sorted gravels and well sorted sands at 1.45 m and graded (lower) contact with between well sorted sands and gravels below.

6.3.6 SECTION 1: INTERPRETATION

All of the units described within Háöldukvísl overdeepening Section 1 are interpreted to have been deposited by fluvial processes. It would appear this section represents three stages of energetic fluvial deposition, interspersed with periods of calmer conditions or erosion.

The lowest sediments from 2.6 to 1.4 m are interpreted as a single unit of normally graded, fluvial sand and gravel. This granular unit is comparable with sediments described by Russell and Knudsen (1999), who interpreted poorly sorted coarse gravel units at Skeiðarárjökull as having been deposited from 'repeated turbulent flow pulses'. The poor sorting and high concentration of fines is believed to be a consequence of rapid deposition from turbulent flow, resulting in high rates of suspended sediment load fallout (Duller et al. 2008) and little or no traction deposition. However, grading from poorly sorted gravels to well sorted sand is inconsistent with multi-pulsed flow, and suggests a gradual, rather than fluctuating, reduction of energy (Collinson et al. 2006). Therefore the lower 0.8 m of this section is interpreted as being deposited from suspension due to rapid energy loss from turbulent flow, or a single turbulent pulse. The upper bounding surface of this well sorted sand unit is sharp and erosive, which is likely to be a result of an increase in flow energy following the deposition of the sand, and possibly a switch from subcritical to supercritical flow.

The silty lamina at 2.4 m is interpreted as a post depositional de-watering or water escape structure. Such structures are common in rapidly deposited sediments as rapid deposition leads to loosely packed grain frameworks which are susceptible to post depositional deformation (Lowe 1975; Russell et al. 2003). Post depositional loading or internal settling then leads to an increase in pore water pressure and liquidised flow, leading to the upwards

movement of water through the sediments (Lowe 1976). Liquidised flow is considered more likely than fluidised flow in this case; as glacier retreat is likely to result in reduced external pressures rather than increased pressures. Thus the potential of fluidised flow through these beds has been rejected (Lowe 1976). In this case, such structures provide further confidence in the interpretation that these sediments were deposited rapidly.

Above these well sorted sands, the middle gravel unit is clearly a product of rapid fluvial deposition much like the unit below. However the dense packing and granular texture, which result from the lack of fines, suggest that this unit may be a product of less viscous, sediment supply limited flows (Duller et al. 2008).

The upper bi-modal cobble unit is again consistent with very high energy, turbulent flows (Nemec and Steel 1984; Russell and Knudsen 1999). The presence of deformed, laminated sands within the otherwise massive sandy matrix suggests rapid sedimentation of sands from suspension occurring concurrently with the deposition of larger clastic sediments. In this case, it is believed that rapid deposition of fines results in the layer on layer formation of laterally restricted, laminated sand beds. These beds then become deformed by larger clasts deposited above. The preservation of such structures supports the interpretation of rapid deposition from suspension, as deposition by traction, or rolling along the bed would likely result in the re-suspension of such fine sands and the structures would be destroyed. Such structures can often be found on delta foresets, where laminated sand beds can become deformed by cobbles rolling down the foreset slope (Shaw and Gorrell 1991). However, in this case, the large proportion of very coarse grains is inconsistent with such a delta foreset environment.

The thin unit of silty clay at 0.8 m, which marks the bounding surface between the upper and middle gravel units, could be interpreted as an indication of a period of relative calm which allowed fine materials in suspension to settle (Collinson et al. 2006). The length of this time period is however difficult to ascertain. The thickness and laminated nature of the sediments may suggest that this could be a sustained period. Depending on the concentration of fines within a water body, such a thick unit of fines may be able to drop from suspension very rapidly and the laminated texture may be a consequence of grain on grain deposition rather than any actual variation in grainsize caused by differential separation in suspension.

However, the lack of lateral continuity and the bifurcation of this bed suggest that this may not be an individual bed in its own right. Due to the diffuse nature of this unit, it is believed that this feature is a de-watering structure (Lowe 1975). This is consistent with the findings of many works where changes in the trajectory of such features are often noted at the bounding surfaces between individual sedimentary units (van de Meer et al. 2009). It is suggested that this structure represents the horizontal limb of a water escape structure which has penetrated upwards through the lower gravels.

In summary, it is believed that this unit was deposited by at least two high energy fluvial episodes separated by periods of incision, resulting in the formation of erosional contacts; or by reductions in flow energy which resulted in variation of sedimentary materials. It is difficult to estimate time constraints between the three sedimentary units and periods of erosion. However it is likely that these periods occurred within quick succession, possibly within the same flood event.

6.3.7 SECTION 2

Section 2 was located on the eastern side of a sharp, tall ridge at the ice marginal end of the Háöldukvísl overdeepening (**Figure 6-4** and **Figure 6-7 - III**). The ridge is located on the northern side of the Háöldukvísl overdeepening and is the only such ridge located adjacent to the landforms northern edge.

As can be seen from **Figure** 6-15 **and Figure** 6-17, the 2.15 m high exposure reveals four distinct sedimentary units.

At the bottom of the section the sediments which make up the lower most unit of the exposure are partially obscured by buried, in-situ glacier ice (**Figure** 6-17**)**. Upon further excavation it is apparent that the ridge was formed within an ice walled 'mould' with a scalloped inner surface. This scalloped surface is made apparent by smooth, moulded diamicton, which appears to be 'pasted' to the gravel face of the ridge along the ice-contact interface.

The lowest sedimentary unit is exposed between a depth of 2.15 m and 1.7 m and is defined by large pebbles and cobbles greater than 100 mm a-axis within a gravelly sand matrix. Some contacts between clasts are evident, resulting in near equal proportions of clast and matrix support and in some places the matrix is composed of large amounts of the diamicton material that appears to have been deposited along the ice contact interface.

Analysis of grainsize distribution from the diamicton deposited along the ice contact shows bi-modal, very poorly sorted, very fine, gravelly, coarse, silty, very fine sand. This sample is very finely skewed and has a leptokurtic kurtosis (**Figure 6-16 - B**).

Between 1.7 m and 1.4 m is a single set of inversely graded triplets. Each of the triplets grades upwards from fine sand to granules and is topped with a thin, open framework clastic bed which is two to three clasts thick. Above these clastic beds there is a rapid aggradation transition into the inversely graded

triplet above. A small proportion of granules can be found in between some of the clasts but their concentration is too low to provide any support to the unit.

The clastic bed at 1.6 m is composed of clasts up to 100 mm a-axis. Some of these clasts are bound by a silty clay matrix and are covered by a silty veneer. The clastic bed at 1.5 m is composed of clasts up to 70 mm a-axis and does not show evidence of the silty veneer seen below. The largest of these clastic beds is found at the top of the top inversely graded triplet at 1.4 m. This is approximately 50 mm thick, but is composed of slightly smaller clasts.

Between 1.4 and 0.4 m, the section comprises alternating rhythmically-bedded units of fine gravel and sandy gravel. These beds incorporate a large proportion of rounded pebble clasts up to 50 mm a-axis. There appears to be little or no fine grained material within the matrix which is evident by the poor cohesion between grains and the granular texture. The only evidence of fine grained material is represented by a thin veneer of silty clay which coats many of the larger clasts. There are also a number of very fine silty clay intra-granular veins found between matrix grains. Grainsize distribution analysis of bulk sediment samples taken from within this unit show a unimodal, very poorly sorted, sandy, medium gravel, with a mesokurtic kurtosis (**Figure 6-16-A**). Between 1.4 and 1.2 m, the size of clasts held within the alternating rhythmically bedded units is considerably greater than the remainder of the unit above with well rounded clasts up to 90 mm a-axis. Many of the larger clasts at this lower level of the unit share numerous points of contact, however there are too few contacts to consider this unit as clast supported.

The upper 0.4 m is composed of very poorly sorted sand to coarse gravel matrix containing rounded to well-rounded cobbles and boulders. There appears to be very little organisation within the upper portion of this unit, however with depth, the sediments become more aligned and grade from a

wholly massive appearance, to having a subtly bedded nature with smaller cobbles and pebbles appearing to been deposited layer on layer. Analysis of clast fabric within these layers shows that as well as some form of lateral organisation, there is also preferential alignment of cobble fabric, with a-axis dips preferentially orientated at near 90° to the orientation of the ridge. In most cases these dips are very shallow with Eigen values of S_1 = 0.531, S_2 = 0.303 and S_3 = 0.1666 **(Figure 6-17)**.

An idealised cross section which depicts the geometry of the gravel ridge in relation to the in-situ glacial ice is shown in **Figure 6-18**.

Figure 6-15

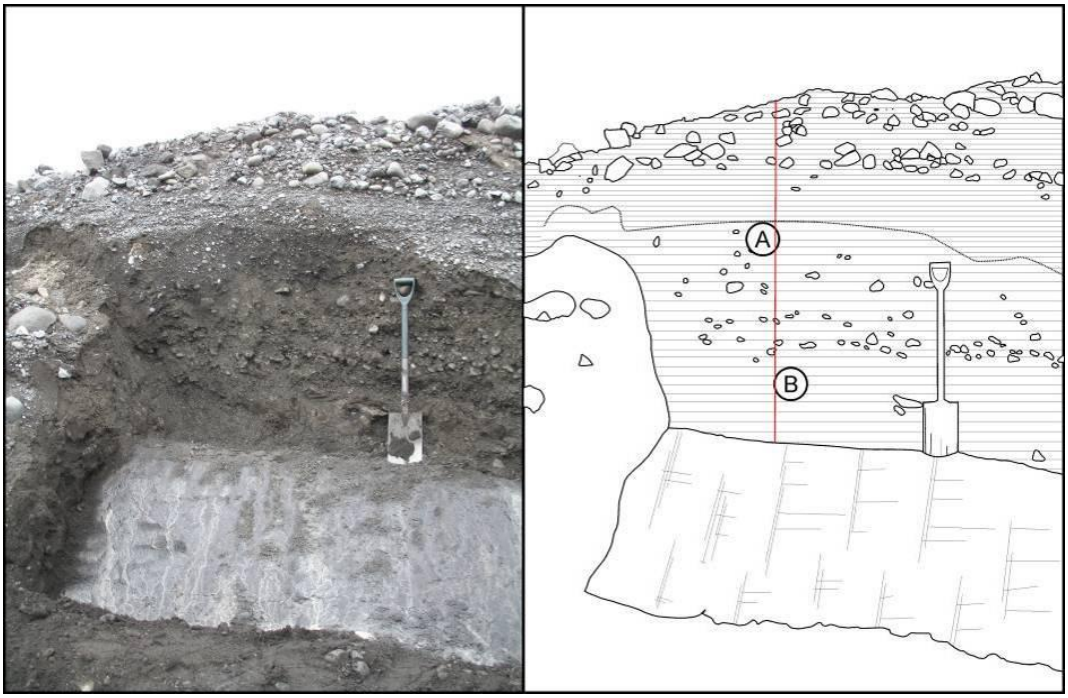

Photograph and panel sketch illustrating the sedimentological architecture of the Háöldukvísl overdeepening section 2. Note spade for scale and red line indicated the location of graphic log Figure 6-17

Figure 6-16

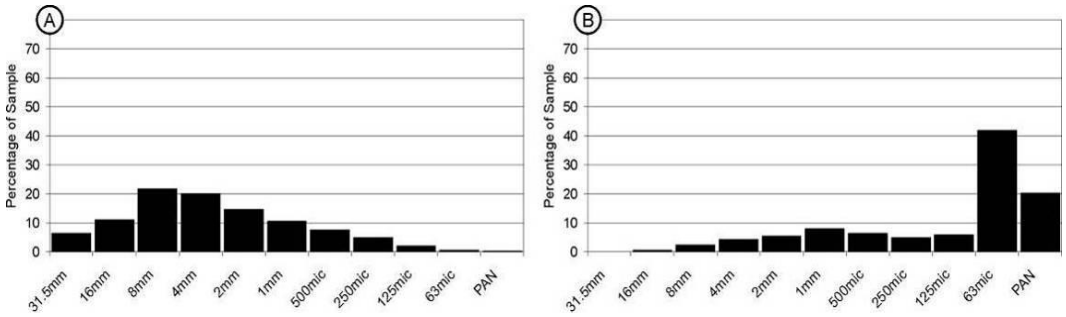

Grainsize distribution histograms of bulk sediment samples taken from the Háöldukvísl overdeepening section 2.

Figure 6-17

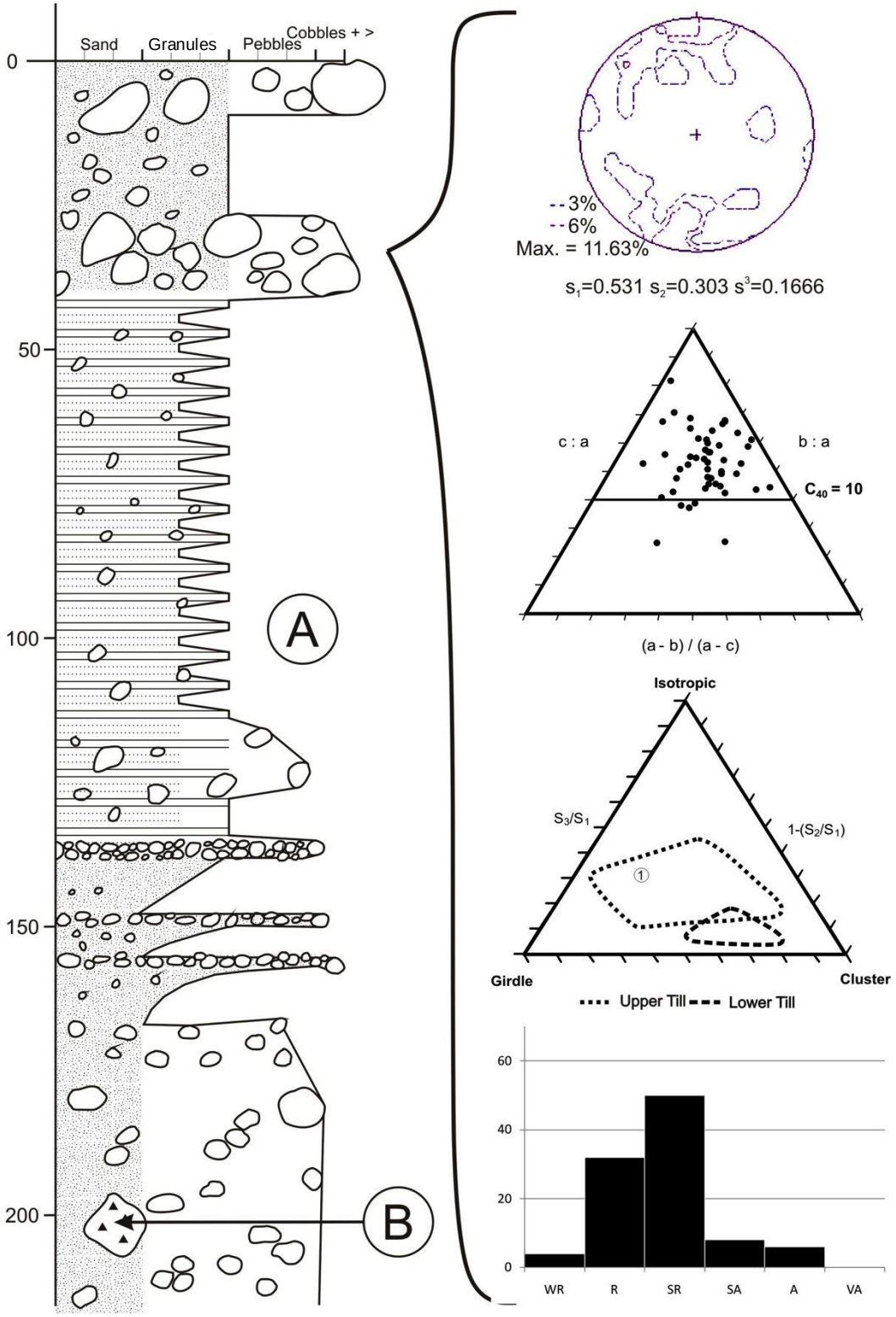

Graphic log of sediments exposed at the Háöldukvísl overdeepening section 2.

Figure 6-18

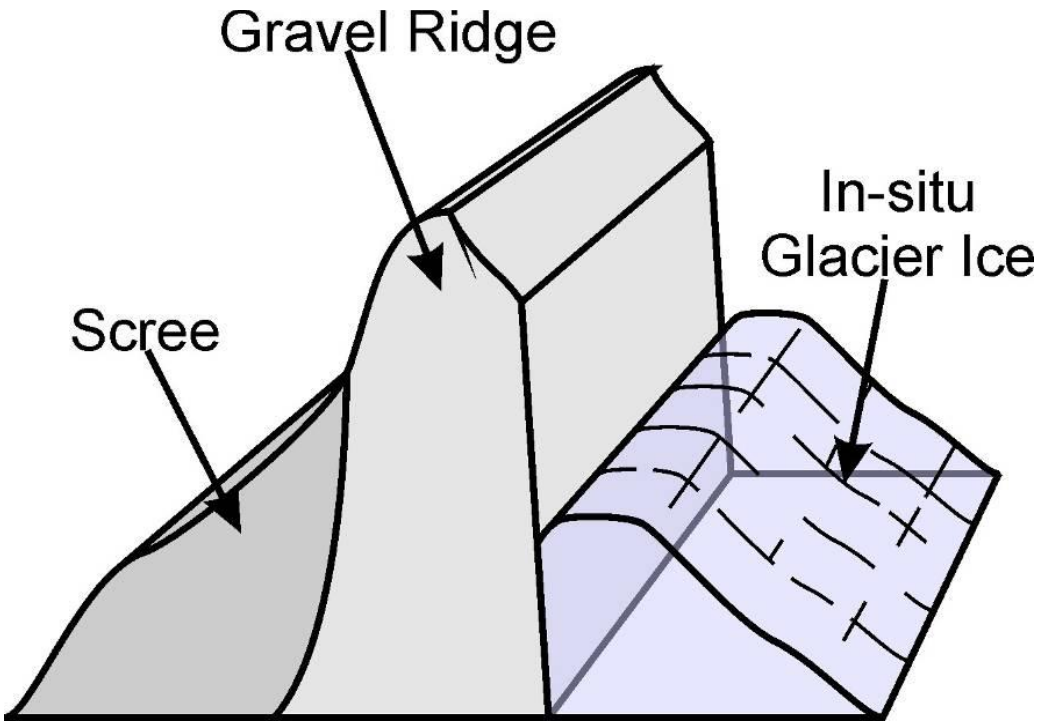

Idealised cross section showing the geometry of the gravel ridge in relation to the in-situ glacial ice at the Háöldukvísl overdeepening section 2.

6.3.8 SECTION 2: INTERPRETATION

As with the sediments of Section 1, the four sedimentary units of Section 2 are all interpreted as having been deposited by high-energy fluvial processes.

The poorly sorted nature of the lowest unit in the exposure is consistent with a highly turbulent flow regime. This has resulted in the formation of a more chaotic, massive unit that does not exhibit any apparent internal structure. The inversely graded triplets directly above are consistent with irregular or pulsating hyperconcentrated flows, where increased viscosity results in the increased density of finer grains, leading to larger grains 'floating' to the surface. The fact that these individual inversely graded packets are intact, demonstrates that the flows were not erosive and that these hyperconcentrated flow conditions did not persist for very long.

The far more ordered character of the bedded coarse sands and gravels suggests a reduction in turbulence. Such structures are consistent with a pulsing flow regime, leading to the deposition of beds of coarse gravels during both the rising and falling limb of each pulse. Such flows have been described in detail by Russell and Knudsen (1999), although the sediments described here have a much finer nature and the individual beds are considerably smaller. Such variations however are likely to be a consequence of reduced discharge and sediment availability, as the sediments described by Russell and Knudsen (1999) were located at the mouth of a large flood water conduit. Based on the geomorphological maps produced in **Section 6.2**, no such conduit has been reported in this location. The increase in cobble size seen in the lower portion of this unit is likely to be a result of variations in sediment availability (Duller et al. 2008) rather that a significant increase in stream power. This interpretation is made on the basis that there is no variation in the nature of the gravelly matrix material.

The upper 0.4 m of well-rounded cobbles are consistent with deposition from a turbulent, high energy, fluvial flow (Russell and Knudsen 1999; Carrivick et al. 2004). Clast fabric analysis from this lower portion is consistent with rolling of clast along the bed in a flow direction that is parallel with the orientation of the ridge. The lack of structure, and clast orientation suggests very rapid dumping of bed load from highly turbulent fluidal flows (Boothroyd and Ashley 1975; Hein 1984). The texture of these sediments is consistent with high-energy deposition from low viscosity, highly turbulent fluidal flows.

The presence of in-situ glacier ice found at the base of this unit suggests that these sediments have been deposited by water flowing englacially within a fracture through the ice. The diamicton, which appears to have been 'pasted' on to the face of the gravels is believed to be a secondary deposit laid down along

the ice contact flowing the initial flood event. The presence of silty veins and veneers found throughout this section are interpreted as diffuse water escape structures and secondary intra-granular flow deposits formed by liquefied flow caused by settling in the main sedimentary body (Lowe 1976).

6.3.9 SECTION 3

Section 3 was located on the north facing side of the most southerly gravel ridge approximately halfway along the length of the Háöldukvísl overdeepening (**Figure 6-4**). In this location the width of each individual ridge is greater than those further towards the ice margin that makes the landscape appear to be dominated by deep gullies rather than tall ridges. A photograph and panel sketch of this excavation is shown in **Figure 6-19** and a graphic log of the excavation is presented in **Figure 6-20.** Although **Figure 6-20** does not include the upper 1 m of the exposure, it is clear that this unit is composed of three primary bedding units. The upper 1 m (not shown in **Figure 6-20**) is composed of cross bedded sands and fine gravels over laying a dense clast supported cobble bed immediately above the top of the cleaned face.

The lower two thirds of this exposure presented in detail in **Figure 6-20** can be divided into two distinct sedimentary units. The upper 0.7 m is defined by numerous thin beds of coarse sand and fine gravel. Between 0.20 - 0.27 m depth, there is a very distinctive bed of matrix supported small pebbles which are up to 12 mm a-axis and very well sorted. This sorting and lack of fines results in very poor cohesion and the whole bed is very unstable. There are numerous inter-granular clay drapes throughout this bed, giving the appearance of the pebbles being coated with a thin veneer of clay. Other inter-granular clay deposits are evident throughout this unit as identified on **Figure 6-20**, especially within the coarse sands.

Figure 6-21 presents grainsize distribution histograms from two of these coarse sand units at shown on **Figure 6-19**. Sample A is defined as a unimodal, poorly sorted, sandy, very fine gravel, with a mesokurtic kurtosis and no skew. Sample B is unimodal, poorly sorted sandy fine gravel with a platykurtic kurtosis and a fine skew.

The lower third of the exposure from 0.7 m to 1.47 m is defined by a significant increase in grainsize. This lower unit is a single normally graded unit with small boulders and large cobbles at its base grading to small cobbles and pebbles at the interface with the upper gravels. The largest cobbles at the base of the unit are clast supported, with a small quantity of sandy gravel matrix material within voids. However the quantity of matrix material increases with elevation in the section. Clay beds within the matrix have been deformed around some of the larger cobbles as well as some of the cobbles having been draped in a thin veneer of clay. Detailed analysis of clast fabric from the clast-supported cobbles shows that there is a considerable a-axis ridge parallel alignment, whilst the matrix-supported cobbles show a-axis' aligned oblique to the ridge (Figure 6-22).

Figure 6-19

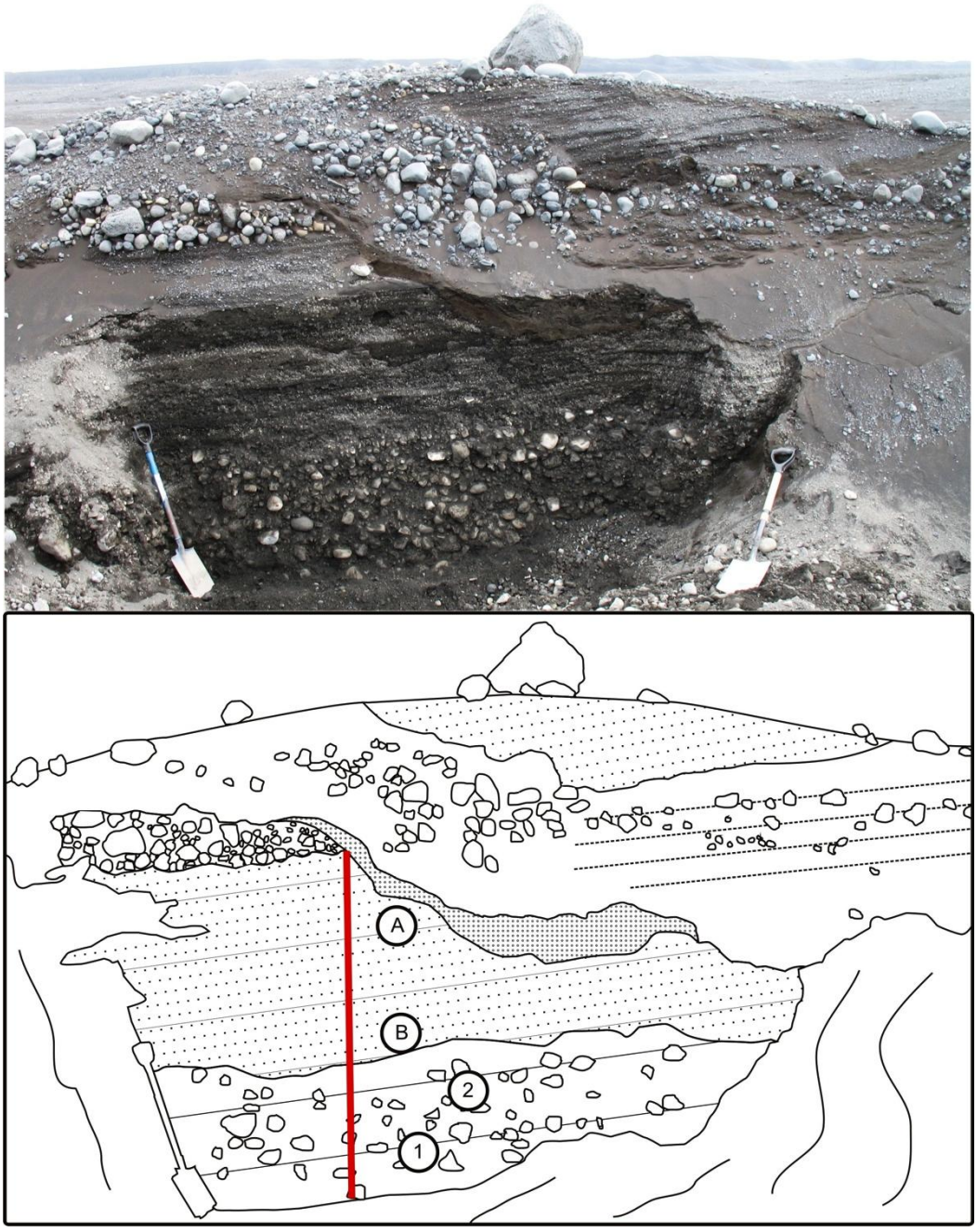

Photograph and panel sketch of the Háöldukvísl overdeepening Section 3. The red line indicates the position of the graphic log shown in Figure 6-20 and circled letters A and B mark the sample locations for sediments collected for grainsize distribution analysis shown in Figure 6-21. Circled numbers so the locations of samples taken for clast fabric analysis presented in Figure 6-22.

Figure 6-20

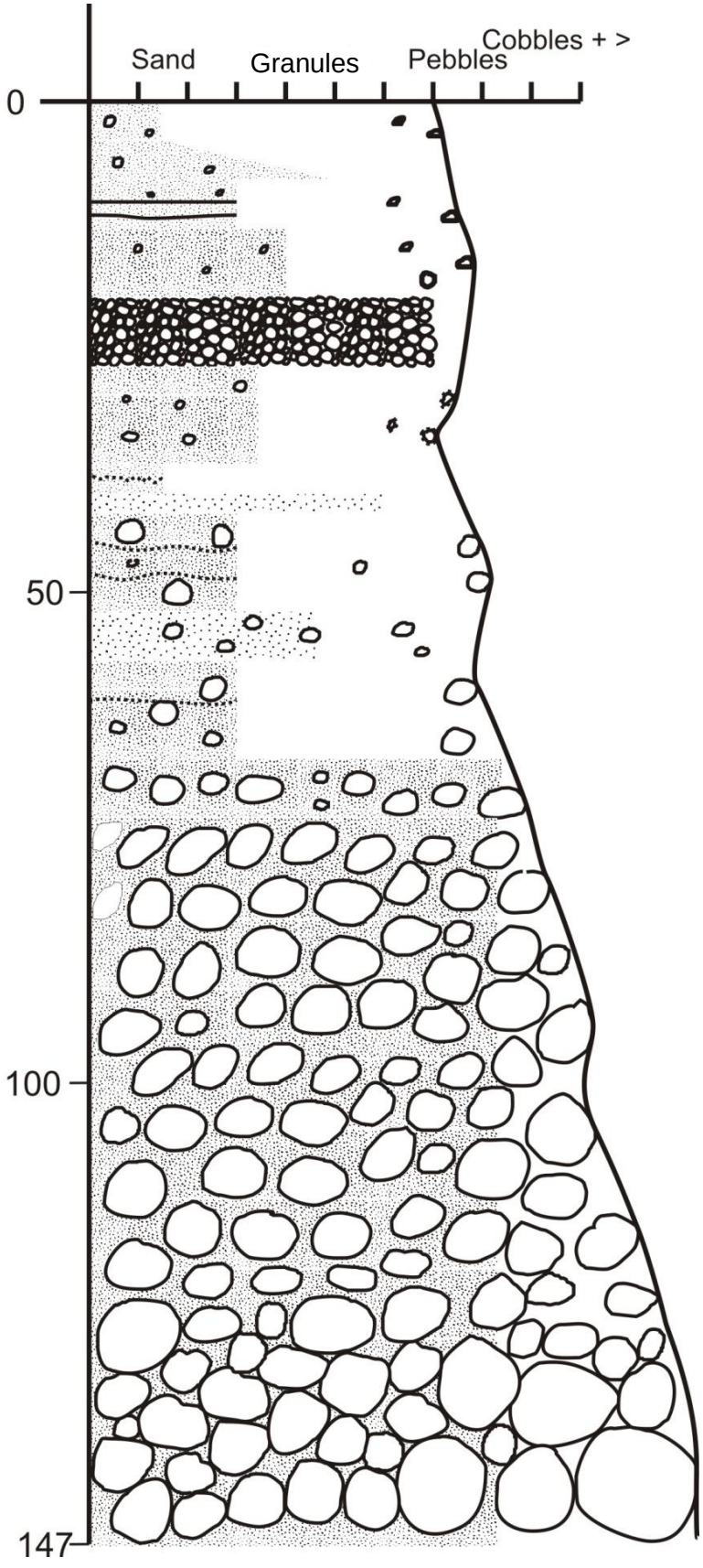

Graphic log of sediments exposed at the Háöldukvísl overdeepening section 3.

Figure 6-21

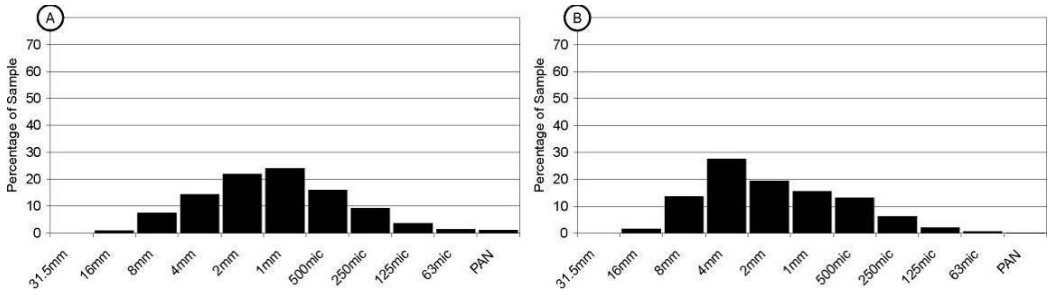

Grainsize distribution histograms of sediments taken from the Háöldukvísl overdeepening section 3

Figure 6-22

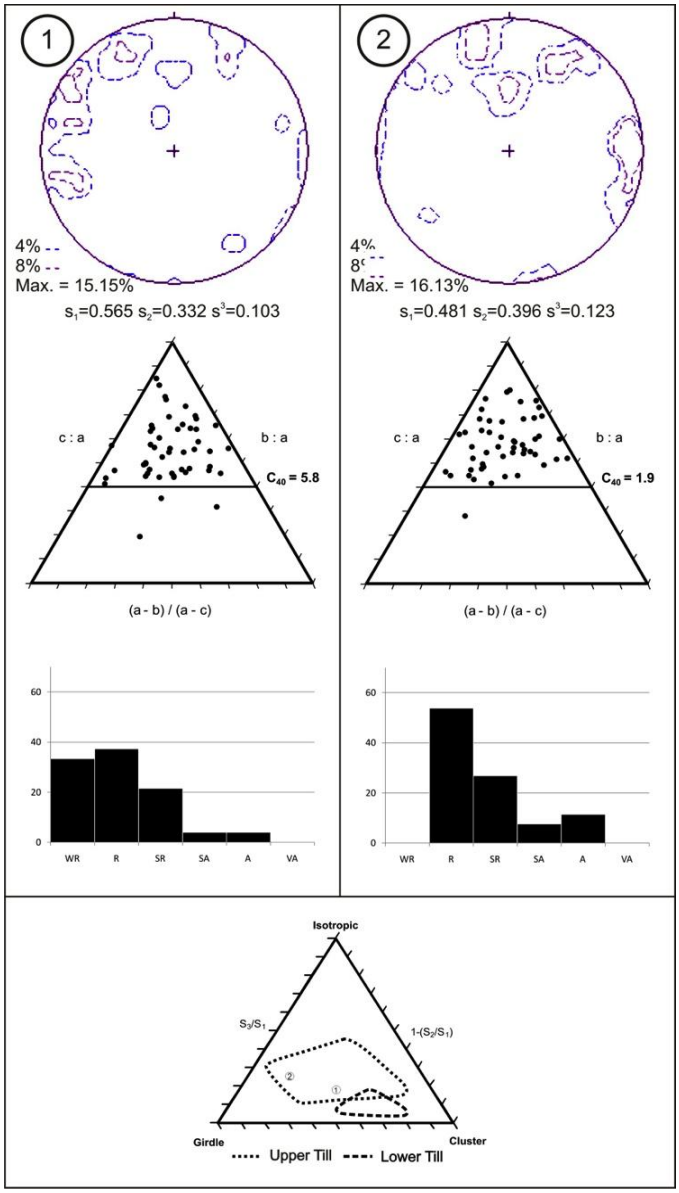

Clast shape and fabric data from the Háöldukvísl overdeepening section 3

6.3.10 SECTION 3: INTERPRETATION

This exposure is interpreted as having been deposited by high-energy fluvial processes. The exposure clearly depicts three primary units (two of which are shown on **Figure 6-20**).

The high degree of rounding and large size of boulders in the lowest unit from 1.47 to 0.65 m is consistent with very high energy fluvial deposition (Powers 1953; Boulton 1978). The switch from clast supported cobbles with ridge parallel clast fabrics at the bottom of the unit, to matrix supported cobbles with ridge oblique clast fabrics higher in the sequence, may be an indication of a rapid switch from hyperconcentrated to more fluidal flow conditions. Hyperconcentrated flows commonly have flow parallel a-axis fabrics, as the increased viscosity of such flows result in the re-alignment of clast's longest axis' parallel to the flow direction, due to the reduced shear stresses associate with this alignment (Hein 1984). As flows become more fluid and less viscous, clast interactions with the bed tend to produce a-axis clast fabrics that are oblique to the orientation of flow (Boothroyd and Ashley 1975) and allow the deposition of fines from suspension.

The coarsely bedded gravels located between 0.65 and 0 m on **Figure 6-19** are consistent with traction deposits from fluidal flows (Brennand 1994). The presence of open framework units suggests rapid fluctuation between laminar and more turbulent conditions while the inter-granular clay drapes present throughout much of this unit are interpreted as post depositional structures deposited by inter-granular ground water flow.

The diffuse sand beds of the top right of this section are indicative of layer on layer deposition from waning stage fluidal flows or pulsating fluidal flows (Carrivick et al. 2004). The lower portion of the upper 1 m of the exposure containing numerous poorly sorted rounded boulders is consistent with having

been rapidly deposited by high energy, turbulent, fluidal or hyperconcentrated flows (Costa 1988).

6.3.11 SECTION 4

Háöldukvísl overdeepening section 4 is located approximately half way along the Háöldukvísl overdeepening's southern edge. It is excavated within the north-facing slope of the southernmost ridge and is composed of three primary sedimentary units (**Figure 6-23 and Figure 6-24**).

The upper 1.25 m of the ridge is composed of very poorly sorted, rounded cobbles and boulders held within a matrix of sands and gravels and a smaller portion of fines. It is clear that the size and concentration of boulders within the upper portion of the exposure reduces considerably with depth until just above the contact with the unit below, where the concentration of clasts increases once more and clusters of clast supported cobbles surrounded by a silty sand matrix are clearly apparent.

The contact with the unit below is erosive and heavily deformed, with evidence of a single load structure in the centre of the panel and pseudo-interbedding towards the right (north) of the section, where the poorly sorted gravels appear below the well sorted sands below.

Below 1.25 m, the section is dominated by well sorted, planar bedded sands. These sands contain no outsized clasts; however there are numerous sub-horizontal silty clay water escape structures which traverse the upper portion of the sand in close proximity to the upper contact. Bulk samples for grainsize analysis of these sands were taken at three locations up the section in-order to identify any subtle variation within the unit (**Figure 6-25 - A, B and C**). All three samples are described as symmetrical, unimodal, very fine gravelly coarse sand. However, variation in mean grainsize does show a very slight normal grading, with the mean grainsize slightly decreasing from 664.0 µm to 550.5 µm

between samples A and C. Grainsize analysis taken from the poorly sorted gravelly interbed on the right of the panel reveals a bimodal, very poorly sorted, sandy very coarse gravel with a platykurtic kurtosis (**Figure 6-25 - D**).

The lower gravel unit shown in **Figure 6-23** is not visible along the whole length of the exposure and this is believed to be a result of the undulating contact between the two units. Where it is exposed in the bottom centre of the panel and again slightly to the left, it is composed of a silty sandy gravel matrix with numerous rounded pebble clasts. The contact with the sands above is very diffuse, made most apparent by a slight lightening of colour and increase in clast concentration. Grainsize analysis of this unit reveals a grainsize distribution very similar to that of sample D, with a unimodal, very poorly sorted sandy coarse gravel with a platykurtic kurtosis (**Figure 6-25 - E**).

Figure 6-23

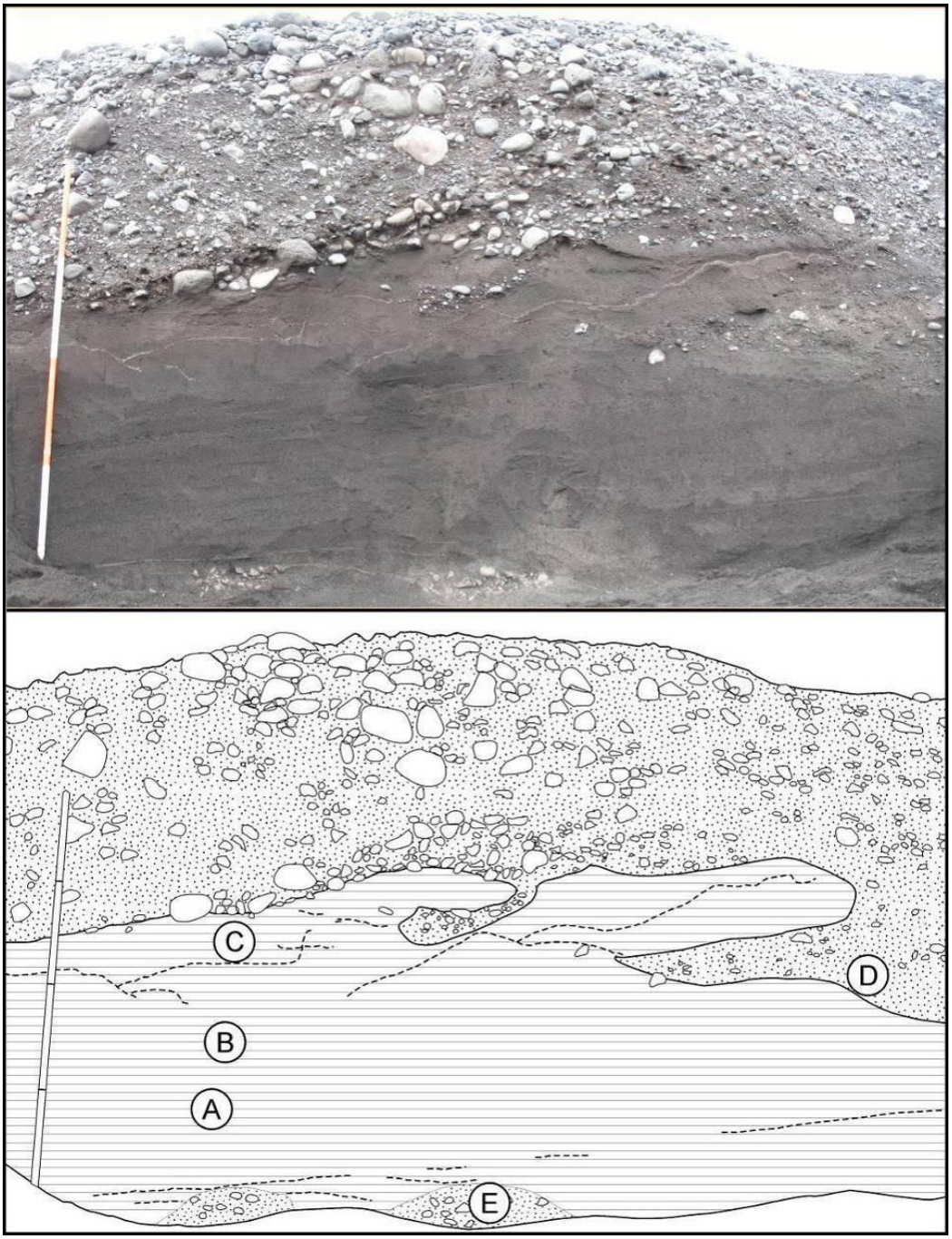

Photograph and panel sketch of Háöldukvísl overdeepening section 4.

Figure 6-24

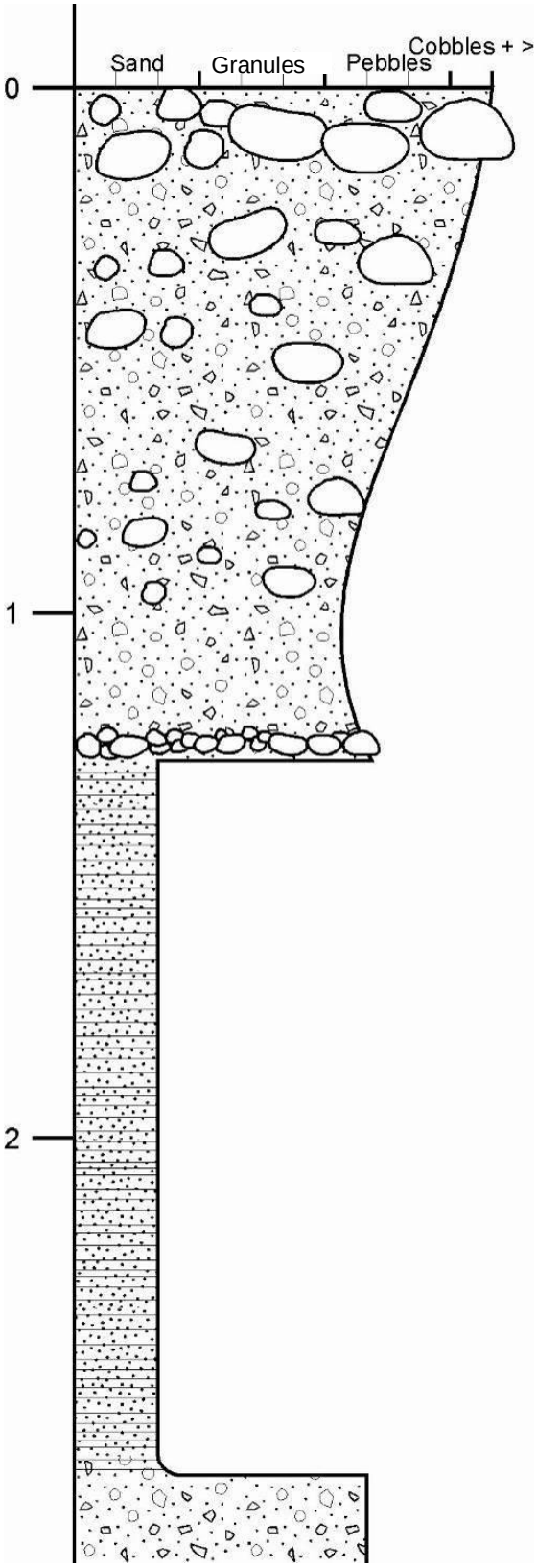

Graphic log illustrating the variation in grainsize between the primary sedimentary units found at Háöldukvísl overdeepening section 4.

Figure 6-25

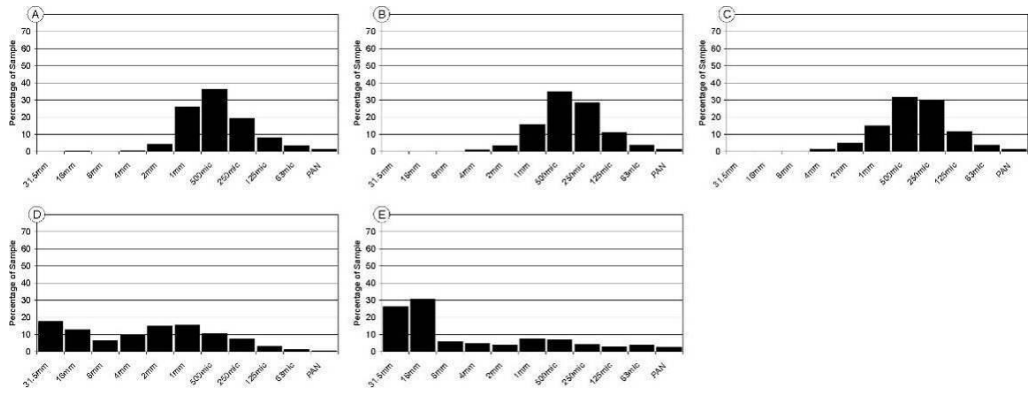

Grainsize distribution histograms illustration the variation if grainsize between samples taken at Háöldukvísl overdeepening section 4.

6.3.12 SECTION 4: INTERPRETATION

Three major units of this ridge are interpreted as having been deposited by high energy fluvial processes. The limited extent of the lowest gravel unit makes interpretation of its origin uncertain. However, the diffuse, none erosive contact between the two units suggest that they were deposited within the same event. The predominantly coarse, finely skewed grainsize distribution and massive appearance are consistent with turbulent, hyperconcentrated flows (Costa 1988; Carrivick et al. 2004).

The planar bedded well sorted fine sands which make up the majority of the lower part of this exposure suggest that these may have been deposited by much lower energy flows than those previously described (Collinson et al. 2006). However, it has also been well documented that sediment availability, as well as flow strength, plays a key role in the grade of fluvial deposits, especially in areas subject to high energy events, (Maizels 1989; Maizels 1997; Duller et al. 2008). In this case, it is considered likely that these planar bedded sands have been deposited by high energy, subcritical flows, possibly in the lee of a hydraulic jump (Russell and Knudsen 1999; Russell and Arnott 2003; Russell et al. 2003; Duller et al. 2008).

The upper surface represents a switch to more turbulent conditions and the rapid deposition of coarse materials. The massive, poor sorting, and well rounded nature of cobbles found in the upper 1.2 m of this exposure are consistent with rapid deposition from high energy hyperconcentrated flows (Costa 1988). The load structures and pseudo-interbedding between the upper gravel and the planar bedded fine sands suggest that the upper gravels were deposited immediately after the deposition of the sands, when water pressures within the sands were high, allowing soft sediment deformation to occur (Lowe 1976; Rijsdijk 2001; Russell et al. 2003).

6.3.13 SECTION 5

The final excavation is located approximately 75 m southeast of excavation 4, within the same ridge. This section is within the east-facing slope of the most western ridge within the ridge network.

The upper 0.37 m of this exposure is composed of moderately well sorted coarse sand to fine gravel matrix which has a distinctive granular texture. Within this matrix there are a few rounded to well rounded, large pebble to small cobble clasts up to 80 mm a-axis. The concentration of clasts is slightly greater towards the top of the unit, however this may be a consequence of windblown removal of fines, increasing the concentration of clasts. Subtle variations in mean grainsize result in alternating coarser and slightly finer beds as shown at the top of **Figure 6-26**.

At 0.37 m, the upper most gravel unit grades to a 60 mm thick unit of very well sorted, massive silty sand. Both the upper and lower contacts of this unit are very sharp, however they do not appear to be erosive (**Figure 6-27 - I**).

Between 0.43 and 0.61 m, there is a massive unit of normally-graded, very well sorted medium to fine sand. This unit contains no outsized clasts except at

its lower bounding surface that is defined by a thin pebble layer 1 - 2 clasts thick (**Figure 6-27 - II**).

Below this pebble layer at 0.67 m, the fine nature of the sediments above become much coarser, well sorted, pebbly, granular gravel with an open framework, clast supported texture. This unit contains a very small proportion of sand sized material (approximately <1%), although some pebbles exhibit a thin surface veneer of silty clay. Most clasts within this unit exhibit a well rounded surface texture, with a small number of these clasts reaching small boulder size (**Figure 6-27 - III**).

At 0.97 m depth, there is another sharp contact with the unit below. This contact does appear to be erosive and is marked by a distinct reduction in the degree of sorting in the underlying sediments. Between 0.97 - 1.29 m, this unit is defined by rounded pebbles and cobbles held within a predominantly granular matrix. This unit has a far greater concentration of sand and fines than the unit above and has a very distinct bi-modal grainsize distribution (**Figure 6-27 - IV**).

The lower bounding surface of the unit above and the upper surface of the unit below are obscured by talus; however the similarities between these two units may indicate that these units grade into one another, although this assumption cannot be confirmed.

The underlying unit, from 1.48 - 1.90 m, is composed of very poorly sorted, rounded to well rounded cobbles up to 250 mm a-axis. Some cobbles appear fractured in-situ and show imbrication dipping towards the northwest (imbrication was identified visually). In a number of locations, cobbles have formed distinct clusters that appear stacked, with distinct points of contact. The matrix material that supports this cobble unit is composed of poorly sorted fine sandy gravel with a small portion of silt (**Figure 6-27 - V**). The lower

bounding surface of this sandy cobble unit is inversely grades from the sand unit below (**Figure 6-27 - VI**)

Between 1.90 - 2.7 m, the unit is composed of normally graded to inversely graded, planar bedded, coarse - fine - coarse sand. This unit contains a small number of rounded outsized clasts and is well sorted. There are also a number of discontinuous silty lamina between fine sand beds.

Between 2.70 - 2.85 m, the grainsize normally grades from sand sized material at the top, to poorly sorted gravels containing a small number of clasts up to cobble size at a depth of 2.85 m (**Figure 6-27 - VII**). These clasts are predominantly sub-rounded and held within a poorly sorted matrix composed of granules, sand, and a small proportion of fines (silt and clay).

Between 2.85 - 3.05 m, the lowest portion of this unit is composed of a massive unit of large rounded cobbles up to 200 mm a-axis held within a poorly sorted, frozen, coarse sand matrix. The matrix has a distinct granular texture that is common where coarse sands are present without the presence of fines. The matrix material of this unit also presents very slight inverse grading (**Figure 6-27 - VIII**).

Figure 6-26

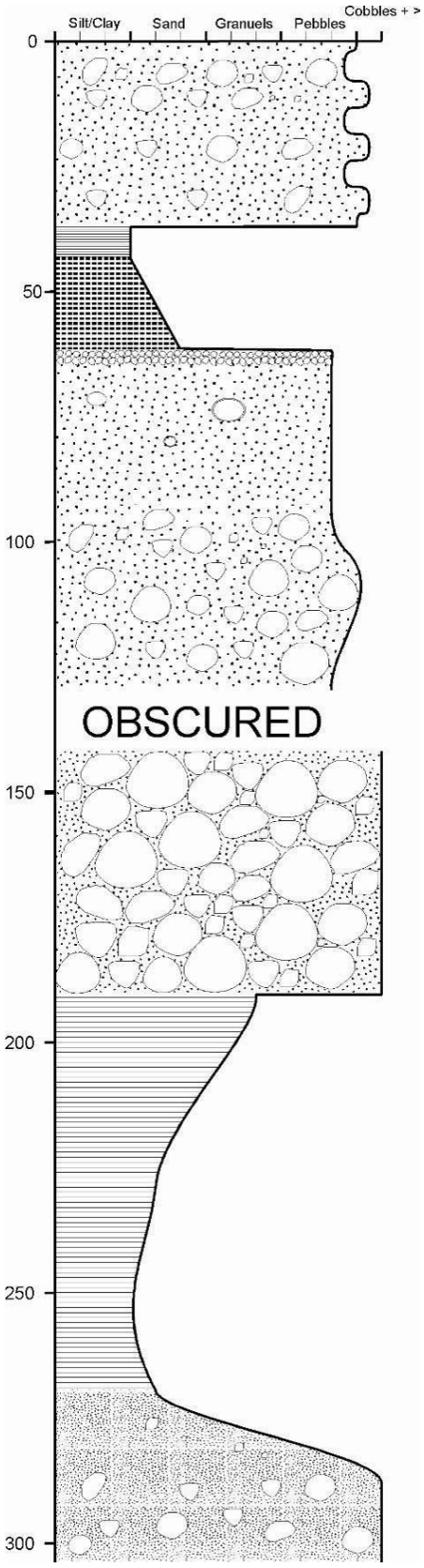

Graphic log illustrating the texture and grainsize of sediments located at the Háöldukvísl overdeepening section 5.

Figure 6-27

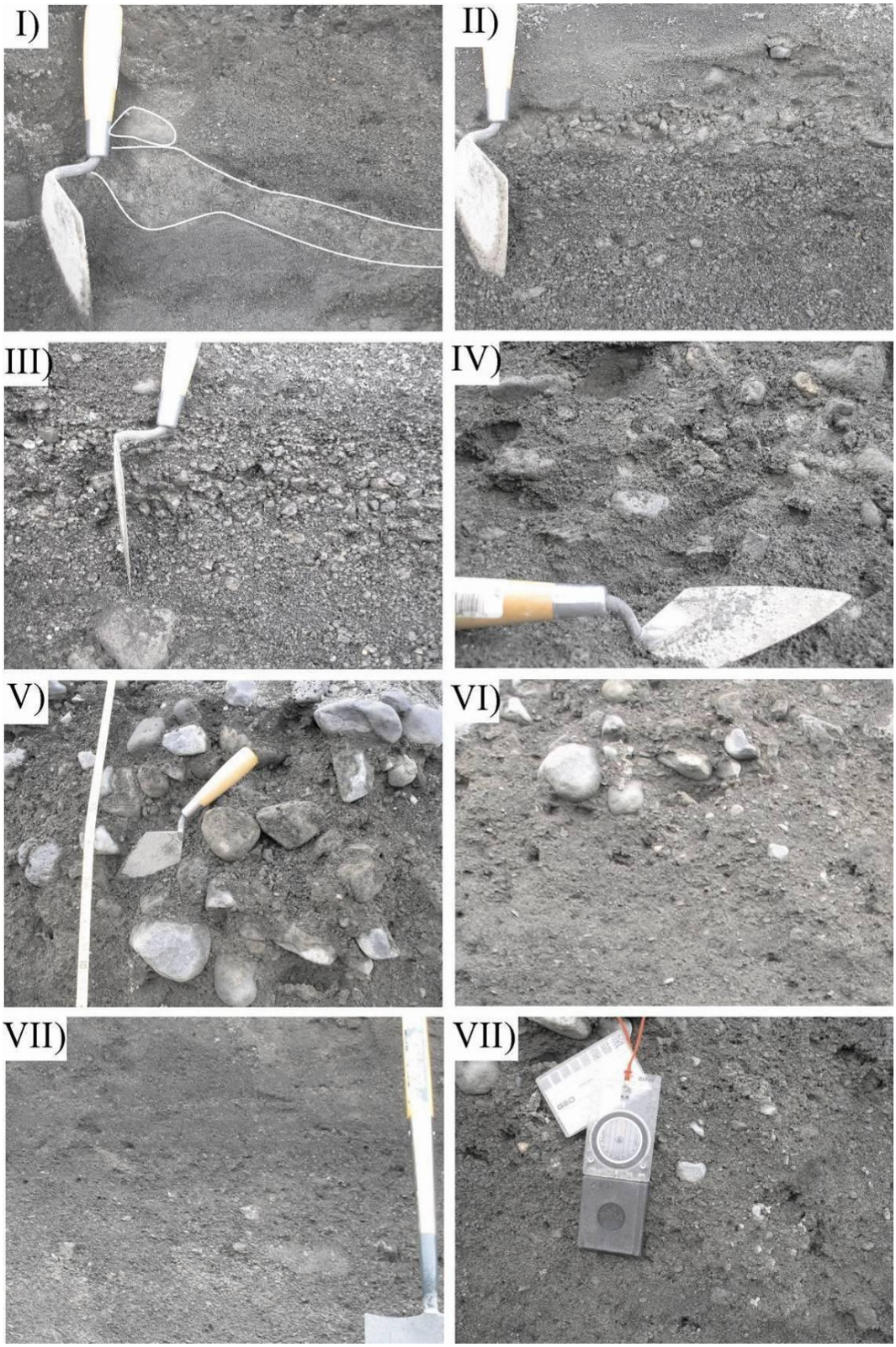

Photographs illustrating the numerous sedimentary facies present at Háöldukvísl overdeepening section 5. I) Diffuse bed of silty sand. II) Well sorted fine sands atop narrow pebble bed. III) Coarse granular gravels. IV) Bi-modal sands with cobbles. V) Bi-modal cobbles with sands. VI) Inversely graded sands to cobbles. VII) Normally graded sands and gravels. VII) Granular, poorly sorted sands and gravels.

6.3.14 SECTION 5: INTERPRETATION

The sediments that make up section 5 are all considered to have been deposited by fluvial processes. The lowest unit of poorly sorted, granular gravels and cobbles, between 3.05 and 2.7 m, are consistent with sediments interpreted by Russell and Arnott (2003) as products of hyperconcentrated flows. Such flows are highly turbulent, resulting in mixing of a wide range of grainsizes. Deposits from such flows are understood to result in rapid fallout from suspension, resulting in massive sedimentary units that show no internal structure.

The normally and inversely graded, planar-bedded sands above, between 2.7 - 1.9 m, have also been associated with hyper concentration. Such laminated deposits have been documented elsewhere along the Skeiðarárjökull ice margin (Russell et al. 2006) and at other glaciers that have been associated with large outburst flood events (Russell and Arnott 2003). In such cases, laminated sands have occurred within expansion bars, downstream of hydraulic jumps associated with large meltwater outlets. Such a switch from massive to laminar bedding is likely to represent a relative reduction in turbulence, possibly associated with antidune migration. The very poorly sorted, fractured, stacked cobble unit over lying these laminar sands between 1.9 - 1.4 m is interpreted as having been deposited by energetic, rapid fallout from suspension which has resulted in the fracturing of numerous clasts. The graded bounding surfaces between the lowest cobble unit, through the normally and inversely graded sands, and into this middle gravel unit at 1.9 m, suggest that the lower portion of the exposure was deposited within a single event. It is likely that initial turbulent conditions deposited the lowest gravel unit, which was then followed by more tranquil, laminar flows resulting in the deposition of the planar graded sands. These were followed by further turbulent conditions. The moderately sorted, granular

sediments with rounded and very poorly sorted cobbles within sands found between 1.29 - 0.67 m are similar to those found at the bottom of the unit and are interpreted as having been deposited from very high energy hyperconcentrated flows (Carrivick et al. 2004). This poorly sorted unit is overlain by a normally graded unit of well sorted sands and then by a bed of silty sand which are interpreted as waning stage fluidal deposits. The upper most unit of alternating moderately sorted gravel beds are consistent with traction bed load deposits as interpreted by Brennand (1994).

The period over which these fluctuations in flow regime may have occurred is difficult to determine. It is considered likely however that they occurred very rapidly, within a pulsating flow. Such pulsating flow behaviour has been documented from numerous glacier outburst events (Maizels 1989; Maizels and Russell 1992; Duller et al. 2008), including the 1996 jökulhlaup at Skeiðarárjökull (Russell and Knudsen 1999).

6.4 DISCUSSION OF THE SEDIMENT - LANDFORM ASSEMBLAGES WITHIN THE HÁÖLDUKVÍSL ICE CONTACT SITE

6.4.1 INTERPRETATION AND FORMATION OF THE HÁÖLDUKVÍSL 'HILL'

Based on the geomorphological and sedimentological descriptions presented above, the streamlined hill to the north of the Háöldukvísl overdeepening is interpreted as a low, broad, gravel cored drumlin (Boulton 1987). Wisniewski et al, (1997) identified a number of outwash fans located in the central part of Skeiðarárjökull in the 1960's that were subsequently overridden when the glacier surged in 1965. It is considered likely that this drumlin was formed during this time, or earlier, as this section of the ice margin has only recently become exposed as a result of glacier melting and ice margin retreat.

It is proposed that the drumlin was formed by processes similar to those described by Boulton (1987), by the overriding of a plastically 'stiff' gravelly alluvial fan. Further support for this hypothesis is provided by the relatively thin carapace of diamicton overlying the fluvial gravels, as seen in **Figure 6-12.** This is consistent with other drumlins which have been interpreted to have been formed by subglacial deformation (Wysota 1994; Hart 1997; Boulton et al. 2001; Clark and Meehan 2001; Evans and Twigg 2002; Fuller and Murray 2002; Waller et al. 2008), and is further supported by the deformation of sands within the diamicton carapace as shown in **Figure 6-10**.

6.4.1.1 Interpretation and formation of ice flow parallel lineations

The ice flow parallel lineations found across the upper surface of the Háöldukvísl drumlin in most cases are interpreted as flutes, easily identified by their association with stoss side, lodged and striated boulders (Rose 1989; Benn 1994). However, in some cases, such lineations are not associated with stoss side lodged boulders. These lineations are difficult to identify from the ground, but are more easily identifiable from the air. They have a very low profile, lineated surface texture not too dissimilar from that of a striated bedrock surface. A similar such lineated surface texture has also been identified by Waller et at; (2008) on the surface of subglacial bed forms interpreted as drumlins recently exposed elsewhere along the Skeiðarárjökull ice margin.

Both types of lineation are interpreted as having been formed as a product of very rapid glacier motion (Benn and Evans 1998; Waller et al. 2008). as this area is known to have been affected by numerous surge events throughout the last century, including well documented events in 1929, 1965 and 1991 (Thorarinsson 1939; Thorarinsson 1943; Wisniewski et al. 1997; van Dijk 2001).

6.4.1.2 Interpretation and formation of ice flow oblique diamicton ridges

The curvilinear lineations composed of diamicton, found adjacent and parallel to the ice margin, on the stoss side of the hill are interpreted as the leading edge of englacial diamicton thrust sheets (controlled moraine) (Gravenor and Kupsch 1959; Evans 2009). These sheets are believed to have become stacked on top of one another as the glacier ramps up the stoss side of the drumlin.

The diamicton within these thrust sheets is believed to have been entrained from the glacier bed into an englacial position as a result of thrusting caused by compression within the glacier margin. This compression is believed to be a result of rapid up glacier ice flow, likely resulting from one of Skeiðarárjökull's many historic surge events, and stress within the ice as a result of a subglacial barrier to that motion, in this case the Háöldukvísl drumlin. This interpretation is favoured over the possibility that the compression was caused by freezing of the glacier margin to the bed as proposed by Hambrey et al,. (1997; 1999) as there is no evidence that this portion of Skeiðarárjökull's ice margin is frozen to its bed.

An alternative interpretation for the formation of these ridges, is that they represent the leading edge of crevasse squeeze ridges, formed by the injection of readily available deformable sediment at the ice bed interface (Evans and Rea, 1999).

However, although it is very difficult to distinguish between crevasse squeeze ridges and thrust sheets without very detailed sedimentological and ice behavioural information, the interpretation of these ridges as thrust sheets is considered more favourable for two reasons.

1) Evans and Rea (1999) state that crevasse squeeze ridges are often found within the ice marginal zone of surge type glaciers. However,

these features are located over 1 km up ice from the 1991 surge limit, and no other such features have been identified within this area of the glacier terminus, which would be expected if the whole ice margin were fractured during the surge as Evans and Rea (1999) suggest.

2) As these landforms have only been identified in the stoss of a subglacial bedform, it is reasonable to suggest that the underlying topographic perturbation was capable of causing sufficient stress in the over-riding ice mass to result in shearing, and the formation of thrust plains.

As stated above, although it is not possible to categorically decipher one from the other with the data available, it is suggested that the simplest interpretation based on the data available is that these features are the result of thrusting caused by ice compression in the lee of a subglacial drumlin.

6.4.1.3 Interpretation and formation of the Háöldukvísl overdeepening gravel ridges

All of the sediments that make up the gravel ridges within the Háöldukvísl overdeepening are interpreted as being deposited by glaciofluvial, rather than glacial, processes. Most of the ridges display a stacked 3-unit stratigraphy, which range from course, poorly sorted gravels at the base, to fine, well-sorted sands in the centre, and are topped with coarse, poorly sorted gravels at the top of the sequence. This stratigraphy has been interpreted as deposited by high-energy hyperconcentrated flows where there has been a switch between turbulent and more laminar flow regimes.

Numerous authors have presented evidence of gravel ridges within both contemporary and Quaternary glacial setting. Such ridges are usually interpreted as eskers (Price 1969; Delaney 2001; Delaney 2002; Burke et al. 2008) or the sedimentary infills of glacial hydrofractures (Roberts et al. 2000; 2001;

Russell et al. 2001; Waller et al. 2001; Roberts et al. 2002). Sedimentologically it is impossible to distinguish between eskers and hydrofractures, as both types of landform are usually composed of stratified or massive glaciofluvial sediments. However, eskers and hydrofracture infills do have distinct morphologies which aid in their identification.

Eskers are often 10's m high / wide, and 100's to 1,000's m long, they often have an anastomosing plan form and may be connected laterally to tributary ridges (Benn and Evans 1998; Delaney 2002). Eskers are formed by the infilling of sub or englacial meltwater channels and their form is governed by the nature of this system (Boulton 1987; Brennand 1994; Burke et al. 2008). As a result, eskers often represent single, well developed conduits which follow efficient hydraulic gradients.

Hydrofractures form when sub or englacial meltwater pressure exceeds the ice overburden pressure, leading to fracturing of the ice (Roberts et al. 2000). Such fracturing may be the result of water exploiting pre-existing weaknesses in the glacier ice, such as closed crevasses, or it may initiate new fractures if water pressures are high enough. Due to the linear nature of crevasses and the crystal structure of ice, fracturing of ice in this manner usually results in the formation of linear structures. Where glacier ice is subject to rapid, intense pressures, large irregular networks have been documented, which lead to the formation of multiple, linear, cross cutting fractures within close proximity(Roberts et al. 2000).

Due to the rectilinear geometry of the ridges, and the presence of *in-situ* glacier ice present at the ice proximal end of the overdeepening, it is believed that the Háöldukvísl ridges were formed by the deposition of sediments within a linear network of hydrofractures (Roberts et al. 2000; Roberts et al. 2001; Roberts et al. 2002).

The preservation of ice and the better condition of sections on the north facing slopes of the ridges is interpreted as a function of ridge aspect. The south side of the ridges is subject to greater amounts of direct sunlight, leading to preferential melting of the south side in comparison to the north, which is somewhat protected by the ridge itself. This causes the southern sides of the ridges to become more rapidly degraded than the north facing sides.

A simplified model of the sedimentation and degradation processes in presented in **Figure 6-28.** This demonstrates how the width of hydrofractures propagates down glacier, leading to the general pattern of widening ridges with distance down ice. Wider accumulations of sediment, and narrower units of ice in between, lead to the pattern of tall ridges at the ice proximal end of the overdeepening and deep gullies at the distal end.

Figure 6-28

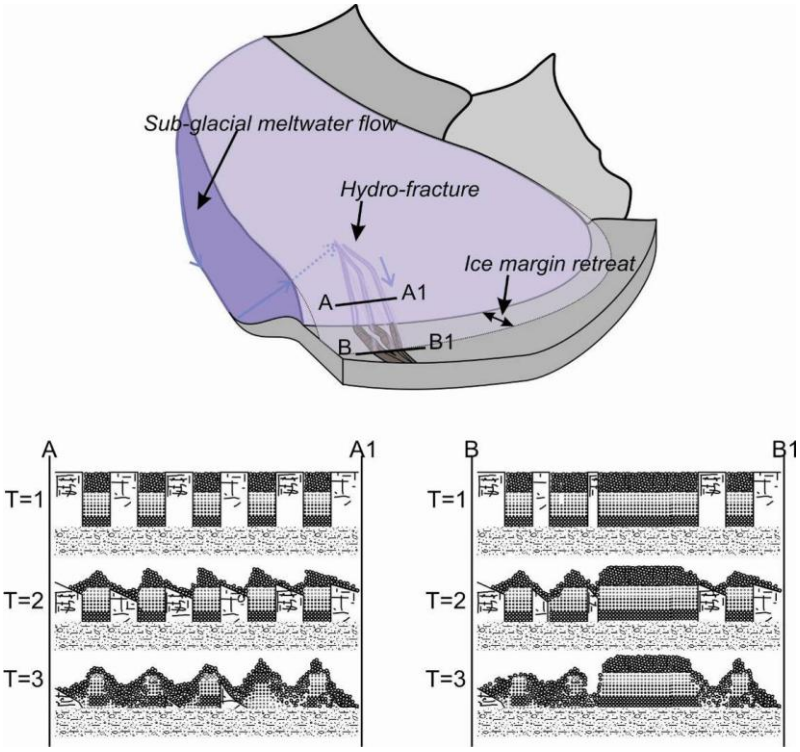

Conceptual model illustration the formation and degradation of fracture fill ridges within the Háöldukvísl overdeepening. Dilation of hydrofractures down ice results in the formation of tall / narrow ridges (A -A1) at the up ice end of the feature and wider ridges at the down ice end. These wider ridges produce a landscape of deep gullies (B - B1).

6.4.2 CONTROLS ON MELTWATER ROUTING

It has been established that the gravel ridges found within the Háöldukvísl overdeepening were formed by the deposition of sediments within hydrofractures. The high discharge required to generate such sub / englacial water pressures suggest that these hydrofractures were formed during one of Skeiðarárjökull's many jökulhlaups. The orientation of the ridges / hydrofractures are consistent with other features along the ice margin which are known to have formed during the November 1996 jökulhlaup (Burke et al. 2008), as such it is considered highly probable that these features also formed during this event.

Most hydrofractures observed at the margin of Skeiðarárjökull, and presented within the literature (Roberts et al. 2000), have an orientation that is oblique to the ice flow direction, and water is shown to flow perpendicular to the orientation of the fracture, (i.e. vertically out of the ice). In this case, the direction of melt water flow appears to be parallel to the orientation of the hydrofracture, at a horizontal angle towards the ice margin. Such flows were proposed by Roberts et al., (2000) as a result of flow along transverse crevasses, however the sedimentary infills of such flows have until now not been recorded.

It would also appear that the routing of meltwater has been significantly influenced by the local subglacial topography (Shreve 1972). Formation of these hydrofractures is clearly concentrated along the sides of the drumlin, suggesting that meltwater has been diverted into the topographically and hydraulically low areas of the glacier bed, rather than flow up and over the drumlins stoss face. This observation clearly demonstrates that the formation of these ridges was directly governed by the nature of the subglacial drainage system (Jørgensen and Sandersen 2006; Russell et al. 2006).

Based on the close spacing and chaotic nature of these ridges, it is believed that these hydrofractures were formed during the rising limb of the 1996 jökulhlaup, when the initial flood wave resulted in the formation of a high number of high pressure distributed conduits (Roberts 2005). During the peak and waning stage, out flows became concentrated upon individual point outlets, resulting in expansion and excavation of meltwater conduits by melting and mechanical excavation (Burke et al. 2008). It is considered unlikely that the hydrofractures which formed the Háöldukvísl ridges would have been preserved during the peak or waning stage of the event as it is considered likely that the ice would have been excavated as seen elsewhere, leading to the formation of a single tunnel.

6.4.3 FORMATION OF THE HÁÖLDUKVÍSL OVERDEEPENING

The morphology of the Háöldukvísl overdeepening and ridge landscape is complex, and without detailed analysis could be misinterpreted as a zone of collapse associated with the melt out of buried ice (Fleisher 1986; Maizels 1992; Fay 2002). However, such analysis has revealed that this landscape is composed of three key components; the Háöldukvísl drumlin, the gravel ridges, and the overdeepening into which the ridges are deposited.

It is clear that for hydrofractures to form in the lee of the Háöldukvísl drumlin, glacier ice must have been present in the lee of the drumlin prior to the onset of the 1996 jökulhlaup. There are a number of hypothesis which could explain the presence of this ice; it is possible that the western flank of the Háöldukvísl drumlin was eroded subglacially by meltwater prior to the 1996 Jökulhlaup, and that the remaining void was subsequently infilled with glacier ice, or it may have been eroded sub-aerially during a previous period of glacier recession. However, such hypotheses require interpretations of glacier dynamics that cannot be justified with the available data. As such, it is considered that the

simplest explanation for the presence of the ice is that it was buried prior to the formation of the drumlin and has been subsequently over ridden.

6.4.4 MODEL FOR THE FORMATION OF THE HÁÖLDUKVÍSL OVERDEEPENING AND GRAVEL RIDGES

Based on the rejection of the above hypotheses, a new polygenetic model for the formation of this landscape has been developed. It has been shown, and is presented in Figure 6-29, that the Háöldukvísl drumlin has formed as a result of ice advance over a proglacial alluvial fan. During the formation of this fan, burial of ice has produced a line of weakness, which would later be exploited by meltwater. Following the drumlinisation of the fan, subglacial flood water – likely associated with the 1996 jökulhlaup, resulted in very high subglacial meltwater pressure that led to fracturing of the buried ice, where the flow of meltwater was controlled by the topography of the glacier bed, routing water around the flanks of the drumlin and through the line of weakness provided by the buried ice. During the waning stage of the flood, sediments within the highly sediment laden meltwater became deposited within the fractures. Upon retreat of the glaciers ice margin, melt out of the hydrofractures has revealed a series of hydrofracture casts, forming of sand and gravel, rectilinear ridges in the lee of the Háöldukvísl drumlin. Differential melting of the ridges has led to their north facing sides being preserved longer and allowed the identification of in-situ glacier ice.

Figure 6-29

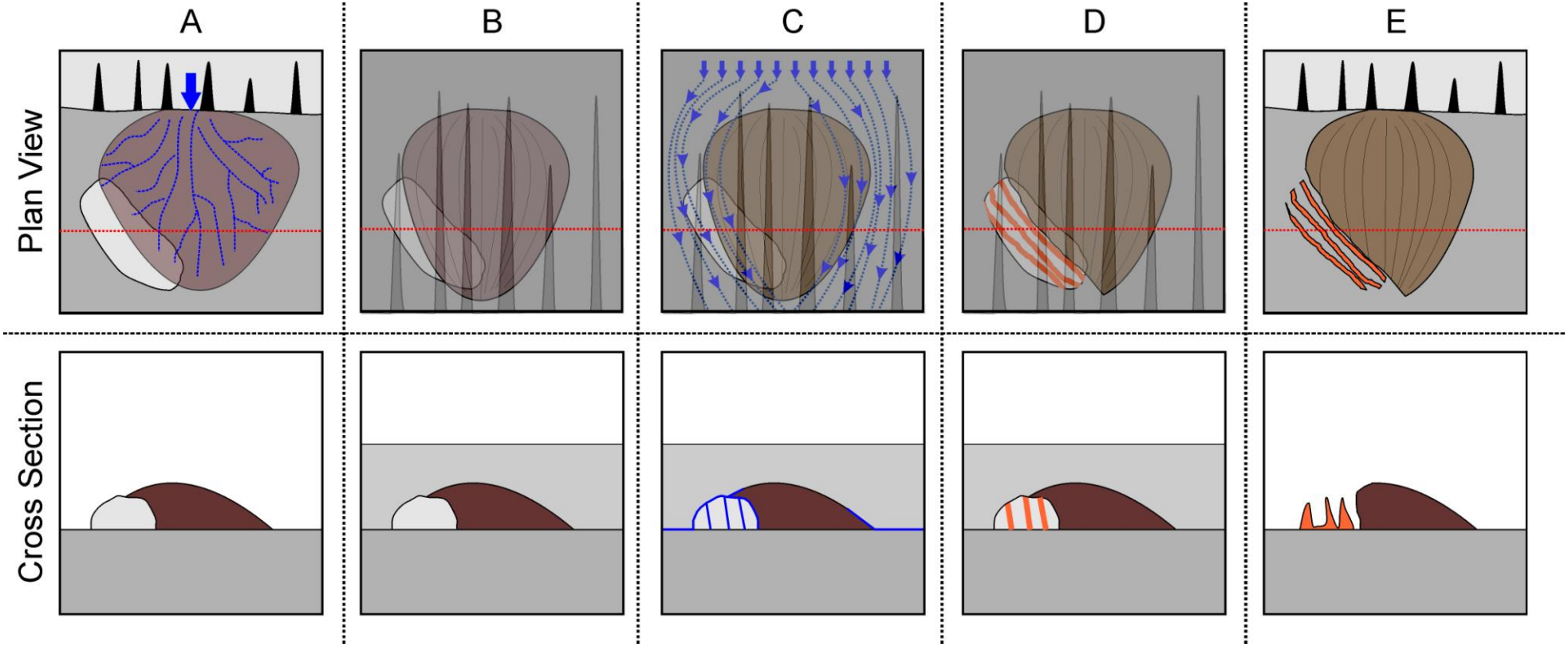

Conceptual model illustrating the processes responsible for the formation of a hydro fracture network in the lee of the Háöld ukvísl drumlin. A) Formation of proglacial alluvial fan and burial of ice. B) Glacier advance and formation of drumlin. C) Onset of flood, meltwater follows the most hydraulically efficient route along the glacier bed, around the flanks of the drumlin, and through the buried ice, forming hydro-fractures. D) Deposition of glaciofluvial sediment with hydrofractures. E) ice margin retreat and melt out of ice, to reveal hydrofracture casts in the form of gravel ridges.

6.5 CHAPTER SUMMERY

This chapter has presented and interpreted a number of geomorphological and sedimentological observations made within the Háöldukvísl ice contact site. These interpretations suggest that this site has been subject to numerous periods of glacier advance and retreat that have contributed to the formation of landforms associated with deformation of the glacier substrate and meltwater routing around subglacial bedforms. It has presented evidence of meltwater flow, at the glacier bed within longitudinal hydrofractures, and that these hydrofractures have formed within pre-existing buried glacier ice. The interactions of these processes are important in the development of overdeepenings at the margins of contemporary glaciers and to the proglacial landsystem as a whole, which are discussed in detail in Chapter 7.

7 DISCUSSION

7.1 INTRODUCTION

The aim of this chapter is to discuss the results presented in the previous chapters of this thesis, within the context of the existing literature and in relation to the aims and objectives of the research set out in **Chapter 1**. This chapter re-assesses literature-based models of overdeepenings using the results of this project. Chapters 4 to 6 present a number of new models developed during this research, which are based on sedimentological and geomorphological investigations carried out at Skeiðarárjökull. These models explore the roles of a number of different processes, including subglacial meltwater erosion, esker formation, ice stagnation, meltwater routing, ice fracturing, and sandur aggradation, in the genesis of overdeepenings at various sites across Skeiðarárjökull's ice margin. This chapter draws on the conceptual / process models which have been developed for three individual sites along the margin of Skeiðarárjökull (Western Sæluhúsavatn, Eastern Sæluhúsavatn, and Háöldukvísl), and provides a discussion of the formation of overdeepenings within the context of the main themes presented within the existing literature. This discussion provides a critical assessment of previous models, while discussing the role of each individual process or combination of processes, which has been found to contribute to the formation of proglacial overdeepenings.

7.2 SUBGLACIAL MELTWATER EROSION AND THE GENESIS OF ICE MARGINAL OVERDEEPENINGS

Chapters 1 and 2 provide a detailed review of current understanding of the processes responsible for formation of ice marginal overdeepenings, and that subglacial meltwater erosion is considered the primary process for the formation of such features within glacierized catchments (Shaw and Gilbert 1990; Ó

Cofaigh 1996; Beaney and Shaw 2000; Sjogren et al. 2002; Gray et al. 2005; Brennand et al. 2007; Smith et al. 2009). Often, this meltwater erosion is the product of catastrophic outbursts or jökulhlaups, and has been interpreted as the primary process for the formation of many Quaternary tunnel channels and tunnel valleys, which are considered overdeepenings in this context (Clayton et al. 1999; Beaney and Shaw 2000; Beaney 2002; Cutler et al. 2002; Kozlowski et al. 2005).

It is well documented that Skeiðarárjökull has been subject to numerous catastrophic jökulhlaups throughout recent history and the Holocene (Guðmundsson et al. 2002; Russell et al. 2005), and such outburst events have been clearly demonstrated to have contributed to the formation of tunnel channels and tunnel valleys during earlier glacial periods (Brennand and Shaw 1994; Clayton et al. 1999; Beaney 2002; Sjogren et al. 2002; Brennand et al. 2007). The presence of an ascending channel, eroded into the glacier's substrate and terminating at the head of an alluvial fan, located at the eastern Sæluhúsavatn basin site, provides support for this subglacial meltwater erosion hypothesis (**Section 2.3.2**) and has been interpreted as a tunnel channel, which formed during the 1996 jökulhlaup (Russell et al. 2007).

However, where evidence for direct subglacial meltwater erosion has been identified, this research has found that this process is only responsible for the erosion and formation of relatively small landform elements, within the wider landscape contexts, which in-turn are dominated by negative topography. This has been shown to be the case at two locations at Skeiðarárjökull; the tunnel channel at the eastern Sæluhúsavatn described above (**Figure 4-9**), and the ascending gully between drumlins in the western Sæluhúsavatn (**Figure 5-22**).

As described above, this study has identified a landform within the eastern Sæluhúsavatn that is characterised as a linear overdeepening, rising from an ice contact lake basin and terminating at the head of a proglacial fan. It has been demonstrated that this feature was formed during the 1996 jökulhlaup as a result of subglacial meltwater erosion and based on the features morphology, geometry, and process of formation; it has been interpreted as a 'Tunnel Channel'. Although this demonstrates that subglacial meltwater erosion has clearly played an important role in parts of this landscape, the formation of the whole eastern Sæluhúsavatn basins landscape cannot be attributed to erosion by subglacial meltwater. Sedimentary evidence collected from the walls of the basins, and the presence of eskers, suggests that the overall landscape has formed as a result of sandur aggradation (**Figure 4-25** and Figure 4-42).

Similarly within the western Sæluhúsavatn, the presence of a subglacially eroded channel which cross cuts a hydrofracture (**Figure 5-22**) provides clear evidence that the channel was formed by subglacial meltwater during the November 1996 Jökulhlaup. However, it is clear from investigations of the surrounding geomorphology and historic aerial photography, that such erosion only occurred within this limited area, and it did not lead to the formation of the wider landscape, which comprises a topographic overdeepening. Further evidence collected during this project has allowed the rejection of the subglacial meltwater erosion hypothesis as the primary agent for the formation of the overall area, whilst supporting other hypothesises such as formation due to sandur aggradation and the melting of buried ice (**Figure 5-23**). Therefore, the findings of this study have demonstrated that the formation of topographic overdeepenings is not exclusively attributed to direct subglacial meltwater erosion.

Importantly, where evidence for subglacial meltwater erosion has been found, this research has been able to improve our understanding of the timing of that erosion. The cross cutting of hydrofractures by a subglacially eroded channel has shown that direct subglacial meltwater erosion of the glacier bed occurred following the deposition of englacial sediments within hydrofractures during the 1996 jökulhlaup. In the western Sæluhúsavatn area, during the later stages of the 1996 jökulhlaup, it is hypothesised that, as water pressures dropped and effective pressures rose, englacial flow through hydrofractures ceased (Roberts 2005), and were followed by the diversion of meltwater along the glacier bed, which resulted in the erosion of the ice – bed interface (**Figure 7-1**).

The observations of the cross cutting of a subglacial channel and hydrofracture at the western Sæluhúsavatn, which link glacier bed erosion with the cessation of flow through hydrofractures, also highlight the importance of ice thickness on the processes of subglacial meltwater erosion during jökulhlaups. Shreve (1972; 1985) clearly demonstrated the positive relationship between ice thickness and subglacial effective pressure, where increases in ice thickness result in an increase in effective pressure, while Roberts (2005) demonstrates that hydrofracturing and the sub-vertical englacial flow of meltwater through hydrofractures is most prominent when the rate of increase in porewater pressure is at its greatest and the rate in the reduction in effective pressure is high. The presence of hydrofracture sediments within a subglacially eroded channel in the western Sæluhúsavatn area has clearly demonstrated a link between the cessation of hydrofracturing and the initiation of subglacial melt water erosion.

Figure 7-1

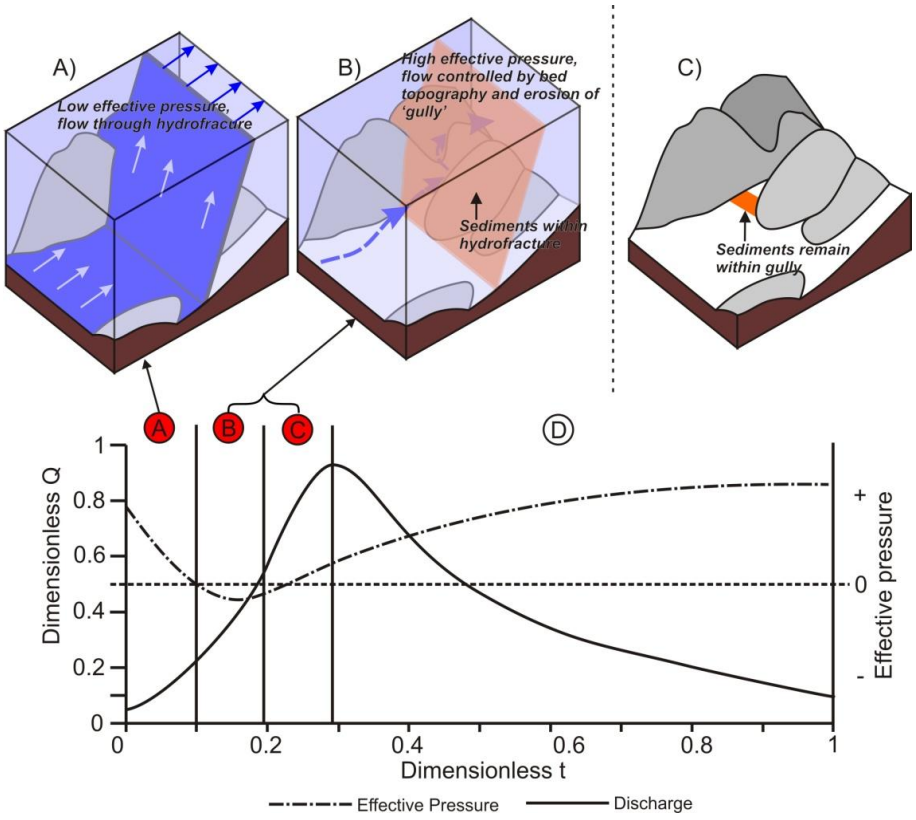

Conceptual models illustrating the impact of discharge and effective pressure at the Western Sæluhúsavatn on sub and englacial meltwater routing during the 1996 Jökulhlaup. A) rapidly falling effective pressure allows the formation of hydrofractures and flow sub-vertically through the ice to the surface. B) as discharge increases, the rate of drop in effective pressure falls and effective pressure begins to increase, flow through hydrofractures cease, leading to deposition of englacial deposits and initiation of fluvial erosion of the glacier bed. C) Following ice retreat and lowering, englacial sediments melt out of the ice and occupy the gully floor. Conceptual hydrograph modified from Roberts (2005) Discharge (solid line) and concomitant effective pressure (dashed line)

Based on the link between the cessation of hydrofracturing and the initiation of subglacial melt water erosion, it could be hypothesised that the thickness of the glacier ice plays an important role in the degree of erosion occurring beneath glaciers. If glacier ice is thicker, subglacial effective pressures are likely to be higher and remain higher for longer during flood events. This would likely result in greater volumes of water flowing through hydrofractures, away from the glacier bed, and reducing the potential for erosion of the glacier substrate. Alternatively, thinner ice would result in lower subglacial effective pressures that would favour topographic control of meltwater flow along the

glacier bed and increasing the potential for subglacial meltwater erosion. This demonstrates the importance of ice thickness, and variations in subglacial meltwater pressure, in controlling the spatial and temporal variations of subglacial meltwater erosion during jökulhlaups.

Considering the absence of any evidence of water exiting the glacier in this location, such as a proglacial channel or fan, prior to or following the 1996 jökulhlaup, it is considered unlikely that this ascending channel was formed prior to the flood, and thus it is unlikely that subglacial meltwater flows utilised this pathway prior to its formation during the peak and waning stages of the 1996 jökulhlaup (Russell et al. 2007). Once formed, it is unlikely that any increase in subglacial discharge would be capable of increasing subglacial water pressures enough to initiate hydrofracturing after a large portal outlet has become established.

7.3 ESKER FORMATION AND THE GENESIS OF TOPOGRAPHIC OVERDEEPENINGS

Eskers have often been directly associated with overdeepenings such as tunnel channels within the glacial system due to the common presence of eskers located along the bottom of tunnel channels (Boulton and Hindmarsh 1987; Christiansen 1987; Moores 1989; Brennand 2000; Sjogren et al. 2002). Eskers often form within overdeepenings as a result of the relative increase in subglacial meltwater which flows through due to their low hydraulic potential (Shreve 1972). This increased flow through such regions of the subglacial system, and the deposition of glaciofluvial sediments from these flows into sub and englacial conduits, results in the formation of eskers (Price 1967; Shreve 1985; Brennand 1994; Fisher et al. 2005). As such, there is a general relationship between eskers and overdeepenings, where esker formation follows the formation of over deepenings such as tunnel channels (and other negative topography), a result of

the pre-existing presence of tunnel channels, with their low hydraulic potential (**Figure 7-2**).

Only one hypothesis presented within the literature has considered the co-formation of eskers and overdeepenings as a single process. This hypothesis was first presented by Boulton and Hindmarsh (1987), and develop by Moores (1989) and Ó Cofaigh (1996) (**Figure 2-12**). This hypothesis considered the synchronous formation of tunnel channels and eskers as a result of subglacial bed deformation into a low-pressure subglacial conduit (**Figure 7-2**). However, very little, if any, corroborative field evidence has been presented in the available literature and the majority of existing literature, e.g. (Price 1967; Shreve 1985; Brennand 1994; Fisher et al. 2005), relating to esker sedimentology provides adequate evidence to critically test and falsify this hypothesis. If eskers were formed by subglacial deformation, the inner core of any esker formed by this process would be composed of subglacially derived, deformed diamicton (Boulton and Hindmarsh 1987; Ó Cofaigh 1996). To falsify this hypothesis, it would be necessary to demonstrate that eskers are not composed of deformed diamicton. This hypothesis can be rejected based on the findings of numerous sedimentological investigations of eskers, where the internal composition is composed of glaciofluvial deposits (Price 1967; Brennand 1994; Huddart et al. 1999), with only a thin diamicton carapace in some cases. Where eskers composed of till have been identified, they have not been associated with tunnel channels (Price 1967; Shreve 1985; Brennand 1994; Fisher et al. 2005; Evans et al. 2010), and are believed to have formed following the evacuation of meltwater from the associated subglacial conduit.

Having demonstrated that the majority of existing models show that eskers form subsequently to tunnel channels (or other overdeepenings) and that the only previous hypothesis for the co-formation of tunnel channels and eskers

has been rejected, this research has added to knowledge by identifying the processes which have lead to a reversal in this relationship, where negative topography forms subsequently to, and as a direct result of the presence of eskers (**Figure 7-2**).

Figure 7-2

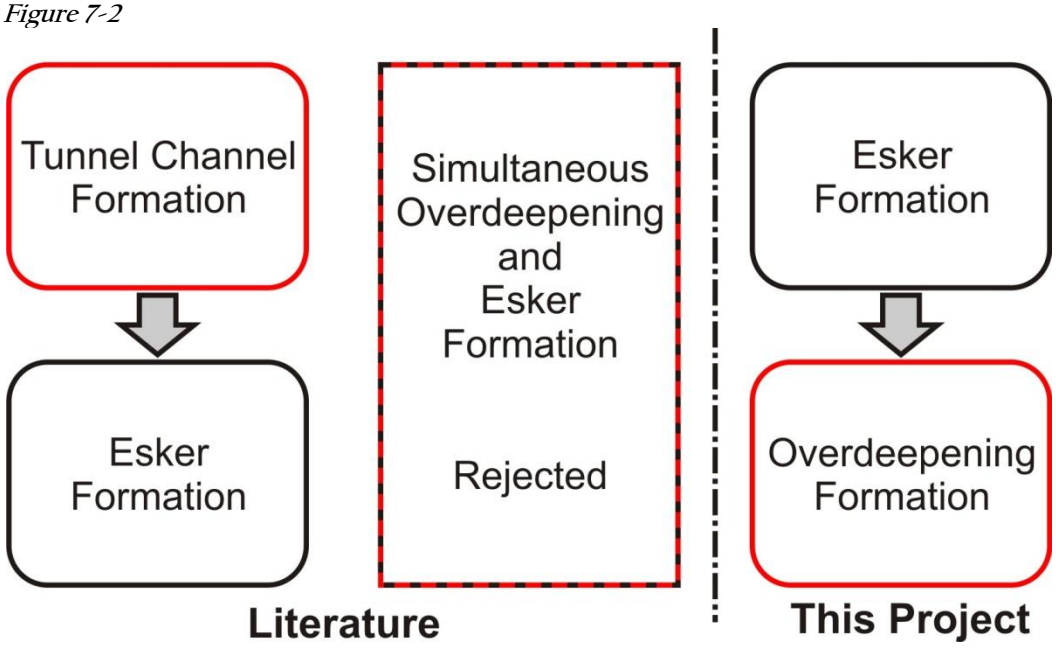

Simplified flow diagrams showing the relationships between tunnel channel and esker formation prior to this study, and the additional understanding resulting from this project.

This project has shown how subglacial eskers can weaken the glacier ice close to the bed by perforation of the ice. The ice reacts to the presence of the eskers in a similar way to that described by Lau, (2005) during laboratory experiments involving the shearing of ice around cones inserted into the ice. Lau, (2005) demonstrated that when steal 'cones' were inserted into ice and forces applied, simulating ice flow, shearing within the ice was largely controlled by the angle of the cone, with greater degrees of shearing occurring with cones that have a high angle of inclination. The findings of Lau's, (2005) work provide support for this research where the presence of eskers (or cones) leads to increased ice shearing. This ice shearing results in a zone or line of decolment within the englacial zone that is in line with the top of the esker ridge. It is

hypothesised that this subglacial shearing results in the detachment of ice at the glacier bed, contributing to the formation of buried ice. The formation of this buried ice is considered key to inhibiting sedimentation within inter esker areas, which enhances the subsequent development of overdeepenings. This research presents the first model for the formation of overdeepenings as the direct result of the presence of eskers (**Figure 7-3**).

Figure 7-3

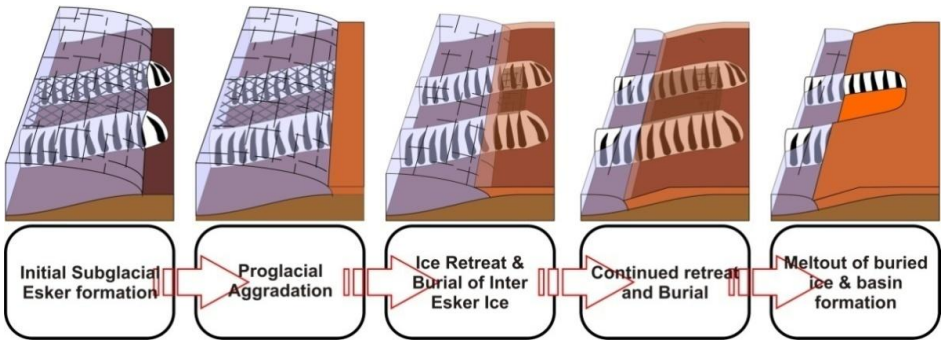

Conceptual model illustrating the development of stagnant ice in-between eskers and the resultant sandur aggradation and melt out of this ice to form topographic basins.

7.4 SANDUR AGGRADATION AND THE GENESIS OF OVERDEEPENINGS

Sandur aggradation plays a key role in the development of proglacial areas (Krigström 1962; Maizels 1991; Gomez et al. 2002), especially at the unconfined margins of large piedmont lobe glaciers such at Skeiðarárjökull (Guðmundsson et al. 2002; Smith et al. 2006). This research has highlighted that sandur aggradation is an important mechanism for the formation of overdeepenings, as the way in which a sandur aggrades is fundamental in controlling the deposition or non-deposition of sediments in the proglacial area, which has been shown to be import in the formation of such landforms.

Piotrowski, (1994); Sjogren et al., (2002); Fisher et al., (2005); and Jørgensen and Sandersen (2006), among others, have highlighted the dominance

of active erosive processes, in the formation of overdeepened landforms such as tunnel channels. Such processes, including meltwater erosion or direct glacial abrasion, create landforms by the mechanical removal of sedimentary or bedrock material. The removal of material by such mechanical processes has obvious implications for the geographical control on the placement of overdeepenings such as tunnel channels, grooves, or basins. The formation of such features is likely to occur where the parent material favours erosion, such as areas surrounded by relatively stronger material, where weaker material will favour preferential erosion (Piotrowski 1994), or where geological characteristics, such as fractures or faulting, provide a weakness which can later be exploited (Rudberg 1973). It is acknowledged that geological characteristics are not the only factor controlling the occurrence of active erosive processes; for example, Russell et al. (2007) demonstrated that meltwater erosion of the glacier bed took place along the path of least hydraulic resistance.

This research has highlighted that such topographic overdeepenings can be formed without any active erosive processes. In this case, preferential deposition and sandur aggradation has contributed to the formation of overdeepenings within areas of 'non-deposition'. This thesis presents the first model of the formation of overdeepenings directly attributed to preferential deposition and sandur aggradation rather than processes of erosion, such as at the eastern Sæluhúsavatn (Figure 4-42) and has clearly demonstrated that overdeepenings at the margins of contemporary glaciers can be formed as a direct result of preferential deposition due to the presence of buried ice occupying inter-esker areas (**Figure 7-3**).

7.5 ESKERS, AGGRADATION, STAGNATING ICE AND THE GENESIS OF OVERDEEPENINGS

This study has highlighted the importance of ice stagnation in the formation of overdeepening. Recent works have highlighted the importance of the melt out of ice at both the micro-scale (Maizels 1992; Fay 2002; Fay 2002) and mega-scale (Fleisher 1986).

Fleisher (1986) interpreted the formation of valley scale dead ice topography as a result of large scale glacier down wasting and burial by glaciofluvial deposits. The finding of this research, from both the eastern Sæluhúsavatn area (Chapter 4) and western Sæluhúsavatn area (Chapter 5) have shown that similar processes have occurred within this contemporary system. At the eastern Sæluhúsavatn, as discussed above (**Section 0**), the presence of esker ridges has resulted in the shearing of basal ice, causing the basal ice zone to become detached from the active glacier. Englacial sedimentation along this plain of decolment helps to protect the underlying ice during glacier retreat, promoting the formation of stagnant ice. As the glacier has melted and retreated, this detached ice has become buried by debris deposited in the proglacial area, protecting the ice from further melting. Further ice advances and melt out have resulted in deposition of sediment at the glacier margin and in the proglacial zone leading to sandur aggradation, however, the presence of buried ice has prevented the infilling of the areas in between eskers. Following further glacier retreat, eventual melting of the stagnant ice has lead to the formation of large areas of negative topography, where previous deposition of sediments had been inhibited. A similar scenario has occurred in the western Sæluhúsavatn area, where glacier bed excavation during the 1965 surge of Skeiðarárjökull (Wisniewski et al. 1997) also contributed to the development of buried ice which led to the development of over deepened topography (Chapter 5).

The addition to knowledge that this research has made under the theme of 'Ice Stagnation', is the identification that the process of ice stagnation has been clearly linked to the presence of eskers, and the process of sandur aggradation. This research has demonstrated that overdeepenings can be formed by preferential deposition during sandur aggradation, and active erosion is not an essential process in their formation. This project has also demonstrated, for the first time, that the classic relationship between eskers and negative topography, where eskers form following the development of negative topography such as tunnel channel, can be reversed. Fleisher, (1986), Fay, (2002; 2002), and Fard, (2003) have demonstrated that buried ice leads to the development of negative topography such proglacial overdeepenings. What has not previously been identified prior to this research, is the link between each of these hypothesises, and how combined together they result in the formation of such overdeepenings (**Figure 7-4**).

Figure 7-4

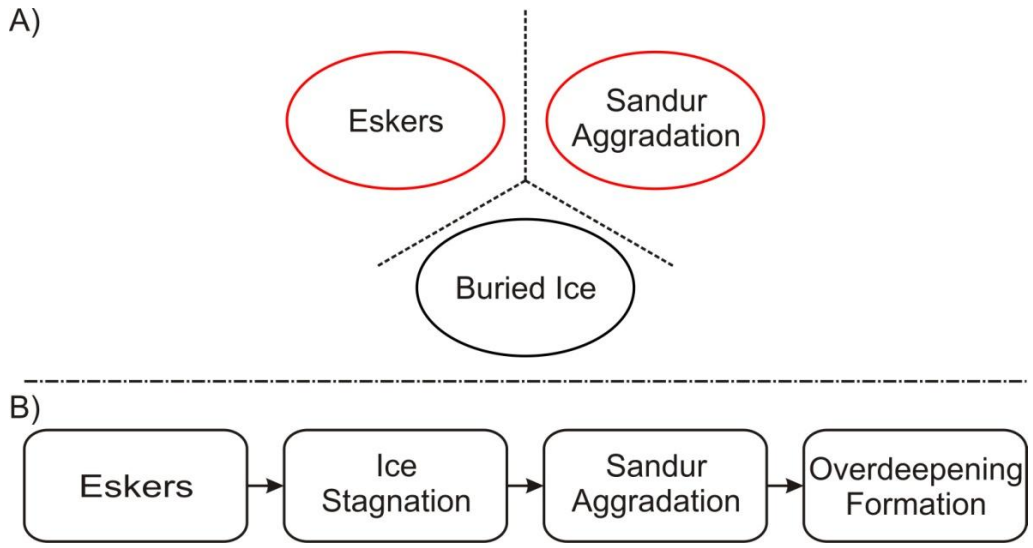

A) Separate hypotheses which have each been shown to contribute to the formation of proglacial overdeepenings, both in this research (red circles) and previously (Black Circle). B) A process illustrating how each of these individual elements have come together at Skeiðarárjökull to result in the formation of overdeepened topography.

7.6 SUBGLACIAL MELTWATER ROUTING AND THE GENESIS OF OVERDEEPENINGS

The route along which meltwaters flow along the glacier bed has long been recognised as an important control mechanism in glacier dynamics (Shreve 1972; Jørgensen and Sandersen 2006). Clear evidence has been presented by Röthlisberger, (1972); Shreve, (1972); and Collins (1998), among others, which demonstrates how subglacial meltwater moving towards the ice margin, can have a significant impact on a number of glaciological processes; such as sediment transport, mass balance and ice flux, on both a local and ice sheet scale. Meltwater routing is controlled by glacier bed topography and ice surface slope, and as such, over-deepenings at the glacier bed greatly influence subglacial meltwater pathways. Examples include the presence of pre-existing subglacial topography which has led to its continued exploitation by subglacial meltwater flow, such as the Tunnel Channels of north Germany described by Piotrowski (1994) where numerous cycles of flood flows have been found to have exploited the presence of this feature in order to transmit subglacial meltwater to the ice margin. Flowers et al. (2003) used a glaciohydraulic model, driven by contemporary observations of the Vatnajökull ice cap, to support the influence of glacier bed and ice surface topography on glacier dynamics. Flowers et al. (2003) found that Brúarjökull, Skeiðarárjökull and Breiðamerkurjökull were the most hydrologically active glaciers draining Vatnajökull, and all occupy low lying drainage basins and have gently sloping surfaces. Simulations of these glaciers predicted early and extensive snowline retreat, which produce high basal water fluxes and low subglacial effective pressures, resulting in complimentary conditions for glacier sliding and sediment deformation (Flowers et al. 2003).

Shreve (1985) and Lawson et al. (1998) have also demonstrated the importance of ice surface slope in controlling variations in ice overburden pressure, and its influence over subglacial meltwater flow, including fluctuations between distributed and channelised drainage patterns and influencing the glaciohydraulic supercooling process, which may influence sediment transport and melt out, through the formation of sediment rich basal ice.

At Skeiðarárjökull, the results of this project have not only successfully confirmed the existing theory that subglacial topography greatly influences meltwater routing, but it has also demonstrated that large scale routing of meltwater also has a significant impact of the formation of new, smaller scale topography. At the Háöldukvísl ice contact site, the deflection of meltwater around the stoss-side and flanks of a subglacial bedform (drumlin) has resulted in the concentration of meltwater along the bedform's southern flank. This controlled meltwater routing was resulted in flow through pre-existing 'ice flow parallel' fractures in the over lying ice. These fractures are orientated parallel to the direction of meltwater flow, and meltwater is believed to have flowed horizontally along these fractures, rather than sub-vertically into the overlying ice, as has been seen previously (Roberts et al. 2000). Thus, deposition of sediments within these fractures has resulted in the formation of new and distinctive landforms that could be interpreted as a hybrid of hydrofracture 'fracture fills' and eskers. Roberts et al., (2001) also inferred this similarity between hydro-fracture fills and eskers. The findings of this research differ from that of Roberts et al., (2001) as the specific routing of meltwater through hydrofractures has been shown to vary significantly from that of Roberts et al., (2001). In this case, it has been shown that these linear gravel ridges have been formed by the lateral flow of water along the glacier bed. Whereas the features identified by Roberts et al., (2001) were interpreted to have formed by the sub-

vertical flow of water from the bed to the ice surface. The interpretation of this previously unidentified flow route in the formation of such features, highlights the importance of large scale meltwater routing in the formation of such features and provides a significant contribution to knowledge which will provide a significant increase in our understanding of the processes of meltwater routing though former glacierized catchments, especially where similar landforms can be identified within the ancient landform record.

7.7 ICE FRACTURING AND THE GENESIS OF TOPOGRAPHIC OVERDEEPENINGS

At Skeiðarárjökull, the processes of ice fracturing and its influence on subglacial erosion has been shown to differ significantly to that presented by Hooke (1991) who first identified the importance of ice fracturing in the development of subglacial overdeepenings. Hooke (1991) demonstrated that subglacial erosion resulted in the formation of minor perturbations in the glacier bed which encouraged fracturing within the overlying ice. These fractures (crevasses) subsequently allowed supraglacial meltwater to enter the glacier and flow towards the glacier bed. Increased amounts of subglacial meltwater enhanced the erosion process, leading to enlargement of the subglacial perturbation and an increase in crevassing within the overlying ice. Thus, a positive feedback cycle of erosion was initiated, where erosion resulted in increased crevassing and ice fracturing, which led to further supraglacial melt water capture, erosion and so on.

This project has provided a new model that further emphasizes the importance of ice fracturing in controlling subglacial erosion. At the western Sæluhúsavatn, it has been clearly demonstrated that subglacial meltwater erosion of the substrate, during the 1996 jökulhlaup, was directly influenced by hydrofracturing of the ice directly above the area of erosion. Sedimentological

and geomorphological investigations of the ascending channel within the western Sæluhúsavatn area, have demonstrated that erosion of the glacier substrate was initiated once flow through the overlying hydrofracture had ceased (**Figure 7-1**). These findings provide a new model, which demonstrates how, where conditions favour hydrofracturing; meltwater may be directed away from the glacier bed, reducing the potential for erosion. However, when discharges are increasing, and effective pressures falling; ice fracturing is less prominent, resulting in enhanced potential for subglacial meltwater erosion and the formation of topographic overdeepenings.

The evidence of hydrofracturing found during this research support the findings of Roberts' (2005), existing model, which demonstrate that ice fracturing is the result of increasing subglacial meltwater pressure. However, this research has also shown how the character of hydrofracturing observed during outburst floods varies from that previously presented. Roberts (2000; 2002; 2005) has shown that the geometry of hydrofractures, and direction of flow within them, is controlled by subglacial meltwater pressure, and thus, hydrofractures commonly form transverse to ice and water flow. As a result, meltwaters flow sub-vertically, englacially through hydrofractures to the glacier surface. However, at the Háöldukvísl ice contact site, sedimentary and geomorphic evidence has shown that these fractures were formed longitudinally, and that flood waters flowed subglacially, horizontally through fractures, towards the glacier margin in a similar manner to water flowing through a sub- or englacial conduit that results in the formation of eskers. However in this case, the nature of the sediments exposed suggests that flow occurred within as open channel at or close to atmospheric pressure, which suggests that the fractures penetrated through the whole ice thickness from the glacier bed to the ice surface.

7.8 CHAPTER SUMMARY

Through detailed sedimentological and geomorphological analysis of overdeepenings identified at the margin of Skeiðarárjökull, this research project has presented a series of new models for the formation of such landforms within the contemporary glacial system. These models provide support for existing models of subglacial erosion such as, subglacial meltwater flow and the importance of ice fracturing. They also demonstrated how previously unidentified variations in such processes further enhance or impede the development of such landforms.

This project has also demonstrated how overdeepenings, which were previously believed to be solely erosional features, can form as a result of preferential deposition within adjacent areas. This research has also identified the importance of subglacial bedforms, such as eskers, in providing the required setting for the development of such topographic features. These new models have been summarised and presented within the context of existing knowledge in **Figure 7-5**.

Figure 7-5

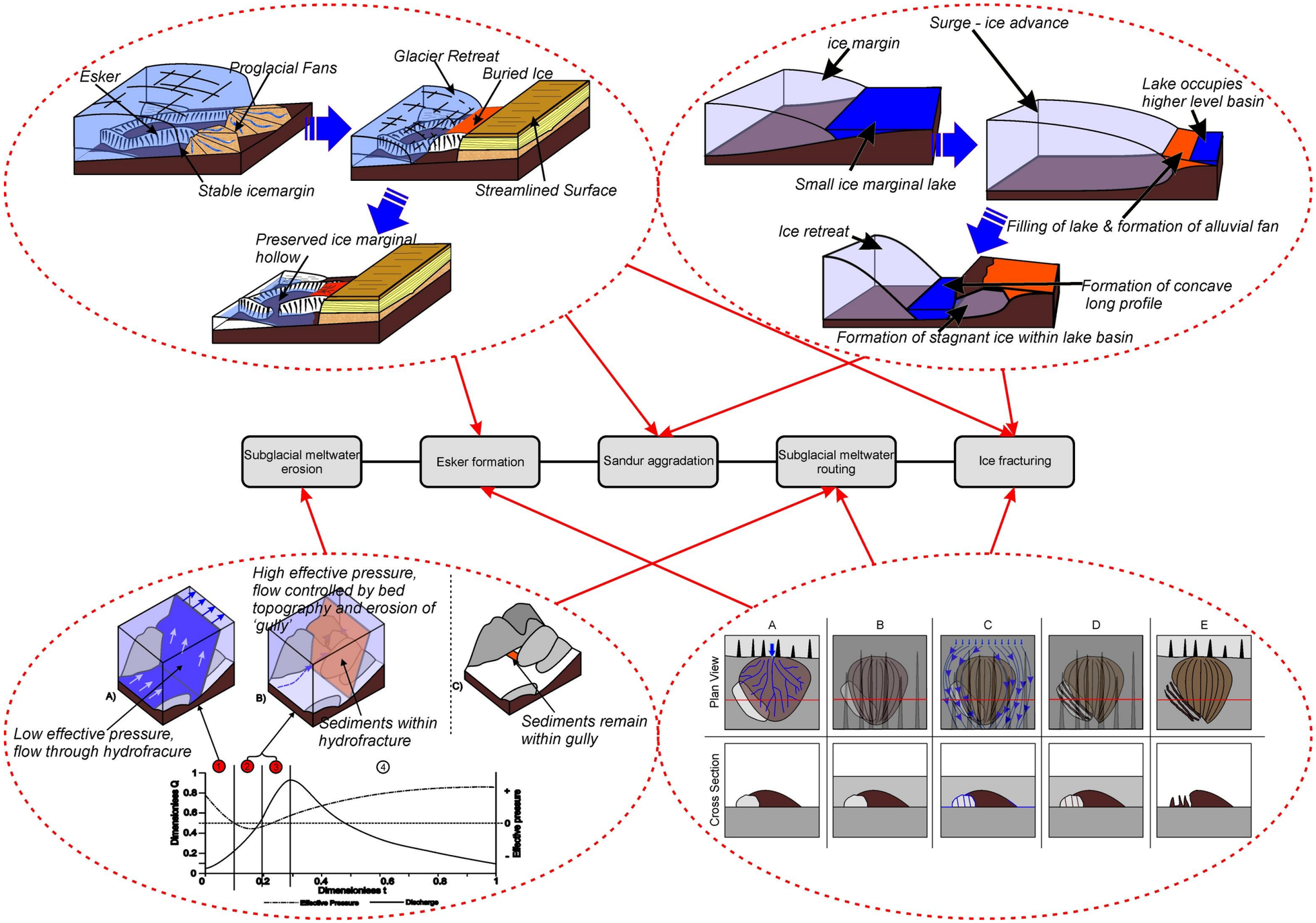

Summary diagram illustrating the four primary modells that have been developed thoughtout this research which highlights the importace of esker formation, sandur aggradation, subglacial meltwater routing and ice fracturing in the formation of ice marginal overdeepenings. The role of subglacial meltwater erosion is less than shown by previous modells.

8 CONCLUSIONS AND WIDER IMPLICATIONS

8.1 INTRODUCTION

This chapter revisits the aims and objectives of this research, demonstrating how each has been successfully accomplished, it summarises the discussion presented in chapter seven and provides a clear synopsis of the contribution to knowledge that this research project has made. This chapter also considers the wider implications of these research findings for future interpretation of contemporary and ancient glacial landscapes, hydrogeology, and the wider earth science community.

8.2 CONCLUSIONS

The aim of this research was to identify the processes that are responsible for the formation of ice marginal overdeepenings within modern glacierized catchments, and to summarise these in the form of conceptual models. This aim has been fulfilled with the production of numerous models presented within chapter seven (**Figure 7-5**). To achieve this aim, a number of specific objectives were met:

Objective 1: This thesis tested existing models and hypotheses of tunnel channel, valley, overdeepening and negative topography formation from existing literature, through geomorphological and sedimentological analysis of landforms identified within the ice proximal zone of Skeiðarársandur, southeast Iceland. These models have been tested against the diagnostic criteria presented in **Error! Reference source not found.**.

Objective 2: a suitable methodology was successfully applied to test these hypothesises (to achieve objective 1), by carrying out well established sedimentological and geomorphological investigative techniques, and by the identification of Skeiðarárjökull as a suitable analogue for the piedmont outlet

glaciers of the large Quaternary ice sheets, which has been clearly and successfully justified.

Objective 3: Based on the results achieved through Objective 2, a number of previously unidentified processes were discussed in the development of a number of refined conceptual models of the formation of overdeepenings within contemporary glacial settings, the details of which are summarised below.

It is clear from this research that overdeepenings at the margin of Skeiðarárjökull are polygenetic landforms, which have formed as the result of a suite of processes including; direct subglacial meltwater erosion, esker formation, subglacial meltwater routing, ice fracturing, ice stagnation, and sandur aggradation.

Direct subglacial meltwater erosion, although previously believed to be the primary agent in the formation of tunnel channels during the Quaternary and earlier glacial periods, has been found to play a secondary role in the formation of similar features at the contemporary margin of Skeiðarárjökull. Although it has been demonstrated that subglacial meltwater erosion has occurred within a number of areas along the ice margin, it is now understood that this processes contributed to the formation of only a small fraction of the landform, and the majority of the features were formed through other previously unattributed processes.

Eskers, which until now have been understood to form after the formation of overdeepening topography such as tunnel channels have, at Skeiðarárjökull, been found to positively contribute to the formation of the overdeepening by contributing to the formation of stagnant ice, which has led to preferential sedimentation within the proglacial area.

This research has found that the stagnation of ice plays a fundamental role in the formation of overdeepenings, by inhibiting the deposition of

sediments, contributing to preferential deposition within the proglacial area and the formation of overdeepenings within areas of 'non-deposition.

It is well documented that the routing of meltwater at the glacier bed is controlled by glacier bed topography and ice thickness. In contrast, this research has demonstrated the importance of the routing of meltwater in the formation of newly described landforms which are described as on a spectrum in-between hydrofracture 'fracture fills' and eskers, and are interpreted to have formed by the sedimentary infilling of longitudinal fractures within the ice.

This thesis has presented new evidence that significantly highlights the importance of ice fracturing in the genesis of overdeepenings, and the initiation of subglacial meltwater erosion. Where ice fracturing is prominent, this research has shown how meltwater can flow transversely along fractures, depositing sediments in a similar manner to that of an esker, and resulting in the formation of overdeepened topography. It has also demonstrated how hydrofracturing can regulate meltwater erosion of the glacier bed.

This research has, for the first time, successfully demonstrated the importance of sandur aggradation as a formative agent in the development of overdeepenings. Where sandar aggrade, the potential for preferential deposition, within one area or another, in association with stagnating ice, can lead to the formation of negative topography as a result of 'non-deposition'.

8.3 WIDER IMPLICATIONS

A full understanding of the processes responsible for the genesis of overdeepenings at contemporary glacier margins is of great importance if we are to fully understand the processes that lead to the formation of similar landforms from the Quaternary and earlier glacial periods. This research has provided a case study, within a well-constrained time frame, which can be used to test hypotheses of the formation of similar landforms in the future.

Until now, overdeepenings had been expected to be found in hydraulically active subglacial environments due to the understanding of formation by subglacial meltwater erosion. However, the finding of this research, which have shown that meltwater erosion is a secondary process, suggest that there are now a significant number of previously unconsidered locations where such features may be found. These include proglacial areas where aggradation rates are high, or where ice fracturing leads to the development of stagnant ice, such as the fracturing which occurs during glacier surges.

The results of this research also have significant implications for future sedimentological investigations. Once infilled, the edges of these features will be preserved as bounding surfaces within the sedimentary record. With no understanding of the formation of such landforms, these geographic 'unconformities' could be interpreted as evidence of a significant climatic shift, especially where ice marginal lake formation leads to the deposition of fines (such as at Skeiðarárjökull). Therefore, the findings of this research will provide a greater understanding to those working within areas where these features could be formed, and will aid in future geological investigations. The infilling of these landforms also has important hydrogeological implications, especially if

infilled with sands and gravels, which could lead to the formation of groundwater aquifers.

All of these implications, when applied to the study of ancient glacial landscapes, will provide greater knowledge of the development of such areas, and thus an unproved understanding of the behaviour of the palaeo ice sheets that moulded them. As our understanding of the behaviour of such palaeo ice sheets improves, we will increasingly improve our ability to predict the behaviour of glaciers in the future, and thus better understand and adapt to changes brought about by global climate change.

The findings of this research also have significant industrial implications. Overdeepenings have often been identified as sources of reservoir rocks that are utilised by the oil and gas industry. The identification of potentially new sources of overdeepenings could have wider implications for this industry. As global oil and gas resources decline, it may become increasingly economical to investigate these smaller, potentially new sources of reservoir rock.

References

Aario, R., Peuraniemi, V., (1992). "Glacial dispersal of till constituents in morainic landforms of different types." Geomorphology **6**: 9–25.

Aber, J. S., D. G. Croot, and M. M. Fenton (1989). "Glacio-tectonic Landforms and Structures". Kluwer, Dordrechi.

Allen, J. R. L. (1982). Sedimentary Structures: Their Character and Physical Basis., Elsevier.

Alley, R. B., G. S. Baker, D. E. Lawson, G. J. Larson and E. B. Evenson (2003). "Stabilizing feedbacks in glacier-bed erosion." Nature **424**(6950): 758-760.

Alley, R. B., G. J. Larson, D. E. Lawson, E. B. Evenson and J. C. Strasser (1998). "Glaciohydraulic supercooling: A freeze-on mechanism to create stratified, debris-rich basal ice: II. Theory." Journal of Glaciology **44**(148): 563-569.

Alley, R. B., D. E. Lawson, E. B. Evenson and G. J. Larson (2003). "Sediment, glaciohydraulic supercooling, and fast glacier flow." Annals of Glaciology **36**: 135-141.

Andrews, J. T., J. Dwyer, J. D. Milliman, A. E. Jennings and N. Rynes (1994). "Sediment thicknesses and Holocene glacial marine sedimentation rates in three East Greenland fjords (ca. 68 degrees N)." Journal of Geology **102**(6): 669-683.

Baker, V. R. (1978). Large-scale erosional and depositional features of the Channelled Scabland. The Channeled Scabland: A Guide to the Geomorphology of the Columbia Basin, Washington. V. R. Baker and D. Nummedal. Washington, National Aeronautics and Space Administration: 17–35.

Baker, V. R. (1984). Flood sediments in bedrock fluvial systems. Sedimentology of Gravels and Conglomerates. E. H. Koster and R. J. Steel, Canadian Society of Petroleum Geologists Memoir. **10:** 87 - 98.

Baker, V. R. (2002). "EARTH SCIENCES: The Study of Superfloods." Science **295**(5564): 2379-2380.

Beaney, C. L. (2002). "Tunnel channels in southeast Alberta, Canada: evidence for catastrophic channelized drainage." Quaternary International **90**: 67-74.

Beaney, C. L. and J. Shaw (2000). "The subglacial geomorphology of southeast Alberta: Evidence for subglacial meltwater erosion." Canadian Journal of Earth Sciences **37**(1): 51-61.

Benn, D., I. (1994). "Fabric shape and the interpretation of sedimentary fabric data." Journal of Sedimentary Research **64**(4a): 910-915.

Benn, D., I. (1994). "Fluted moraine formation and till genesis below a temperate glacier: Slettmarkbreen, Jotunheimen, Norway." Sedimentology **41**: 279 - 292.

Benn, D., I. and D. J. A. Evans (1998). Glaciers & Glaciation. New York, Arnold.

Benn, D. I. (1995). "Fabric signature of subglacial till deformation, Breiðamerkurjökull, Iceland." Sedimentology **42**(5): 735-747.

Benn, D. I. and C. K. Ballantyne (1994). "Reconstructing the transport history of glacigenic sediments: a new approach based on the co-variance of clast form indices." Sedimentary Geology **91**(1-4): 215-227.

Benn, D. I. and D. J. A. Evans (1996). "The interpretation and classification of subglacially-deformed materials." Quaternary Science Reviews **15**(1): 23-52.

Bennett, M. R. and N. F. Glasser (1996). Glacial Geology: Icesheets and Landforms. Chichester, John Wiley & Sons Ltd.

Bennett, M. R., R. I. Waller, N. F. Glasser, M. J. Hambrey and D. Huddart (1999). "Glacigenic clast fabrics: genetic fingerprint or wishful thinking?" Journal of Quaternary Science **14**(2): 125-135.

Berry, F. G. (1979). "Late Quaternary scour-hollows and related features in central London." Quarterly Journal of Engineering Geology and Hydrogeology **12**(1): 9-29.

Björnsson, H. (1996). "Scales and rates of glacial sediment removal: a 20 km long, 300 m deep trench created beneath Breiðamerkurjökull during the Little Ice Age." Annals of Glaciology **22**: 141-146.

Björnsson, H., F. Palsson and E. Magnusson (1999). "Skeiðarárjökull: Lansdlag og rennslisleðir vants undir spirði." Raunvisindastofnun Haskolans: 10 - 20.

Björnsson, H., F. Pálsson, O. Sigurðsson and G. E. Flowers (2003). "Surges of glaciers in Iceland." Annals of Glaciology **36**: 82-90.

Bluemle, J. P. (1970). "Anomalous Hills and associated depressions in central North Dakota". Geological Society of America, Abstracts with Programs **2**, 325 - 326.

Bluemle, J. P. and Clayton, L (1984). "Large-scale glacial thrusting and related processes in North Dakota". Boreas **13**: 279 - 299.

Boothroyd, J. and G. M. Ashley (1975). "Processes, bar morphology, and sedimentary structures on braided outwash fans, northern Gulf of Alaska". Glaciofluvial and Glaciolacustrine Sedimentation. A. V. Jopling and B. C. McDonals, SEPM Special Publication. **23:** 193 - 222.

Boulton, G. S. (1974). Processes and Patterns of Glacial Erosion. Glacial Geomorphology. D. R. Coates, State University of Binghampton. : 41 - 87.

Boulton, G. S. (1978). "Boulder shapes and grain-size distributions of debris as indicators of transport paths through a glacier and till genesis." Sedimentology **25**(6): 773-799.

Boulton, G. S. (1982). Subglacial processes and the development of glacial bedforms. Research in glacial, glacio-fluvial, and glacio-lacustrine systems. Proc. 6th Guelph symposium on geomorphology, 1980. R. Davidson-Arnott, W. Nickling and B. D. Fahey, Geo Books: 1-31.

Boulton, G. S. (1987). "A theory of drumlin formation by subglacial sediment deformation." In Rose, J. Menzies, J. (Eds.), Drumlin Symposium. Balkema, Rotterdam. 194 - 159.

Boulton, G. S. and P. E. Caban (1995). "Groundwater flow beneath ice sheets: Part II - Its impact on glacier tectonic structures and moraine formation." Quaternary Science Reviews **14**: 563-587.

Boulton, G. S., P. E. Caban and K. Van Gijssel (1995). "Groundwater flow beneath ice sheets: Part I — Large scale patterns " Quaternary Science Reviews **14**(6): 545-562

Boulton, G. S., K. E. Dobbie and S. Zatsepin (2001). "Sediment deformation beneath glaciers and its coupling to the subglacial hydraulic system." Quaternary International **86**(1): 3-28.

Boulton, G. S., P. Dongelmans, M. Punkari and M. Broadgate (2001). "Palaeoglaciology of an ice sheet through a glacial cycle: the European ice sheet through the Weichselian." Quaternary Science Reviews **20**(4): 591-625.

Boulton, G. S. and R. C. A. Hindmarsh (1987). "Sediment deformation beneath glaciers: rheology and geological consequences." Journal of Geophysical Research **92**(B9): 9059-9082.

Boyce, J. I. and N. Eyles (1991). "Drumlins carved by deforming till streams below the Laurentide ice sheet." Geology **19**(8): 787-790.

Boyd, R., D. B. Scott and M. Douma (1988). "Glacial tunnel valleys and Quaternary history of the outer Scotian shelf." Nature **333**(6168): 61-64.

Brennand, T. A. (1994). "Macroforms, large bedforms and rhythmic sedimentary sequences in subglacial eskers, south-central Ontario: implications for esker genesis and meltwater regime." Sedimentary Geology **91**(1-4): 9-55.

Brennand, T. A. (2000). "Deglacial meltwater drainage and glaciodynamics: Inferences from Laurentide eskers, Canada." Geomorphology **32**(3-4): 263-293.

Brennand, T. A., H. A. J. Russell and D. S. Sharpe (2007). Tunnel Channel Character and Evolution in Central Southern Ontario. Glacier Science and Environmental Change (First Edition). G. K. Peter: 37-39.

Brennand, T. A. and J. Shaw (1994). "Tunnel channels and associated landforms, south-central Ontario: their implications for ice-sheet hydrology." Canadian Journal of Earth Sciences **31**(3): 505-522.

Burke, M. J., J. Woodward, A. J. Russell, P. J. Fleisher and P. K. Bailey (2008). "Controls on the sedimentary architecture of a single event esker: Skeiðarárjökull, Iceland." Quaternary Science Reviews **27**: 1829 - 1847.

Carrivick, J. L., A. Russell, F. S. Tweed and D. R. Twigg (2004). "Palaeohydrology and sedimentary impacts of Jökulhlaups from Kverkfjöll, Iceland." Sedimentary Geology **172**: 19 - 40.

Cassidy, N. J., Ó. Knudsen, E. L. Rushmer, T. A. G. P. Van Dijk, A. J. Russell, P. M. Marren and H. Fay (2003). "GPR derived architecture of November 1996 jökulhlaup deposits, Skeiðarársandur, Iceland." Geological Society Special Publication(211): 153-166.

Chinn, T. J. (1996). "New Zealand glacier responses to climate change of the past century." New Zealand Journal of Geology and Geophysics **39**(3): 415-428.

Christiansen, E. A. (1987). "Verendrye valley and the Glidden esker, Saskatchewan: subglacial and ice-walled features in southwestern Saskatchewan, Canada." Canadian Journal of Earth Sciences **24**(1): 170-176.

Church, M. & Gilbert, R. (1975). "Proglacial fluvial and lacustrine environments." In: Jopling, A. V. & McDonald, B. C. (Eds) Glaciofluvial and Glaciolacustrine Sedimentation. The Society of Economic Palaeontologists and Mineralogists, Special Publication **23**, 22 - 100.

Clark, C. D. (1997). "Reconstructing the evolutionary dynamics of former ice sheets using multi-temporal evidence, remote sensing and GIS." Quaternary Science Reviews **16**(9): 1067-1092.

Clark, C. D., J. K. Knight and J. T. Gray (2000). "Geomorphological reconstruction of the Labrador Sector of the Laurentide Ice Sheet." Quaternary Science Reviews **19**(13): 1343-1366.

Clark, C. D. and R. T. Meehan (2001). "Subglacial bedform geomorphology of the Irish Ice Sheet reveals major configuration changes during growth and decay." Journal of Quaternary Science **16**(5): 483-496.

Clapperton, C. M (1989). "Asymetrical drumlins an Patagonia, Chile." Sedimentary Geology **62**: 387 - 398.

Clayton, L., Moran, S. R. and Bluemle, J. P. (1980). "Explanatory text to accompany the Geologic Map of North Dakota". North Dakota Geological Survey, Report of Investigation No. 69.

Clayton, L., J. R. Teller and J. W. Attig (1985). "Surging of the southwestern part of the Laurentide Ice Sheet." Boreas **14** (3): 235 - 241.

Clayton, L., J. W. Attig and D. M. Mickelson (1999). Tunnel Channels formed in Wisconsin during the last glaciation. Glacial Processes Past and Present. D. M. Mickelson and J. W. Attig, Geological Society of America Special Paper. **337:** 69 - 82.

Collins, D., N. (1998). "Outburst and rainfall-induced peak runoff events in highly glacierized Alpine basins." Hydrological Processes **12**(15): 2369-2381.

Collinson, J., N. Mountney and D. Thompson (2006). Sedimentary Structures. Harpenden, England, Terra Publications.

Costa, J. E. (1988). Rheologic, geomorphic and sedimentologic differentiation of water flows, hyperconcentrated flows and debris flows. Flood Geomorphology. . V. R. Baker, R. C. Kochel and P. C. Patton. New York, Wiley**:** 113– 122.

Cutler, P. M., P. M. Colgan and D. M. Mickelson (2002). "Sedimentologic evidence for outburst floods from the Laurentide Ice Sheet margin in Wisconsin, USA: Implications for tunnel-channel formation." Quaternary International **90**: 23-40.

Delaney, C. (2001). "Esker formation and the nature of deglaciation: the Ballymahon Esker, Central Ireland." North West Geography **1**(2): 23 - 23.

Delaney, C. (2002). "Sedimentology of a glaciofluvial landsystem, Lough Ree area, Central Ireland: implications for ice margin characteristics during Devensian deglaciation." Sedimentary Geology **149**: 111– 126.

Dionne, J.C. (1987). "Tadpole rock (rocdrumlin): a glacial streamlined form, In Rose, J. Menzies, J. (Eds.), Drumlin Symposium. Balkema, Rotterdam. 194 - 159.

Dobracki, R. and D. Krzyszkowski (1997). "Sedimentation and erosion at the Weichselian ice-marginal zone near Golczewo, northwestern Poland." Quaternary Science Reviews **16**(7): 721-740.

Dowdeswell, J. A., M. A. Maslin, J. T. Andrews and I. N. McCave (1995). "Iceberg production, debris rafting, and the extent and thickness of Heinrich layers (H-1, H-2) in North Atlantic sediments." Geology **23**(4): 301–304.

Dowdeswell, J. A. and M. J. Sharp (1986). "Characterization of pebble fabrics in modern terrestrial glacigenic sediments." Sedimentology **33**(5): 699-710.

Drewry, D. J. (1986). Glacial Geologic Processes. London, Edward Arnold.

Duller, R. A., N. P. Mountney, A. J. Russell and N. J. Cassidy (2008). "Architectural analysis of a volcaniclastic jökulhlaup deposit, southern Iceland: sedimentary evidence for supercritical flow." Sedimentology **55**: 939 - 964.

Dyke, A. S. and V. K. Prest (1987). "Late Wisconsinan and Holocene History of the Laurentide Ice Sheet". Géographie physique et Quaternaire. **41** (2): 237-263

Ehlers, J. and G. Linke (1989). "The origin of deep buried channels of Elsterian age in NW Germany." Journal of Quaternary Science **4**(3): 255 - 265.

Evans, I.S., (1996). "Abraded rock landforms (whalebacks) developed under ice streams in mountain areas." Annals of Glaciology **22**: 9–16.

Evans, D. J. A. (2000). "A Gravel Outwash/Deformation till Continuum, Skalafellsjokull, Iceland." Geografiska Annaler. Series A, Physical Geography **82**(4): 499-512.

Evans, D. J. A. (2009). "Controlled moraines: origins, characteristics and palaeoglaciological implications." Quaternary Science Reviews **28**: 183 - 208.

Evans, D. J. A. and D. Benn, I. (2004). A practical guide to the study of glacial sediments. London, Arnold.

Evans, D. J. A., D. S. Lemmen and B. R. Rea (1999). "Glacial landsystems of the southwest Laurentide Ice Sheet: modern Icelandic analogues". Journal of Quaternary Science **14 (7):** 637 - 691.

Evans, D. J. A., C. D. Nelson and C. Webb (2010). "An assessment of fluting and "till esker" formation on the foreland of Sandfellsjökull, Iceland." Geomorphology **114**(3): 453-465.

Evans, D. J. A., B. R. Rea, J. F. Hiemstra and C. O Cofaigh (2006). "A critical assessment of subglacial mega-floods: a case study of glacial sediments and landforms in south-central Alberta, Canada." Quaternary Science Reviews **25**(13-14): 1638-1667.

Evans, D. J. A. and D. R. Twigg (2002). "The active temperate glacial landsystem: A model based on Breiðamerkurjökull and Fjallsjökull, Iceland." Quaternary Science Reviews **21**(20-22): 2143-2177.

Evans, D. J. A & Wilson, S. B (2006). "Scottish Landform example 39: The lake of Menteith glacitectonic hill- hole pair." Scottish Geographical Journal, **122:4**, 352-364

Everest, J. and T. Bradwell (2003). "Buried glacier ice in southern Iceland and its wider significance." Geomorphology **52**(3-4): 347-358.

Eyles, N. (2006). "The role of meltwater in glacial processes." Sedimentary Geology **190**(1-4): 257-268.

Eyles, N. and P. de Broekert (2001). "Glacial tunnel valleys in the Eastern Goldfields of Western Australia cut below the Late Paleozoic Pilbara ice sheet." Palaeogeography, Palaeoclimatology, Palaeoecology **171**: 29-40.

Fairchild, H.L. (1907). "Drumlins of central New York. New York State Museum Bulletin **111**: 391 - 443.

Fairchild, H.L., (1929). "New York drumlins." Rochester Academy of Sciences Bulletin **7**:1–37.

Fard, A. M. (2003). "Large dead-ice depressions in flat-topped eskers: Evidence of a Preboreal jökulhlaup in the Stockholm area, Sweden." Global and Planetary Change **35**(3-4): 273-295.

Fay, H. (2002). Formation of ice-block obstacle marks during the November 1996 glacier-outburst flood (jökulhlaup), Skeiðarársandur, southern Iceland. Flood and Megaflood Processes and Deposits: Recent and Ancient Examples. International Association of Sedimentologists Special Publication Number 32. I. P. Martini, V. R. Baker and G. Garzonón: 85-97.

Fay, H. (2002). Formation of kettle holes following a glacial outburst flood (jökulhlaup), Skeiðarársandur, southern Iceland. The Extremes of the Extremes: Extraordinary Floods. Á. Snorrason, H. P. Finnsdóttir and M. E. Moss, IAHS Publication no. 271: 205-210.

Fisher, T. G., H. M. Jol and A. M. Boudreau (2005). "Saginaw Lobe tunnel channels (Laurentide Ice Sheet) and their significance in south-central Michigan, USA." Quaternary Science Reviews **24**(22): 2375-2391.

Fisher, T. G., and Shaw, J. (1992). "A depositional model for Rogen moraine, with examples from the Avalon Peninsula, Newfoundland." Canadian Journal of Earth Sciences **29**: 669 - 686.

Fleisher, P. J. (1986). "Dead-ice sinks and moats: Environments of stagnant ice deposition." Geology **14**: 39 - 42.

Fleisher, P. J., D. H. Cadwell and E. H. Muller (1998). "Tsivat Basin conduit system persists through two surges, Bering Piedmont Glacier, Alaska." Bulletin of the Geological Society of America **110**(7): 877-887.

Flowers, G. E., H. Björnsson and F. Pálsson (2003). "New insights into the subglacial and periglacial hydrology of Vatnajökull, Iceland, from a distributed physical model." Journal of Glaciology **49**(165): 257-270.

Fuller, S. and T. Murray (2002). "Sedimentological investigations in the forefield of an Icelandic surge-type glacier: Implications for the surge mechanism." Quaternary Science Reviews **21**(12-13): 1503-1520.

Gale, S. J. and P. G. Hoare (1991). Quaternary Sediments: Petrographic Methods for the Study of Unlithified Rocks. London Belhaven Press.

Ghienne, J. F. and M. Deynoux (1998). "Large-scale channel fill structures in Late Ordovician glacial deposits in Mauritania, western Sahara." Sedimentary Geology **119**(1-2): 141-159.

Glasser, N. F. and M. R. Bennett (2004). "Glacial erosional landforms: origins and significance for palaeoglaciology." Progress in Physical Geography **28**: 43-75.

Goldthwait, R. P. (1979). "Giant grooves made by concentrated basal ice streams." Journal of Glaciology **23**: 297- 307.

Gomez, B., A. J. Russell, L. C. Smith and Ó. Knudsen (2002). "Erosion and deposition in the proglacial zone: The 1996 jökulhlaup on Skeiðarársandur, southeast Iceland." IAHS-AISH Publication(271): 217-222.

Gomez, B., N. D. Smith, L. C. Smith, F. J. Magilligan and L. A. K. Mertes (2000). "Glacier outburst floods and outwash plain development: Skeiðarársandur, Iceland." Terra Nova **12**(3): 126-131.

Graham, D. J. and N. G. Midgley (2000). "Graphical representation of particle shape using triangular diagrams: an excel spreadsheet method." Earth Surface Processes and Landforms **25**: 1473–1477.

Graham, A.G.C., Larter, R.D., Gohl, K., Hillenbrand, C.-D., Smith, J.A., Kuhn, G., (2009). "Bedform signature of a West Antarctic palaeo-ice stream reveals a multitemporal record of flow and substrate control". Quaternary Science Reviews **28**: 2774–2793.

Gravenor, C. P. and W. O. Kupsch (1959). "Ice disintegration features in western Canada." Journal of Geology **67**: 48 - 64.

Gray, L., I. Joughin, S. Tulaczyk, V. B. Spikes, R. Bindschadler and K. Jezek (2005). "Evidence for subglacial water transport in the West Antarctic Ice Sheet through three-dimensional satellite radar interferometry." Geophys. Res. Lett. **32**(3): L03501.

Guðmundsson, M. T., A. Bonnel and K. Gunnarsson (2002). "Seismic soundings of sediment thickness on Skeiðarársandur, SE-Iceland." Jökull **51**: 53 - 64.

Guðmundsson, M. T., F. Sigmundsson and H. Bjornsson (1997). "Ice-volcano interaction of the 1996 Gjalp subglacial eruption, Vatnajökull, Iceland." Nature **389**(6654): 954-957.

Gurnell, A. M., P. J. Edwards, G. E. Petts and J. V. Ward (2000). "A conceptual model for alpine proglacial river channel evolution under changing climatic conditions." CATENA **38**(3): 223-242.

Hallet, B. (1979). "A theoretical model of glacial abrasion." Journal of Glaciology **23**: 23 - 28.

Hambrey, M. J., D. Huddart, M. R. Bennett, J. A. Dowdeswell and N. F. Glasser (1999). "Debris entrainment and transfer in polythermal valley glaciers." Journal of Glaciology **45**(149): 69-86.

Hambrey, M. J., D. Huddart, M. R. Bennett and N. F. Glasser (1997). "Genesis of 'hummocky moraines' by thrusting in glacier ice: evidence from Svalbard and Britain." Journal of the Geological Society **154**(4): 623 - 632.

Hanvey, P. M., (1989). "Stratified flow deposits in a late Pleistocene drumlin in northwest Ireland." Sedimentary Geology **62:** 211–221.

Hart, J. K. (1995). "Drumlin formation in southern Anglesey and Arvon, northwest Wales." Journal of Quaternary Science **10** (1): 3–14.

Hart, J. K. (1997). "The relationship between drumlins and other forms of subglacial glaciotectonic deformation." Quaternary Science Reviews **16**(1): 93-107.

Hein, F. J. (1984). Deep-sea and fluvial braided channel conglomerates: a comparison of two case studies. Sedimentology of Gravels and Conglomerates. E. H. Koster and R. J. Steel, Canadian Society of Petroleum Geologists Memoir. **10:** 33 - 49.

Hirst, J. P. P., A. Benbakir, D. F. Payne and I. R. Westlake (2002). "Tunnel valleys and density flow processes in the upper Ordovician glacial succession, Illizi Basin, Algeria: Influence on reservoir quality." Journal of Petroleum Geology **25**(3): 297-324.

Hoffmanna, K. and J.A. Piotrowski (2001). "Till melange at Amsdorf, central Germany: sediment erosion, transport and deposition in a complex, soft-bedded subglacial system." Sedimentary Geology **140:** 215-234.

Hooke, R. L. (1991). "Positive feedbacks associated with erosion of glacial cirques and overdeepenings." Geological Society of America Bulletin **103**(8): 1104-1108.

Hooke, R. L. and N. R. Iverson (1995). "Grainsize distribution in deforming subglacial tills: Role of grain fracture." Geology **23**(1): 57 - 60.

Hooke, R. L. and C. E. Jennings (2006). "On the formation of the tunnel valleys of the southern Laurentide ice sheet." Quaternary Science Reviews **25**(11-12): 1364-1372.

Howarth, P. J. (1968) Geomorphological and Glaciological Studies, Eastern Breiðamerkurjökull, Iceland. Unpublished Ph.D. Thesis, University of Glasgow.

Howarth, P. J. (1971) Investigations of two eskers at eastern Breiðamerkurjokull, Iceland. Arctic and Alpine Research, 3, 305-318

Hubbard, B. and N. F. Glasser (2005). Field techniques in glaciology and glacial geomorphology, Wiley.

Huddart, D., M. R. Bennett and N. F. Glasser (1999). "Morphology and sedimentology of a high-arctic esker system: Vegbreen, Svalbard." BOREAS **28**: 253 - 273.

Inman, M. (2005). "Antarctic Drilling: The Plan to Unlock Lake Vostok." Science **310**(5748): 611-612.

Iseya, F. and H. lkeda (1987). "Pulsations in bedload transport rates induced by a longitudinal sediment sorting : a flume study using sand and gravel mixtures." Geografiska Annaler **69A**: 227-253.

Jakobsen, P. R. (1996) "Distribution and intensity of glaciotectonic deformation in Denmark." **Bulletin of the Geological Society of Denmark. 42**: 175—185. -

Jóhannesson, H. (1985) "The advances and retreats of the Skeiðarársandur glacier in southeast Iceland in the last 250 years." Náttúrufræðingurinn, 54, 31-45.

Johansson, M., P. Migon and M. Olvmo (2001). "Development of joint-controlled rock basins in Bohus granite, SW Sweden." Geomorphology **40**(1-2): 145-161.

Johnson, P. G. (1992). "Stagnant Glacier Ice, St. Elias Mountains, Yukon." Geografiska Annaler. Series A, Physical Geography **74**(1): 13-19.

Johnson, M.D., Schomacker, A., Benediktsson, Í.Ö., Geiger, A.J., Ferguson, A., Ingólfsson, Ó., (2010). "Active drumlin field revealed at the margin of Múlajökull, Iceland: a surge-type glacier." Geology **38** (10): 943–946.

Jørgensen, F. and P. B. E. Sandersen (2006). "Buried and open tunnel valleys in Denmark-erosion beneath multiple ice sheets." Quaternary Science Reviews **25**(11-12): 1339-1363.

Kamb, B. (1964). "Glacier Geophysics." Science **146**: 353 - 365.

Kamb, B. (1987). "Glacier surge mechanisms based on linked cavity configuration of the basil water conduit system." Journal of Geophysical Research **92**: 9083 - 9100.

Kehew, A. E., S. P. Beukema, B. C. Bird and A. L. Kozlowski (2005). "Fast flow of the Lake Michigan Lobe: evidence from sediment-landform assemblages in southwestern Michigan, USA." Quaternary Science Reviews **24**(22): 2335-2353.

Kerr, M., and Eyles, N., (2007). "Origin of drumlins on the floor of Lake Ontario and in upper New York State." Sedimentary Geology **193**: 7–20.

Kirkbride, M. P. (1993). "The temporal significance of transitions from melting to calving termini at glaciers in the central Southern Alps of New Zealand." Holocene **3**(3): 232-240.

Kirkbride, M. P. and C. R. Warren (1999). "Tasman Glacier, New Zealand: 20th-century thinning and predicted calving retreat." Global and Planetary Change **22**(1-4): 11-28.

Kjaer, K. H., E. Larsen, J. van der Meer, O. Ingolfsson, J. Kruger, I. Orn Benediktsson, C. G. Knudsen and A. Schomacker (2006). "Subglacial decoupling at the sediment/bedrock interface: a new mechanism for rapid flowing ice." Quaternary Science Reviews **25**(21-22): 2704-2712.

Knighton, D. (1998). Fluvial Forms & Processes. London, Arnold.

Kozlowski, A. L., A. E. Kehew and B. C. Bird (2005). "Outburst flood origin of the Central Kalamazoo River Valley, Michigan, USA." Quaternary Science Reviews **24**(22): 2354-2374.

Krigström, A. (1962). "Geomorphological Studies of Sandur Plains and Their Braided Rivers in Iceland." Geografiska Annaler **44**(3/4): 328-346.

Kupsch, W.O., (1955). "Drumlins with jointed boulders near Dollard, Saskatchewan." Geological Society of American Bulletin **66**: 327–338.

Lau, M. (2005). Preliminary modeling of ice failure on cones due to edge shear. 18th International Conference on Port and Ocean Engineering under Arctic Conditions, Potsdam, New York.

Lawson, D. E., G. J. Larson, S. A. Arcone, J. C. Strasser, E. B. Evenson and R. B. Alley (1998). "Glaciohydraulic supercooling: A freeze-on mechanism to create stratified, debris-rich basal ice: I. Field evidence." Journal of Glaciology **44**(148): 547-562.

Le Heron, D. P. and J. L. Etienne (2005). "A complex subglacial clastic dyke swarm, Sólheimajökull, southern Iceland." Sedimentary Geology **181**(1-2): 25-37.

Lingle, C. S., A. Post, U. C. Herzfeld, B. F. Molnia, R. M. Krimmel and J. J. Roush (1993). "Bering Glacier surge and iceberg-calving mechanism at Vitus Lake, Alaska, U.S.A." Journal of Glaciology **39**(133): 722-727.

Lowe (1975). "Water escape structures in coarse-grained sediments." Sedimentology **22**(2): 157-204.

Lowe, D. R. (1976). "Subaqueous liquefied and fluidized sediment flows and their deposits." Sedimentology **23**: 285-308.

Lundqvist, J. L. Clayton and D. M. Mickelson (1993). "Deposition of the Late Wisconsin Johnstown Moraine, South-Central Wisconsin" Quaternary International **18**: 53 - 59.

Magilligan, F. J., B. Gomez, L. A. K. Mertes, L. C. Smith, N. D. Smith, D. Finnegan and J. B. Garvin (2002). "Geomorphic effectiveness, sandur development, and the pattern of landscape response during jökulhlaups: Skeiðarársandur, southeastern Iceland." Geomorphology **44**(1-2): 95-113.

Mahlmann, A. (2002). Flood Dates in the river Skeidará (almost exceptionally from Grímsvötn). GLACIORISK.

Maizels, J. (1989). "Sedimentology, paleoflow dynamics and flood history of Jokulhlaup deposits: paleohydrology of Holocene sediment sequences in southern Iceland sandur deposits." Journal of Sedimentary Petrology **59**(2): 204-223.

Maizels, J. (1990). "Sand intraclasts within a diamicton mélange, southern Niagara Peninsula, Ontario, Canada." **Journal of Quaternary Science 5** (3): 189–206.

Maizels, J. (1991). The origin and evolution of Holocene sandur deposits in areas of jokulhlaup drainage, Iceland. Environmental change in Iceland. J. K. Maizels. Glaciology & Quaternary Geology, 7, Kluwer: 267-302.

Maizels, J. (1992). "Boulder ring structures produced during Jokulhlaup flows: origin and hydraulic significance." Geografiska Annaler, Series A 74 **A**(1): 21-33.

Maizels, J. (1997). "Jokulhlaup deposits in proglacial areas." Quaternary Science Reviews **16**(7): 793-819.

Maizels, J. and A. Russell (1992). "Quaternary perspectives on jokulhlaup prediction." Quaternary Proceedings **2**: 133-152.

Maizels, J. K. (1993). "Lithofacies variations within sandar deposits: the role of runoff regime, flow dynamics and sediment supplycharacteristics." Sedimentary Geology **85**: 299– 325.

McCabe, A. M., (1989). "The distribution and stratigraphy of drumlins in Ireland". In: Ehlers, J., Gibbard, P. L., Rose, J. (Eds.), Glacial Deposits in Great Britain and Ireland. Balkema, Rotterdam, pp. 421–435.

McKenzie, G. D. (1969). "Observations on a collapsing kame terrace in Glacier Bay National Monument, southeast Alaska." Journal of Glaciology **8**: 413– 414.

Menzies, J. (1979). "A review of literature on the formation and location of drumlin". Earth Science Reviews **14:** 315 - 359.

Menzies, J. (2002). Modern and past glacial environments. Oxford, Arnold.

Menzies, J., and Brand, U., (2007). "The internal sediment architecture of a drumlin, Port Byron, New York State, USA." Quaternary Science Reviews **26**: 322–335.

Molewski, P. (1996). "Nowe fakty dotyczace genezy zaglebien wytopiskowych na sandrach przedpola lodowca Skeidarar (Islandia) New facts relating genesis of the kettle holes on the sandurs of the Skeidarar glacier (Iceland) foreland." Przeglad Geograficzny **68**(3-4): 405-426.

Moores, H. D. (1989). "On the formation of the tunnel valleys of the Superior lobe, central Minnesota." Quaternary Research **32**(1): 24-35.

Munro-Stasiuk, M. J., T. G. Fisher and C. R. Nitzsche (2005). "The origin of the western Lake Erie grooves, Ohio: implications for reconstructing the subglacial hydrology of the Great Lakes sector of the Laurentide Ice Sheet." Quaternary Science Reviews **24**(22): 2392-2409.

Nemec, W. and R. J. Steel (1984). Alluvial and Coastal Conglomerates: Their significant features and some comments on gravelly Mass-Flow deposits. Sedimentology of Gravels and Conglomerates. E. H. Koster and R. J. Steel, Canadian Society of Petrolium Geologists. **Memoir 10:** 1 - 30.

Nenonen, J., (1994). "The Kaituri drumlin stratigraphy in the Kangasniemi area, Finland." Sedimentary Geology **91:** 365–372

Newman, W. A. and D. M. Mickelson (1994). "Genesis of Boston Harbor drumlins, Massachusetts." Sedimentary Geology **91**(1-4): 333-343.

Nye, J. F. (1976). "Plasticity solution of a glacier snout." Journal of Glaciology **6**: 695 - 715.

O'Connor, J. E. (1993). "Hydrology, Hydraulics, and Geomorphology of the Bonneville Flood." Geological Society of America Special Paper (274).

O'Connor, J. E. and V. R. Baker (1992). "Magnitudes and implications of peak discharges from glacial Lake Missoula." Geological Society of America Bulletin **104**(3): 267-279.

Ó Cofaigh, C. (1996). "Tunnel valley genesis." Progress in Physical Geography **20**(1): 1-19.

Orwin, J. F. and C. C. Smart (2004). "Short-term spatial and temporal patterns of suspended sediment transfer in proglacial channels, Small River Glacier, Canada." Hydrological Processes **18**(9): 1521-1542.

Pálsson, S., S. Zóphóníasson, O. Sigmarðsson, H. Kristmannsdóttir and H. Aðalsteinsson (1992). "Skeiðarárhlaup Og Framhlaup Skeiðarárjökuls 1991." Orkustofnun: 5 - 12.

Patterson, C.J., Hooke, L.H., (1995). "Physical environment of drumlin formation." Journal of Glaciology **41** (137): 30–38.

Philips, E. R., D. J. A. Evans and C. A. Auton (2002). "Polyphase deformation at an oscillating ice margin following the Loch Lomond readvance, central Scotland, UK." Sedimentary Geology **149**: 157 - 182.

Piotrowski, J. A. (1994). "Tunnel-valley formation in northwest Germany - geology, mechanisms of formation and subglacial bed conditions for the Bornhöved tunnel valley." Sedimentary Geology **89**(1-2): 107-141.

Piotrowski, J. A. (1997). "Subglacial groundwater flow during the last glaciation in northwestern Germany." Sedimentary Geology **111**(1-4): 217-224.

Piotrowski, J. A. (1997). "Subglacial hydrology in north-western Germany during the last glaciation: groundwater flow, tunnel valleys and hydrological cycles." Quaternary Science Reviews **16**(2): 169-185.

Powell, R. D. and E. Domack (1995). Modern Glaciomarine Environments. Glacial Environments, vol 1: Modern Glacial Environments: Processes, Dynamics and Sediments. J. Menzies. Oxford, Butterworth-Heinemann: 445-486.

Powers, M., C. (1953). " A new roundness scale for sedimentary particles." Journal of Sedimentary Petrology **23**: 117 - 119.

Praeg, D. (2003). "Seismic imaging of mid-Pleistocene tunnel-valleys in the North Sea Basin-high resolution from low frequencies." Journal of Applied Geophysics **53**(4): 273-298.

Prest, V. K. (1969). "Retreat of Wisconsin and recent ice" in North American Geological Survey of Canada. Map 1257A.

Price, R. J. (1967). Fluvioglacial features and esker formation near Casement Glacier. Observed processes of glacial deposition in Glacier Bay, Alaska. P. J. Anderson. Miscellaneous Publication, 236, Ohio State University, Byrd Polar Research Center: 94-98.

Price, R. J. (1969). "Moraines, Sandar, Kames and Eskers near Breiðamerkurjökull, Iceland." Transactions of the Institute of British Geographers(46): 17-43.

Proudfoot, D. N., R. W. May, N. W. Rutter and J. Shaw (1982). Glacialand Postglacial Sediments Edmonton-Jasper-Banff-Calgary area, Alberta., International Association of Sedimentologists 11 International Congress, Excursion Guide 2OB.

Rains, R. B., J. Shaw, D. B. Sjogren, M. J. Munro-Stasiuk, K. Robert Skoye, R. R. Young and R. T. Thompson (2002). "Subglacial tunnel channels, Porcupine Hills, southwest Alberta, Canada." Quaternary International **90**(1): 57-65.

Riggs, E. and C. Lindemann (2008). Fractured cobbles and outcrop-scale deformation reflect stresses associated with brittle regional detachment faulting: Titus Canyon formation, Death Valley region, California/Nevada, United States. International Geological Congress, Oslo.

Rijsdijk, K. F. (2001). "Density-Driven Deformation Structures in Glacigenic Consolidated Diamicts: Examples from Traeth y Mwnt, Cardiganshire, Wales, U.K." Journal Of Sedinentary Research **71**(1): 122-135.

Roberts, M. J. (2005). "Jökulhlaups: a reassesment of floodwater flow through glaciers. ." Reviews of Geophysics **43**(1 - 21).

Roberts, M. J., D. E. Lawson, G. J. Larson, E. B. Evenson, H. Björnsson, F. S. Tweed, A. J. Russell and Ó. Knudsen (2002). "Glaciohydraulic supercooling in Iceland." Geology **30**(5): 439-442.

Roberts, M. J., F. lsson, M. Gudmundsson, T. s, Bj, H. rnsson and F. S. Tweed (2005). "Icewater interactions during floods from Grænalón glacier-dammed lake, Iceland." Annals of Glaciology **40**: 133-138.

Roberts, M. J., A. J. Russell, F. S. Tweed and O. Knudsen (2000). "Ice fracturing during Jökulhlaups: Implications for englacial floodwater routing and outlet development." Earth Surface Processes and Landforms **25**(13): 1429-1446.

Roberts, M. J., A. J. Russell, F. S. Tweed and Ó. Knudsen (2001). "Controls on englacial sediment deposition during the November 1996 jökulhlaup, Skeiðarárjökull, Iceland." Earth Surface Processes and Landforms **26**(9): 935-952.

Roberts, M. J., A. J. Russell, F. S. Tweed and Ó. Knudsen (2002). "Controls on the development of supraglacial floodwater outlets during jökulhlaups." IAHS-AISH Publication(271): 71-76.

Rose, J. (1989). "Glacier stress patterns and sediment transfer associated with superimposed flutes." Sedimentary Geology **62**: 151 - 176.

Rose, J. and Letzer, J.M. (1977) "Superimposed Drumlins." Journal of Glaciology **18**: 471 - 480.

Röthlisberger, H. (1972). "Water pressure in intra- and subglacial channels." Journal of Glaciology **11**(62): 177–203.

Rudberg, S. (1973). "Glacial erosion forms of medium size — a discussion based on four Swedish case studies." Zeitschrift Fur Geomorphologie Suppliment Band **17**: 33 - 48.

Russell, A. (2005). The geomorphological & sedimentary impact of Jökulhlaups Skeiðarársandur. In: Rekonstrukcja Procesow Glacjalnych W Wybranych Strefach Marginalnych Lodowcow Islandii - Formy I Osady Islandia (Reconstruction of glacial processes in the chosen marginal zones of the Icelandic Glaciers - forms and deposits), sierpnia 2005. Torun, Poland: Instytut Geografii UMK, : 73-96.

Russell, A., J, H. Fay, P. M. Marren, F. S. Tweed and O. Knudsen (2005). Icelandic jökulhlaup impacts. Iceland: modern processes and past environments. C. Caseldine, A. Russell, J, J. Harðardóttir and O. Knudsen, Elsevier: 397.

Russell, A. and O. Knudsen (1999). "An ice-contact rhythmite (turbidite) succession deposited during the November 1996 catastrophic outburst flood (Jökulhlaup), Skeiðarárjökull , Iceland." Sedimentary Geology **127**: 1 - 10.

Russell, A. J., A. R. Gregory, A. R. G. Large, P. J. Fleisher and T. D. Harris (2007). "Tunnel channel formation during the November 1996 jökulhlaup, Skeiðarárjökull, Iceland." Annals of Glaciology **45**: 95 - 103.

Russell, A. J., P. G. Knight and T. A. G. P. Van Dijk (2001). "Glacier surging as a control on the development of proglacial, fluvial landforms and deposits, Skeiðarásandur, Iceland." Global and Planetary Change **28**(1-2): 163-174.

Russell, A. J. and Ó. Knudsen (1999). "An ice-contact rhythmite (turbidite) succession deposited during the November 1996 catastrophic outburst flood (jökulhlaup), Skeiðarárjökull, Iceland." Sedimentary Geology **127**(1-2): 1-10.

Russell, A. J. and Ó. Knudsen (2002). "The effects of glacier-outburst flood flow dynamics on ice-contact deposits: November 1996 jökulhlaup, Skeiðarársandur, Iceland." International Association of Sedimentologists Special Publications(32): 67-83.

Russell, A. J., O. Knudsen, J. K. Maizels and P. M. Marren (1999). "Channel cross-sectional area changes and peak discharge calculations in the Gígjukvísl river during the 1996 Jökulhlaup, Skeiðarárjökull, Iceland." Jökull **47**: 45-58.

Russell, A. J., P. M. Marren, J. Heinz, J. Tronicke, Ó. Knudsen and H. Fay (2001). "Morphology and sedimentology of a giant supraglacial, ice-walled, jökulhlaup channel, Skeiðarárjökull, Iceland: Implications for esker genesis." Global and Planetary Change **28**(1-2): 193-216.

Russell, A. J., M. J. Roberts, H. Fay, P. M. Marren, N. J. Cassidy, F. S. Tweed and T. Harris (2006). "Icelandic jökulhlaup impacts: Implications for ice-sheet hydrology, sediment transfer and geomorphology." Geomorphology **75**(1-2): 33-64.

Russell, H. A. J. and R. W. C. Arnott (2003). "Hydraulic-jump and hyperconcentrated-flow deposits of a glacigenic subaqueous fan: Oak ridges Moraine, southern Ontario, Canada." Journal of Sedimentary Research **73**(6): 887-905.

Russell, H. A. J., R. W. C. Arnott and D. R. Sharpe (2003). "Evidence for rapid sedimentation in a tunnel channel, Oak Ridges Moraine, southern Ontario, Canada." Sedimentary Geology 160(1-3): 33-55.

Ruszczynska-Szenajch, H (1976). "Glacitektoniczne depresjie i kry lodowcowe na tle budowy geologicznej poludniowo-wschodniego Mazowsza i poludniowego Podlasia (Glacitectonic depresions and glacial rafts in mid-eastern Poland)". Studia Geologica Polonica **50**: 1 - 106.

Sandersen, P. B. E., Joslash and F. rgensen (2003). "Buried Quaternary valleys in western Denmark-occurrence and inferred implications for groundwater resources and vulnerability." Journal of Applied Geophysics **53**(4): 229-248.

Saunderson, H. C. (1977). "The sliding bed faciès in esker sands and gravels: a criterion for full-pipe (tunnel) flow? ." Sedimentology **24**: 623-638.

Sharp, M. (1985). "'Crevasse-fill' ridges—a landform characteristic of surging glaciers?" Geographiska Annaler **67a**: 213 - 220.

Sharpe, D. R., (1987). "The stratified nature of drumlins from Victoria Island and Southern Ontario, Canada." In: Rose, J., Menzies, J. (Eds.), Drumlin Symposium. Balkema, Rotterdam, pp. 185–214.

Sharpe, D. R., A. Pugin, S. E. Pullan and G. Gorrell (2003). "Application of seismic stratigraphy and sedimentology to regional hydrogeological investigations: an example from Oak Ridges Moraine, southern Ontario, Canada." Canadian Geotechnical Journal **40**(4): 711–730.

Sharpe, D. R. and J. Shaw (1989). "Erosion of bedrock by subglacial meltwater, Cantley, Quebec." Geological Society of America Bulletin **101**(8): 1011-1020.

Shaw, J. (1983). "Drumlin formation related to inverted melt-water erosional marks." Journal of Glaciology **29**(103): 461-479.

Shaw, J. (1988). "Glacio-fluvial sediment transfer: An Alpine perspective : edited by A.M. Gurnell and M.J. Clark, 1987, J. Wiley and Sons Ltd, Chichester, ISBN 0-471-90929-7, [UK pound]42.50 hardback, 524 pp." Quaternary Science Reviews **7**(1): 107.

Shaw, J. (1988). "Subglacial erosional marks, Wilton Creek, Ontario." Canadian Journal of Earth Sciences **25**(8): 1256-1267.

Shaw, J. (2002). "The meltwater hypothesis for subglacial bedforms." Quaternary International **90**(1): 5-22.

Shaw, J. and J. Archer (1979). Deglaciation and glaciolacustrine sedimentation conditions, Okanagan valley, British Columbia, Canada. Proc. INQUA symposium on genesis and lithology of Quaternary deposits, Zurich, 10-20 September 1978. Moraines varves: origin, genesis, classification. C. Schluchter, A.A. Balkema: 347-356.

Shaw, J., G. Douglas R, G. Jean-Pierre, A. Thane W and P. D. Russell (2000). "Submarine and onshore end moraines in southern Newfoundland: implications for the history of late Wisconsinan ice retreat." Boreas **29**(4): 295-314.

Shaw, J. and R. Gilbert (1990). "Evidence for large-scale subglacial meltwater flood events in southern Ontario and northern New York State." Geology **18**(12): 1169-1172.

Shaw, J. and G. Gorrell (1991). "Subglacially Formed Dunes with Bimodal and Graded Gravel in the Trenton Drumlin Field, Ontario." Géographie physique et Quaternaire **45**(1): 21-34.

Shaw, J., G. Jean-Pierre, A. Thane W and P. D. Russell (2000). "Submarine and onshore end moraines in southern Newfoundland: implications for the history of late Wisconsinan ice retreat." Boreas **29**(4): 295-314.

Shoemaker, E. M. (1992). "Water sheet outburst floods from the Laurentide Ice Sheet." Canadian Journal of Earth Sciences **29**: 1250 - 1264.

Shreve, R. L. (1972). "Movement of water in Glaciers." Journal of Glaciology **11**: 205 - 214.

Shreve, R. L. (1985). "Esker characteristics in terms of glacier physics, Katahind esker system, Maine." Geological Society of America Bulletin **96**: 639 - 646.

Sigurðsson, O. (2005). Variations of termini of glaciers in Iceland in recent centuries and their connection with climate. Iceland – Modern Processes and Past Environments,

Developments in Quaternary Science. C. Caseldine, A. Russell, J. Harðardóttir and Ó. Knudsen. **5:** 241-255.
Singh, I. B. (1977). "Bedding Structures in a Channel Sand Bar of the Ganga River Near Allahabad, Uttar Pradesh, India." Journal of Sedimentary Research **47**(2): 747 - 752.
Sjogren, D. B., H. M. Jol, M. J. Munro-Stasiuk, T. G. Fisher and L. D. Taylor (2002). "Incipient tunnel channels." Quaternary International **90**: 41-56.
Smed, P. (1962). "Studier over den fynske øguppes glaciale landskabsformer". Meddelelser fra Dansk Geologisk Forening **15**: 1-74.
Smith, J. A., C.-D. Hillenbrand, R. D. Larter, A. G. C. Graham and G. Kuhn (2009). "The sediment infill of subglacial meltwater channels on the West Antarctic continental shelf." Quaternary Research **71**(2): 190-200.
Smith, L. C., L. A. K. Mertes, N. D. Smith, J. B. Garvin, D. E. Alsdorf, F. J. Magilligan and B. Gomez (2000). "Estimation of erosion, deposition, and net volumetric change caused by the 1996 Skeiðarársandur Jökulhlaup, Iceland, from synthetic aperture radar interferometry." Water Resources Research **36**(6): 1583-1594.
Smith, L. C., Y. Sheng, F. J. Magilligan, N. D. Smith, B. Gomez, L. A. K. Mertes, W. B. Krabill and J. B. Garvin (2006). "Geomorphic impact and rapid subsequent recovery from the 1996 Skeiðarársandur Jökulhlaup, Iceland, measured with multi-year airborne lidar." Geomorphology **75**: 65–75.
Smith, L. N. (2004). "Late Pleistocene stratigraphy and implications for deglaciation and subglacial processes of the Flathead Lobe of the Cordilleran Ice Sheet, Flathead Valley, Montana, USA." Sedimentary Geology **165**(3-4): 295-332.
Smith, N. (1978). "Sedimentation processes and patterns in a glacier-fed lake with low sediment input." Canadian Journal of Earth Sciences **15**(5): 741–756.
Sneed, E. D. and R. L. Folk (1958). "Pebbles in the lower Colorado River, Texas, a study of particle morphogenesis." Journal of Geology **66**(2): 114–150.
Snorrason, Á., P. Jónsson, S. Pálsson, S. Árnason, O. Sigurðsson, S. Víkingsson, A. Sigurðsson and S. Zóphóníasson (1997). HLAUPIÐ Á SKEIÐARÁSANDI HAUSTIÐ 1996 Útbreiðsla, rennsli og aurburður. Vatnajökull Gos og hlaup 1996. R. H. Haraldsson, Vegagerðin: 79 - 137.
Snorrason, Á., P. Jónsson, S. Sigurðsson, S. Pálsson, S. Árnason, S. Víkingsson and I. Kaldal (2002). "November 1996 jökulhlaup on Skeiðarásandur outwash plain, Iceland." Spec. Publs int. Ass. Sediment. **32**(55-65.).
Stea, R.R., and Brown, Y., (1989). "Variation in drumlin orientation, form and stratigraphy relating to successive ice flows in southern and central Nova Scotia." Sedimentary Geology **62**: 223–240.
Stokes, C. R. and C. D. Clark (2001). "Palaeo-ice streams." Quaternary Science Reviews **20**(13): 1437-1457.
Stokes, C. R., M. Matteo., and C. Clark (2011). "The composition and internal structure of drumlins: Complexity, commonality, and implications for a unified theory of ther formation" Earth Science Reviews 107: 398 - 422.
Sugden, D. E., John, B. S., (1976). "Glaciers and Landscape: A Geomorphological Approach. "Edward Arnold, London. 375 pp.
Summerfield, M. (1991). Global Geomorphology. Harlow, Pearson Education Ltd.
Thorarinsson, S. (1939). "The ice dammed lakes of Iceland with particular reference to their values as indicatirs of glacier oscillations." Geografiska Annaler **21**: 216 - 242.
Thorarinsson, S. (1943). "Vatnajokull: Scientific results of the Swedish-Icelandic Investigations. 1936-37-38." Geografiska Annaler 25: 1 - 54.
Thorarinsson, S., (1956). "On the variations of svínafellsjökull, skaftafellsjökull and kviárjökull in oræfi". Jökull **6**, 1–15.
Þórarinsson, S. (1974). Vötnin stríð - Saga Skeiðaráhaulp og Grímsvatnagosa. Reykjavík Bókaútgáfa menningsjóðs.
Thoroddsen (1893). "Dr. Thoroddsen's Explorations in Iceland." The Geographical Journal **2**(2): 154-158.
Thwaites, F. T. (1926). "The Origin and Significance of Pitted Outwash." The Journal of Geology. 34 (4): 308 -319
Tikku, A. A., R. E. Bell, M. Studinger and G. K. C. Clarke (2004). "Ice flow field over Lake Vostok, East Antarctica inferred by structure tracking." Earth and Planetary Science Letters **227**(3-4): 249-261.
Todtmann, E.M., (1960). "Gletscherforschungen auf Island (Vatnajokull). Abhandlung aus dem Gebiet der Auslandskunde". Hamburg. Bd 65, Rh. C, Bd 19.
Tucker, M. (1988). Techniques in sedimentology. Oxford, Blackwell Scientific Publications.
Tweed, F. S., M. J. Roberts and A. J. Russell (2005). "Hydrologic monitoring of supercooled meltwater from Icelandic glaciers." Quaternary Science Reviews **24**(22): 2308-2318.

Tweed, F. S. and A. J. Russell (1999). "Controls on the formation and sudden drainage of glacier-impounded lakes: Implications for jökulhlaup characteristics." Progress in Physical Geography **23**(1): 79-110.

Upham, W,. (1892) "Conditions of the accumulation of drumlins". American Geologist **10:** 339 - 362.

Upham, W. (1894). "The Madison type of drumlins." American Geologist **14**: 69–83.

van de Meer, J. J. M., K. H. Kjaer, J. Kruger, J. Rabassa and A. A. Kilfeather (2009). "Under pressure: clastic dykes and glacial settings." Quaternary Science Reviews **28**: 708 - 720.

van Dijk, T. (2001). Glacier surges as a control on the development of proglacial, fluvial landforms and deposits, Keele University. **Unpublished Ph. D**.

van Dijke, J. J. and A. Veldkamp (1996). "Climate-controlled glacial erosion in the unconsolidated sediments of northwestern Europe, based on a genetic model for tunnel valley formation." Earth Surface Processes and Landforms **21**(4): 327-340.

Veillette, J. J. (1986). "Former southwesterly ice flows in the Abitibi-Temiskaming region: implications for the configuration of the late Wisconsinan ice sheet. ." Canadian Journal of Earth Sciences **23**: 1724-1741.

Wadell, H. (1935). "Ice Floods and Volcanic Eruptions in Vatnajökull." Geographical Review **25**(1): 131-136.

Waller, R. I., A. J. Russell, T. A. G. P. Van Dijk and Ó. Knudsen (2001). "Jökulhlaup-related ice fracture and supraglacial water release during the November 1996 Jökulhlaup, Skeiðarárjökull, Iceland " Geografiska Annaler, Series A: Physical Geography **83**(1-2): 29-38.

Waller, R. I., T. A. G. P. Van Dijk and O. Knudsen (2008). "Subglacial bedforms and conditions associated with the 1991 surge of Skeiðarárjökull, Iceland." Boreas **37**(2): 179 - 194.

Warburton, J. (1990). "An alpine proglacial fluvial sediment budget." Geografiska Annaler, Series A 72 **A**(3-4): 261-272.

Warren, C. and M. Aniya (1999). "The calving glaciers of southern South America." Global and Planetary Change **22**(1-4): 59-77.

Whipple, K. X., G. S. Hancock and R. S. Anderson (2000). "River incision into bedrock: Mechanics and relative efficacy of plucking, abrasion, and cavitation." Geol Soc Am Bull **112**(3): 490-503.

Wildt, M. S., E. J. Klok and J. Oerlemans (2003). "Reconstruction of the mean specific mass balance of Vatnajökull (Iceland) with a Seasonal Sensitivity Characteristic." Geografiska Annaler, Series A: Physical Geography **85**(1): 57-72.

Wingfield, R. (1989). "Glacial incisions indicating middlena and upper Pleistocene ice limits off Britain." Terra Nova **1**: 538 - 548.

Wingfield, R. (1990). "The origin of major incisions within the Pleistocene deposits of the North Sea." Marine Geology **91**(1-2): 31-52.

Wisniewski, E., L. Andrzejewski and P. Molewski (1997). "Fluctuations of the snout of Skeiðarárjökull in Iceland in the last 100 years and some of their consequences in the central part of its forefield." Landform Analysis **1**: 73 - 78.

Woodward, J., T. Murray and A. McCaig (2002). "Formation and reorientation of structure in the surge-type glacier Kongsvegen, Svalbard." Journal of Quaternary Science **17**(3): 201-209.

Wright, H.E., (1962). "Role of the Wadena lobe in the Wisconsin glaciation of Minnesota." Bulletin of the Geological Society of America **73**, 73–100.

Wright, H. E., Jr. (1971). "Retreat of the Laurentide Ice Sheet from 14,000 to 9,000 years ago." Quaternary Research **1**: 316-330.

Wright, H. E., Jr (1973). "Tunnel valleys, glacial surges and subglacial hydrology of the superior lode, Minnesota." Geological Society of America Memoir, **136**: 251 - 276.

Wysota, W. (1994). "Morphology, internal composition and origin of drumlins in the southeastern part of the Chelmno-Dobrzyn Lakeland, North Poland." Sedimentary Geology **91**(1-4): 345-364.